CHARACTERISATION OF THE PROGENITORS FOR THE MOUSE ANTEROPOSTERIOR AXIS

Noemí Cambray

Thesis presented for the degree of Doctor of Philosophy
Institute for Stem Cell Research
University of Edinburgh
2006

To mama Roser, for always putting us first, and for her unconditional support and encouragement.

ABSTRACT

Elongation of the mouse anteroposterior axis depends on a small population of progenitors initially located in the primitive streak and later in the tail bud. Gene expression and lineage tracing have shown that there are many features common to these progenitor tissues throughout axial elongation. Retrospective single cell marking experiments indicate a stem cell progenitor for the myotome and the spinal cord in the primitive streak and its descendant, the tail bud. However, the identity and exact location of the progenitors is unclear from these analyses.

First, I performed a detailed gene expression analysis using genes known to play a role in axis elongation (*T* (*Brachyury*), *Fgf8* and *Wnt3a)* and the homologues of genes expressed in the *Xenopus* tail (*Evx1* (*Xhox3*), *Foxa2* (*Pintallavis*) and *Cdx2* (*Xcad3*). Comparison of the gene expression patterns showed a consistent set of expression domains that was continuous throughout axis elongation. This gives further support to the idea that tail bud formation in the mouse, as shown in other vertebrates, is a continuation of gastrulation. However, in the mouse, we have not detected a new wave of gene expression coinciding with tail elongation, as seen in *Xenopus*. Furthermore, the different domains of gene expression described in *Xenopus* do not always match the domains in mouse. In addition, we have found that up to 2 days before the end of axial elongation, expression of the majority of tail bud markers decreases drastically. Intriguingly, high level of *T* expression continues until 13.5 dpc when axial elongation stops. Since *Fgf8* and *Wnt3a* are thought to maintain *T* expression, this implies either a very slow loss of these proteins or compensation by other family members.

Secondly, from experiments started during my MRes and finished during my PhD, we have shown that ingression of ectodermal cells to the mesoderm layer continues even after posterior neuropore closure around the 35-somite stage, as previously observed in chick. Furthermore, grafts of one of the regions of the tail bud, named the chordoneural hinge (CNH) region by analogy to an equivalent structure in *Xenopus* and chick, showed it had properties expected of a stem cell population. When transplanted to

earlier (8.5 dpc) embryos, which were then cultured in vitro during a period of extensive axis elongation, the CNH could incorporate to all dorsal host axial tissues and still retain progenitor cells in the tail bud. Indeed, these cells could be serially passaged through 3 successive generations of embryos without apparent loss of their ability to differentiate and retain progenitors in the tail bud. Therefore, the CNH has the characteristics of a population of axial stem cells.

A third set of experiments was then performed to localise the putative axial stem cells at earlier stages. Using isotopic grafts to 8.5 dpc embryos, I tested the fate of the node region itself, the region just posterior to it that represents the border between the node and streak (named border) and the anterior primitive streak (APS) region, and found that only cells from the border region contribute to all the dorsal axial tissues and to the CNH, while its neighbours showed a much restricted set of fates. Furthermore, the border was able to give rise to all the derivatives of node and APS when transplanted to these regions, while node and APS had very restricted potency. Consistent with the above results, grafting these sub-regions to a neutral site, the kidney capsule, showed that, the border and CNH, but not neighbour tissues, differentiate to a wide range of axial derivatives. Taken together, these results point to the existence of axial stem cells with equivalent gene expression that reside in the border region at primitive streak stages and later in the CNH in the tail bud.

COMMON ABBREVIATIONS

AER	apical ectodermal ridge
A/P	anteroposterior
APS	anterior primitive streak
AVE	anterior visceral endoderm
βgal	β-galactosidase
BMP	bone morphogenetic protein
BSA	Bovine Serum Albumin
°C	degrees centrigrade
cDNA	complementary DNA
CNH	chordoneural hinge
CNS	central nervous system
CO_2	carbon dioxide
DEPC	diethyl pyrocarbonate
dH_2O	distilled water
DiI	1,1'-dioctadecyl-3,3,3',3-tetramethylindocarbocyanine
DNA	deoxyribonucleic acid
dNTP	dinucleotide triphosphate
dpc	days *post coitum*
D/V	dorsoventral
ES	embryonic stem
EtOH	ethanol
Fgf	fibroblast growth factor
g	grams
GFP	green fluorescent protein
GMEM	Glasgow's modified Eagle's medium
hr	hours
ICM	inner cell mass
Kb	kilobase
l	litre
LB	Luria-Broth
lfng	*lunatic fringe*
LIF	leukemia inhibitor factor

LPM	lateral plate mesoderm
L/R	left/right
m	milli
μ	micro
M	molar
min	minutes
mRNA	messenger RNA
NaOAc	sodium acetate
PBS	phosphate buffered saline
PBT	phosphate buffered saline + 0.1% Tween 20 solution
PCR	polymerase chain reaction
PFA	paraformaldehyde
PGCs	primordial germ cells
PS	primitive streak
PSM	presomitic mesoderm
RNA	ribonucleic acid
RNAse	ribonuclease
rpm	revolutions per minute
RT	room temperature
SE	surface ectoderm
sec	seconds
Shh	*sonic hedgehog*
TB	tail bud
TBM	tail bud mesoderm
TF	transcription factor
TGF	transforming growth factor
UV	ultraviolet
VE	visceral endoderm
VEG	ventral ectodermal groove
VER	ventral ectodermal ridge
v/v	volume:volume
w/v	weight:volume
Xgal	5-bromo-4-chloro-3-indolyl-b-d-galactoside

TABLE OF CONTENTS

Chapter 2. Gene expression in the axial progenitors

LIST OF FIGURES

Chapter 3

Chapter 4

LIST OF TABLES

Chapter 1

INTRODUCTION

Perhaps the most crucial aspect in the development of vertebrates is the formation and elongation of the anteroposterior axis of the embryo from its inception at gastrulation, at 6.5 days post coitum (dpc), to its termination 7 days later in the mouse. Although it is well established that the anterior structures (head) derive from the transit of cells through the primitive streak and their subsequent migration towards the anterior end of the embryo; the formation of the posterior tissues, namely the posterior trunk and tail has been controversial over the years. The basis for this controversy and the key recent experiments in vertebrates that have attempted to readdress this issue are presented in this introductory chapter. The use of molecular markers and labelling experiments, aiming to follow cell behaviour, have led to the conclusion that the formation of the posterior tissues is a direct continuation of the processes begun at gastrulation. Interestingly, some experiments have also suggested the existence of axial stem cells for the formation of the axis in the mouse. The localisation of these axial stem cells during anteroposterior axis development in the mouse is the main focus of my PhD. Therefore the evidence for their existence will be discussed in detail at the end of this introduction.

1.1 AXIAL ELONGATION

Axial elongation is accomplished by the progressive allocation of progenitors to the differentiating axial tissues in a rostrocaudal sequence. During the early stages of gastrulation, formation of the anterior embryonic and extraembryonic mesoderm and endoderm results from movement en masse towards and through the primitive streak of cells located over a large proportion of the epiblast (Lawson, 1991). At later stages these mass movements cease and the mesoderm progenitors are instead located close to the primitive streak and its descendant the tail bud. These two structures, the primitive streak and the tail bud, share many common features. Firstly, they produce similar axial tissues: somites, notochord and neural tube. Secondly, in vertebrates, the sites of mesoderm formation at gastrulation and later at tail bud stages share expression of many genes (Gawantka et al, 1998; Pollet et al. 2005). Thirdly,

18

a number of genes such as *T* (*Brachyury*) and *Wnt3a*, which have a critical role in primitive streak morphogenesis revealed by null mutations, affect only tail development when function is partially lost (Chesley, 1935; Wilson *et al.*, 1995; Greco *et al.*, 1996). Thus in these respects, the extension of the anteroposterior axis caudal to the head in the mouse can be viewed, as a continuum throughout the formation of about 65 somites. However, although this view of axial elongation seems most accepted now; in the past, two extreme views coexisted in the literature unresolved for many years. By the early 90's, new attention was given to tail development in the different vertebrates and new work was done trying to readdress both views.

Two extreme views of tail development

Holmdahl in 1925, from studies in chick, concluded that the tail formed by a separate and distinct process from that of the trunk. He suggested that the tail bud constitutes a blastema of undifferentiated cells with little or no regional specification of the progenitors. This suggested that cells in the tail bud not only have different potency, but also differentiate according to different rules from those that pertain to the streak. This view was not shared by Pasteels (1937, 1943) who proposed a different conception of the tail bud, which he considered to be formed by a mosaic of cellular populations already endowed with differential potentials from gastrulation. However, no clear experimental data had so far permitted to discern between these two views.

In the 1990's, with the use of molecular markers, these two views have been directly addressed in different organisms. Different lines of evidence seem to corroborate Pasteels' idea that the different tissues of the tail derive from distinct cells populations. However, there is also strong evidence to suggest the existence of self-renewing pools of progenitors with more than one tissue fate (Selleck and Stern, 1991), reminiscent of Holmdahl's idea of the tail tissues being formed by a blastema of undifferentiated cells. Nonetheless, all these experiments suggest that the formation of the posterior tissues is a direct continuation of the processes begun at gastrulation.

I will firstly review the gene expression studies carried out to date, and show that most genes expressed in the region of mesoderm formation at early stages continue to be expressed in the tail bud. Secondly, I will examine lineage studies to date, and show that these point to the existence of regionalised progenitors in the blastopore/primitive streak that will form the tissues of the tail. Thirdly, these lineage analyses also indicate that the cell movements during gastrulation, continue during tail formation. Fourthly, I will describe the organizer grafts done so far, and show that the tip of the tail, named the CNH, retains organizer activity as its earlier precursor the node or dorsal blastopore. Finally, I will describe the evidence in the mouse for the continuity of gene function from gastrulation to tail formation.

From gastrulation to the tail bud

1. Gene expression

<u>Xenopus</u>

Gont *et al.* in 1993, working in *Xenopus* embryos, compared the expression of two markers that are expressed in distinct regions of the blastopore of the early gastrula and whose expression can be followed continuously as they become localized to distinct populations in the tail bud. The markers used were *Xnot2* a homeobox gene expressed in the dorsal lip of the blastopore, and *Brachyury*, expressed in the entire blastoporal ring (stages 10.5 to 13) (see Table 1.1 for *Xenopus* developmetal stages). In the developing tail, *Xnot2* is expressed in a U-shaped region, which consists of the posterior ventral spinal cord and posterior notochord as well as the region of continuity between these two tissues. The latter region was designated the chordoneural hinge (CNH) by Pasteels, 1943 (see Fig. 1.1 top panel for *Xenopus* anatomy; see Fig. 1.2 top panel for *Xenopus* gene expression). The expression of *Xnot2* in the notochord decreases in the posterior notochord as the tail develops and becomes restricted to the CNH region and ventral spinal cord by stage 28. *Brachyury* transcripts are found in the notochord and the CNH and in the mass of cells that lies posteriorly, ventrally and laterally to the CNH (stage 22). Cells expressing *Xbra* are also found in the roof of the spinal cord,

	Xenopus	Chick	Mouse
gastrulation	Stage 10-10.5 - early gastrula	Stage 2 - initial streak	6.5-7.25 dpc - early streak
	Stage 11-11.5 - middle gastrula	Stage 3 - intermediate streak	7.0-7.75 dpc - mid-streak
	Stage 12 - late gastrula	Stage 4 - definitive streak (Hensen's node present)	7.25-7.75 dpc - late streak (node present)
	Stage 13 - early neurula	Stage 5 - head-process	7.25-8.0 dpc - early allantoic bud
	Stage 13.5 - formation neurenteric canal		
	Stage 14 neurulation begins	Stage 6 - head-fold	7.5-8.0 dpc - head-fold stages
	Stage 19 neural tube closure	Stage 7 - one somite	8.25 dpc - one somite
organogenesis	Stage 20 ↓ Stage 25	Stage 11 (13 somites) - TB condensation	
		Stage 13 (19 somites) - posterior neuropore closure	9.0 dpc (17-18 somites) - VER appears in ventral SE
	Stage 26 - early TB stage	Stage 15 (24-27 somites) - TB transformation complete	
tail bud extension	Stage 27 - TB outgrowth starts	Stage 16 (26-28 somites) - tail outgrowth starts	10.0 dpc (30 somites) - tail outgrowth starts
	Stage 35 - neurenteric canal collapses		10-10.5 dpc (30-35 somites) - posterior neuropore closure
	Stage 41 (~50 somites) - somite formation stops	Stage 27 (~5days, ~52 somites) - tail elongation stops	13.5 dpc (~65 somites) - tail elongation stops

Legend:

— non-equivalence between stages in different organisms

--- equivalent stages between organisms

→ neuropore closure, occurring at unequal developmental stages between organisms

Table 1.1 Comparison of stages between *Xenopus*, chick and mouse (*Xenopus* stages taken from Sive *et al.*, 2000; Beck and Slack 1998; Gont *et al.*, 19993; Niewkoop and Faber, 1967; chick stages taken from a reprint of Hamburger and Hamilton (1951); Knezevic *et al.*, 1998; Catala *et al.*, 1995; Pourquié et al., 2004; mouse stages taken from Downs and Davies, 1993; Wilson and Beddington, 1996; Gofflot *et al.*, 1997, Goldman *et al.*, 2000). VER: ventral ectodermal ridge, TB: tail bud, SE: surface ectoderm.

Xenopus

Stage 13

A
- dorsal blastopore lip
- lateral blastopore lip
- ventral blastopore lip
- lateral blastopore lip

B
- neural tube floorplate
- notochord
- dorsal blastopore / CNH
- blastopore
- yolk plug
- blastopore

endoderm

Stage 28

C

D spinal cord
roof floor
- CNH
- neurenteric canal
- fin
- posterior wall
- hindgut cavity
- anus
notochord

Chick

Stage 6

E

F
- presomitic mesoderm
- neural tube
- notochord
- node
- PS

Stage 15

G

H
- somite
- presomitic mesoderm
- notochord
- neural tube
- node / CNH
- PS/TB

Mouse

8.5 dpc

I

J
- allantois
- PS
- node
- notochord
- endoderm
- somite
- neurectoderm

10.5 dpc

L
- neurectoderm
- presomitic mesoderm
- closed neuropore
- TB
- notochord
- somite
- hindgut

K

Figure 1.1 Anatomy of *Xenopus*, chick and mouse

Top panel shows two different stages of *Xenopus laevis* development: stage 13 (late gastrula, early neurula) on the left and stage 28 (tail bud) on the right, **A** and **C**: illustrations taken from www.xenbase.org, **B**: diagram modified from Beck and Slack (1998), **A** and **B**: posterior dorsal view and sagittal section, respectively, of a stage 13 embryo, **C** and **D**: lateral view of a stage 28 embryo, **D**: magnified sagittal section diagram of the tail bud region marked in C. Anterior is to the left. **Middle panel** shows a stage 6 (0-1 somites, headfold) chick embryo on the left and stage 15 (24-28 somites, tail bud) on the right, **E** and **G**: illustration taken from a reprint of Hamburger and Hamilton (1951), **E**: dorsal view of a stage 6 embryo, **F**: diagram showing a close up of the primitive streak region marked in E, **G**: dorsal view of a stage 15 embryo, **H**: diagram showing a close up of the tail bud region marked in G. Anterior is dorsal. **Bottom panel** shows an 8.5 dpc (2-8 somites) mouse embryo on the left and 10.5 dpc (30 somites) on the right, **I** and **K**: lateral view of an 8.5 dpc and 10.5 dpc embryo, respectively expressing *T (Brachyury)*, **J**: sagittal section diagram of an 8.5 dpc embryo, **L**: close up lateral view diagram of the tail bud region of a 10.5 dpc embryo. Anterior to the left. PS: primitive streak, CNH: chordoneural hinge, TB: tail bud, dpc: days post coitum. Bar: 150µm in I; and 500µm in K.
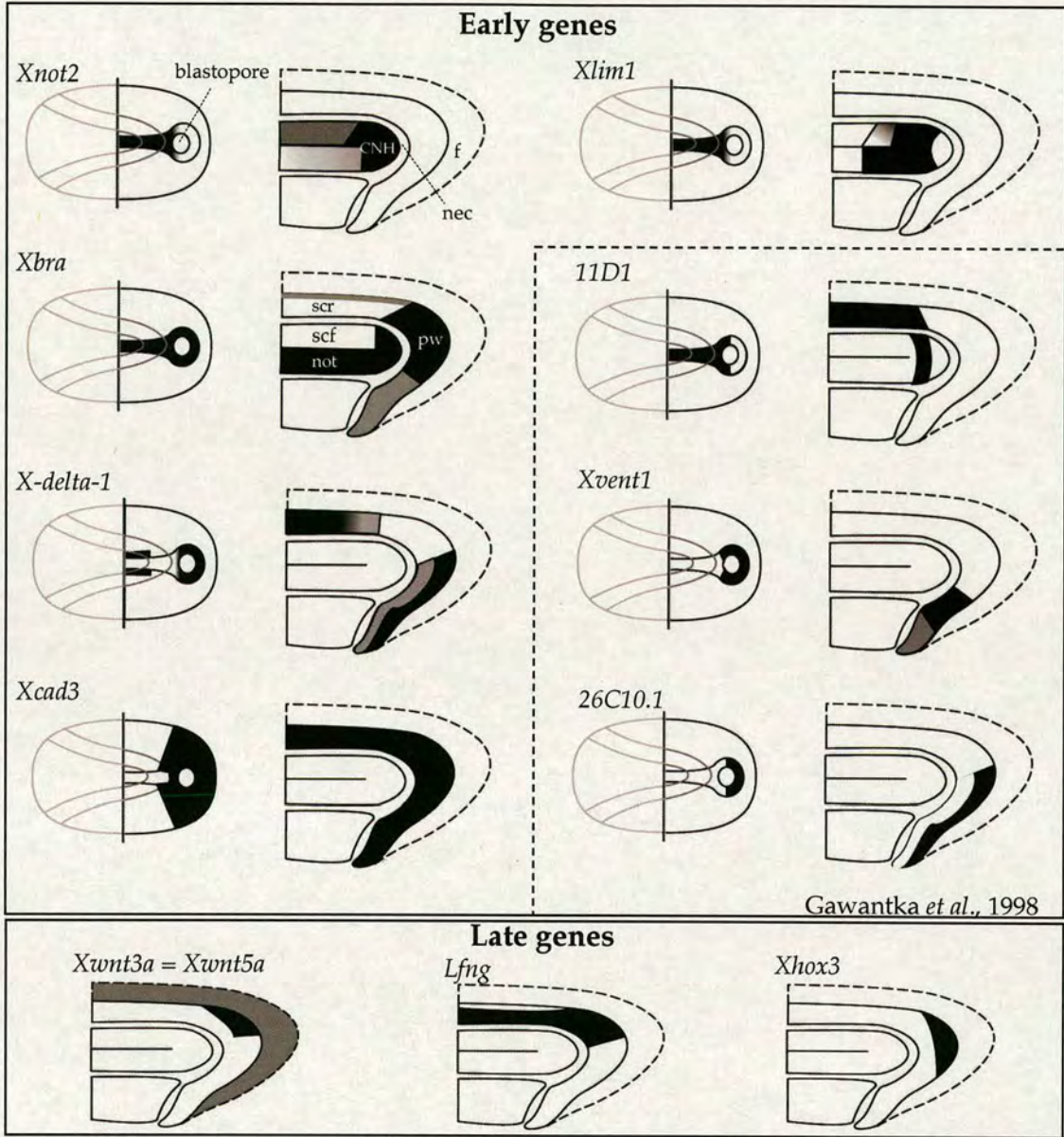
Figure 1.2 *Xenopus* regions of gene expression
Top panel shows diagrams of the regions of gene expression described by the so called "early genes" as described by Beck and Slack (1998) as they are expressed from gastrulation to tail bud formation (for each gene, left shows a posterior dorsal view of a late gastrula stage 13 and right shows mid-sagital view of a tail bud stage 28), Gawantka *et al*. (1998) added 3 more genes to this list. **Bottom panel** shows the so called "late genes" that are only expressed at the time of tail bud outgrowth (stage 28 represented). CNH: chordoneural hinge, f: fin, nec: neurenteric canal, scr: spinal cord roof, scf: spinal cord floor, not: notochord, pw: posterior wall. Anterior is to the left.

23

which appears to be continuous with the posterior mass of cells expressing *Xbra*. This posterior mass of cells (referred as posterior wall), which is *Xbra+* and *Xnot2-* is separated from the CNH (*Xbra+*, *Xnot2+*) by a structure called the neurenteric canal, which in amphibians connects the lumen of the spinal cord to that of the gut and it is formed at stage 13.5 by the closure of the lateral blastopore lips over the blastopore and collapses at stage 35. While there is no evidence in the literature for the existence of a neurenteric canal in the chick or the mouse embryo, this structure probably represents an ancestral chordate feature, for it is present in Amphioxus (Hopper and Hart, 1985), shark (Kingsbury, 1932), amphibian (Nieuwkoop and Faber, 1967), gecko (kerr, 1919), turtle (Yntema, 1968) and human embryos (Moore, 1977).

From these studies, at least three different cell populations were distinguishable in the developing *Xenopus* tail bud (stage 13-28):

1. the CNH, which is positive both for *Xnot2* and *Xbra*,
2. the posterior wall cells and cells in the roof plate of the spinal cord which are *Xbra*-positive but *Xnot2*-negative,
3. the ventral spinal cord which is *Xnot2*-positive but *Xbra*-negative.

By stage 30, *Xnot2* expression has decreased in the ventral spinal cord and has become restricted to the CNH, whereas *Xbra* expression has decreased in the posterior notochord and has become restricted to the CNH and posterior wall.

In 1998, Beck and Slack extended Gont *et al.*'s gene expression studies, describing seven distinct domains in the developing tail bud of *Xenopus*. The genes that were studied in this report were chosen based on one of two criteria: genes that had previously been reported in the tail bud, but without precise location, and/or genes with possible association with other systems involving distal outgrowth. They observed two distinct temporal phases of gene expression in tail development:

Early genes

The early phase involves expression of genes that are already expressed in the tail bud region before its determination at stage 13 and are subsequently restricted in the extending tail bud by stage 30 (Fig. 1.2

top panel). They include: the Notch ligand *X-delta-1*, which is expressed specifically in the posterior wall of the neurenteric canal but is excluded from the CNH at stage 30, thus maintaining its earlier expression in the lateral and ventral blastopore lips. *Xlim1* is expressed in the notochord and dorsal blastopore lip at the end of gastrulation, and is maintained in the CNH and the posterior tip of the differentiated notochord in later stages. Interestingly, *Xlim1* transcripts are barely detectable or absent at the tip of the CNH. *Xnot2* is expressed as described by Gont *et al.* (1993). The posterior notochord therefore represents a novel expression domain by stage 30, marked by *Xlim1* but not *Xnot2* transcripts. *Xbra* is expressed in the CNH and posterior wall as described by Gont *et al.* (1993). *Xcad3* expression in the posterior neural plate is later maintained in the posterior wall and posterior dorsal neural tube.

Late genes

The second, later, phase of gene expression begins at stage 27 and correlates with the onset of tail outgrowth. These genes were not expressed in the tail bud region at stage 13, before its determination (Fig. 1.2 bottom panel). They include *Xwnt3a* and *lunatic fringe (lfng)*, expressed in the dorsal roof domain of the tail bud. The posterior extent of the dorsal roof region is marked by a sharp limit of *Xwnt3a* and *lfng* expression within the posterior wall, which corresponds to the future tip of the tail bud. In contrast, the expression of these genes fades gradually towards the anterior limit. Although the posterior boundaries match exactly, expression of *lunatic fringe* extends further towards the anterior than that of *Xwnt3a*. *Xwnt5a* expression is weaker than that of *Xwnt3a* but is restricted to an identical region of the tail bud roof. Another novel late region is the distal tip of the tail, marked by the expression of *Xhox3*, which corresponds to the most distal part of the posterior wall and partially overlaps dorsally with the domain defined by *Xwnt3a, Xwnt5a* and *lfng*. *Xhox3* expression therefore marks the most distal cells of the tail bud in *Xenopus*.

As described by Gont *et al.* (1993) and Beck and Slack (1998), the *Xenopus* tail contains different regions of gene expression, which might

represent different subpopulations of cells. Some of these populations might have originated during gastrulation, as they show gene expression continuous from gastrulation to tail development. However, some genes are expressed *de novo* at the onset of tail outgrowth, reminiscent of Holmdahl's idea that the tail grows by a different mechanism from the trunk. However, the homologues of these *de novo* expressed genes: *Xwnt3a, Xwnt5a, lunatic fringe* and *Xhox3* are expressed as a continuum from gastrulation to tail development in chick and mouse.

In the same year, Gawantka *et al.* (1998) performed a large-scale gene expression screen where 1765 randomly picked cDNAs were analysed by whole-mount *in situ* hybridisation also in *Xenopus*. Approximately 30% of cDNAs analysed represent differentially expressed genes and about 5% show highly regionalized expression. Novel marker genes and potential developmental regulators were found. Most interestingly, marker genes were used to study regionalization of the entire gastrula as well as the tail forming region and the epidermis of the tail bud embryo. These experiments identified 3 new regions in the tail bud, bringing the total to 10. The new domains described in this article include new territories in the CNH, in the posterior wall and in the post anal gut (Fig. 1.2 top panel, inside broken box). The CNH had been divided by Beck and Slack (1998) into two domains: the most posterior part that is negative for *Xlim1* expression and the anterior part, which is *Xlim1* positive. Gawantka *et al.* (1998) define a new territory in the middle of these that expresses a novel gene named *11D1*, which forms a stripe in continuity with the spinal cord roof. Interestingly, the expression of this gene in the roof of the spinal cord is also continuous with expression of the gene in the posterior-most presomitic mesoderm. Within the posterior wall, three domains are now distinguishable: a dorsal domain, expressing *Xbra* alone, a medial/posterior domain, expressing *Xbra* and *Xhox3*, and a ventral one expressing *Xvent1* and *Xbra*. An additional domain in the tail is the post anal gut expressing *26C10.1*.

These three genes described by Gawantka *et al.* show continuous expression from gastrulation to tail development. Therefore in amphibians, which lack an apparent mesenchymal condensation in the tail

bud, analysis of the distribution of molecular markers have shown the continuity of gene expression from gastrulation to tail formation. In addition, they have shown that the *Xenopus* tail bud is regionalized, ten different domains of gene expression have been described: the roof of the spinal cord that expresses: *Xdelta1, Xcad3, 11D1,* and exclusively *Xwnt3a* and *lunatic fringe*; the floor of the spinal cord that expresses *Xnot2*; the posterior notochord that expresses *Xbra* and *Xlim1*; the CNH region that expresses *Xbra* and *Xnot2* broadly, but is divided in three domains: an anterior region expressing *Xlim1*, a middle region expressing *Xlim1* and a novel gene *11D1* and a posterior region *Xlim1* negative, *Xbra* and *Xnot2* positive; the posterior wall is divided in three regions of gene expression: *Xcad3, X-delta-1* and *Xbra* are expressed broadly, *Xhox3* is expressed at its most posterior tip and the ventral region expresses *Xvent1*; the post-anal gut region expresses the novel gene *26C10.1* exclusively.

Chick

In amniotes, during tail development, a process called secondary neurulation has been described. In the chick, four major events can be distinguished. First, dorsally in the developing tail, cells of the primitive streak/tail bud aggregate to form a solid medullary cord. Then, this cord differentiates into peripheral and central cells, after which, multiple isolated lumina appear. Finally, all lumina coalesce to form a single central cavity, which makes contact with the lumen of the primary neural tube (Schoenwolf and Delongo, 1980). Therefore, the primitive streak and tail bud are replaced by a bulb-like structure, consisting of a morphologically uniform mass of mesenchyme directly continuous with axial (neural tube, notochord, gut) and paraxial (segmental plate) structures formed during the earlier phases of gastrulation. This appearance led to the proposal that structures in the tail were formed directly from a blastema without segregation of cells into germ layers (Holmdahl, 1925; reviewed by Griffith *et al.*, 1992). However, Knezevic *et al.* (1998) performed a very similar analysis in the chick to that performed by Gont *et al.* in the frog. They examined the regional distribution of three markers at gastrulation stages and tail bud stages. Previously, it had been reported that *Gnot1* and

27

Tbx6L were expressed in complementary domains during gastrulation. *Gnot1* is expressed in Hensen's node and notochord and *Ch-Tbx6L* in the primitive streak and segmental plate, while *Ch-T* is expressed in node, notochord and primitive streak, in all nascent mesoderm (see Fig 1.1 middle panel for chick anatomy; see Fig. 1.3 for chick gene expression). Formation of the tail bud in the chick starts in the 13-somite embryo (stage 11) as cells of Hensen's node and primitive streak begin to accumulate caudally in this mass of apparently uniform mesenchyme (see Table 1.1 for chick developmental stages). By 19-somite stage (stage 13) the posterior neuropore is closed. This transformation into tail bud is completed by the 24-28 somite stage (stage 15). Surprisingly, despite its uniform morphological appearance, gene expression in the forming tail bud suggested a segregation of Hensen's node and primitive streak-derived cells. Expression patterns were shown to be comparable throughout this transitional period (stage 11-16). *Gnot1* expression is detected in the formed and nascent notochord at stage 15, but does not extend very posteriorly from this region compared to *Ch-T*. The caudal limit of *Gnot1* expression corresponded to the CNH region (point where caudal neural tube and notochord unite), located between the residual Hensen's node (*Gnot1* and *Ch-T* positive) and primitive streak (*Ch-T* positive). Tail bud formation is followed by elongation. During stages 16-35, the tail bud elongates posteriorly, leaving behind organized tail structures. Although the tail bud eventually occupies a small region at the tip of the growing tail, distinct regional domains of gene expression are still visible at these later times. *Gnot1* expression continues in the CNH region and adjacent caudal notochord as described in the frog (Gont *et al.* 1993), while *Ch-T* and *Ch-Tbx6L* are expressed in the ventral rim of tail bud mesenchyme. *Ch-T* expression also continues in CNH and notochord, and *Ch-Tbx6L* in the tail segmental plate. The distribution of these markers in the tail bud compared with gastrulation suggests a direct continuity of different cell identities and conservation of spatial relationships between these cells. Therefore, in chick as in frog, most of the cells of the tail bud cannot constitute a blastema.
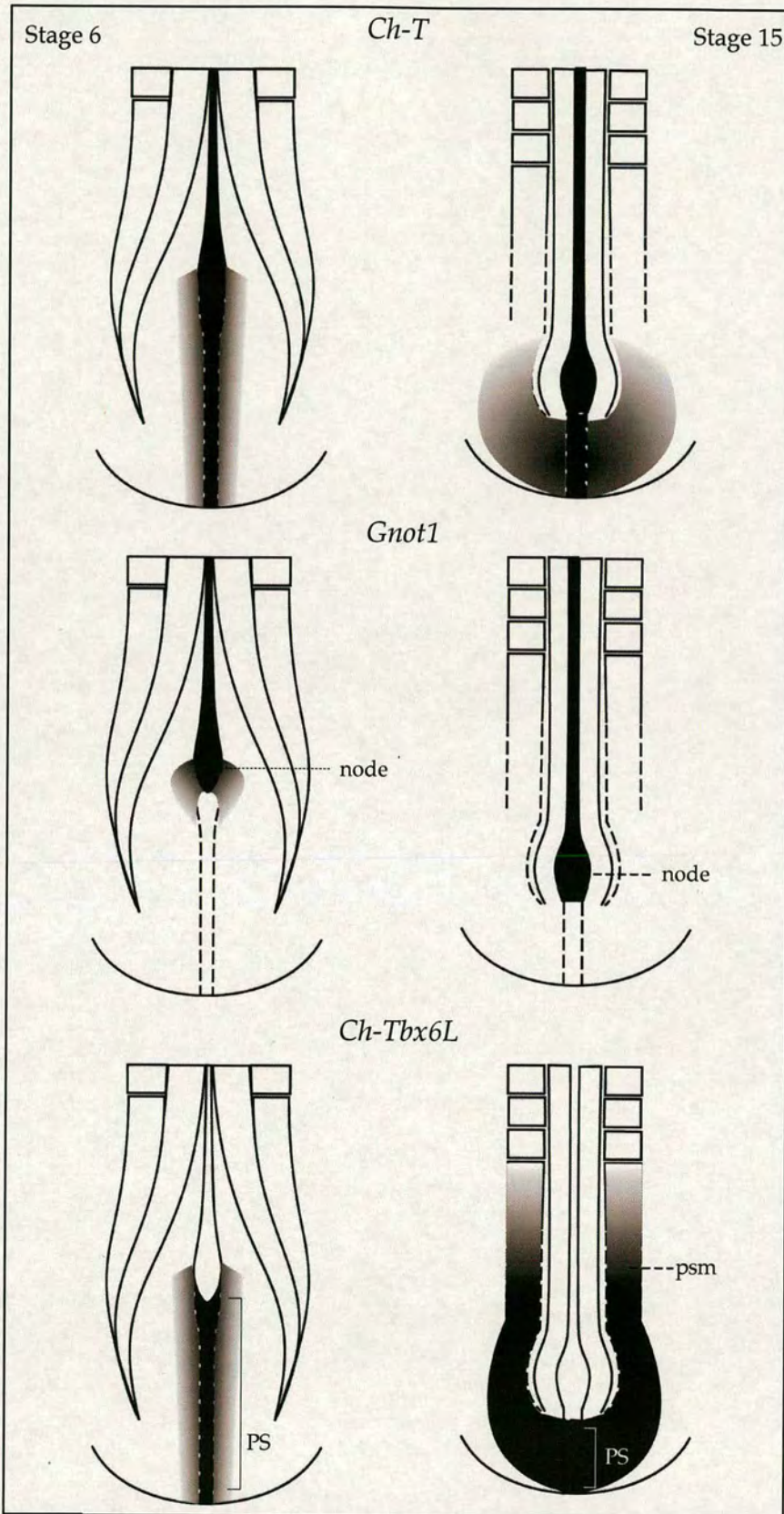
Figure 1.3 Chick regions of gene expression
Dorsal view diagrams of the chick primitive streak at head fold stage, 0-1 somites (stage 6) on the left and TB stage (stage 15) on the right representing genes described by Knezevic *et al.* (1998). PS: primitive streak, psm: presomitic mesoderm.

Mouse

In the mouse, primary and secondary neurulation are indistinguishable at the morphological level, unlike in the chick embryo where formation of multiple lumina has been observed and where primary and secondary neurulation overlap transiently in the region of the posterior neuropore where the primary neural tube is located dorsally to the forming secondary neural tube. Primary neurulation finishes in the mouse with the closure of the posterior neuropore at approximately the 28-32 somite stage (10.5 dpc) (see Table 1.1 for mouse developmental stages). Gofflot *et al.* (1997), decided to perform a gene expression study at day 10, just before neuropore closure, using genes known to be involved in the key events of gastrulation and neurulation at earlier stages, as previously done in frog and chick. The continuity of function from the epiblast, primitive streak and node to tail bud is reflected in a continuity of expression of the genes: *Wnt5a, Wnt5b, Evx1, RARγ, Brachyury (T), Hoxb1, Foxa2 (Hnf3β), Foxa1 (Hnf3α), Shh* and *Fgf8* from the node/primitive streak region to specific patterns within the tail bud (see Fig. 1.1 bottom panel for mouse anatomy; see Fig. 1.4 for summary of expression patterns). *Brachyury,* and *Hoxb1* are expressed throughout the tail bud, whereas *Wnt5b, Evx1, RARγ* and *Fgf8* are expressed preferentially within the dorsal and central tail bud cells, which differentiate to form the neural tube, notochord, and hindgut. *Fgf8* expression decreases in a dorsal to ventral gradient in the tail bud. *Wnt5a* shows a lower level of expression in the central (presumptive notochordal) cells of the tail bud, consistent with the absence of its expression in the notochord and the node during gastrulation. Genes involved in induction, formation, and maintenance of the notochord (*Foxa2, Shh,* and *Brachyury*) are all present at a high level in the notochordal cells of the tail. In contrast, three patterns of expression were shown in the hindgut: *Foxa1, Wnt5b, Wnt5a,* and *RARγ* showed uniform transcript levels in all cells. Dorsal cells express higher levels of *Foxa2, Brachyury,* and *Fgf8* than ventral cells, whereas *Shh* and *Evx1* showed the reverse pattern. In the neuroepithelium, whereas *Wnt5b, RARγ, Brachyury, Hoxb1,* and *Fgf8* are expressed throughout the neural plate of the posterior open neuropore, *Evx1* and *Wnt5a* expression reveal
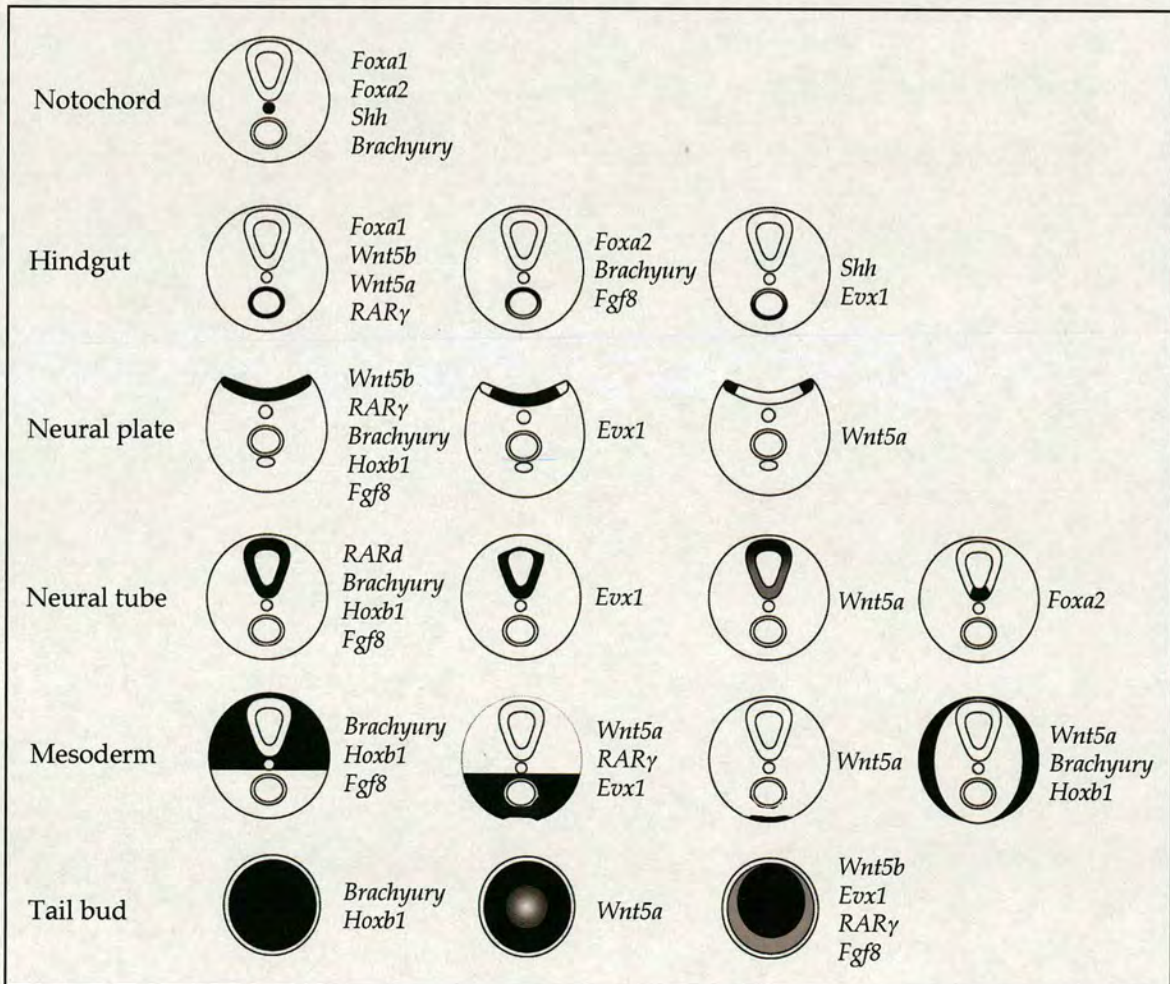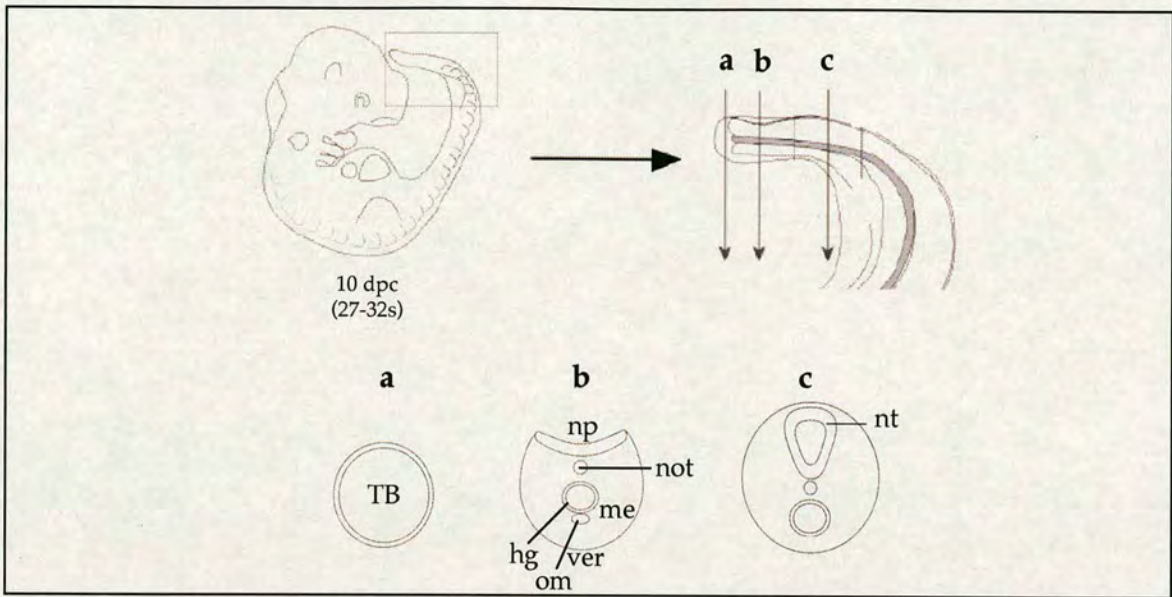
Figure 1.4 Patterns of gene expression in the tail tissues during posterior neuropore closure (10-10.5 dpc) in the mouse

Top panel shows the 3 levels of sections (a-c) which were used to define and illustrated the different regions of gene expression in the tail tissues (modified from Gofflot *et al.*, 1997). **Bottom panel** shows diagrams summarising the different patterns observed in the different tissues and the genes that define those patterns (Based on Gofflot *et al.*, 1997). TB: tail bud, np: neuropore, not: notochord, :me: mesenchyme, ver: ventral ectodermal ridge, hg: hindgut, om: omphalomesenteric artery, nt: neural tube.

31

distinct cell populations. *Evx1* is expressed medially, in a domain larger than the future floorplate, and *Wnt5a* is expressed complementarily at the lateral tips of the folds. In the closed neural tube these two patterns evolve so that *Evx1* is primarily expressed in the ventral and lateral walls, whereas *Wnt5a* is expressed in dorsal cells forming the roof of the neural tube. The cells of the floorplate of the recently closed neural tube are specifically labelled by *Foxa2*. This gene has been proposed as a regulator of floorplate development (Sasaki and Hogan, 1994). The transient expression of *Brachyury* throughout the caudal neuroepithelium observed in the mouse is in agreement with data reported in chick embryos (Kispert *et al.*, 1995), but different from the described expression of *Xbra* specifically in the roof of the caudal spinal cord in *Xenopus* embryos (Gont *et al.*, 1993). Before the formation of somites, the caudal mesoderm presents a morphologically uniform mesenchymal appearance. With respect to gene expression, however, the mesoderm is the most complex of the caudal tissues. Four domains were revealed: paraxial, ventrolateral, ventromedial, and subectodermal. Genes seem to be expressed in one or more domains of these domains in dynamic patterns according to the axial level. The paraxial domain clearly corresponds to the segmental plate. In this domain, expression of *Brachyury*, *Hoxb1*, and *Fgf8* is strong caudally and disappears at a cranial boundary coinciding with early somatic condensation. The ventromedial domain is a small block of tissue adjacent to the tail bud. It lies between the hindgut and the ventral ectodermal ridge (VER) and narrows progressively in more cranial sections, with its cranial boundary just caudal to the cloacal membrane. A recent study in chick (Liu *et al.*, 2004) showed that this ventral tail bud mesoderm domain (at tail bud stage 17) is able to induce the formation of elongated paraxial mesoderm extensions when grafted to the area pellucida or area opaca of an early chick host (stage 3+). Thus, this domain might be acting as a signalling centre specific for paraxial mesoderm induction. This mesodermal domain is specifically labelled by *Wnt5a*, *RARγ* and *Evx1*. At a more cranial level, the expression of these three genes divides the tail mesoderm into two regions: the paraxial mesoderm expressing high levels of *Wnt5a* and destined for somitogenesis, and the ventrolateral mesoderm,

which expresses *RARγ* and *Evx1*. *Wnt5a*, *Brachyury*, and *Hoxb1* demarcate a subectodermal domain of gene expression in the mesoderm. No obvious embryonic structure derives from the cells of this region. In Gofflot *et al.*'s study (1997), only *Wnt5a* was observed to be expressed in the ventral ectodermal ridge (VER), and this expression did not extend to the ventral ectodermal groove (VEG). The VER is a thickening of the ectoderm present at the ventral surface of the tail bud and tail region immediately cranial to the tail bud (Gajovic and Kostovic-Knezevic, 1995). More cranially it is continuous with the VEG that ends at the cloacal membrane. Based on morphological evidence, it had been suggested that the VER is analogous to the apical ectodermal ridge (AER) of the limb buds in being a site of epithelial-mesenchymal interaction (Gajovic and kostovic-Knezevic, 1995). However, Goldman *et al.* (2000) showed that these two structures although similar in morphology, are not strictly analogous structures with equivalent functions. The AER does not appear to be able to substitute for the VER in tail explants. Moreover, unlike the AER, the VER does not appear to influence cell proliferation or cell survival in the underlying mesoderm. Nevertheless, VER ablated tails tend to grow much shorter, thicker and contain less number of somites than intact tail explants. In addition, the ablated tails lose the expression of the BMP antagonist *Noggin* in the ventral tail bud mesoderm after culture. This shows that VER ablation compromises tail explant development and suggests that this structure might have a role in providing signals to regulate BMP activity, which in turn controls somitogenesis. These authors also showed that the VER expresses *Bmp2* and *Ffg17*, in addition to *Wnt5a*, as reported by Gofflot *et al.* (1997).

In conclusion, Gofflot *et al.* showed that in the mouse embryo, the tail bud at stage 10.0 dpc has distinct domains of gene expression, even within the same tissue type. Moreover, genes expressed at gastrulation stages continue to be expressed at tail bud stages at the time of neuropore closure. Thus, their study complements others performed in the chick and frog embryo, concluding that the gene expression domains observed during gastrulation continue during tail formation. Therefore, in vertebrates, cells in the tail bud cannot all constitute a blastema of

undifferentiated cells. However, Gofflot's study focuses only on a small time window at the time of neuropore closure at the end of primary neurulation. Therefore, the expression of these genes after neuropore closure remains to be analysed. Moreover, is there a conserved difference in gene expression coinciding with the transition from primary to secondary neurulation, at the time when the tail starts to elongate? In the mouse, there is no apparent distinction at a morphological level between these two processes. In *Xenopus*, however, a new wave of gene expression was described by Beck and Slack (1998) at the time of tail bud elongation. However, homologues of these *Xenopus* genes (*Xwnt3a*, *Xwnt5a*, *Xhox3* and *lfng*) in chick and mouse are expressed as a continuum from gastrulation to tail bud elongation. Thus, are gene expression domains in the tail bud equivalent among the different vertebrates? These questions will further discussed in Chapter 2.

2-3. Fate mapping studies (describing cell progeny and cell movements)

Given that gene expression domains can be followed continuously from the node or the blastopore to the tail bud, are these regions lineally related? To answer this, lineage tracing experiments can be done using, for example, the fluorescent carbocyanine dye DiI or performing isotopic grafts of quail and chick embryos. After microinjection into embryonic tissues, DiI, being lipophilic, intercalates in the cell membrane, marking small groups of cells (Selleck and Stern, 1991; Izpisúa-Belmonte *et al.*, 1993) and their descendants after a period of culture. In the case of the quail-chick chimaera system, isotopic and isochronic reciprocal exchanges of precisely defined regions of the tail bud were performed. As quail cells can be distinguished from chick cells by the structure of their interphase nucleus (Le Douarin, 1969) or using antibody staining, the quail-chick chimaera technique allows the fate of the grafted cells to be followed until completion of development, thus leading to the construction of a precise fate map. These fate maps not only allow us to follow cell progeny, but also to start drawing conclusions about the movements that the cells undertake during tail formation.

34

Xenopus

Gont *et al.* (1993) used DiI to label cells of the late blastopore (stage 13) in *Xenopus* embryos, and showed that these cells are fated to form specific tissues of the tail bud. Initially, they marked dorsal blastoporal lips of mid to late gastrulae (stage 11-12.5) and found that the lineage tracer did not mark the tail bud (at stage 33), but instead marked the mesoderm of the trunk. This indicated that involution movements are the main activity taking place at the dorsal lip even as late as stage 12.5. However, when they marked blastoporal lips at the early neurula stage (stage 13), just as the blastopore starts to elongate, labelling of the tail bud proper was consistently observed. Their interpretation of these results was that at stage 13 in the frog, an important change takes places in the movements of cell layers at the blastopore: the ectodermal and mesodermal cells layers stop involuting, attach to each other, and move together towards the posterior of the embryo (Fig. 1.5 top panel). Therefore, not until the blastopore starts to elongate at stage 13, can one mark cells that will remain as resident cells populating the developing tail bud. Three populations were identified. Firstly, the dorsal lip, which gives rise to the CNH, the ventral spinal cord and the notochord; secondly, the lateral lip, which gives rise to the posterior wall and somites; and thirdly, the ventral lip, which gives rise to the lateral plate mesoderm and the stretch of post anal gut spanning the region between the anus and the tail bud.

Thus, different parts of the blastopore lip give rise to different parts of the tail. The interspersion of labelled and unlabelled cells in the notochord region indicates that cell intercalation continues at least until the swimming tadpole stage. This is of interest because cell intercalation along the dorsal midline starts much earlier in development and is considered one of the main driving forces of gastrulation movements: convergence-extension (Shih and Keller, 1992; Keller *et al.*, 1991). Therefore, Gont and collegues although they believe that involution movements stop at stage 13 in the frog embryo, show that intercalation movements continue during tail elongation. They also conclude that this posterior movement of the
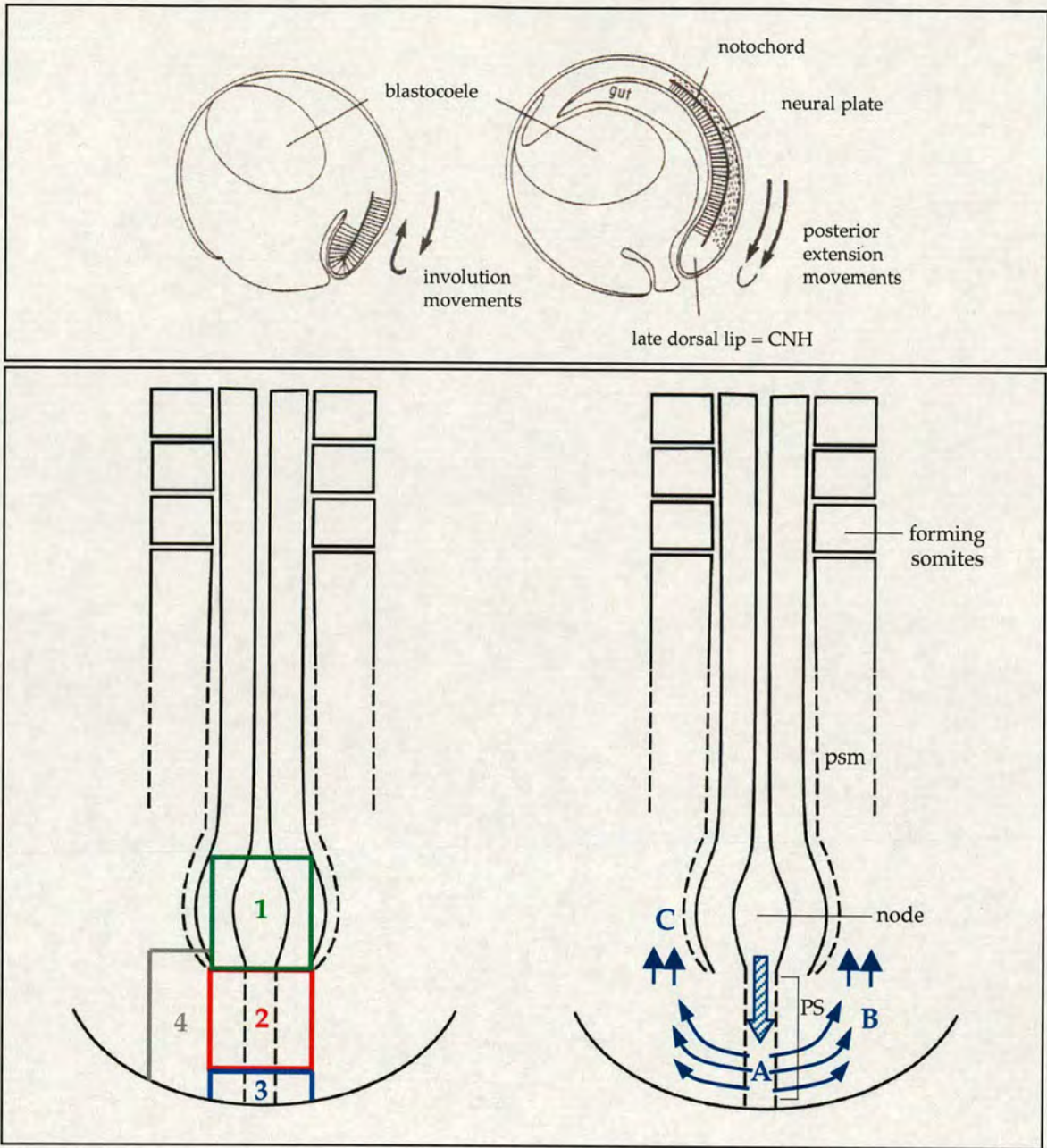
Figure 1.5 Morphogenetic movements during axis elongation in *Xenopus* and chick
Top panel shows two diagrams of *Xenopus* morphogenetic movements at mid-gastrula (stage 11) and at late gastrula/early neurula (stage 13), respectively. Note that involution movements have stopped by stage 13, at which stage both ectoderm and mesoderm of the late blastopore lip move towards the posterior. Reproduced from Gont *et al.*, 1993. **Bottom panel on the left**, dorsal view diagrams of the chick primitive streak at TB stage (stage 15, 25 somites) showing the different regions grafted by Catala *et al.* (1995). Region 1 includes the CNH, region 2 includes the rostral two-thirds of the PS/TB, region 3 includes the caudal third of the PS/TB, and region 4 is located laterally and corresponds to the caudal-most level of the presumptive segmental plate. **Bottom panel on the right**, same stage diagram showing the proposed morphogenetic movements described by the fate maps: the axial structures, notochord and neural tube, undergo an elongation allowing their growth in a rostrocaudal direction (arrow A). In contrast, somitic precursors in the primitive streak undergo a lateral divergence (arrows B), before being added to the already formed presomitic mesoderm allowing the body growth by an accretion mechanism (arrows C). CNH: chordoneural hinge, PS: primitive streak, psm: presomitic mesoderm. Based on Catala *et al.*, 1995.

CNH in *Xenopus* may be analogous to the regression of the late Hensen's node in the chick embryo.

Later, Tucker and Slack (1995a) produced a similar fate map of the neurula stage embryo. In this case they used orthotopic grafts of tissue from embryos that had been labelled with the fluorescent lineage label FDA (fluorescein dextran amine) shortly after fertilisation. They complemented this fate map by producing a specification map, which shows how a region develops if cultured in isolation from the embryo. Some information about specification can also be gained by studying the development of the complementary ablated embryo. To create the fate map they extirpated the tissue of interest of a stage 18 embryo, cutting through all the cell layers, and replacing these with similar labelled pieces of tissue. The *Xenopus* tail is defined as the tissue located posterior to the proctodaeum. It was clear from comparison of the labelled regions at stage 18 and stage 24 that the proximal two thirds of the tail axial tissue is derived from the trunk of the embryo and is displaced into the tail as a result of anterior movement of the proctodaeum during extension of the body. The tail bud itself gives rise to the distal third of the tail. For this reason Tucker and Slack (1995a) distinguish between the 'tail bud', which is the region of apparently homogeneous cells at the posterior extreme of the embryo, visible as a bulge from stage 27 onwards; and the 'tail-forming region', which is the larger area that forms the complete tail of the stage 40 embryo. In this paper they characterised the tail-forming region, assessing how it moves and changes shape as the tail develops. The fate map defined the tail-forming region at the mid-late neurula stage (stage 18) as a rectangle 700 μm wide by 600 μm long, 100 μm anterior to the base of the proctodaeum. Prior to neural tube closure (stage 13) the tail-forming region occupies an area of similar length but 800 μm wide. In terms of tissue contributions, the tail-forming rectangle can be seen to make up the whole axial portion of the tail: notochord, myotomes and neural tissue, but it is only responsible for the very tip section of the epidermis, and some neural crest-derived mesenchyme, which has moved out of the labelled neural tube. This implies that the bulk of the epidermis and neural crest-derived mesenchyme responsible for fin formation must be

located in areas outside the rectangle grafted. In order to determine the fate of subdivisions of this tail-forming region, the standard rectangle was cut in half, and either the anterior or the posterior half being grafted orthotopically. The grafts were followed from stage 24 to 40. The posterior part of the rectangle, which would be predicted to include the CNH, forms the mesoderm for most of the tail, as well as being a source for some of the ventral posterior fin. The anterior section of the rectangle contributes only to a small segment of more anterior mesoderm above the proctodaeum, as well as some of the dorsal posterior fin. The area posterior to the tail-forming rectangle, lying directly above the proctodaeum did not contribute a great deal to the tail tissue. The fluorescence was restricted to the area around the proctodaeum by stage 40, and to small amount of ventral fin. Specification of the same region was studied by explanting the same pieces at the same stage (stage 18) in culture. The explants were often difficult to score after culture due to the fact that they only grew to approximately a quarter of the size of the corresponding regions in controls. This size reduction was proved to be due to the lack of any food in reserve in the explants, which do not contain yolky tissue, as when grafted to a putative neutral site on a host embryo (ventral side of mid-late neurula), the grafts did indeed grow to approximately half the size of controls. The isolated anterior halves formed non-elongated blocks of mesoderm, covered in a small amount of fin. The embryos lacking this anterior section had a deficit of mesoderm from above the proctodaeum, visible as a thinning in the tail at this point, and were shorter than controls. The posterior halves, by comparison, consisted of elongated, tapered structures, with some somite patterning and again a small amount of fin. The embryos lacking this posterior region did not possess a tail, similar to the phenotype obtained on removal of the complete tail-forming region. This highlights the importance of the CNH region in *Xenopus* tail formation. Gont *et al.*'s lineage analysis had already shown that this region was the descendant of the dorsal blastopore lip of the late gastrula and was directly responsible for the formation of the notochord and ventral spinal cord. Tucker and Slack studies now showed that without the CNH the embryos do not develop a tail.

The importance and special nature of the CNH region in *Xenopus* was emphasized by other studies by Davis and Kirschner (2000). They created another fate map but this time at late tail bud stages (stage 31), using a technique that allows higher resolution than conventional studies using DiI. They used photoactivation of fluorescence to label small numbers of adjacent tail bud cells in the developing embryo. Embryos were injected at the 2-cell stage with caged fluorescein dextran conjugate (CFD). Caged fluorophores are colourless and nonfluorescent until photolysed with ultraviolet light. By stage 31, the embryos were mounted on an inverted microscope and photoactivation of fluorescence was performed by brief long-wavelength ultraviolet light exposure through a fixed circular aperture. Embryos were imaged immediately to record photoactivation marks, and then kept in the dark, until they reached stage 45-46, when they were imaged again to record the fate of progeny cells. They labelled groups of 9 cells in three different regions; two of these regions are known from Gont *et al.*'s fate maps (1993) to have been derived from different cell populations at gastrulation: the dorsal and ventral part of the CNH region derive from the dorsal blastopore lip and give rise to the notochord and ventral neural tube in the frog and the notochord and floor plate in the chick; and the posterior wall of the neurenteric canal that derives from the lateral blastopore lips and gives rise to the most posterior tail somites. Cells in the ventral part of the CNH or posterior wall regions gave rise largely to muscle (ventral myotome) and epidermis, and some unidentified cell types; only a small fraction showed label in the notochord or neural tube. This finding is consistent with other fate map studies showing that fate in the tail bud is regionalized. The majority of embryos labelled in the dorsal CNH showed progeny in multiple tissues: the dorsal myotome, neural tube and notochord. Only 17/56 embryos showed label in a single tissue and no embryos had label in the notochord alone. This suggested either that progenitors with different fates were located very close together, or that some multipotent cells exist in the dorsal CNH. To confirm these results they then reduced the photoactivation aperture in order to label groups of up to three adjacent cells in the equivalent of the dorsal region in stage 36 embryos. The

distribution of label was remarkably similar to that of the dorsal region with the larger aperture. 10 of 23 embryos had label in three or four cell types, including notochord, neural tube, myotome, epidermis and other unidentified cells. Interestingly as well, in the case of the neural tube labelling, they found that floor plate, lateral wall or roof plate could be labelled; suggesting that neural precursors are not committed to particular regions of the neural tube at the time of photoactivation, in contrast to other fate maps where CNH only gives rise to the ventral part of the tail neural tube (Gont *et al.*, 1993). Therefore, these experiments in part support the idea that the tail bud is regionalized, but they also show that small groups of cells can give rise to progeny populating several tissues in a single embryo, in support of the existence of multipotent cells in the CNH region of the tail bud. However, the fact that the epidermis (known to be a lineage that segregates earlier in this organism (Dale and Slack, 1987) was labelled together with notochord, neural tube and myotome, suggests that cells in different planes might have been consistently labelled. The existence of multipotent cells had already been observed in early mouse fate maps (Lawson *et al.*, 1991), this will be analysed in detail later in this introductory chapter.

Chick

In the chick embryo, the early fate maps pointed to the view of the tail bud as a blastema because in all cases, the tail bud was studied by grafting it as a whole. Therefore, Catala *et al.* (1995) applied the quail-chick marker system to perform small size grafts of selective tail bud areas, in order to study the developmental potentials of the avian tail bud and the morphogenetic movements that affect this region at the 25-somite stage (stage 15) (neuropore closed at the 19-somites stage, stage 13). They found that, caudal to the posterior limit of the neural tube and notochord, the territory designated by Pasteels as the CNH (region 1, Fig. 1.5 left bottom panel) is of prime importance for secondary body formation in the chick, as I have already described in *Xenopus*. It moves in a rostro-caudal direction and gives rise to the notochord and the floor plate. It corresponds to what remains of Hensen's node, as shown by the same

authors in their fate map of Hensen's node at the 6-somite stage (Catala *et al.*, 1996). The laterodorsal walls of the neural tube originate from a region caudal to the CNH (region 2), again similar to what the same authors observed at the 6-somite stage. Interestingly this region 2 also gave rise to somitic derivatives as far as the tip of the tail. At each level however, cells originating from the donor and the host were intermingled meaning that this labelled territory participates in somite formation together with a different host's territory. The most rostral level of the neural tube arising from the graft was located more caudally than the rostralmost level of the somitic mesoderm, as observed before (Schoenwolf, 1977). Therefore, in this region posterior to the CNH, mesodermal and neural potentialities coexist. Posterior to this region (region 3) the graft gave rise only to the most caudal somites. All these somites were mixed with cells coming from both the graft and the host. In contrast, when labelling a lateral region of the tail bud (region 4), which would correspond to the caudalmost level of the presumptive segmental plate, the graft gave rise to all the cells forming somites 34 to 36 and their derivatives, no cell mixing was observed with the host. Therefore, the grafts involving regions 2, 3 and 4 allowed them to deduce the morphogenetic movements leading to the formation of the caudal somites (Fig. 1.5 right bottom panel). Cells originating from the medial caudal part of the tail bud, namely regions 2 and 3 intermingle and diverge laterally and add caudally to the already formed mesoderm (region 4); meaning that the divergent movements of cells from the primitive streak occurring during gastrulation after ingression (Catala *et al.*, 1996) are still occurring at tail bud stages.

This morphogenetic movements were furthermore analysed by Knezevic *et al.* (1998) by DiI labelling different surface regions of the tip of the tail bud either at stage 11 (13 somites, tail bud condensation just visible; posterior neuropore open) or at stage 13 (19 somites, distinct tail bud condensation; posterior neuropore closed). They showed that ingression of somitic precursors from the dorsal surface started at gastrulation continues after neuropore closure and during tail bud formation. Once internalized, both Knezevic *et al.*'s and Catala *et al.*'s results suggest that these somitic precursors first move posteriorly and

turn ventrally in the distal tail bud, and then move laterally and anteriorly to contribute to newly formed segmental plate. Similar movements have also been described for the zebrafish tail bud by Kanki and Ho (1997), who termed this "subduction" as distinct from gastrulation movements, which are primarily in a forward direction. However, taking into account the bulky hemispherical shape of the tail bud compared to the flat early embryo, the movements are not dissimilar to those during gastrulation.

These results (Catala *et al.*, 1995,1996; Knezevic *et al.*, 1998) clearly show that the avian tail bud is a heterogeneous structure similar to that of amphibians. Moreover, they showed that the surface ingression movements followed by lateral divergence of presomitic precursors originating at gastrulation continue during tail formation after neuropore closure in the chick. In contrast, Gont *et al.* (1993) observed that involution movements are reported to stop at stage 13 in the frog embryo, because from this stage onwards they found that labelling cells of the blastopore gave rise to progeny contributing as far as the tip of the tail, thus supposing that by this point there is a resident population at the blastopore supplying the mesoderm of the tail. However, in this organism it has long been known that the posterior part of the neural plate gives rise to tail somites, rather than to spinal cord as might have been expected (Bitjel, 1936). The question whether these somite fated cells are being produced by an ongoing process of specification to mesoderm as cell ingression or merely differentiation of a previously committed population has not yet been answered. In the chick embryo, Knezevic *et al.* (1998) have shown that continuation of surface ingression contributing to somitic mesoderm can occur, even though it has been proved that by this stage there is already an existing population of presomitic precursors residing in the tail bud (Catala *et al.*, 1995). However, in the chick, the issue of whether the cells still ingressing from ectoderm to mesoderm are, in fact, already specified as mesoderm, has not been addressed.

Mouse

In the mouse, Wilson and Beddington (1996) constructed a fate map of the primitive streak in the 6-somite stage embryo (8.5 dpc). They used

the lineage marker DiI to label groups of cells in the node or the primitive streak. Embryos were scored after a period of 48 hours culture. They also looked at ingression movements by labelling cells on the surface of the primitive streak before and after neuropore closure (from 8.5 to 11.0 dpc) (neuropore closes at 10.5 dpc, at about 30 somites in the mouse). As seen in the chick, Wilson and Beddington found that apparently resident mesoderm populations already exist in the node and primitive streak at the 6-somite stage in mouse embryos. Labelling cells of the ventral and dorsal node, progeny are found in the axial mesoderm until the tip of the tail. The same is observed when labelling anterior primitive streak: labelled paraxial mesoderm cells are found in the somites of the axis and also in the tail bud mesoderm. By this time ingression of cells via the primitive streak from the epiblast is still underway and continues until neuropore closure. Thus, resident populations and ingression are not necessarily exclusive in the mouse and chick embryo.

4. Organizer activity

So far, in mouse as in chick and *Xenopus*, fate maps have shown that the different regions of the blastopore lip and primitive streak during gastrulation have exact or near-exact equivalents in the tail bud. In addition, genes expressed in regions of the streak continue their expression in subpopulations of the tail bud. The dorsal blastopore lip whose equivalent in chick and mouse is the node is not only the source of notochord and ventral neural tube, but also shows organizer activity: the ability to induce secondary neural axes in naïve ectodermal tissue on ectopic transplant. Therefore, it is pertinent to ask whether the CNH, as the descendant of the dorsal blastopore lip or node also retains organiser activity.

Xenopus

Gont *et al.* (1993) performed a series of transplantation experiments trying to answer this question. In *Xenopus*, the dorsal blastopore lip has inducing activities that change over time: the early dorsal lip acts as a head organizer while the late dorsal lip of the gastrula behaves as a trunk-

tail organizer (Spemann, 1931). The morphogenetic potential of tissue fragments can be tested by implanting them into the blastocoele of a *Xenopus* gastrula by the Einsteck procedure of Mangold (Spemann and Mangold, 1924). Therefore, in order to test the persistence of organizer activity through late stages of development, two types of grafts were performed. First, the inducing potential of the CNH from tail buds was tested at stage 25. Second, they tested if the inducing activity persists at stages in which the tail has already formed, at stage 35. By this stage the neurenteric canal has collapsed making the dissection of the hinge from the posterior no longer possible, thus instead tail tips were dissected and transplanted. When CNH was implanted into a host gastrula, tail-like structures were produced in 13 out of 14 grafts. When stage 35 tail tips were tested, the embryo developed tail-like structures in 19 out of 27 grafts. The structures formed by both types of implants are typical tails, as indicated by the presence of dorsal and ventral fins and of well-organized notochords flanked by paired muscle blocks and neural tissue. The fundamental property of the organizer is that it is able to recruit cells from the host into a twinned axis (Spemann and Mangold, 1924). In order to determine whether the graft was able to induce host tissues to form axial structures, lineage-traced transplantations were performed. When the donor CNH or tail tips were uniformly labelled with fluorescein dextran (FDA) they contributed to only a small part of the secondary tail. The secondary axis consists mostly of cells derived from the host. Induced cells include notochord and muscle blocks and some neural tissue, while the tip of the secondary axis and the neural tube are mostly derived from the graft. Interestingly, the notochord in the secondary tails can derive from both the host and the graft, because it is known that organizer tissue can induce the formation of notochord in neighbouring cells (Stewart and Gerhart, 1991) as well as self-differentiating into notochord (Hamburger, 1988). Therefore, from this experiments we can conclude that the CNH and the tip of the tail, even at late stages of development, retain Spemann's tail organizer activity in the frog.

Chick

In the chick embryo, the same experiment was performed by Knezevic *et al.* (1998). Stage 17/18 quail tail tips (tip mesenchyme only) or region just anterior to it (caudal end of the medullary cord region) were grafted to stage 4⁻ chick embryo recipients that are competent to respond to Hensen's node graft by ectopic axis induction. Grafts to the lateral mid-area pellucida usually contained a morphologically discrete second neural tube or neural plate of chick origin (5/5), as well as loose mesenchyme that sometimes included morphologically distinguishable somites of both chick and quail origin (3/5) and notochord of quail origin (2/5), whereas grafts derived from regions anterior to the tail tip only formed structures of graft origin. However, grafts to the area pellucida are situated on tissue that will contribute to the host embryonic axis and so are likely to recruit host epiblast cells already committed to form neural tissue into an ectopic axis. To further test whether the grafts could caudalise existing neural tissue the grafts were placed adjacent to the forming head region of the host embryo (anterolateral area pellucida). In this case, nearby neural-committed host cells that are recruited into the ectopic axis would normally form anterior neural tissue (forebrain to hindbrain). Neural tissue in the ectopic axis was of host origin in all the cases examined (28/28) and pan-neural markers were always expressed. However, the induced neural tissue failed to express any anterior regional markers (*Otx-2*, and *En-1,2*) while the consistent expression of *Pax-3* and *Hoxb-8* was most consistent with caudal (posterior spinal cord) regionalization. Most importantly, a second set of experiments showed that grafts were also able to induce neural plate, when grafted to the area opaca (uncommitted, non-neural ectoderm that forms only extra-embryonic tissue). As before, in the majority of the cases, the ectopic neural tissue expressed selectively caudal markers. In summary, the tip of the elongating tail tip at stage 17/18 still retains neural inducing as well as caudalising activity in the chick.

Mouse

The tail bud in the mouse still remains to be tested for organizer activity. However, there is good reason to suppose that there is a

functional continuum between the organizer activity in the gastrulating mouse embryo and the late tail bud stage embryo, as I will discuss in the next section.

5. *Evidence for continuity of gene function in the mouse*

The continuity of gene expression from gastrulation and during tail formation suggests that gene function should be continuous through axial elongation. Evidence supporting this hypothesis comes from study of spontaneous induced or targeted mutations: *Brachyury (T)* and *Wnt3a*, have a crucial role in primitive streak morphogenesis as revealed by null mutations, but affect only the tail bud and tail development when function is partially lost in the mouse.

The *T* gene is a T-box containing transcription factor. It is expressed in the primitive streak from the onset of gastrulation and persists in the tail bud for the entire period of axis elongation (6.5-12.5 dpc). It is also expressed in the node and notochord (Wilkinson *et al.*, 1990; Herrmann, 1991; Kispert and Herrmann, 1994). Homozygous null mice for *T*, as described for the mouse *Brachyury* mutant (Hermann *et al.*, 1990), have somites posterior to the seventh absent or abnormal and usually die at mid-gestation (11 dpc). They have prominent defects in the notochord, the allantois and the primitve streak. The allantois fails to grow and the primitive streak is abnormally thickened. Heterozygous mice are viable, but have a reduction in tail length or tail kinks (Chesley, 1935; Gruneberg, 1958). A means of exploring the developmental capacity of individual mutant cells was to use chimaeric analysis, where *T/T* cells experience a wild-type environment sufficient to support their development until there is an absolute requirement for cell autonomous *T* function (Rashbass *et al.*, 1991). Wilson *et al.* (1995) used this system with *lacZ* expressing *T/T* ES cells injected into wild-type host blastocysts. The resulting embryos displayed a range of phenotypes depending on the level of contribution of *T/T* cells. A high contribution of *T/T* cells produced detectable abnormalities by early somite stages reminiscent of the intact *T/T* phenotype. Chimaeras with a low *T/T* cell contribution exhibited tail and allantoic deformities, most evident from approximately 10.0 dpc., similar to *T/+* embryos. A characteristic abnormality of chimaeras composed of

wild-type and *T/T* mutant ES cells was the aggregation and accumulation of mutant cells in the primitive streak and its descendant, the tail bud (Wilson *et al.*, 1995). As a consequence, there is a deficit of mutant cells in definitive mesodermal derivatives particularly in the notochord and somites posterior to somite 9. This accumulation of cells is likely to be due to a downstream effector of the *T* gene product that alters cell surface (probably adhesion) properties as cells pass through the primitive streak. Thus, the *Brachyury* deletion also affects either primitive streak or tail bud morphogenesis, depending on the level of T protein. The defect (exit from the progenitor zone) remains the same throughout axis elongation.

     Wnt3a is a member of the Wnt family of secreted signalling molecules. Its expression starts in the primitive streak and continues to be expressed in the tail bud (Takada *et al.*, 1994). *Wnt3a* null mutants remain alive until 12.5 dpc; however, they lack all somites caudal to somite 9 and fail to form a tail bud. Therefore, the body axis usually terminates between the fore- and hindlimbs (Takada *et al.*, 1994). On the basis of this severe somitic phenotype and the absence of tail bud formation it was suggested that *Wnt3a* signalling might regulate somite fate and establishment or maintenance of the tail bud (Takada *et al.*, 1994). A hypomorphic mutant named vestigial tail (vt) was described by Heston (1951) and Gruneberg (1957, 1974). It is an autosomal recessive mutation that results in viable animals with reduced and/or kinked tails. Typically, many caudal vertebrae are absent, and those that remain exhibit severe morphological abnormalities. Greco *et al.* (1996) showed that the defect in *vt/vt* animals resulted from the generation of a hypormorphic allele of *Wnt3a*. These authors then generated embryos carrying different allelic combinations, thereby progressively lowering the levels of *Wnt3a* expression, somitogenesis and subsequent axial skeleton development was correspondingly arrested at increasingly more anterior positions. As mentioned above, homozygotes for the null allele exhibit no somite development posterior to somite 9. Because most of these embryos die by 12.5 dpc, prior to vertebral formation, data on the skeleton are limited. However, somite 9 gives rise to the fifth and sixth cervical vertebrae; therefore, it is likely that the vertebral formation would terminate in the

neck. In $Wnt3a^{neo/vt}$ compound heterozygotes, the small amounts of $Wnt3a$ produced from one vt allele is sufficient for prenatal viability and normal development of most thoracic vertebrae. Higher levels of $Wnt3a$ produced in vt/vt individuals completely rescue the postnatal viability and are sufficient for normal development of the lumbar and sacral region, though not for the posterior tail vertebrae. Finally, there is evidence that the reduced dosage of $Wnt3a$ in $vt/+$ mice is not always sufficient for the formation of all vertebrae, sometimes resulting in fewer caudal vertebrae and morphological irregularities that produce tail kinks (Gruneberg and McLaren 1972). Fate mapping in the mouse suggests that the first somites formed are derived from mesodermal precursors arising at the anterior limit of the primitive streak (Tam and Beddington, 1987; Tam 1989). As development continues, the tail bud replaces the primitive streak (by stage 9.0 dpc, 24-26 somites) and continues contributing to the mesodermal precursors that generate all the remaining somites (Schoenwolf 1977; Tam 1986; Tam and Tan 1992). Thus, the occipital, cervical, and thoracic vertebrae are probably derived from the primitive streak, whereas lumbar, sacral and caudal vertebrae of the tail are derived from the tail bud. These data suggest that $Wnt3a$ is required during primitive streak stages and throughout tail bud development for the elaboration of new somites, as disruption of this gene can affect both primitive streak and tail bud. Moreover, the alteration of gene dosage suggests that increasing levels of $Wnt3a$ activity are necessary for the development of more posterior somites. Interestingly, Yoshikawa (1997) reported that in the absence of $Wnt3a$ cells adopt ectopic neural fates. Therefore, $Wnt3a$ is thought to modulate the transition from ectoderm to mesoderm cell fates at primitive streak stages and later in the tail bud upstream of T and $Tbx6$ (Yamaguchi et al., 1999b).

In summary, T and $Wnt3a$ genes are expressed from gastrulation through axis elongation. When these two genes are mutated they affect the two structures responsible for trunk and tail formation: primitive streak and the tail bud. However, the head tissues seem intact. Null mutations of either of these genes result in early defects in primitive streak morphogenesis and embryonic lethality; whereas in partial loss mutations:

increased amounts of Wnt3a (cell non-autonomous) or high proportion of T protein (cell autonomous) result in higher pre-natal viability and defects affecting only the tail bud and the formation of more posterior regions of the axis. Therefore, primitive streak and its descendant, the tail bud share many similarities in mouse. It is likely that the tail bud, particularly the CNH region in mouse conserves organizer activity as its counterpart the node, as seen in chick and frog. However, this hypothesis remains to be tested in the mouse.

In conclusion, all these experiments suggest that in amniotes, development of the caudal body results from a direct continuation of events initiated during the earlier phase of gastrulation, as it does in amphibians. Therefore, this corroborates Pasteels' idea that the cell populations of the tail originated during primitive streak stages. Furthermore, the persistence of organizer properties in the chick tail reveals evolutionary conservation of a feature found in amphibians (Gont *et al.* 1993) and suggests an important role for continuing caudal organizer function in the formation of the posterior body and elongation of the tail in amniotes, as well as amphibians. However, there is also evidence from some of these studies that some of these cell populations of the tail, in particular the CNH and its precursor the anterior streak or node, might contain multipotent progenitors for the trunk and tail tissues; reminiscent of Holmdahl's idea of a blastema giving rise to different tissues of the tail.

Different models for axial extension

Although so much attention has focused on proving that axial elongation is a continuum from its inception at gastrulation to its termination at the tail bud, the mechanism by which axis elongation, including tail formation, occurs achieving different body length in different vertebrates is still not clear. In different organisms, authors have followed different observations to study axis elongation and tail formation, which have led to different models: in *Xenopus*, Tucker and Slack (1995b) focused on why exogastrulae did not form a tail structure despite having all the right tissues expressing the right genes. This led to the proposal of the N/M/C model for trunk (which will later become

incorporated in the tail) and tail formation. So far, this model has not yet been demonstrated in other vertebrates. On the other hand, studies in mouse focused on the observation made from early fate maps that resident populations existed in the primitive streak at the mid/late gastrula, derivatives of which can populate the whole axis, leading to the proposal of the existence of self-renewing axial stem cells. Apparently resident populations have been observed in fate maps of *Xenopus* (Gont *et al.*, 1993) and chick (Catala *et al.*, 1995). So far, the most significant evidence comes from studies in the mouse, where two structures, the myotome and the spinal cord, appear to be derived from self-renewing precursors probably residing in the primitive streak and later in the tail bud. I will now describe these two approaches in more detail.

N/M/C model in Xenopus

Tucker and Slack (1995b) proposed the N/M/C model for tail determination in *Xenopus*. Based on exogastrulae and neural plate manipulations, they proposed that three regions needed to be in contact in order to initiate a tail bud. These regions are the most posterior 100 μm of the neural plate (M) destined to form tail somites, the neural plate anterior to this (N), and the most caudal ~200 μm of the notochord (C) (Fig. 1.6 A). In this model, a tail bud that is capable of distal growth is induced by an interaction, occurring at about the end of gastrulation (neurula stage, stage 13), between the two territories in the posterior neural plate: N and M, and the posterior mesodermal territory, C. Once an N/M junction has been exposed to C, it will form a tail bud even if subsequently is grafted away from C. Hence, N/M junctions from the C domain will form tails if grafted elsewhere at/or after stage 13, and new N/M junctions created over the C domain will produce an extra tail, but N/M junctions created away from C domain will not form a tail. This was shown firstly, by folding the waist region of an exogastrula (formed from an amphibian blastula placed in an isotonic salt solution, the gastrulation movements result in the eversion of the meso-endoderm instead of its invagination into the interior, which forms a structure with the mesoendoderm and the ectoderm joined posterior-to-posterior by a narrow waist region), before folding, on an
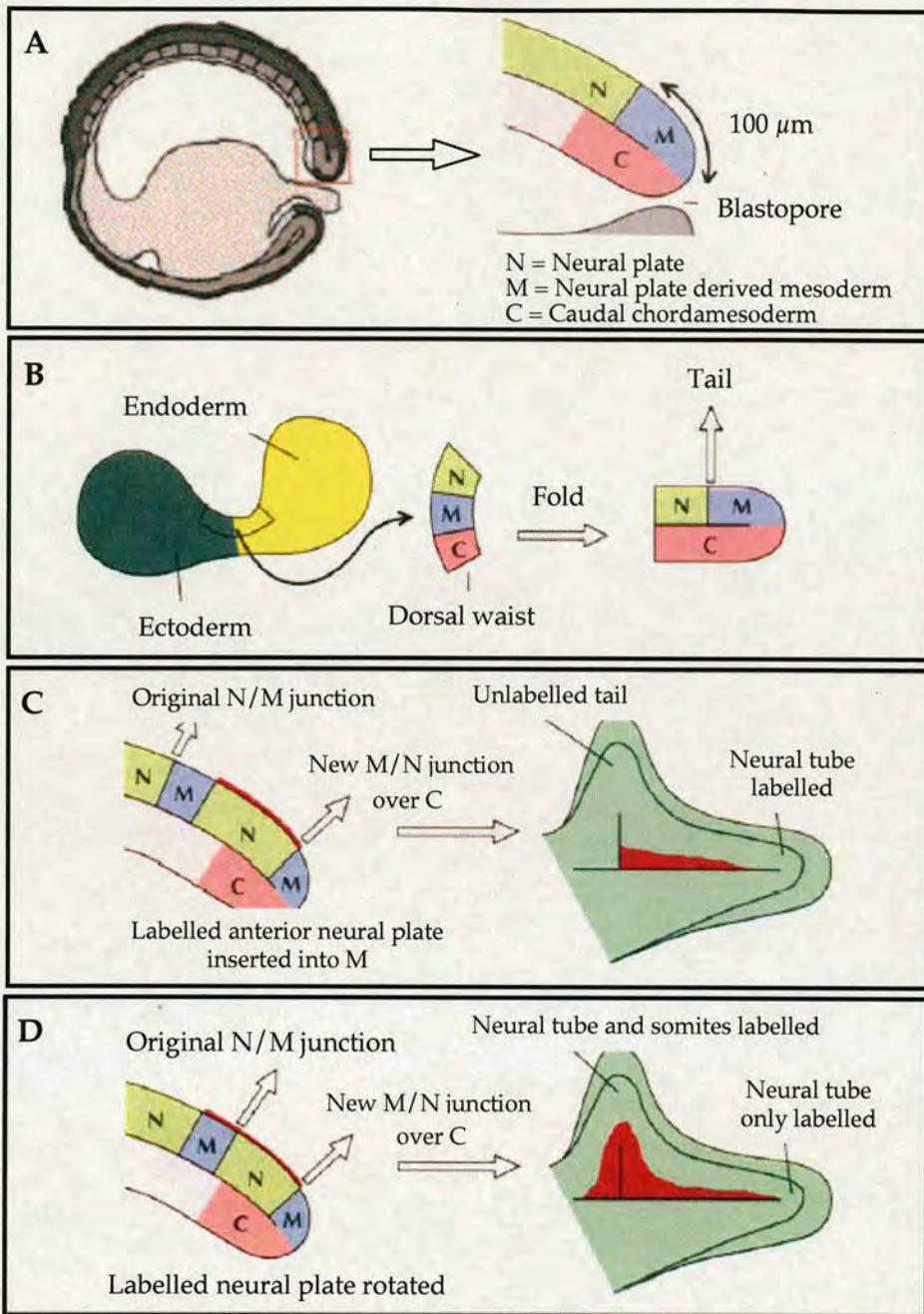
Figure 1.6 N/M/C model for tail formation in *Xenopus*

A) Diagram depicting the tail bud-forming zone at stage 13. The three regions important for tail development, N, M and C, are shown. In this model, C is restricted to about 200 μm from the blastopore, and M runs from the blastopore to a point about 100 μm along the neural plate.
B) Folding of the dorsal waist region of an exogastrula causes the N/M junction to come into contact with C so that a tail can form. **C)** Insertion of a piece of anterior neural plate into a slit in the posterior neural plate, dividing the M region (surface red colour indicates fluorescent labelling). The insertion causes the original tail N/M junction to be pushed anteriorly away from its original position. This N/M boundary was previously over C, and so has already received a signal from this region. A tail can thus form, which has no labelling from the graft. The insertion of the new N tissue creates two new N/M boundaries. The more posterior one is located over C, so a tail would be expected to form here, the neural tube of which should be labelled. If the middle N/M boundary is formed over C, a third tail would be predicted, but the inserted piece of N would have to be extremely small for this to occur. **D)** Rotation of a piece of posterior neural plate by 180°. The rotation shifts the original N/M boundary anteriorly, but it can form a tail as it has been previously in contact with C. This tail would be expected to be labelled. The rotation forms two new N/M boundaries. The most posterior is found over C, so a tail forms, the neural tube of which is labelled. The anterior boundary, however, has no contact with C so does not form a tail. Modified from Tucker and Slack (1995).

51

exogastrula the posterior part of the neural plate, N and M, and the posterior part of the axial mesoderm, C, lie end-to-end rather than one on top of the other. When the exogastrula waist is folded, C is brought in contact with N/M and so a tail forms (Fig. 1.6 B). Secondly, manipulation of the posterior neural plate of neurulae, by graft insertion or rotation, led to the formation of supernumerary tails (see Fig. 1.6 C-D and figure legend for more details). This model stresses the importance of a signal from the underlying C region that would affect the neural plate above, but there must also be a reciprocal signal from the neural plate, once the tail bud has been set up, to allow recruitment of the notochord. Thus, tails formed by N/M junctions moved from the C region to a more anterior level include notochord that has split off from the main axis of the host.

To confirm this model Beck and Slack (1998) looked for the specific expression of genes in the N/M/C regions at the end of gastrulation, but failed to find any specific gene for each region, which might indicate that these regions are defined not by individual genes, but by unique combinations of gene activity at stage 13. Instead, they observed two distinct temporal phases of gene expression in tail development. The early phase involves expression of genes that are already localised in the prospective tail bud region at the end of gastrulation, thus when the N/M/C interaction occurs. These early genes remain associated with specific regions of the tail bud throughout tail development. The second, later, phase of expression begins at stage 27 and correlates with the onset of tail outgrowth. The expression of this late phase genes depends on the correct alignment of the N/M/C regions at the stage of initiation (stage 13). As discussed in the previous section (Fig. 1.2), their results showed that the early and late gene domains together defined seven distinct regions of the tail bud, and this was increased to ten regions following the study of additional genes (Gawantka et al. 1998). Interestingly, they found a small region of overlap between X-Notch-1 and X-delta-1 (early genes), expressed together in the posterior wall (M), and lunatic fringe (lfng), expressed in the dorsal roof on the neural tube (N). The region of overlap corresponds to the junction between N and M territories in the posterior of the embryo, which defines the direction of tail outgrowth. At around the

same time, *Xhox3* (a *Xenopus* homologue of Drosophila *evenskipped* gene) is expressed in a subset of cells of the overlap region corresponding to the caudal tip, or most distal cells, of the future tail bud. By analogy with other systems undergoing outgrowth such as the Drosophila wing disc and the chick limb (Fleming *et al.*, 1997; Laufer *et al.*, 1997; Panin *et al.*, 1997; Rodriguez-Esteban *et al.*, 1997), Notch signalling may be restricted by *lfng* to the overlap region, and this could be the molecular basis of the N-M interaction in the posterior wall that leads to outgrowth of the tail bud (Fig. 1.7 top panel).

In 1999, Beck and Slack designed an assay for tail-forming ability in which a piece of animal cap tissue expressing the test gene is grafted into the posterior neural plate of a host embryo at stage 13. The grafts become incorporated into the neural plate, and if they contain an appropriate mRNA, will develop into a tail-like structure with axial tissues formed from the graft and a fin formed from the host. This assay was used to test the effect of the ectopic expression and inhibition of the above late tail bud genes. They showed that ectopic tail-like projections could be formed by grafts expressing a constitutively active cytoplasmic domain of *X-Notch-1* (*Notch ICD*). The resulting buds express *Xhox3* as well as many other tail bud markers. Furthermore, grafts expressing *Xhox3* form identical ectopic tails, suggesting that *Xhox3* is a downstream target of Notch signalling. Evidence that *Xhox3* is actually a critical step in *Xenopus* bud outgrowth is provided by the use of an antimorphic form of *Xhox3*, which prevents ectopic formation by *Notch ICD*, and also prevents tail development in intact embryos. These results provided evidence that the N-M interaction initiates a new molecular pathway controlling tail bud outgrowth, involving activation of Notch signalling at the future tail tip and consequent activation of *Xhox3*. They also showed that expression of *Xwnt3a*, in the most extreme posterior dorsal roof and distal tip of the tail bud is required in addition to Notch signalling to turn on *Xhox3* at stage 26 and that Wnt expression might be acting as a posterior competence factor in tail morphogenesis. In support of this, in the mouse, *Wnt3a* expression is also localised to the tail bud (Takada *et al.*, 1994), although in this organism, *Wnt3a* is expressed from early gastrulation stages in the
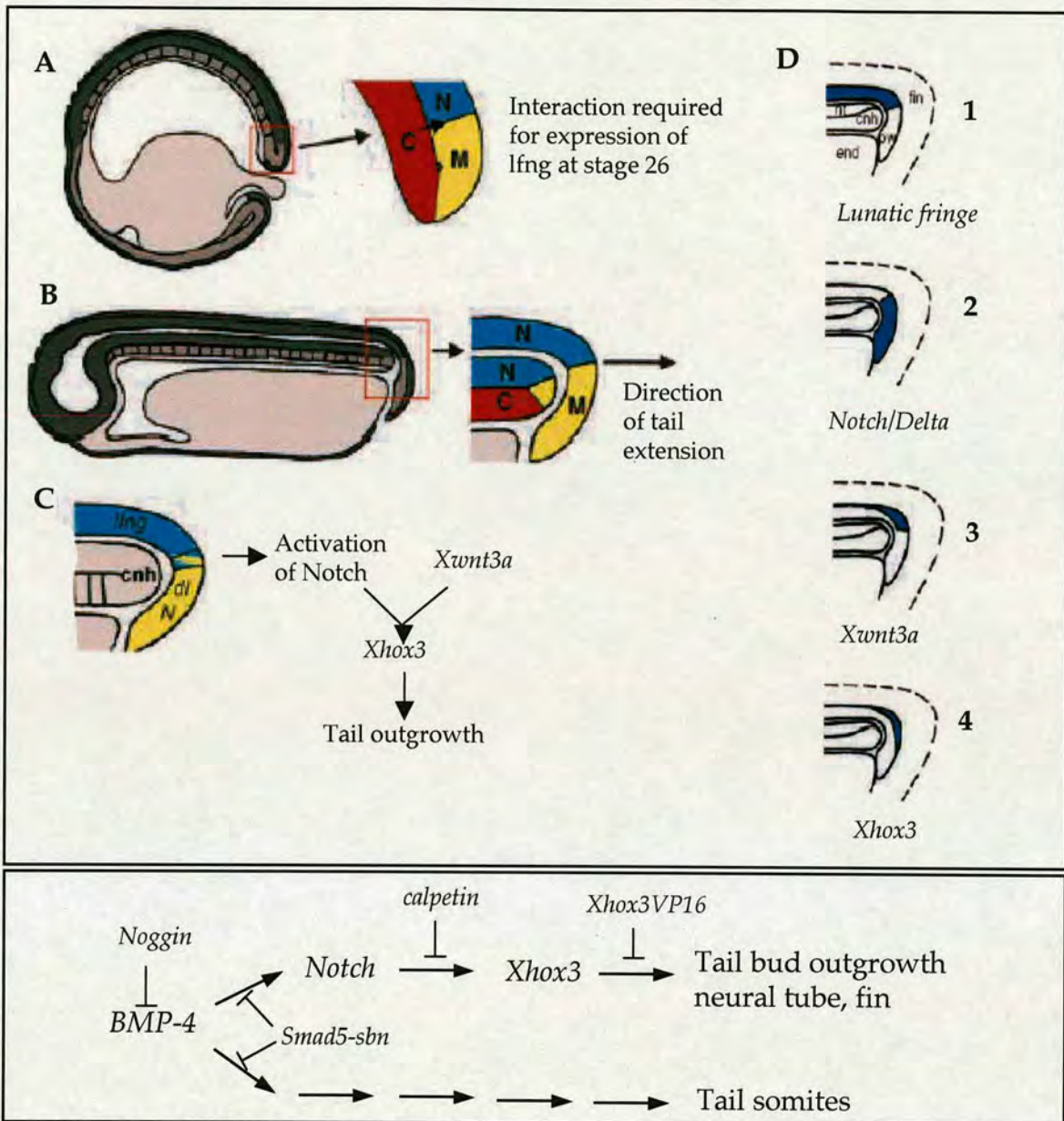
Figure 1.7 A model for tail outgrowth in *Xenopus*

Top panel: A) At stage 13, the three regions: N, M and C need to come into alignment so that the junction of N and M overlies C. This interaction is essential for tail formation and is also required for onset of expression of *lfng* and *Xwnt3a* at stage 26. **B)** By stage 26, closure and extension of the neural tube results in formation of the posterior wall of the neural tube from the lateral blastopore lips, and movement of the N-M junction to the tip of the tail bud. **C)** A mechanism for tail bud outgrowth mediated by Notch signalling. At around stage 26, *lfng* expression begins in the dorsal roof of the neural tube (**D.1**). Expression terminates at the posterior of the embryo in a sharp boundary, which slightly overlaps expression of the early genes *X-Notch-1* and *X-delta-1* in the posterior wall (**D.2**). This arrangement results in localised activation of Notch signalling at the leading edge of the tail bud. In the presence of *Xwnt3a* (**D.3**), also turned on at sage 26 in the extreme posterior dorsal roof and distal tip of the tail bud, this results in *Xhox3* (**D.4**) expression in the distal tip of the tail bud. **D)** Summary of key genes at the time of tail outgrowth. Tail bud expression of *lfng, Notch, Delta* and *Xhox3* is shown in blue for comparisison. Adapted from Beck and Slack, 1999. **Bottom panel:** Model for the role of BMP signaling in tail development. BMP is activated in the M region upstream of *Notch/Xhox3* causing tail outgrowth. Moreover, BMP independently of Notch might trigger tail somite formation. *Xhox3VP16*: antimorphic *Xhox3* construct that has the repressor domain replaced by a transactivation domain from the VP16 protein; *Smad5-sbn*: zebrafish mutant *somitabun (sbn)* that acts as a dominant negative, specific to BMP signalling. Reproduced from Beck *et al.*, 2001.

primitive streak and continues in the tail bud as axial elongation takes place.

However, ectopic tails generated in this way contain neural tube and fin, but not somites or notochord. A modification of the above model was therefore proposed (Beck and Slack in 2001), using an antibody that detects the phosphorylated form of Smads 1/5/8 (Faure *et al.*, 2000), they showed that BMP signalling is activated in the M region corresponding to the future ventral posterior wall of the tail bud. This activity is present from the end of gastrulation and persists at least until the tail bud begins to emerge. This region of the tail bud is fated to give rise to posterior somites (Gont *et al.*, 1993). Using the same grafting test as for Notch, they showed that *BMP4* mRNA, activated BMP receptor *Alk3*, or and activated *Smad 5* mutant all produced ectopic tails, and these contain somites in addition to neural tube and fin. However, the tails were never found to contain notochord. Epistasis experiments suggest the requirement for BMP signalling upstream of *Notch/Xhox3* in tail outgrowth; one possible explanation given by the authors is that BMP, as well as causing activation of Notch which will trigger neural tube formation, also activates a second Notch independent pathway that results in the formation of somites from the ventral tail bud (see Fig. 1.7 bottom panel for BMP signalling model for tail outgrowth).

In summary, the formation of the tail of *Xenopus laevis*, depends on an initial tail determination event, which requires the interaction between the mesodermal (M) and neural (N) regions of the posterior neural plate, and the underlying caudal notochord (C), which first come into contact at the end of gastrulation. This correct interaction will allow a new wave of gene expression later around stage 27, among those the expression of lunatic fringe in the dorsal tail bud region (N), leads to an activation of Notch signalling also activated by *BMP4* at the dorsal/ventral boundary of the tail bud. This in turn leads to localised *Xhox3* expression in the distal tip of the tail bud as the neural tube begins to extent. On the other hand, *BMP4* triggers somite formation from the posterior wall. Given that *Notch, Wnt3a, BMP4* and *evenskipped*-related genes are expressed in the tail bud of the mouse (Takada *et al.*, 1994; Gofflot *et al.*, 1997) and zebrafish (Joly *et al.*,

1993; Westin and Lardelli, 1997) embryo, Beck and Slack propose that this may provide a general mechanism for the formation of the tail in all vertebrates. However, there are discrepancies in the time of expression of the genes and also the regions of expression in the tail bud, between mouse and *Xenopus*. As I will further describe in chapter 2, the homologues of genes expressed as a new wave of expression in the *Xenopus* tail bud such as *lfng, Xwnt3a, Xhox3* and *BMP4*, are expressed as a continuum from gastrulation until the end of tail elongation in the mouse embryo. Moreover, the expression domains of these genes in the tail bud do not always coincide between these two organisms. Furthermore, Beck *et al.* (2001) proposed that BMP as well as causing activation of Notch that produces tail outgrowth, activates a second, Notch independent pathway that results in the formation of somites from the ventral tail bud. However, there is no evidence from mutants in the Notch signalling pathway in mouse that tail eversion is specially blocked. On the contrary, periodic activation of Notch in the presomitic mesoderm is thought to act as the initiation of somite boundary specification and is needed for somite formation in mouse and chick (reviewed by Pourquié, 2004; Huppert *et al.*, 2005). As a result, it seems unlikely that the model proposed for *Xenopus* tail outgrowth is able to account well for tail formation in amniotes, particularly in the mouse.

Self-renewing precursors in the mouse

Clonal analysis (by labelling with horseradish peroxidase and culturing for up to 36h) of the pre-streak and early streak embryo at the onset of gastrulation (Lawson *et al.*, 1991; Lawson and Pedersen, 1992) showed that morphogenetic movements occur in the presence of extensive, although not indiscriminate, cell mixing in the epiblast. It also showed that growth in the epiblast was rapid, noncoherent and in most regions anisotropic and directed towards the primitive streak. With respect to axial progenitors, it showed that clonal descendants were not necessarily confined to a single germ layer or to extraembryonic mesoderm, indicating that these lineages are not separated at the beginning of gastrulation and that a high degree of pluripotency exists

(Fig. 1.8). Indeed it suggested that each epiblast cell maintained this ability until it has reached, or gone through, the streak. Pluripotency seems to be common for all the cells of the early gastrulation epiblast, as only 56% of the clones had descendants in only one germ layer. In particular, in one area the incidence of contributing to more that one layer was higher than the rest (76%). This region is situated anteriorly to the forming streak at prestreak and early streak stages. It also differs from others in that cells that were in or near it (zone X, Fig. 1.9) at the early streak stages have descendants at the neural plate stage in the anterior part of the streak and node, as well as in more anteriorly located mesoderm and endoderm. This suggests that a subpopulation of cells in or near the anterior end of the early streak maintains its position in that part of the streak until late in gastrulation and might form a stem cell population whose progeny will populate successively more posterior regions of the embryo.

The existence of resident cells in the primitive streak and node has also been inferred from labelling and grafting studies on both early (Tam and Beddington, 1987; Lawson *et al.*, 1991) and late (Tam and Tan, 1992) embryos. Wilson and Beddington (1996) showed using DiI labelling, that most of embryos labelled in the primitive streak and node at 8.5 dpc retain labelled cells in the primitive streak and tail bud, even after 48h development in vitro. However, it is difficult to prove the full duration of their persistence in the streak due to the limited time span of normal development in vitro, and it remained a possibility that these apparently resident cells are merely delayed in their exit from the primitive streak.

The most striking evidence for the existence of self-renewing populations in the primitive streak has come from retrospective single cell marking analysis. Cell clones are labelled in embryos by a random genetic event in a *lacZ* reporter gene (Bonnerot and Nicolas, 1993). This reporter construct (Bonnerot *et al.*, 1987) contains an internal duplication of the *nls lacZ* gene (*laacZ*) that inactivates β-galactosidase activity (Fig. 1.10 top panel). If an intragenic homologous recombination occurs between the duplicated sequences of the *laacZ* (β-gal⁻) transgene, it reestablishes the *lacZ* (β-gal⁺) reading frame and results in functional β-gal expression. By analogy with Drosophila, where homologous recombination in somatic
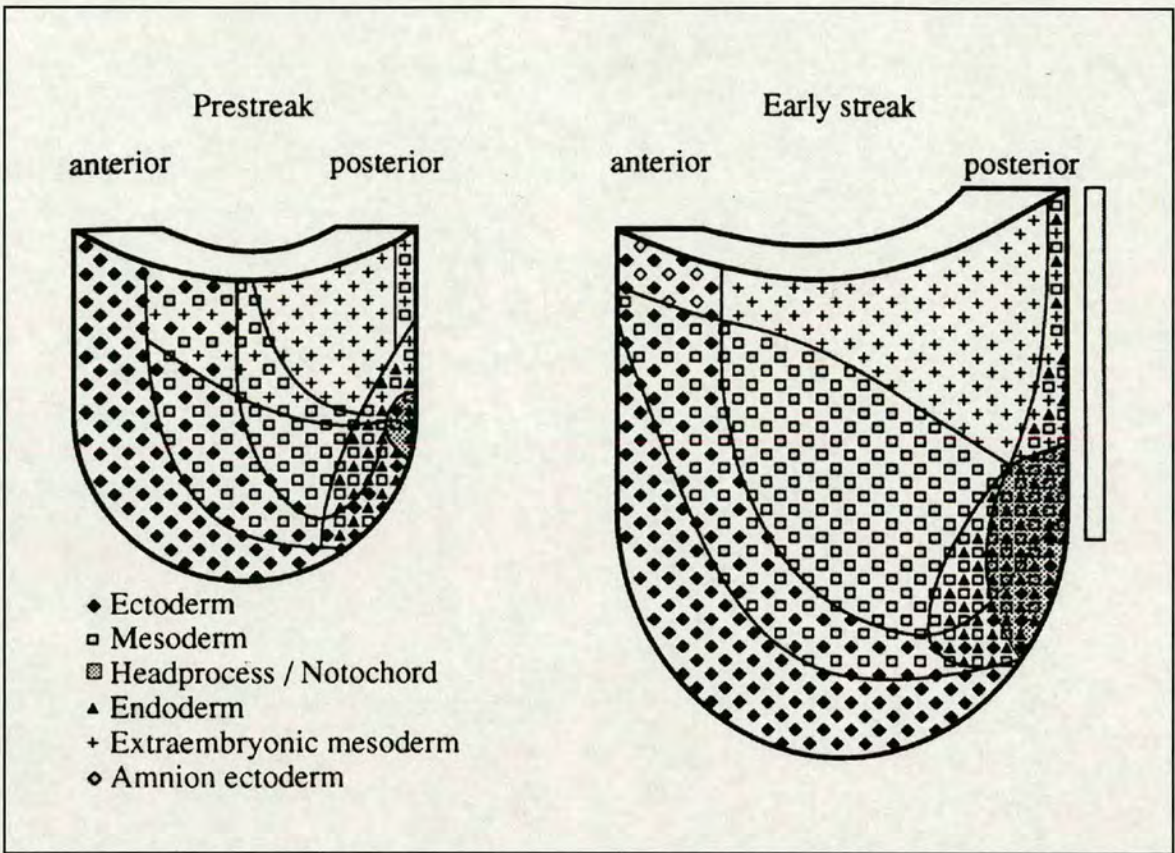
Figure 1.8 Fate map of the early epiblast of the mouse embryo
Diagrams of the prestreak and early-streak stages showing the derivation of the germ layers up to
the mid- to late-streak and neural plate stages respectively. The approximate extent of the primitive
streak is indicated by the white bar. Reproduced from Lawson *et al.*, 1991.
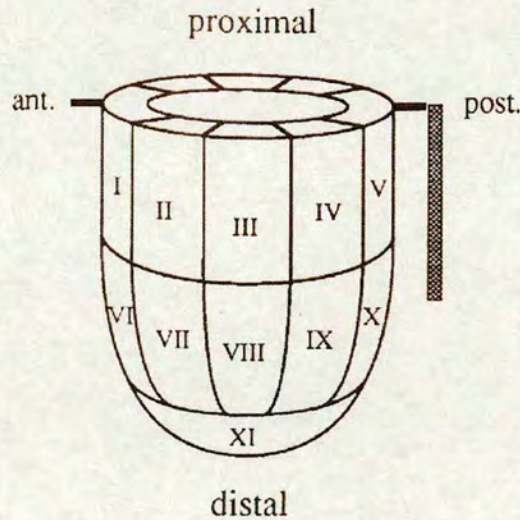
**Figure 1.9 Diagram of the epiblast zones injected by Lawson *et al.* (1991) at the
early streak stage**
The extent of the primitive streak is indicated with a hatched bar. Reproduced from Lawson and
Pedersen, 1992.
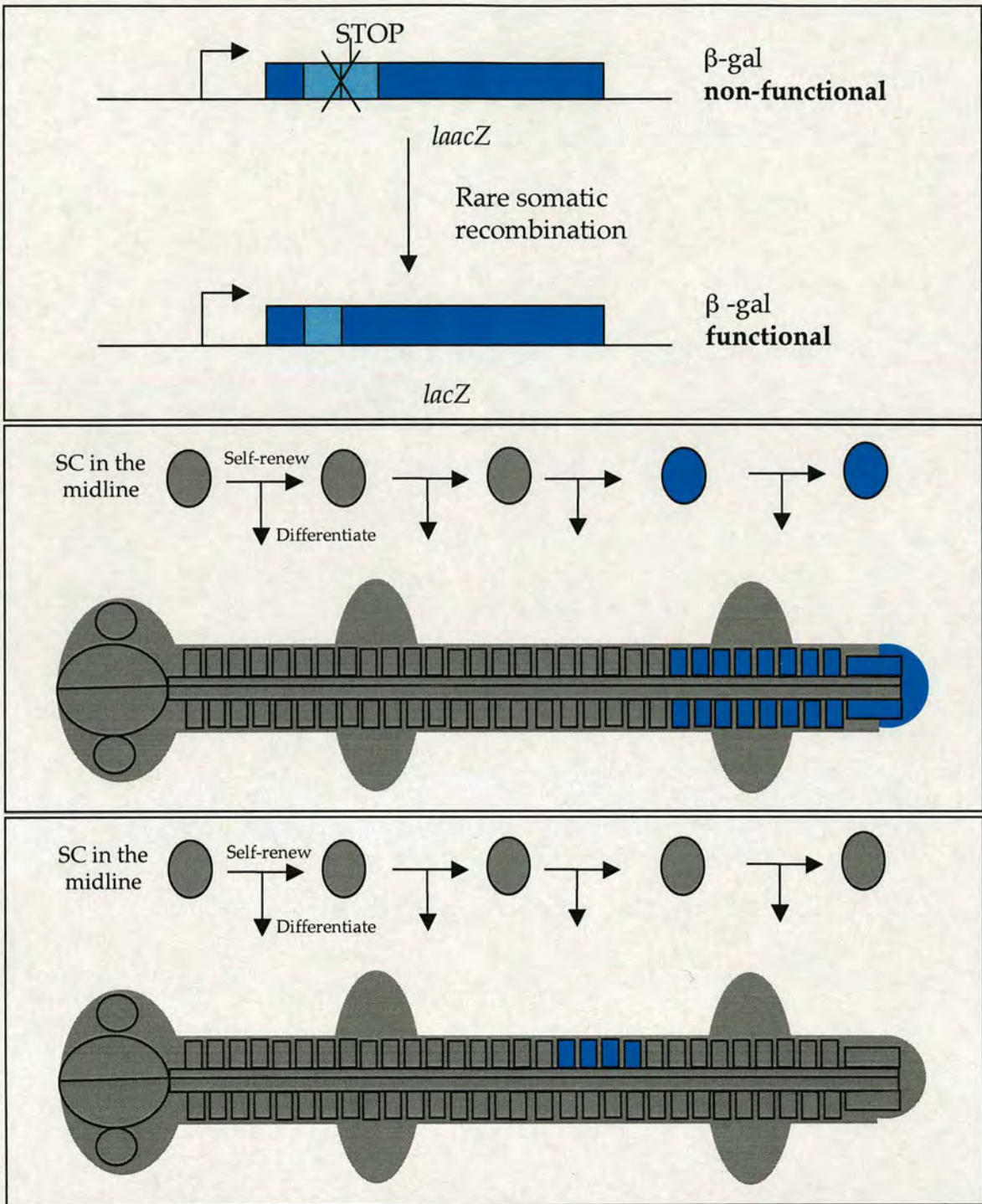
Figure 1.10 Retrospective clonal analysis performed using the *laacZ* system to define progenitor fate in the myotome and spinal cord

Top panel shows that if a rare intragenic homologous recombination occurs between the duplicated sequences of the *laacZ* (β-gal⁻) transgene, it reestablishes the *lacZ* (β-gal⁺) reading frame and results in functional β-gal expression. This can happen in all cells at any time during development. The probability of generating a clone, at any give time, is dependent on the number of precursor cells that give rise to the structure examined. **Middle panel** shows the outcome of recombination in a myotome stem cell. All the progeny becomes labelled bilaterally, as far as the posterior end, creating a long clone. **Bottom panel** shows the outcome of recombination in a more committed descendant (non-stem cell), only the progeny of the limited cell divisions will be labelled, creating a unilateral short clone. This self-renewing mode has been also proposed for the spinal cord. SC: stem cells. (Based on Nicolas *et al.*, 1996; Mathis and Nicolas, 2000).

59

cells is detected by mitotic recombination (e.g. twin spots), the frequency of detection of a spontaneous recombination event in somatic mouse cells will be dependent on the rate of cell division (Panthier and Condamine, 1991). Moreover, the probability of generating a clone, at any given time, is dependent on the number of precursor cells that give rise to the structure examined.

Consequently, this retrospective clonal approach allows for an investigation of the modes of proliferation, dispersal and differentiation of cells *in situ*. The recombination event in the *lacZ* reporter gene generates an intrinsic long-term marker (β-galactosidase) that allows visualisation of the descendants of the ancestral cell even in a mature differentiated structure and should permit an analysis of all cells at the origin of this structure (Bonnerot and Nicolas, 1993). This method was applied to the study of two structures: the myotome (Nicolas *et al.*, 1996) and the spinal cord (Mathis and Nicolas, 2000).

The myotome is a structure that is derived from the paraxial mesoderm and is organised at embryonic day 11.5 into 37 to 42 segments along the A-P axis corresponding to the dorsal part of the somites. In order to analyse the lineage of cells in the myotome, the expression of the *laacZ* gene was driven by the promoter of the α subunit of the acetylcholine receptor (αAchR), which limits expression specifically to cells of this compartment (Klarsfeld *et al.*, 1991). The frequency of 11.5 dpc embryos exhibiting β-gal$^+$ cells was 153 of 3000, or about one out of twenty embryos. This low frequency verifies that most of the positive embryos contained only β-gal$^+$ cells from a single recombinant clone, because the probability of more than one recombination event occurring in cells of the myotome of the same embryo is $1/20^2$. Two categories of clones were found: long clones that contributed to more than 6 somites and short clones that contributed to 6 or less. The longitudinal organisation of myotome formation is polarised from anterior to posterior as the number of long clones contributing to any one somite increases from rostral to caudal. Long clones also contributed predominantly to segments on both sides of the myotome, indicating that the clone arose at the midline (corresponding to the primitive streak or tail bud) (Fig. 1.10 middle panel).

Short clones contributed to only a small number of segments. The majority of clones shorter than 4 somites are unilateral, i.e. they arise in the presomitic mesoderm after divergence of these cells to left and right halves of the embryo (Fig. 1.10 bottom panel). The observation of these two types of clones with those characteristics fits a model that postulates axis formation from a pool of permanent progenitors. The orientation of the polarity indicates the direction of the movement of this pool. Shorter clones are also expected from this model, which correspond to the descendants of those progenitors deposited along the axis by the permanent pool. The contribution of long clones to both sides of the myotome means that the progenitors cells must be located in a structure that includes both right and left segments. Because there are examples of long clones contributing from the first visible somite as far as the most posterior one that has formed a myotome, the pool of progenitors must arise at the beginning of somite formation and derive from a pool of cells that self-renews and which follows axis formation during development. Thus, they postulate that a likely site of localisation for the progenitors is at the anterior part of the primitive streak at 8 dpc and that they would continuously contribute to the future segments of paraxial mesoderm during the formation of the axis from the primitive streak and then from the tail bud. From the numerical data, it was also possible for the authors to approximate the size of the pool of self-renewing precursors to about 100-150 cells.

In the case of the central nervous system (CNS), they used mice expressing the *laacZ* reporter gene under the control of the neuron specific enolase promoter (NSE-1) (Forss-Petter *et al.*, 1990), which allows visualisation of the descendants of the precursors in the ventromedial cells of the CNS. They harvested embryos at 12.5 dpc, when the *laacZ* transgene is strongly expressed along the entire CNS (Mathis *et al.*, 1999). They found 163 CNS clones exhibiting β-gal^{+} cells from a total of 3000 embryos. As seen for the myotome, this low frequency verifies that most of the β-gal^{+} cells derived from a single recombination event, since the probability of more than one recombination event in the same embryo is about $1/20^2$. To study the contribution of labelled cells, they divided the anterior CNS

(brain) and spinal cord in 64 segments of equal length. They found a group of very long clones that contributed from the most anterior segments in the brain to the most posterior spinal cord. Surprisingly and unlike the myotome long clones, which were mostly bilateral, half of the CNS long clones were bilateral and half unilateral. This suggests that the midline is a clonal boundary for the CNS from very early on, and so there is not extensive intermingling (at least not mediolateral) in the ectoderm; in contrast to the bilaterality of even small myotome clones, consistent with the migratory nature of mesoderm precursors.

However, from the distribution of the clones, the brain and the spinal cord appear to be formed by two different modes. The brain was populated either by very long clones that spanned the whole axis, or by very short clones. This fits with an ordered (coherent) intermingling mode of growth, in which cells can rearrange only with their closest neighbours. The spinal cord, however, was mainly populated by long clones restricted to this structure, whose polarity suggests growth from a population of self-renewing precursors that moves posteriorly with axial development, as seen for the myotome. However, the observation of long clones contributing from the anterior segments of the brain to the posterior spinal cord suggest that both structures derived from a common population of founder cells that originated in the epiblast (5-6.5 dpc). In about two cell divisions (6-7 dpc), the two modes of growth would have probably become separated between anterior and posterior neural system precursors, probably due to the anterior to posterior regression of a pool of self-renewing cells and to a relatively coherent growth in the brain. These results are in broad agreement with the early fate maps of the neural plate in the mouse (Lawson *et al.*, 1991; Lawson and Pedersen, 1992). The more coherent cell behaviour in the brain, and the caudal polarity in the spinal cord are consistent with descriptions of neurulation movements in other species (Schoenwolf and Smith, 1990; Woo and Fraser, 1995), illustrating the significant conservation of the cell movements of gastrulation and neurulation during vertebrate evolution.

In summary, these experiments have shown that at least two of the axial tissues, the myotome and the spinal cord, are produced by pools of

progenitors, which would be localised early in the anterior primitive streak and later in the tail bud. The authors propose that these progenitors remain the same throughout axial elongation, in a self-renewing mode. However, an additional explanation would be that the progenitors are differentiating to a more posterior precursor after each cell division. Therefore, more posterior progenitors could only give rise to posterior tissues. These two possibilities remain to be addressed.

1.2 AIMS OF THE PROJECT

Although the clonal lineage studies show the strongest evidence for the existence of axial stem cells in the mouse, the use of promoters specific only to each compartment means that they cannot give detailed information on the position of the putative precursors, neither do they distinguish between the possibility of separate stem cell populations, and a common one supplying all lineages, nor whether they are self-renewing progenitors.

My PhD project intended to address these questions by performing grafting experiments in the mouse embryo. Thus, the aims of my project were to:

1. Search for candidate gene products that might control the maintenance or differentiation of the putative stem cell progenitors for the axial tissues.

2. Locate the exact position of these putative stem cells along the axis at early (primitive streak) and late (tail bud) stages.

3. Define their potency.

Chapter 2 describes gene expression: we have focused on genes known to be expressed at primitive streak stages, to follow their expression in the different regions of the tail bud; genes known to be expressed in the *Xenopus* tail bud and genes involved in maintaining pluripotency and self-renewal. Chapter 3 and 4 present the grafting experiments performed aiming to locate the axial stem cells at late stages (tail bud) and early stages (primitive streak) consecutively. Chapter 4 also

looks at the potency of the putative regions containing the progenitors at primitive streak stages, by grafting them to a neutral site. Finally, Chapter 5 contains concluding remarks and perspectives.

Chapter 2

GENE EXPRESSION IN AXIAL PROGENITORS

2.1 INTRODUCTION

Despite our current understanding of tail morphogenesis as outlined in the introduction, and of gene expression during early stages of gastrulation, little is known of genetic patterning and the potential morphogenetic role of regulatory molecules in the mouse tail. As discussed in the introductory chapter we know from gene expression studies mainly performed in *Xenopus* and chick that the expression of some genes can be followed from gastrulation to tail bud stages (Gont *et al.*, 1993; Knezevic *et al.*, 1998). Moreover, lineage studies have shown that these regions of gene expression correspond to different subpopulation of cells in the node and primitive streak and their derivatives in the tail bud. Therefore, the tail bud is regionalised and ten different expression domains have been described in the *Xenopus* tail bud (Beck and Slack, 1998; Gawantka *et al.*, 1998). In the mouse, Gofflot *et al.* (1997), aiming to find factors involved in defective spinal neurulation, performed a detailed analysis of gene expression in the tail at the time of neuropore closure. Their study complements others performed in the chick and frog embryos and presents evidence of defined distinct domains within the mouse tail. The use of genes known to be important during gastrulation proved that in mouse, as in other vertebrates, gene expression is continuous from gastrulation to tail elongation. However, the time scale of their analysis was very short, spreading over a period spanning the formation of only 6 somites and concentrating at the stage just prior to neuropore closure (10 dpc). The short time window and the use of some but not all the same genes used in other studies in frog and chick leaves questions still unanswered for the mouse embryo:

-Is gene expression continuous from gastrulation until the end of tail elongation in the mouse?

-Are gene expression domains, at primitive streak/blastopore stages and tail bud stages, equivalent among the different vertebrates?

-Is there a change in gene expression coinciding with the start of secondary neurulation and tail elongation in the mouse (10.0 dpc), reminiscent to the new wave of gene expression described in *Xenopus* at the start of tail elongation?

-Does the end of axial elongation in the mouse (13.5 dpc) coincide with a decrease of gene expression in the tail bud?

The observation of different domains of gene expression in the tail bud of the different vertebrates shows that the cells of the tail bud cannot all constitute a blastema of undifferentiated cells. On the other hand, lineage analysis and more recently retrospective single cell marking analysis in the mouse have proven the existence of progenitor pools for the myotome and the spinal cord located earlier in the primitive streak and later in the tail bud.

-Is there a cell population in the mouse primitive streak and tail bud expressing genes characteristic of pluripotent stem cells?

2.2 AIMS AND EXPERIMENTAL APPROACH

To answer the questions just mentioned, this results chapter describes a gene expression analysis performed on mouse embryos from gastrulation stages (7.5 dpc) until the end of tail elongation (13.5 dpc). I have focused on: genes known to be expressed at early primitive streak stages and to be important for streak morphogenesis, to follow their expression into the different regions of the tail bud; genes known to be expressed in the *Xenopus* tail bud, where a model of tail outgrowth has already been proposed (Tucker and Slack, 1995b; Beck and Slack, 1999); and genes involved in maintaining pluripotency and self-renewal to find markers for the putative axial progenitors (see Table 2.1, for description and function of genes used). The riboprobes that I used are: *T* (Herrmann, 1991), *Fgf8* (Mahmood et al., 1995), *Cdx2* (Tanaka et al., 1998), *Wnt3a* (Takada et al., 1994), *Evx1* (Dush and Martin, 1992), *Foxa2* (Sasaki and Hogan, 1993), *Nodal* (Conlon et al., 1994), *Sox1* (Aubert et al., 2003; probe made by Su Ling Zhao in Meng Li's lab), *Oct-3/4* (Scholer et al., 1990b), and *Nanog* (Chambers et al., 2003).

I have described in detailed two representative time points during axial elongation: 8.5 dpc (primitive streak stage), as the start of trunk formation when gastrulation finishes; and 10.5 dpc (tail bud stage), after neuropore closure and start of tail elongation. These are also the stages mainly used in our grafts, as I will describe in chapter 3 and 4.

Gene	Gene description	Null phenotype	Function	References
T Brachyury	T-box transcription factor[1]	Die at 11 dpc, truncated axis, defects in NCH (absent), PS (thickened) and allantois (not formed)[2-3]	Needed for axis elongation-role in migration of cells from the streak and/or tail bud[4-5]	[1]Kispert and Herrmann, 1993; [2]Chesley, 1935; [3]Herrmann *et al.*, 1990; [4]Wilson *et al.*, 1995; [5]Wilson and Beddington, 1997
Fgf8	FGF family, secreted molecule[1]	Die at 9.5 dpc, truncated axis, cells undergo EMT but fail to migrate from the streak, no mesoderm or endoderm formed[2]	Needed for gastrulation and axis elongation-role in segmentation and PSM differentiation[3]	[1]Crossley and Martin, 1995; [2]Sun *et al.*, 1999; [3]Dubrulle and Pourquié, 2004
Cdx2	Caudal-like homeobox TF[1]	Die at 3.5-5.5 dpc[2]; if rescued*: survive until 11.5 dpc, but truncated posterior to the forelimb bud[3]	Possible role in regulating cell proliferation and tissue production as the axis elongates[3]	[1] James and Kazenwadel, 1991; [2]Chawengsaksophak *et al.*, 1997; [3]Chawengsaksophak *et al.*, 2004
Wnt3a	Wnt family, secreted molecule[1]	Die at 12.5 dpc, truncated axis, lack somites caudal to somite 9, cells fail to migrate from PS[2], ectopic neural tube[3]	Modulate a balance between mesoderm and neural fates[3], also needed to control segmentation[4]	[1]Roelink and Nusse, 1991; [2]Takada *et al.*, 1994; [3]Yoshikawa *et al.*, 1997; [4]Aulehla *et al.*, 2003
Evx1	Homeobox TF[1]	Die at 5 dpc, before gastrulation, the extraembryonic tissues fail to differentiate, egg cylinder does not form[2]	Expressed in cells that will form the PS[3]; its homolog in *Xenopus* has been implicated in tail outgrowth[4]	[1]Bastian and Gruss, 1990; [2]Spyropoulos and Capecchi, 1994; [3]Dush and Martin, 1992; [4]Beck and Slack, 1999
Foxa2	Winged-helix TF[1]	Die at 10-11 dpc, fail to form a distinct node and lack notochord, floor plate and gut, and have a truncated PS[2-3], if rescued* PS morphogenesis is restored[4]	2 separate roles: 1) in VE to promote PS morphogenesis, 2) specification of the node and its derivatives[4]	[1]Weigel and Jäckle, 1990; [2] Ang and Rossant, 1994; [3]Weinstein *et al.*, 1994; [4]Dufort *et al.*, 1998;
Nodal	TGFβ family secreted molecule[1]	Arrest shortly before gastrulation, fail to establish a PS and lack most mesoderm[1-2]	Required in the epiblast for the specification of the AVE[3], promotes the formation of the PS and node correctly[4-5]	[1]Zhou *et al.*, 1993; [2]Conlon *et al.*, 1994; [3]Brennan *et al.*, 2001; [4]Lowe *et al.*, 2001 [5]Perea-Gomez *et al.*, 2002;
Sox1	HMG box TF from SOXB1 family[1]	Viable, lens defects[2] and epileptic seizures[3], lack of telencephalic neurons that form the ventral striatum[4]	Earliest and most specific TF to mark neural progenitors[5], involved in their maintenance[6]	[1]Gubbay *et al.*, 1990; [2]Nishiguchi *et al.*, 1998; [3]Malas *et al.*, 2003; [4]Ekonomou *et al.*, 2005; [5]Wood and Episkopou, 1999; [6]Pevny *et al.*, 1998
Oct-3/4	POU TF (class V)[1,2,3]	Die at the time of implantation due to a failure to form the ICM that differentiates to trophectoderm[4]	Essential to maintain the pluripotent lineage of the ICM and ES cells[4]	[1]Schöler *et al.*, 1990; [2]Rosner *et al.*, 1990; [3]Okamoto *et al.*, 1990; [4]Nichols *et al.*, 1998
Nanog	Homeobox TF[1,2]	Die at the time of implantation due to a failure by the ICM to generate epiblast, ICM differentiates to parietal endoderm[1]	Essential to maintain pluripotency in the ICM and ES cells independent of LIF-*Stat3*[1,2]	[1]Mitsui *et al.*, 2003; [2]Chambers *et al.*, 2003;

Table 2.1. Description of genes used in our gene expression analysis *by tetraploid aggregation with null mutant ES cells. NCH: notochord, PS: primitive streak, FGF: fibroblast growth factor, EMT: epithelial to mesenchymal transformation, PSM: presomitic mesoderm, VE: visceral endoderm, TGF: transforming growth factor, AVE: anterior visceral endoderm, TF: transcription factor, ICM: inner cell mass, ES: embryonic stem, LIF: leukaemia inhibitor factor, HMG: high mobility group.

Patterns of gene expression were studied by *in situ* hybridisation on whole embryos up to 9.5 dpc, after this stage tails were isolated from the embryos by a cut just posterior to the hindlimb buds. At least ten 8.5 dpc and 10.5 dpc embryos were hybridised with each probe, and no less than two embryos were used for the other stages. Subsequently, the whole embryos or tails were embedded in wax and sectioned. In the case of the *Sox1* gene, I complemented the mRNA analysis by studying mice that carry a targeted insertion of GFP in the *Sox1* locus (*Sox1*-GFP; Ying *et al.*, 2003). In this case the embryos were embedded in gelatin-albumin and sectioned at 100 *μ*m using a vibratome. These sections were analysed using confocal microscopy.

All the descriptions focus mainly on the node and primitive streak areas at early stages and the tail bud at late stages.

2.3 RESULTS

All genes used in this study have a published, restricted expression pattern. In all cases shown in this chapter, the expression patterns observed closely resembled these published patterns, suggesting that background due to non-specific probe hybridisation was not problematic in these experiments.

Table 2.1 contains the gene description, null phenotype and gene function of all the genes described in the results. Figure 2.1 shows in situ hybridisation results for all the genes described from 7.5 dpc to 13.5 dpc. Figures 2.2, 2.3, 2.4, 2.5, 2.6, 2.7, 2.8, 2.10, 2.11 show in situ hybridisation results for all the genes described at 8.5 dpc and 10.5 dpc. Figure 2.9 shows the confocal microscopy results for the Sox1-GFP protein from 8.5 dpc to 11.5 dpc.

Genes expressed at primitive streak stages continue to be expressed as the tail bud elongates

T (Brachyury)

T is expressed in the ectodermal and mesodermal layers of the primitive streak as mesoderm is being produced at 7.5 dpc and 8.5 dpc

(Fig. 2.1 a1, a2). In the node expression is observed in the ventral layer of prospective notochord (Fig. 2.2 B, d). In the ectodermal layer of the node, the anterior part does not express the transcript, whereas expression is detected in the most posterior part (compare the node ectoderm in Fig 2.2 d with e). By 8.5 dpc, *T* expression can also be seen in the differentiated notochord (Fig 2.2 A, B). By 9.0 dpc expression becomes restricted to the posterior end of the embryo, where expression is observed in the most posterior neural tube and newly formed mesoderm, in the gut and in all the cells of the notochord (Fig. 2.2 H, I). From 10.5 dpc until 12.5 dpc, expression resembles that of 9.0 dpc (Fig. 2.1 a3-a6). However, although *T* is expressed broadly in the tail bud ectoderm, transverse sections through this structure show *T* transcripts are expressed more strongly in the dorsal part, as well as the nascent notochord and the tip of the hindgut (data not shown). By 13.5 dpc when axial elongation is about to stop, *T* transcripts remain high in a very small region at the end of the notochord and levels are lower in what looks like the mesoderm adjacent to it (Fig. 2.1 a7).

Fgf8

Fgf8 is expressed in the ectodermal and mesodermal layers of the primitive streak, like *T* at 7.5 dpc and 8.5 dpc (Fig. 2.1 c1, c2). The unsegmented paraxial mesoderm also expresses *Fgf8* at this stage. Intriguingly, as seen with *T* expression, the most posterior part of the node ectoderm expresses *Fgf8*, whereas the anterior part does not (compare the node ectoderm in Fig 2.3 c with d). At tail bud stages, continues to be expressed in all the proliferating tissues as *T*: neurectoderm, the end of the notochord, the gut and the surrounding tail bud mesoderm (Fig. 2.3 G, H; Fig. 2.1 c3-c6). However, although *Fgf8* is expressed broadly in the tail bud ectoderm, transverse sections through this structure show *Fgf8* transcripts are expressed more strongly in the dorsal part, as well as the nascent notochord and the tip of the hindgut, as *T* transcripts (Fig. 2.3 i-l). Other sites of expression are the limbs, where it is expressed in the apical ectodermal ridge (AER) (Fig. 2.3 G), and the midbrain-hindbrain junction (Fig. 2.3 B).
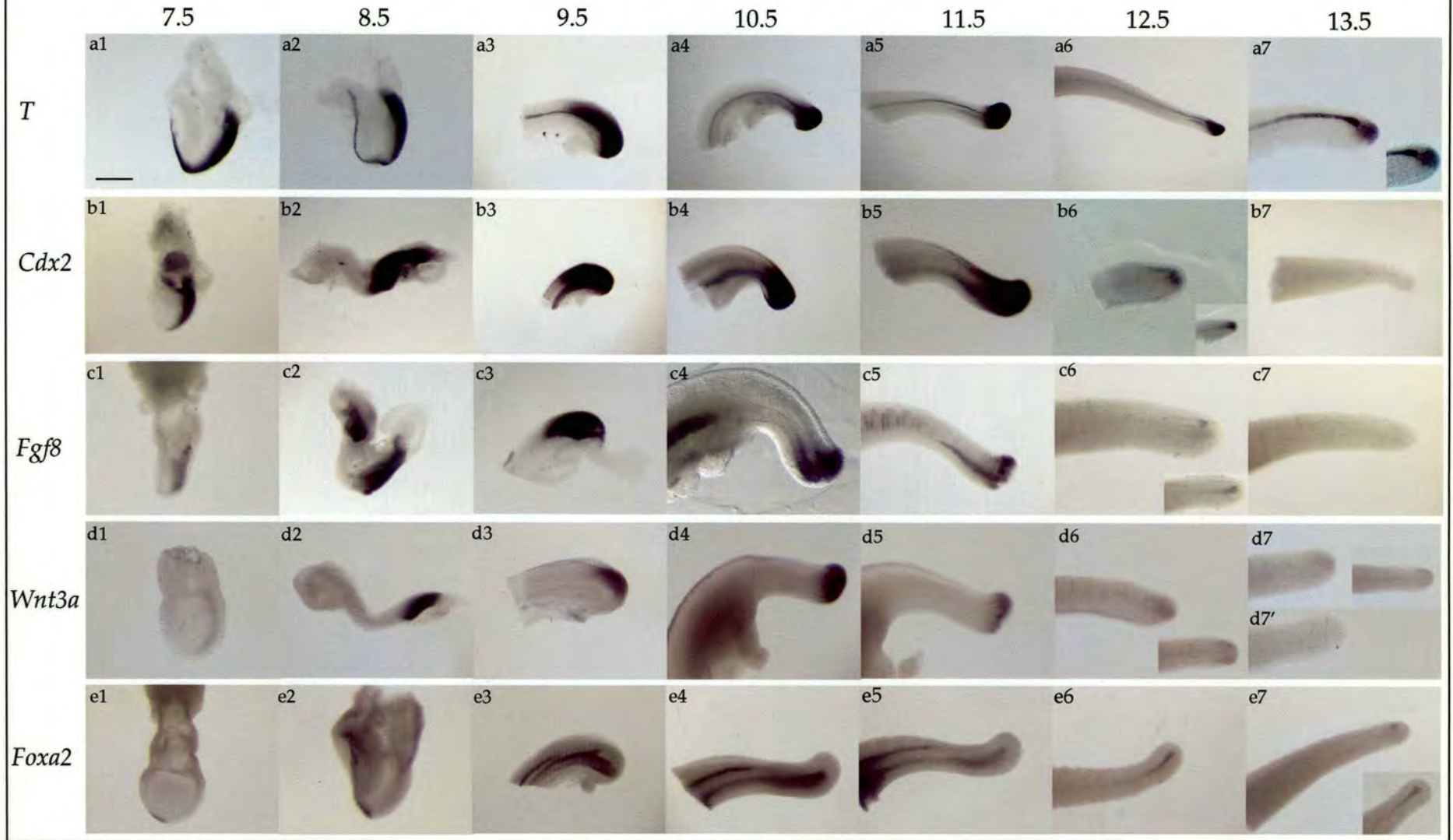
Figure 2.1 Expression of the genes described from 7.5 dpc to 13.5 dpc

a1-2, b1-2, c1-2, d1-2, e1-2) Lateral view of the whole embryo. **a3-7, b3-7, c3-7, d3-7, e3-7)** Lateral view of the end of the tail of the embryo. Insets in **a7, b6, c6, d6, d7, e7** show a dorsal view of the same tail. **d7, d7′)** show two different tails hybridised with *Wnt3a*, very low expression of the gene is expressed in d7 compared to no expression seen in d7′. PS: primitive streak, TB: tail bud. Anterior is to the left. Bar: 300µm in a1-2, b1-2, c1-2-4, d1-2, e1-2; 400µm in a3-7, b3, c3-7, d3-7-7′, e3; 600µm in a4-5, b4-7, e7; 500µm in b5-6, c5-6, d4-5-6, e4-5-6; and 1.5mm in a6.
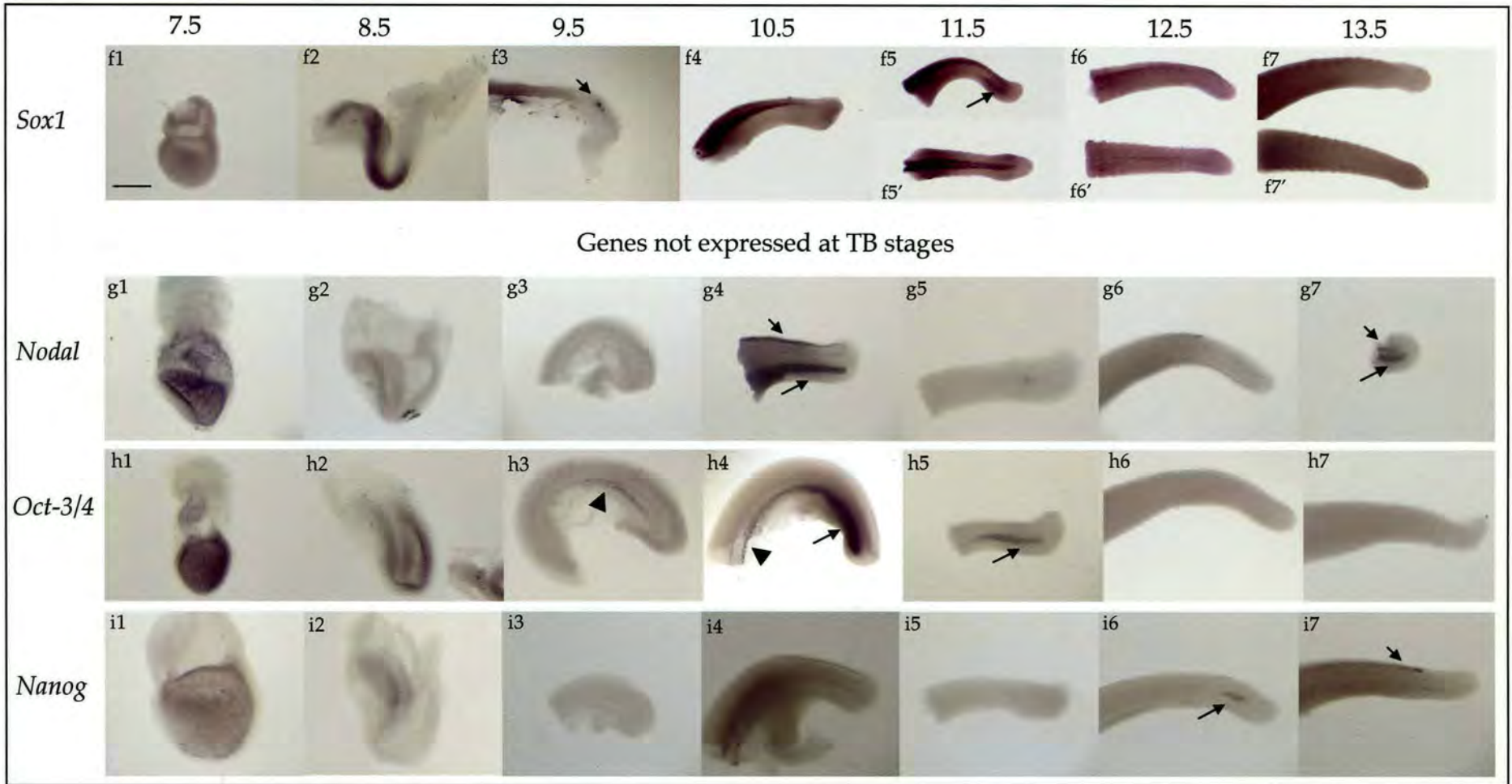
Figure 2.1 Expression of the genes described from 7.5 dpc to 13.5 dpc (continuation)
f1-2, g1-2, h1-2, i1-2) Lateral view of the whole embryo. **f3-7, g3-7, h3-7, i3-7)** Lateral view of the end of the tail of the embryo. Inset in h2 shows a posterior dorsal view of the same embryo, showing the expression of *Oct-3/4* in the PGCs. Arrowheads in h3, h4 show migrating PGCs in the hindgut. **f5', f6', f7')** show a dorsal view of the same tail as in f5, f6, f7, respectively. Note that *Nodal, Oct-3/4* and *Nanog* are not expressed in the tail bud, however in some of the tails we found some trapping either in the neural tube or hindgut or in both as shown by arrows in g4, g7, h4, h5, i6, i7. Trapping can also be observed in the hindgut of a 11.5 dpc tail expressing *Sox1* (arrow in f5). Arrow in f3 also shows some non-legitimate staining in the primitive streak of a 9.5 dpc tail expressing *Sox1*. TB: tail bud, PGCs: primordial germ cells. Anterior is to the left. Bar: 300µm f1-2, g1-2, h1-2, i2; 180µm in i1; 400µm in f3, g3-7, h3, i3; 600µm in f4-7-7', g5, h5-7, i5-7; 500µm in g4, h4, i4; 1mm in f5-5'-6-6'; and 750µm in g6, h6, i6.
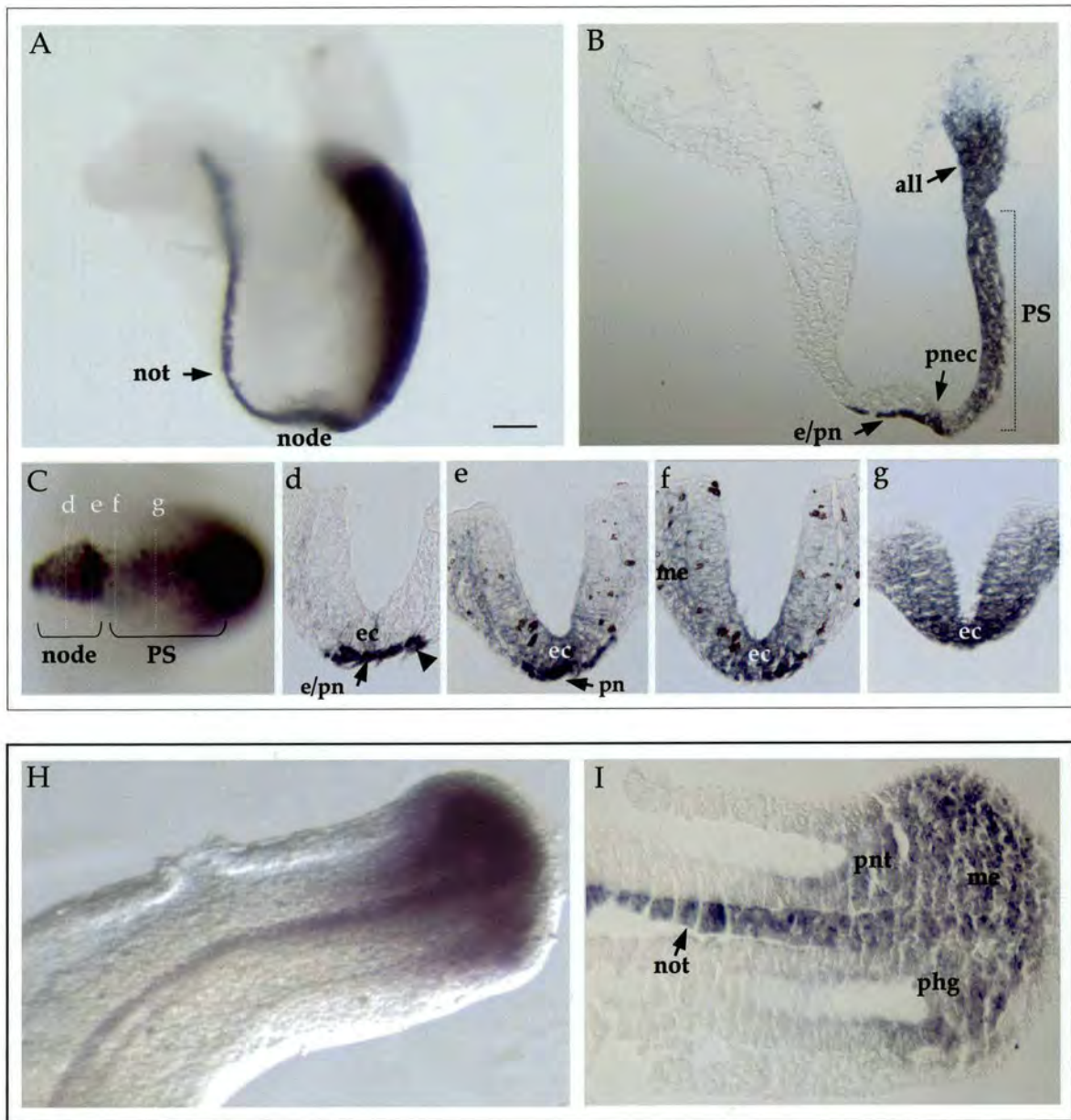
Figure 2.2 *T* expression at 8.5 dpc and 10.5 dpc

A) Lateral view of an 8.5 dpc embryo. **B)** Sagittal section through embryo in A. **C)** posterior dorsal view of an 8.5 dpc, showing expression in the node and primitive streak. **d-g)** transverse sections of embryo in C. **d)** anterior node, **e)** posterior node, **f)** anterior PS, **g)** PS. Arrowhead in d) marks a group of *T* expressing cells that also express *Nodal*. **H)** Lateral view of the end of the tail of a 10.5 dpc embryo. **I)** Sagittal section through tail in H. not: notochord, e: endoderm, pn: pre-notochordal cells, all: allantois, pnec: posterior node ectoderm, PS: primitive streak, ec: ectoderm, me: mesoderm, pnt: posterior neural tube, phg: posterior hindgut. Anterior is to the left. Bar: 100μm in A, B, C, H; 60μm in d, e, f, g; and 75μm in I.

72
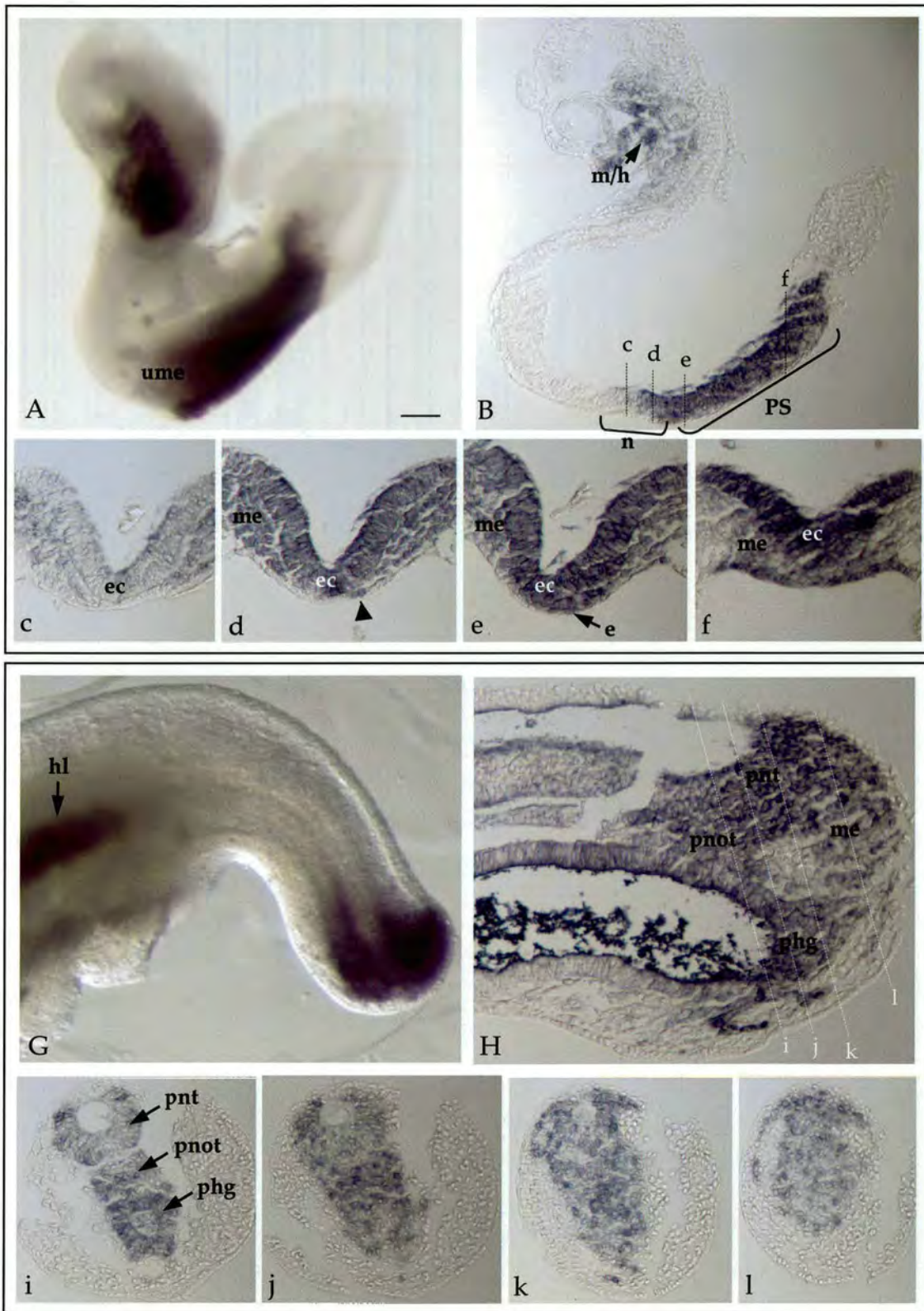
Figure 2.3 *Fgf8* **expression at 8.5 dpc and 10.5 dpc**
A) Lateral view of an 8.5 dpc embryo. B) Sagittal section through embryo in A. c-f) transverse
sections of an 8.5 dpc embryo. c) anterior node, d) posterior node, e) anterior PS, f) posterior PS.
Arrowhead in d) marks a group of *Fgf8* expressing cells that also express *Nodal*. G) Lateral view of
the end of the tail of a 10.5 dpc embryo. H) Sagittal section through tail tip in G. i-l) transverse
sections through a 10.5 dpc embryo at the levels marked in H. ume: unsegmented paraxial
mesoderm, n: node, PS: primitive streak, ec: ectoderm, me: mesoderm, e: endoderm, hl: hindlimb
bud, pnt: posterior neural tube, pnot: posterior notochord, phg: posterior hindgut. Anterior is to
the left. Bar: 100μm in A, B; 60μm in c, d, e, f, H; 150μm in G; and 86μm in i, j, k, l.

Cdx2

Cdx2 is expressed in the ectodermal and mesodermal layers of the primitive streak as *T* and *Fgf8* (Fig. 2.1 b1, b2). *Cdx2* mRNA was expressed in both layers of the node as well as the mesoderm immediately adjacent to it. Unlike *T* and *Fgf8, Cdx2* transcripts were expressed in both anterior and posterior node ectoderm (Fig. 2.4 F, G). At this stage, *Cdx2* transcripts can also be observed in the unsegmented paraxial mesoderm and the hindgut (Fig. 2.4 A, B). At tail bud stages, *Cdx2* is expressed in all the gut endoderm and in all the tissues at the posterior end of the tail: the posterior neurectoderm, notochord, unsegmented paraxial mesoderm and tail bud mesoderm (Fig 2.4 F, G; Fig. 2.1 b3-b6). The anterior limit of expression of *Cdx2* in the neural tube and notochord seems to expand further than that of *T* and *Fgf8* (compare tail bud staining in Fig. 2.4 F and Fig. 2.3 G, Fig 2.2 H). *Cdx2* transcripts are expressed in decreasing intensity from dorsal to ventral in the newly formed unsegmented mesoderm (Fig. 2.4 h-k).

Evx1 and *Wnt3a* are expressed in a complementary domain to *Foxa2*

Wnt3a and *Evx1*

Wnt3a and *Evx1* are expressed in the ectodermal and mesodermal layer of the primitive streak and in the unsegemented paraxial mesoderm at 8.5 dpc (Fig. 2.5 A; Fig. 2.1 d1, d2; Fig. 2.6 B). These two genes are also expressed in a similar manner to *T* and *Fgf8* in the node ectoderm: posterior but not anterior node expresses the gene (Fig. 2.5 A; Fig. 2.6 B). In the tail bud *Wnt3a* and *Evx1* transcripts are expressed at the tail tip: in the most posterior region of the neurectoderm and tail bud mesoderm (Fig. 2.5 F, G; Fig. 2.6 D,F; Fig. 2.1 d3-d6). In the neurectoderm the anterior domain of *Evx1* expands more anteriorly than that of *Wnt3a* (compare posterior neurectoderm in Fig. 2.5 G and Fig. 2.6 in F). At early and late stages *Wnt3a* mRNA is also seen in the cells of the roof of the spinal cord along the axis (Fig. 2.5 C, F).

74
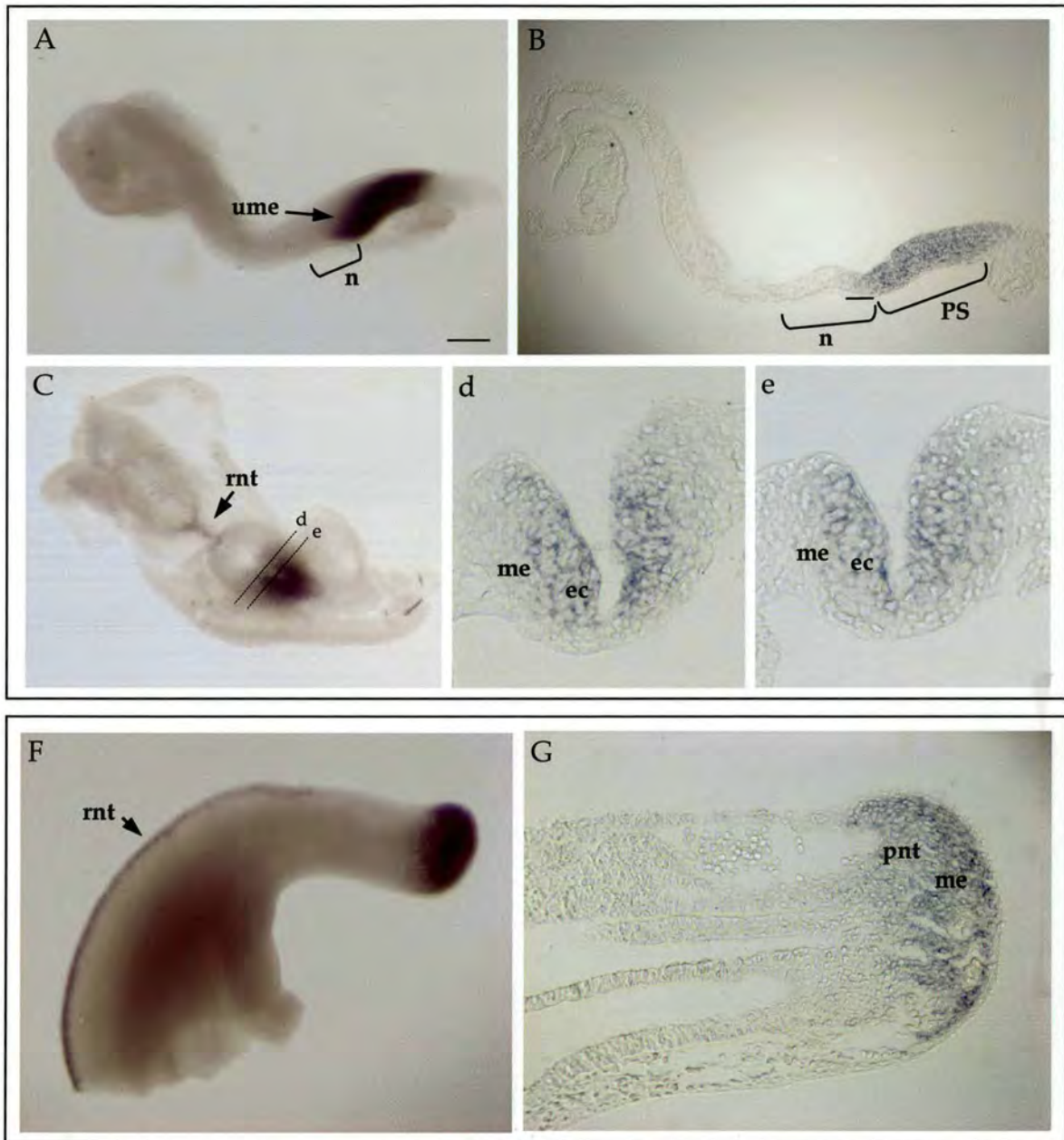
Figure 2.5 *Wnt3a* expression at 8.5 dpc and 10.5 dpc
A) Lateral view of an 8.5 dpc embryo. **B)** Sagittal section through embryo in A. Bar in B marks the extent of the posterior part of the node. **C)** Dorsal view of an 8.5 dpc. **d, e)** transverse sections of embryo in C. **d)** posterior node, **e)** primitive streak. **F)** Lateral view of the end of the tail of a 10.5 dpc embryo. **G)** Sagittal section through tail tip in F. ume: unsegmented paraxial mesoderm, n: node, PS: primitive streak, rnt: roof of the neural tube, ec: ectoderm, me: mesoderm, pnt: posterior neural tube. Anterior is to the left. Bar: 150μm in A; 100μm in B; 300μm in C; 38μm in d, e; 250μm in F; and 75μm in G.
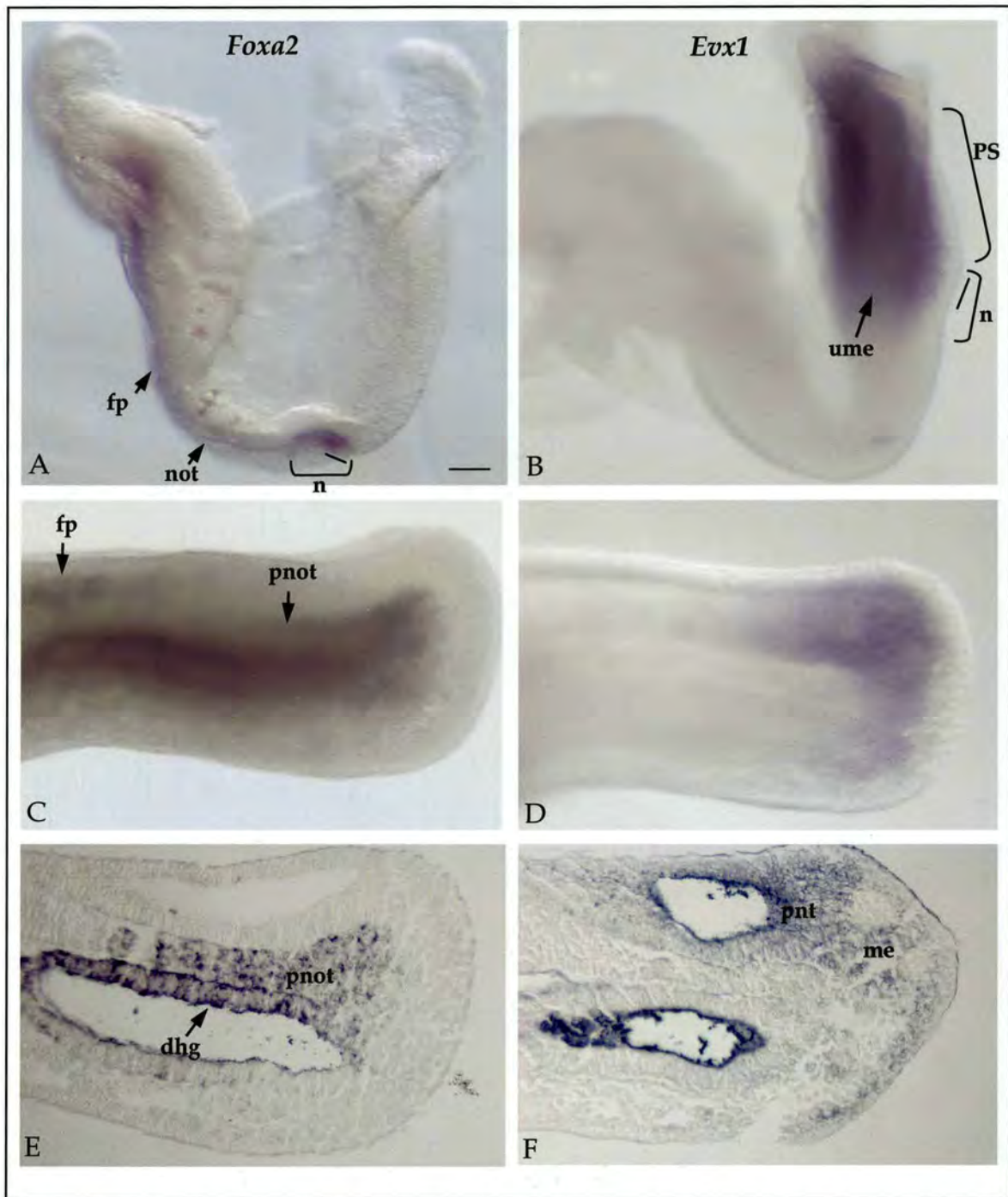
Figure 2.6 Complementary domains of expression of *Foxa2* and *Evx1* at 8.5 dpc and 10.5 dpc

A-B) Lateral view of an 8.5 dpc embryo expressing *Foxa2* and *Evx1*, respectively, showing complementary domains of gene expression. *Foxa2* is express in the node and the notochord, whereas *Evx1* is expressed as *Wnt3a* in the primitive streak. Bar in A, B mark extent of the posterior part of the node. **C-D)** Lateral view of the end of the tail of a 10.5 dpc embryo expressing *Foxa2* and *Evx1*, respectively. *Foxa2* is expressed in the posterior notochord and dorsal hindgut, whereas *Evx1* is express in the posterior-most neural tube and tail bud mesoderm. **E-F)** Sagittal sections through the tail tips in C and D, respectively. not: notochord, n: node, PS: primitive streak, ume: unsegmented paraxial mesoderm, fp: floorplate, pnot: posterior notochord, dhg: dorsal hindgut, pnt: posterior neural tube, me: mesoderm. Anterior is to the left. Bar: 86μm in A, B; 75μm in C, D; and 67μm in E, F.

Foxa2

Foxa2 is expressed in the ventral layer of the node and its derivative, the newly formed notochord (Fig. 2.6 A; Fig. 2.1 e1, e2). It is also expressed in the floorplate just anterior to the end of this notochord domain by 8.5 dpc (Fig. 2.6 A). At tail bud stages, *Foxa2* continues to be expressed at the posterior end of the notochord and the floorplate just anterior to the end of this notochord expression domain and in the dorsal gut (Fig. 2.6 C, E; Fig. 2.1 e3-e7).

Therefore, *Wnt3a* and *Evx1* are expressed in complementary domains to *Foxa2* in the primitive streak and tail bud.

Nodal is expressed in clusters of cells surrounding the node

Nodal

In the head-fold stage (7.5 dpc), *Nodal* mRNA is expressed in the node up to its caudal-most extent in two very small domains on each side of the prospective notochord cells inserted in the endoderm layer (Fig. 2.1 g1). These two domains seem to include both mesodermal and endodermal cells. By early somite stage, *Nodal* mRNA expression has become markedly asymmetrical, with more intense staining seen on the left (Fig. 2.1 g2; Fig. 2.7 A-e). By this stage, transcripts can also be seen in an asymmetric domain confined to a subpopulation of lateral mesoderm cells on the prospective left side of the embryo (data not shown), which has been associated to the role of *Nodal* in defining left-right asymmetry (Collignon *et al.* 1996; Lowe *et al.*, 1996, Tabin and Vogan, 2003). By 9.0 dpc, *Nodal* expression has disappeared and no expression is observed in the tail bud (Fig. 2.1 g3-g7; Fig. 2.7 F-h).

Interestingly, *T* and *Cdx2* are also strongly expressed in these mesodermal domains in both sites of the node region (arrowheads in Fig. 2.2 d, and Fig. 2.4 d), while *Fgf8* is also expressed in the same cells at the caudal-most region of the node (Fig. 2.3 arrowhead in d).

Sox1-GFP is expressed in the neurectoderm all along the axis and the mesoderm of the tail.

Sox1 mRNA

Sox1 mRNA is expressed in the anterior neurectoderm at 8.5 dpc (Fig. 2.8 A; Fig. 2.1 f2), its most posterior domain of expression being the anterior part of the node (compare node ectoderm in Fig. 2.8 e and f). By tail bud stages, Sox1 transcripts continue to be expressed in all the axial neurectoderm (Fig. 2.8 H-m; Fig. 2.1 f3-f7). In the tail bud, the intensity of expression decreases in the most posterior neurectoderm, and sagittal sections show that it is very low in the tail bud mesoderm (Fig. 2.8 J-m).

Sox1-GFP

Ying *et al.* (2003) showed that mice carrying the targeted insertion of GFP in the Sox1 locus overall reflected Sox1 mRNA expression. Sox1-GFP is expressed in the most anterior neurectoderm at 8.5 dpc, as seen by RNA *in situ* hybridisation (Fig. 2.9 B′). In the primitive streak very low expression was barely detectable (Fig. 2.9 B′). However, at tail bud stages, Sox1-GFP expression in the most posterior neurectoderm is as strong as the rest of the neurectoderm and a distinct, though lower intensity domain of expression is seen in the tail bud mesoderm (Fig. 2.9 C, F, I).

Interestingly, transverse sections of the tail bud of 9.5-11.5 dpc Sox1-GFP mice revealed expression in single cells or small clusters either continuous with the ventral neural tube or separated and intermingled with the partially condensed notochord territory. These appear at either side of the ventral neural tube and are similar in staining intensity to neurectoderm rather than the GFP expression in the tail bud mesoderm (Fig. 2.9 arrowheads in D, H, K).

ESC markers of pluripotency and self-renewal are not expressed in the mouse tail bud

Oct-3/4

Oct-3/4 is initially expressed in all blastomeres of the developing embryo, later gene expression becomes restricted to the inner cell mass (ICM), and is downregulated at gastrulation in an anterior-posterior
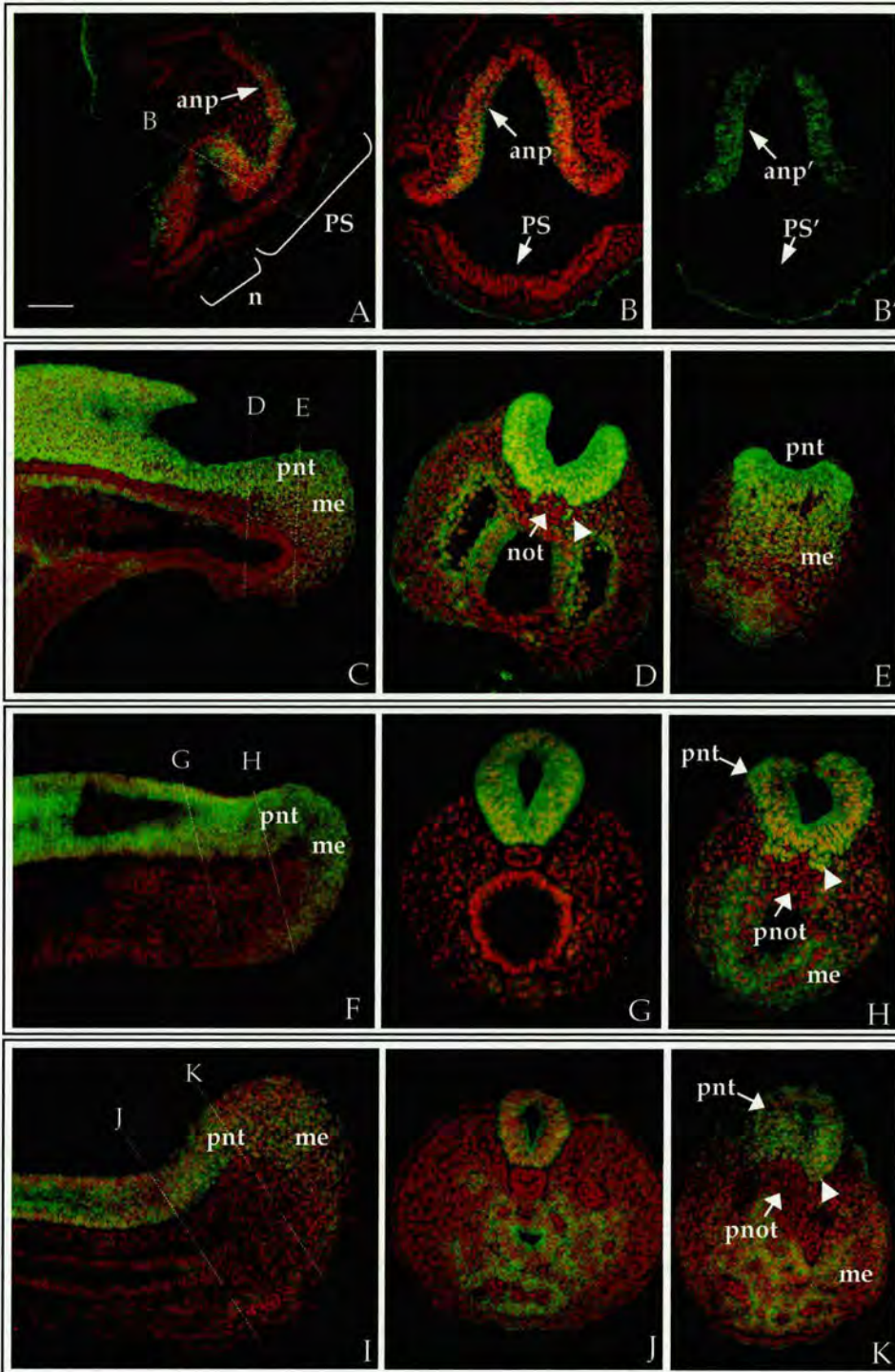
Figure 2.9 Confocal images of *Sox1*-GFP expression from 8.5 dpc to 11.5 dpc
A) Sagittal section of an 8.5 dpc embryo. B-B') Transverse section of an 8.5 dpc embryo at the level mark in A. B) shows *Sox1*-GFP expression in green and the cell counter TO-PRO-3 expression in red, whereas B') shows only *Sox1*-GFP expression, expression is high in the anterior neural plate but barely detectable in the primitive streak. C) Sagittal section through the tail of a 9.5 dpc embryo. D-E) Transverse sections through the tail tip of a 9.5 dpc embryo at the level marked in C. F) Sagittal section through the tail of a 10.5 dpc embryo. G-H) Transverse sections through the tail tip of a 10.5 dpc embryo at the level marked in F. I) Sagittal section through the tail of a 11.5 dpc embryo. J-K) Transverse sections through the tail tip of a 11.5 dpc embryo at the level marked in I. Note in C-K *Sox1*-GFP expression can be seen in the posterior neurectoderm, as expected, and also in the contiguous tail bud mesoderm, which might result from the slow decay of the GFP protein. Arrowheads in D,H,K mark a *Sox1*-GFP positive population of cells in the notochord. PS: primitive streak, n: node, anp: anterior neural plate, pnt: posterior neural tube, me: mesoderm, not: notochord, pnot: pre-notochordal cells. Anterior is to the left. Bar: 150µm in A; 100µm in B, B'; 120µm in C, F, I; and 86 µm in D, E, G, H, J, K.

pattern (Nichols *et al.*, 1998). By 8.5 dpc, *Oct-3/4* transcripts can be detected by *in situ* hybridisation at the anterior neurectoderm and the ectodermal layer of the primitive streak and node (Fig. 2.10 A, B; Fig. 2.1 h2). Cells expressing *Oct-3/4* in the ectoderm seem to be situated in the dorsal part of this tissue (Fig. 2.10 d-f). *Oct-3/4* is also expressed in the primordial germ cells (PGCs) situated at the base of the allantois at this stage (Fig. 2.10 g; Fig. 2.1 inset in h2). By 9.0 dpc, the gene has been switched off in the ectoderm. Therefore, no expression could be seen in the tail bud (Fig. 2.10 H, I; Fig. 2.1 h3-h7)). Only the PGCs, which migrate through the gut from 9.5 dpc until 10.5 dpc express *Oct-3/4* (Fig. 2.10 H; Fig. 2.1 arrowheads in h3 and h4).

Nanog

Nanog is expressed firstly in the inner cells of the morula prior to blastocyst formation, then is restricted to the cells of the ICM of the blastocyst. *Nanog* transcripts are no longer detectable at implantation. Expression reappears in the proximal epiblast at 6 dpc and remains restricted to the epiblast as development progresses (Fig. 2.1 i1). Expression is lost as the cells enter the streak and differentiate to form mesoderm (Chambers *et al.*, 2003; Mitsui *et al.*, 2003). By 8.5 dpc, expression in the ectodermal layer of the primitive streak has been lost, *Nanog* transcripts can only be seen in the isthmus (Fig. 2.11 A, B; Fig. 2.1 i2) and the PGCs (data not shown). No expression can be detected in the tail bud (Fig. 2.11 C, D; Fig. 2.1 i3-i7).

Towards the end of axial elongation, tail bud gene expression decreases drastically

Strong tail bud expression of *Wnt3a*, *Fgf8*, *T* and *Cdx2* is continuous from primitive streak stages to the tail bud (Fig. 2.1 a1-a7, b1-b6, c1-c6, d1-d6). However, from 10.5 dpc to 11.5 dpc, a noticeable decline in the expression of *Wnt3a* and *Fgf8* was observed (compare Fig. 2.1 c4, d4 with c5, d5, respectively). From 11.5 dpc to 12.5 dpc, a major decrease in expression was observed in *Cdx2*, *Wnt3a* and *Fgf8* transcripts (compare Fig. 2.1 b5, c5, d5 with b6, c6, d6, respectively). On the other hand, the *T*
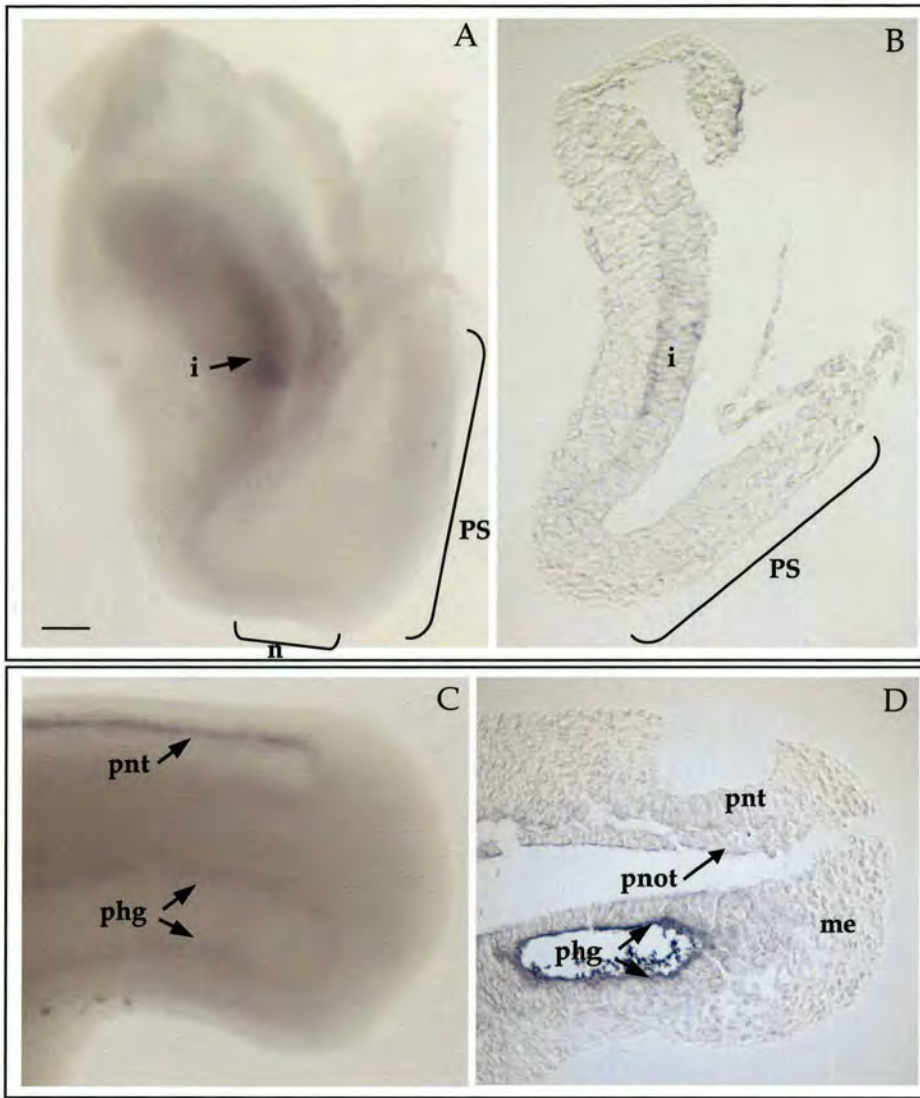
Figure 2.11 *Nanog* expression at 8.5 dpc and 10.5 dpc
A) Lateral view of an 8.5 dpc embryo. B) Sagittal section through an 8.5 dpc embryo, showing expression in the isthmus. C) Lateral view of the end of the tail of a 10.5 dpc embryo. D) Sagittal section through the tip of the tail in C. Note the trapping inside the neural tube in C and the hindgut in C and D. i: isthmus, n: node, PS: primitive streak, pnt: posterior neural tube, phg: posterior hindgut, pnot: posterior notochord, me: mesoderm. Anterior is to the left. Bar: 75μm in A, B, C, D.

expression remains high at 12.5 dpc, and is reduced only just prior to the end of axis elongation at 13.5 dpc (compare Fig. 2.1 a5, a6 with a7).

Wnt3a and Fgf8 are expressed in the most posterior neurectoderm and tail bud mesoderm at 10.5 dpc (Fig. 2.1 c4, d4). By 11.5 dpc expression has slightly declined, and it is strongly seen in the most posterior neurectoderm and the most adjacent mesoderm (Fig. 2.1 c5, d5). By 12.5 dpc, Wnt3a and Fgf8 domains of expression have reduced drastically, and their expression seems to be restricted to the most posterior neurectoderm and newly formed mesoderm just adjacent to it (Fig. 2.1 c6, d6). The Fgf8 domain is smaller than that of Wnt3a, and might be restricted just to the neurectodermal layer (compare gene expression domain in Fig. 2.1 c6 with d6). By 13.5 dpc their domains are further reduced and in some embryos are not seen (Fig. 2.1 c7, d7, d7').

Cdx2 is expressed in all tissues of the tail by 10.5 dpc, with its anterior domain expanding more anteriorly than T, Wnt3a and Fgf8 (compare domains of expression in Fig. 2.1 b4 with c4, d4). Cdx2 continues to be expressed in a similar manner by 11.5 dpc (Fig. 2.1 b5). However, by 12.5 dpc its expression becomes considerably reduced to a domain in the most posterior newly formed mesoderm and the roof of the most posterior neurectoderm (Fig. 2.1 b6). By 13.5 dpc, no expression was detectable by in situ hybridisation (Fig. 2.1 b7).

On the other hand, T transcripts are expressed in all the tissues of the tail by 10.5 dpc and continue until 12.5 dpc (Fig. 2.1 a4-a6). By 13.5 dpc, its expression becomes restricted to the end of the newly formed notochord and the mesoderm adjacent to it (Fig. 2.1 a7).

2.4 DISCUSSION

Continuous regions of gene expression from PS and tail bud are conserved among different vertebrates

In the present gene expression analysis, I have found that transcripts of genes known to play a role in axis elongation such as T (Brachyury), Fgf8 and Wnt3a are expressed from gastrulation stages and during tail elongation, as are the homologues of genes expressed in the Xenopus tail such as Evx1 (Xhox3), Foxa2 (Pintallavis) and Cdx2 (Xcad3) (Fig.

2.1). This gives further support to the idea that, as previously shown in other vertebrates, tail bud formation in the mouse is a continuation of gastrulation, as both processes are controlled by similar gene expression. Moreover, I have shown that the primitive streak and tail bud are regionalised, and these domains of gene expression are consistent with previous fate maps marking different cell populations (Wilson and Beddington, 1996).

Next, it was interesting to find out if these different domains of gene expression of the early blastopore/primitive streak and tail bud of *Xenopus* and chick were conserved in mouse. As described in the general introduction, Gont *et al.* (1993) compared the expression of two markers: *Xnot2* and *Brachyury*. *Xnot2* is expressed in the dorsal lip of the blastopore, while *Brachyury* is expressed in the entire blastoporal ring (stages 10.5-13). In the developing tail, *Xnot2* is expressed in a U-shaped region, which consists of the posterior ventral spinal cord and posterior notochord as well as the region of continuity between these two tissues. The latter region was designated the chordoneural hinge (CNH) by Pasteels (1943). The expression of *Xnot2* in the posterior notochord weakens as the tail develops. *Brachyury* transcripts are found more broadly: in the posterior notochord, the CNH, the roof of the spinal cord and posterior wall (see Fig. 1.2 of the introduction).

In chick, Knezevic *et al.*, performed a similar analysis using *Ch-T* (homologue of *Xbra*) and *Gnot1*, a homologue of the *Xenopus* Xnot genes: *Xnot2*, just mentioned and described by Gont *et al.* (1993) and *Xnot*, a gene described by Von Dassow *et al.*, in the same year that has a 90% identical amino acid sequence to *Xnot2* (Von Dassow *et al.* 1993). *Xnot* and *Xnot2* are expressed in the same tissues at early and late stages. The chick *Gnot1* is expressed in equivalent tissues to the ones in *Xenopus*: Hensen's node, which is the equivalent to the dorsal blastopore and in the newly formed notochord, at gastrulation stages; and the CNH region at tail bud stages. The CNH in chick was described as the point where caudal neural tube and notochord unite and it is located between the residual Hensen's node (*Gnot1* and *Ch-T* positive) and primitive streak (*Ch-T* positive), which would be equivalent to the posterior wall in *Xenopus*. *Ch-T* is expressed in

a much broader manner: the node, notochord, primitive streak at gastrulation stages and all nascent mesoderm in the tail bud are positive (see Fig. 1.3 of the introduction). Therefore, similar regions to the ones in *Xenopus* can be described by gene expression in chick: the node and its descendant the CNH expressing both *Ch-T* and *Gnot1* on one hand, and the primitive streak and its descendant the tail bud mesoderm, expressing only *Ch-T*. However, the most posterior ventral spinal cord in the tail bud, which was positive for *Xnot2* but negative for *Xbra* in *Xenopus*, is negative for *Gnot1* and positive for *Ch-T* in chick (Kispert *et al.*, 1995; Knezevic *et al.*, 1998). Moreover, as we mentioned above, the roof of the spinal cord expresses *Xbra* in *Xenopus*, whereas no *Ch-T* expression was observed in this region in chick. Therefore, the most posterior neurectoderm at tail bud stages, seems to be a point of discrepancy between these two organisms.

At the time of choosing our markers, the *Not* gene had not been described in the mouse, but it has been subsequently published. *Not* expression in the mouse resembles that of the chick and *Xenopus*: it is expressed in the node and notochord at primitive streak stages and continues to be expressed in the posterior notochord and CNH in the tail bud (Plouhinec *et al.*, 2004; Abdelkhalek *et al.*, 2004). *T* is expressed more broadly: in the node, notochord and primitive streak at early stages and continues in the CNH, notochord and tail bud mesoderm in the tail bud (Fig 2.2). Similarly to chick but different from *Xenopus*, the mouse most posterior ventral neurectoderm is positive for *T* and negative for *Not* at tail bud stages.

Therefore, similar regions to the ones in *Xenopus* and chick can be described by gene expression in mouse. Furthermore, in the chick embryo the comparison of *Gnot1* and another Tbox gene *Ch-Tbx6L* showed that these two genes were expressed in complementary domains at early and late stages. As described above, *Gnot1* is expressed in the node and notochord at gastrulation stages, while *Ch-Tbx6L* is expressed in the primitive streak and segmental plate. In the tail, *Gnot1* is expressed in the recently formed notochord and the CNH, whereas *Ch-Tbx6L* is expressed in the tail bud mesoderm and segmental plate.

In mouse, a similar segregation of node and primitive streak-derived cells was seen when looking at different markers: *Foxa2* is expressed as *Not*, in the recently formed notochord and node (Fig. 2.6; Plouhinec *et al.*, 2004; Abdelkhlek *et al.*, 2004); whereas *Evx1* and *Wnt3a* are expressed as *Tbx6*, the homologue of the gene *Ch-Tbx6L* in mouse, in the primitive streak and segmental plate (Fig. 2.5; Fig. 2.6; Chapman *et al.*, 1996). In the tail bud, *Foxa2* is expressed at the end of the notochord and in the CNH, whereas *Evx1, Wnt3a* and *Tbx6* are expressed in the surrounding tail bud mesoderm and segmental plate. The distribution of these markers in the tail bud compared to their distribution at gastrulation stages suggest a direct continuity of different cell lineages and conservation of spatial relationships between cells of different origin, conserved in the different vertebrates.

Gene expression domains in the mouse do not always match the domains in *Xenopus*

As described above for the roof and floor of the spinal cord, not all the gene expression domains described for the *Xenopus* tail bud coincide with that of the mouse.

Evx1 is the mouse homologue of the *Xenopus* homeobox gene *Xhox3*. *Xhox3* has two different periods of expression: during the early period (gastrula and neurula stages) transcripts are found in a graded fashion along the anteroposterior (AP) axis in the mesoderm and are most concentrated at the posterior pole. The late period begins at the tail bud stage (stage 27) and is characterised by new expression of *Xhox3* in the central nervous system and in the most distal cells of the posterior wall in the tail bud (see Fig. 1.2 bottom panel of the introduction; Ruiz i Altaba, 1989). This late expression in the tail bud is reported to represent a new site of activation of the gene (Ruiz i Altaba, 1989; Beck and Slack, 1998) and seems to be associated with the mechanism of the tail bud outgrowth (Beck and Slack, 1999). In contrast, in the mouse embryo, *Evx1* is expressed continuously from gastrulation to tail bud stages, where its expression is much broader than that of the *Xenopus* tail bud. It is

expressed in the most posterior neurectoderm and tail bud mesoderm (Fig. 2.6 D, F).

Lhx1 (Lim1) is the mouse homologue of the *Xenopus* homeobox factor *Xlim1* (Taira *et al.*, 1992). In *Xenopus Xlim1* is expressed in the dorsal blastopore lip and in the notochord at the end of gastrulation, and is maintained at later stages in the posterior tip of the differentiated notochord and in the CNH (see Fig. 1.2 top panel of the introduction). In contrast, in the mouse *Lhx1* is an early organizer specific gene needed for proper cell movement during gastrulation (Hukriede *et al.*, 2003). *Lhx1* is only expressed during gastrulation. By 8.5 dpc its expression has declined and no expression is detected in the tail bud by *in situ* hybridisation (Shawlot and Behringer, 1995; Barnes *et al.*, 1994). We confirmed these results by *in situ* hybridisation (data not shown).

Wnt3a is the mouse homologue of *the Xenopus Xwnt3a. Xwnt3a*, as described by Beck and Slack (1998) is expressed in a novel domain in the dorsal roof domain of the tail bud by stage 27, which corresponds to the future tip of the tail bud (see Fig. 1.2 bottom panel of the introduction; Beck and Slack, 1998). In contrast, in the mouse tail bud, *Wnt3a* is expressed in the posterior end of the neurectoderm and the newly formed tail bud mesoderm. This tail bud expression marks a much broader domain than the one described for the *Xenopus* tail bud. At early and late stages *Wnt3a* mRNA is also seen in the cells of the roof of the spinal cord along the axis, but its posterior limit finishes before the tail bud, and therefore it does not match to the domain described in *Xenopus* (Fig. 2.5 F, G).

Three class V POU domain proteins: Xlpou25, Xlpou60, Xlpou91, have been described in *Xenopus* and are related to the mammalian Oct-3/4. These proteins can substitute for Oct-3/4, to a greater or lesser extent in maintaining ES cell self-renewal, with Xlpou91 giving the best rescue. Depletion using morpholino oligonucleotides in *Xenopus* results in reduction of the AP axis and gives anterior defects, which are more severe when the 3 proteins are depleted (Gillian Morrison, personal communication). Interestingly, two of these genes, *Xlpou25* and *Xlpou91*, are expressed in a region in the middle of the spinal cord at the tail tip as

the tail elongates (Cao *et al.*, 2004; Pollet *et al.*, 2005; Gillian Morrison, personal communication). In contrast, mouse *Oct-3/4* gene expression was not detected in the tail bud by *in situ* hybridisation (Fig. 2.10 H, I; Fig. 2.1 h3-h7). Oct-3/4 is the only class V POU protein known to be expressed in the embryo, only one other class V POU protein exists, Sperm1, only detected during spermatogenesis.

Xcad3 is the closest *Xenopus* CDX family member to *Cdx2*. At tail bud stages, *Xcad3* transcripts form a gradient in the neural tube with highest levels in the tail bud. It is also expressed in the posterior wall. However, interestingly, transcripts are absent from the notochord at tail bud stages. The CNH and the ventral neural tube are also negative, where *Xnot2* is expressed (see Fig. 1.2 bottom panel of the introduction; Beck and Slack, 1998). In contrast, in the mouse *Cdx2* is expressed in all tissues of the tail: expression is seen in the posterior notochord and neural tube, both dorsally and ventrally with its anterior limit extending further than that of *Fgf8* transcripts (Fig. 2.4 F-k).

Gene expression domains that led to the *Xenopus* model of tail bud outgrowth do not match those in mouse

Beck and Slack (1998) showed that a new wave of gene expression starts at stage 27 coinciding with the beginning of tail outgrowth in *Xenopus*. This gene expression study described 7 different domains in the *Xenopus* tail. Later, in 1999, Beck and Slack showed that some of these domains were needed functionally to come into contact to form a tail. In their model, the small region of overlap between *X-Notch-1* and *X-delta-1*, expressed together in the posterior wall, region M, and *lunatic fringe*, expressed in the dorsal roof of the neural tube, region N, corresponds to the junction between N and M territories in the posterior of the embryo, which defines the direction of tail outgrowth and turns on *Xhox3* in a subset of cells of the overlap region corresponding to the caudal tip, or most distal cells of the future tail bud. *Xwnt3a* expression also in the roof of the neural tube is required in addition to Notch signalling to restrict tail outgrowth to the posterior of the embryo (see Fig. 1.7 of the introduction). All these genes define strongly restricted domains in the *Xenopus* tail.

However, in the mouse, as described above, *Xhox3* homologue *Evx1* is expressed in a much broader domain than *Xhox3* and the same is true for *Wnt3a* gene compared with *Xwnt3a*. The Notch receptors: *Dll1* and *Dll3* are expressed broadly in the tail bud, but their contribution to the tail tissues has not been described in detail; the Notch ligands: *Notch1* and *Notch2*, and *lunatic fringe* seem absent from the tail bud or in the case of *Notch1* reported to be expressed broadly at very low levels. Instead, *Notch1* is expressed in the unsegmented paraxial mesoderm, whereas *Notch2* and *lunatic fringe* are expressed in the most recently formed somite (Koizumi *et al.*, 2001; Aulehla *et al.*, 2003; Wong *et al.*, 1997). Rather than inducing tail outgrowth, Notch signalling is required for in a number of processes during axis elongation in the mouse: *Notch1*, *Notch2*, *Dll3* and *lunatic fringe* regulate segmentation in mouse, as they apparently do in chick and *Xenopus* embryos (Jen *et al.*, 1999; Dale *et al.*, 2003; Conlon *et al.*, 1995; Zhang and Gridley, 1998), Notch signalling through the *Dll1* receptor is involved in controlling the decision between floor plate and notochord development. Notch activation expands the floor plate domain of *Shh* and *Pintallavis* and represses the notochordal markers *Chordin* and *Brachyury* in *Xenopus* (Lopez *et al.*, 2003; Lopez *et al.*, 2005) and a similar reduction in notochordal cells has been shown in mouse *Dll1* mutants (Przemeck *et al.*, 2003).

Therefore, the homologues of the genes needed for tail outgrowth in *Xenopus* are expressed in broader domains in the mouse tail or not expressed at all, showing no resemblance to the domains in *Xenopus*. From these results, it is unlikely that the model proposed for *Xenopus* tail outgrowth (Tucker and Slack, 1995b; Beck and Slack, 1998; Beck and Slack, 1999; Beck *et al.*, 2001) is also true for the mouse. Nevertheless, expression of the Notch family members remains to be described in detail in the mouse tail bud.

The present gene expression study complements that of Gofflot *et al.* (1997), which concentrated on the expression of genes just prior neuropore closure. Both studies show that gene expression in the mouse is a continuum from gastrulation to tail bud stages. No new expression of genes starts at the time of tail bud elongation as seen in the *Xenopus* tail.

Moreover, as I mentioned above, genes that are expressed in specific domains in the *Xenopus* tail tend to be expressed broadly in the mouse tail bud.

Interestingly, no change in gene expression was observed in the transition from primary to secondary neurulation, a process described in the chick. Together with the fact that these two processes are undistinguishable morphologically proposes the question whether they are indeed such distinct mechanisms in the mouse.

Three putative novel domains of expression were found in our analysis:

Fgf8, Cdx2, T and Sox1-GFP define a region of mesoderm production in the apparently undifferentiated tail tip

Fgf8, Cdx2 and *T* transverse sections through the tip of the tail reveal strong expression of these genes in the medial and dorsal regions of the extreme distal tail tip, and this domain is continuous with the rosette of the neural tube, the gut and the notochord (Fig. 2.3 i-l; Fig. 2.4 h-k). These genes are expressed continuously from the most posterior neurectoderm to the adjacent mesoderm, as seen by sagittal sections (Fig. 2.2 I; Fig. 2.3 H; Fig. 2.4 G). This pattern of expression is also seen in *Sox1-*GFP sagittal sections (Fig. 2.9 C, F, I). As described in the next chapter, cells in this region of the most posterior neurectoderm continue to undergo ectoderm to mesoderm transition, corresponding to the remnant of the primitive streak in the tail bud. Furthermore, lower *Cdx2* transcripts are found in gradually declining intensity from the most posterior neurectoderm to the adjacent mesoderm in the tail and from dorsal to ventral in the unsegmented paraxial mesoderm (Fig. 2.4 h-k). The differential intensity of gene expression observed from the neurectoderm to the mesoderm and towards the paraxial mesoderm resembles the movements undertaken by mesodermal cells described by Catala *et al.* (1995) and Knezevic *et al.* (1998) in the avian tail: somitic precursors after ingressing, first move posteriorly and turn ventrally in the distal tail bud, and then move laterally and anteriorly to contribute to newly formed segmental plate (see Fig. 1.5 bottom panel on the left of the introduction).

Cells surrounding the newly formed notochord express Nodal at primitive streak stages and Sox1-GFP at tail bud stages

Two genes, *Nodal* at early stages, and *Sox1* at tail bud stages are expressed in two domains, which morphologically seem very similar and might be related to one another. *Nodal* is expressed in the node at 8.5 in a few cells on each side of the pre-notochordal cells (Fig. 2.7 A-e). These two domains seem to include mesodermal and endodermal cells expressing also *Cdx2, T* and *Fgf8* (Arrowheads in Fig. 2.2 d; Fig. 2.3 d; Fig. 2.4 d). Together with the domain of *Nodal* expression in the lateral plate mesoderm, these domains are associated in defining left-right asymmetry in the mouse and they are conserved among vertebrates: *Nodal* related genes in *Xenopus* (*Xnr1*) and chick (*Cnr1*) are expressed in similar domains (Collignon *et al.*, 1996; Lowe *et al.*, 1996, Tabin and Vogan, 2003).

However, *Sox1*-GFP is also expressed in two domains at either side of the newly formed notochord from 9.5 dpc onwards (arrowheads in Fig. 2.9 D, H, K). These may either represent evidence of ventral neural tube contribution to the notochord, or may consist of static populations of cells. If the latter is the case, their location at either side of the posterior notochord would be ideal for a population of cells that are involved in the maintenance of the notochord or the CNH. These domains appear to be similar in staining intensity to the neurectoderm rather than the GFP expression in the tail bud mesoderm, presumed to have recently emerged from the ectoderm (compare Fig. 2.9 arrowhead in H with the adjacent tail bud mesoderm expression). In chick a similar *CSox1* expression domain has been described. However, Charrier *et al.* (2002) propose that this is due to the floor plate (*Csox1* negative in this organism) being inserted in the neural tube, although in their experiments there is little to support this hypothesis more than the others I have proposed above.

The most posterior region of the node has a different gene expression than the rest of this structure

Surprisingly, the most posterior region of the node ectoderm displays a different gene expression to the anterior part. At 8.5 dpc, it expresses *T, Fgf8, Wnt3a* and *Evx1* in the ectodermal layer, as the adjacent

primitive streak, whereas the anterior region is negative for these genes (compare node ectoderm in Fig. 2.2 d, Fig. 2.3 c, with Fig. 2.2 e, Fig. 2.3 d, respectively; Fig. 2.5 B; Fig. 2.6 B). *T* and *Foxa2* expression is also seen strongly in the ventral layer of this caudal region, which is known to contain precursors for the notochord (see Fig. 2.2 e; Fig. 2.6 A; Wilson and Beddington, 1996). Therefore, the posterior region of the node seems to represent a region of heterogeneous expression with closely apposing expression of genes characteristic of prospective notochord, and of prospective paraxial mesoderm. Furthermore, LacZ expression, in heterozygous mice carrying a *Nodal-LacZ* reporter allele, is observed specifically in this caudal region of the node, revealing a novel domain of *Nodal* expression not seen by RNA in situ hybridisation, which probably reflects the persistence of β-gal activity. It strongly suggests that some descendants of the *Nodal* expressing cell population are displaced caudally around the periphery of the node (Collignon *et al.*, 1996), and might imply a role of *Nodal* in the regulation of mesoderm production in this region around the node, as initially proposed by Zhou *et al.* in 1993. Therefore, it would be very interesting to know in which layer of the posterior node the *Nodal* descendants become incorporated. Interestingly, the homeobox gene *Lhx1* is also expressed in this region of the caudal node between 7.5 dpc and 8.5 dpc (Barnes *et al.*, 1994). *Lhx1* expression resembles that of *Nodal-LacZ*, as it is also seen in the cells surrounding the middle part of the node. It would be interesting to know if both domains coexpress.

Interestingly, the descendant of the node in the tail bud, the CNH (described in the next chapter), expresses similar genes to that of the posterior node: its ectodermal layer also expresses *T, Fgf8, Wnt3a* and *Evx1*, whereas the underlying posterior notochord expresses *T* and *Foxa2*.

I will discuss the implications of this analogous gene expression in these two structures, posterior node and CNH, together with the results of grafting experiments trying to locate the axial progenitors in Chapter 3 and 4.

Arrest of axial elongation coincides with the decrease of gene expression in the tail

Axial elongation stops in the mouse at 13.5 dpc, when the tip of the tail bud and the most posterior tissues formed are thought to die by apoptosis (Nievelstein *et al.*, 1993). However, the mechanism by which tail elongation arrests and the genes involved in this process remains to be described. In the present study, tails from 11.5 dpc until 13.5 dpc were included, aiming to see if there were changes in gene expression patterns and levels as tail elongation comes to an end. Genes known to be important for axis elongation like *Wnt3a, Fgf8, Cdx2* and *T* are expressed broadly until 10.5 dpc. By 11.5 dpc, *Wnt3a* and *Fgf8* expression has started to decline. However, the most drastic decrease in the domains of gene expression of *Wnt3a, Fgf8* and *Cdx2* is seen from 11.5 dpc to 12.5 dpc, whereas *T* expression continues until 13.5 dpc, although by this stage its domain of expression is reduced to the most posterior end of the notochord and adjacent mesoderm (Fig. 2.1). It has been previously described that cells in the notochord lacking Brachyury (T) protein die by apoptosis (Chesley, 1935). Kispert and Herrmann (1994) after studying T protein expression in wild-type and mutant embryos proposed that somitic mesoderm formation in the tail might require less T activity than notochord formation (Kispert and Herrmann, 1994). However, in notochordless tails, the neural tube, gut, and somites, which are initially formed from the tail bud, disintegrate. This may be due to a lack of signalling from the notochord or insufficient T activiy in cells forming somitic mesoderm, or both (Kispert and Herrmann, 1994). Therefore, decreasing levels of T in the notochord and mesoderm of the 13.5 tail tip might be the cause of axial elongation arrest and death.

However, the fact that *Wnt3a* and *Fgf8* expression in the tail bud starts to decline almost two days before *T* expression, presents a paradox. Ciruna and Rossant (2001) showed that Fgf signalling through *Fgfr1* is needed for appropriate Wnt signalling, which in turn is needed for *T* function in the primitive streak but not in the node. Therefore, *T* needs Fgf and Wnt signalling to function. *Fgfr1, Fgf8, Wnt3a* and *T* mutants all share in common defects in cell adhesion and migration of cells in the primitive

streak. Mutant cells do not migrate and accumulate in the primitive streak, due to a failure of epithelial to mesenchymal transformation, in the place of mesoderm, neural tissue is produced (Ciruna *et al.*, 1997; Ciruna and Rossant, 2001; Sun *et al.*, 1999; Takada *et al.*, 1994; Yoshikawa *et al.*, 1997; Yamaguchi *et al.*, 1999b). These authors showed that this is due to a failure in *Fgfr1* mutants to activate *Snail*, which is needed to repress E-cadherin levels, to allow the release of free β-catenin, which can then enter the nucleus and allow appropriate Wnt signalling to occur by activating *T*, which in turn activates *Tbx6* and allows correct paraxial mesoderm formation (Ciruna and Rossant, 2001). Therefore, by 12.5-13.5 dpc, other gene family members might be compensating for the loss of *Fgf8* and *Wnt3a* expression, to maintain *T* expression in the tail bud.

Although *Fgf8* is been proposed to be important for survival and proliferation of the tail bud progenitors during axial elongation, as its transcripts are specifically expressed in the chick tail bud, and cells differentiate as they move away from its domain of expression (Dubrulle and Pourquié, 2004), other Fgf genes are also known to be expressed in the tail bud: *Fgf3, Fgf4, Fgf9, Fgf15, Fgf16, Fgf17, Fgf18* (Wilkinson et al., Niswander and Martin, 1992; McWhirter *et al.*, 1997; Maruoka *et al.*, 1998; Colvin *et al.*, 1999; Yamaguchi *et al.*, 1999b; Goldman *et al.*, 2000). However, their expression at these late stages of tail development needs to be further investigated.

In the case of Wnt signalling *Wnt3a* is the prime candidate to assure continued *T* expression, as *Wnt3a* hypomorphs have a *T*-like defect (Heston, 1951; Gruneberg, 1957, 1974). However, another Wnt family member, *Wnt5a*, is expressed in a similar manner to *Wnt3a* in the primitive streak and tail bud. Furthermore, Yamaguchi *et al.* (1999a), showed that *Wnt5a* might be involved in regulating proliferation of the progenitor cells in several structures, including the primitive streak and its descendant the tail bud. More importantly, *Wnt5a* does not appear to signal via the canonical β-catenin dependent signalling pathway in a zebrafish assay (Slusarski *et al.*, 1997). *Wnt5a* is expressed in the tail bud until 13.5 dpc, when axis elongation stops. *Wnt5a* null homozygote mice lack a tail and have progressively severely reduced somite size in the axis and lack sacral

and tail vertebrae. Therefore, other mechanisms in conjunction with Ciruna and Rossant's model might insure appropriate tail elongation. Interestingly, *Wnt5a* might be downstream of Hox genes (Yamaguchi *et al.* 1999a).

The Hox cluster genes such as *Hoxb13*, have also been implicated in cell proliferation and survival of progenitor cells. Economides *et al.* (2003) showed that the most 5' gene in the HoxB cluster, *Hoxb13*, might act as an inhibitor of cell proliferation and an activator of programmed cell death in the tail, thereby setting up a chain of events leading to cessation of tail outgrowth. *Hoxb13* expression starts around 10.5 dpc in the most posterior regions of the developing embryo, in the neural tube and tail bud mesoderm. While many Hox mutations result in loss of structures, *Hoxb13* null homozygous mice show longer and thicker tails with longer and wider spinal cord and overgrowth in vertebrae, probably due to an increase in cell proliferation and decreased level of apoptosis. The authors compared the expression of *Wnt3a* in wild-type and mutant *Hoxb13* embryos and found no difference in the level of expression of this gene. But the relationship between *Hoxb13* and *Wnt5a* remains to be studied. However, this increase in cell proliferation observed in *Hoxb13* mutants is general for the whole tail, and not specific for the tail bud progenitors.

Finally, another gene suggested to be involved in controlling apoptosis is *Shh*, which is expressed in the notochord and floor plate. In chick, the neural tube dies by apoptosis, on experimental blockage of notochord and floor plate formation by excision of the axial-paraxial hinge at the 6-somite stage (Charrier *et al.*, 1999). However, neural tube formation can be rescued by adding cells producing *Shh* a day later, when dramatic apoptosis is already present (Charrier *et al.*, 2001). Therefore, this gene is needed in the spinal cord for survival of the neuroepithelial cells. *Shh* anti-apoptotic function is accomplished by blocking the signal of its own receptor *Patched (Ptc)*, which in absence of *Shh* induces apoptotic cell death (Thibert *et al.*, 2003). Therefore, arrest of tail bud outgrowth, could also be related with a decrease of Shh activity. This remains to be investigated further.

'Stemness' genes are not expressed in the mouse tail

The observation of different domains of gene expression in the tail bud of the different vertebrates shows that the cells of the tail bud cannot all constitute a blastema of undifferentiated cells. On the other hand, lineage analysis and more recently retrospective single cell marking analysis have proven the existence of progenitor pools for the myotome and the spinal cord located earlier in the primitive streak and later in the tail bud. In the next 2 chapters I will describe the evidence I found for the existence of axial stem cells and their restricted location within the primitive streak and tail bud. In this gene expression analysis we included two genes known to be essential for the self-renewal and pluripotency of embryonic stem (ES) cells, trying to find out whether the axial progenitors would share the characteristics of ES cells. However, *Oct-3/4* and *Nanog* were not found to be expressed in the mouse tail bud by *in situ* hybridisation (Fig. 2.1, h3-h7, i3-i7). Moreover, most of the genes studied are expressed all over the newly forming tail bud tissues. Genes that are known to provoke truncations in the axis when mutated such as *T*, *Wnt3a*, and *Cdx2* are expressed broadly in the tail. *Foxa2* was expressed exclusively in the notochord, whereas *Evx1* and *Wnt3a* were expressed in complementary tissues: the posterior neurectoderm and the tail bud mesoderm, but even among these two domains there might be a region of overlapping which remains to be tested. Therefore, so far we have found no unique markers for a putative population of axial stem cells, which leaves two possibilities: either we have not found yet the exclusive marker gene or these progenitors are described by a combination of different markers.

2.5 SUMMARY

In the present gene expression analysis, I have found that transcripts of genes known to play a role in axis elongation such as *T (Brachyury)*, *Fgf8* and *Wnt3a* are expressed from gastrulation through tail elongation, as the homologues of genes expressed in the *Xenopus* tail such as *Evx1 (Xhox3)*, *Foxa2 (Pintallavis)* and *Cdx2 (Xcad3)*. This supports the hypothesis that mouse tail elongation is broadly similar to that of other

vertebrates. Moreover, I have shown that the primitive streak and tail bud are regionalised, and these domains of gene expression are consistent with previous fate maps marking different cell populations (Wilson and Beddington, 1996). Some of these domains coincide among different vertebrates. However, in the mouse there is not a new wave of gene expression coinciding with secondary neurulation or tail elongation as seen in *Xenopus*. Furthermore, the different domains of gene expression described in *Xenopus* do not always match the domains in mouse. Therefore, it is unlikely that the model proposed for *Xenopus* tail outgrowth (Tucker and Slack, 1995b; Beck and Slack, 1998; Beck and Slack, 1999; Beck *et al.*, 2001) is also true for the mouse.

In addition, we have found that towards the end of axial elongation, tail bud gene expression decreases drastically. However, intriguingly, *T* expression continues intensely until 13.5 dpc when axial elongation stops, at this stage, the levels of other genes are almost undetectable. It is known that *T* requires Wnts and Fgfs for axial elongation (Ciruna and Rossant, 1998), yet *T* expression levels are apparently unaffected by the decline in expression of *Wnt3a* and *Fgf8*, which might be due to the compensating effect of other family members.

Three putative novel domains of expression were found in our analysis:

-*Fgf8, Cdx2, T* and *Sox1*-GFP define a region of mesoderm production in the apparently undifferentiated tail tip.

-Two genes, *Nodal* at early stages, and *Sox1*-GFP at tail bud stages are expressed in two domains surrounding the newly formed notochord, which morphologically seem very similar and might be related to one another.

-The most posterior ectodermal region of the node has a different gene expression than its anterior and middle regions, analogous to the CNH.

Finally, the primitive streak and tail bud do not express 'stemness' markers. Therefore, a putative axial progenitor population/s residing in these two tissues have different characteristics from those of ES cells and may be defined only by a combination of markers.

The focus of the next two chapters will be to discuss the nature and localisation of the axial progenitors.

Chapter 3

LOCALISATION OF AXIAL
PROGENITORS AT TAIL BUD STAGES

3.1 INTRODUCTION

As described in chapter 2, gene expression domains in the mouse are continuous from gastrulation to tail formation. This gives further support to the idea that tail formation in vertebrates is a continuation of gastrulation, as both processes are controlled by similar gene expression. Moreover, we have shown that the primitive streak and tail bud are regionalised, and these domains of gene expression are consistent with previous fate maps marking different cell populations (Wilson and Beddington, 1996). However, are these cell populations self-renewing? And/or is there one axial stem cell population supplying all the others? As described in the introduction, lineage studies have proven the existence of apparently self-renewing progenitor pools for the myotome and the spinal cord (Lawson *et al.*, 1991; Beddington, 1981; Tam and Beddington, 1987; Tam and Tan, 1992; Wilson and Beddington, 1996; Nicolas *et al.*, 1996; Mathis and Nicolas, 2000).

Although these studies show the strongest evidence for the existence of axial stem cells in the mouse, the use of promoters specific to each compartment means that they cannot give detailed information on the position of the putative precursors, neither do they distinguish between the possibility of separate stem cells populations, and a common one supplying all lineages, nor whether they indeed are self-renewing progenitors.

In this introduction, I am going to discuss next the results of the experiments done during part of my MRes project aimed at locating the exact position of the progenitors for the mouse axial tissues at tail bud stages and defining their potency by performing grafting experiments. This work was continued during my PhD. The results of the work done during my PhD will be discussed in the results section of this chapter. The work described in this chapter was published in Development (Cambray and Wilson, 2002; for full article see reprint attached (Appendix II).

We first aimed to refine previous fate maps to show that the tail bud contains regionally separated descendants of cells in the streak using topically applied lipophilic dyes. We then used a transgenic mouse strain that expresses the green fluorescent protein GFP (Okabe *et al.*, 1997)

ubiquitously to explore the potency of these cells. We showed that descendants of cells in the vicinity of the node are found in an equivalent structure to the *Xenopus* and chick CNH. These cells fulfilled criteria expected of stem cells: they are able to self-renew, shown by their capacity to contribute to both anterior and posterior differentiated tissues and their ability to be serially passaged. By contrast, cells in the more ventrally located tail bud mesoderm (TBM) were more limited in their potency, a characteristic expected of a more committed CNH derivative.

All host embryos used in this study were dissected for labelling or grafting at 8.5 dpc (two to eight somites) and cultured for 48h, forming a total of 30-35 somites, as described previously (Wilson and Beddington, 1996).

Regionalisation of primitive streak descendants in the tail bud

Previous lineage analyses have shown that some descendants of cells in the node and primitive streak at 8.5 dpc are present in the tail bud at 10.5 dpc (Wilson and Beddington, 1996). To determine whether there is any relationship between origin of the cells in the streak and their subsequent location in the tail bud, two distinct sites were labelled: the ventral layer of the node and the anterior primitive streak (Fig. 3.1 A, B). In accordance with previous fate-mapping studies, the descendants of cells in the node were located in the notochord, whereas those of the anterior streak were predominantly somitic. Descendants of anterior streak were also located in the ventral neurectoderm, but not notochord. The anterior limit of labelling was around somite 12. In the tail bud after node labelling, the labelled notochord widened and ended abruptly beneath the neural tube, anterior to the end of the tail such that the mesoderm in the tail bud was unlabelled. Descendants of the anterior streak were located in the tail bud in two domains: the posterior ectoderm continuous with the ventral posterior neural tube (termed posterior neural plate) and the tail bud mesoderm (TBM).

We next compared this fate map information with the contribution of GFP transgenic node and primitive streak cells when grafted to stage-matched embryos. These were grafted to the anteriormost extreme of the

103

primitive streak, touching the outer rim of the node, to allow incorporation of the grafted tissue in either the host node or streak (Fig. 3.1 C, D). In general, these grafts mirrored the tissue contribution seen after DiI labelling, showing that, when grafted to this position, cells can incorporate efficiently in either tissue from this site, and that the pattern of incorporation reflects the site of origin of the cells. Grafts of node contributed predominantly to notochord and anterior streak to somites, although in eight embryos, contribution from grafted node to predominantly medial paraxial mesoderm was observed. This is consistent with fate maps of the chick node, where cells in lateral regions of the node contribute to somites (Psychoyos and Stern, 1996; Selleck and Stern, 1991). However, the majority of embryos receiving node grafts contained little or no contribution to somites, indicating that it is possible to physically separate somite from notochord progenitors. In the tail bud, the contribution from GFP transgenic cells was essentially as seen with the fluorescent lineage tracers.

Therefore the mouse tail bud is regionalised and different regions containing the different progenitors could be dissected. The CNH in the mouse, in analogy to *Xenopus* and chick, consists of the most posterior neural plate and underlying notochord together with the condensed axial mesoderm adjacent to it (the mouse CNH shows no union of the notochord and most posterior neurectoderm as seen in frog and chick), whereas the TBM is composed of loose mesenchyme. It was therefore possible to dissect apart the loose tail bud mesoderm (TBM) from the CNH, morphologically (Fig. 3.2 B). As shown above, the ventral node descendants at the tail bud label the end of the notochord, whereas anterior streak descendants labelled the posterior neural plate. Therefore, the CNH contains descendants of ventral node and anterior streak, while the TBM contains only anterior streak descendants (Fig. 3.1 E, F). The contribution of these cells to the tail bud suggests that they may constitute a self-renewing subset of the labelled or grafted tissue. This was tested in two ways: (1) grafting the CNH and TBM from tail buds up to 12.5 dpc into 8.5 dpc embryos and (2) the labelled 10.5 dpc CNH or TBM were serially passaged into successive 8.5 dpc embryos. In each case, a

self-renewing population would be expected to contribute descendants both to the differentiated axial tissues formed by the host and the tail bud itself.

The CNH, but not TBM, is capable of incorporating in all host axial tissues and still retains cells in the tail bud, when grafted to younger embryos

We compared the capacity of dissected 10.5-12.5 dpc CNH or TBM to differentiate relative to control isochronic grafts described above, when grafted to the 8.5 dpc primitive streak/node border (Fig. 3.2). The donor tissues were derived from GFP transgenic embryos, *Zin 40* embryos (expressing LacZ ubiquitously) (Munsie *et al.*, 1998) or wild-type tissue labelled with DiI. Although a high proportion of control isochronic grafts had incorporated well in the axis, we observed a reduction in the proportion of grafts from the TBM that incorporated correctly, with cells remaining predominantly as morphologically undifferentiated clumps (Fig. 3.3 A, B). Only one out of 11 heterochronic grafts of TBM contributed to labelled cells in the axis. However, the labelled cells were restricted to a short unilateral stretch of somitic mesoderm and did not populate the tail bud.

By contrast, a high proportion of embryos receiving up to 12.5 dpc CNH cells showed extensive contribution to the axis (Fig. 3.4 A-C). Most successfully grafted embryos contained label in somites, with a lower proportion showing label in notochord and /or neural tube. All embryos showed bilateral contribution from the labelled cells. In general, the anterior limit of contribution tended to be more posterior than in isochronic grafts (approx. somite 17 onwards). Unlike TBM, they also populated the tail bud with high frequency, and were located in both the CNH and in TBM.

Taken together, these results suggested that the grafted CNH is at least partially equivalent to its earlier counterpart in the node and anterior streak. These results showed that the CNH has the potential both to contribute widely to the axis, and to repopulate the CNH itself and the TBM.

107
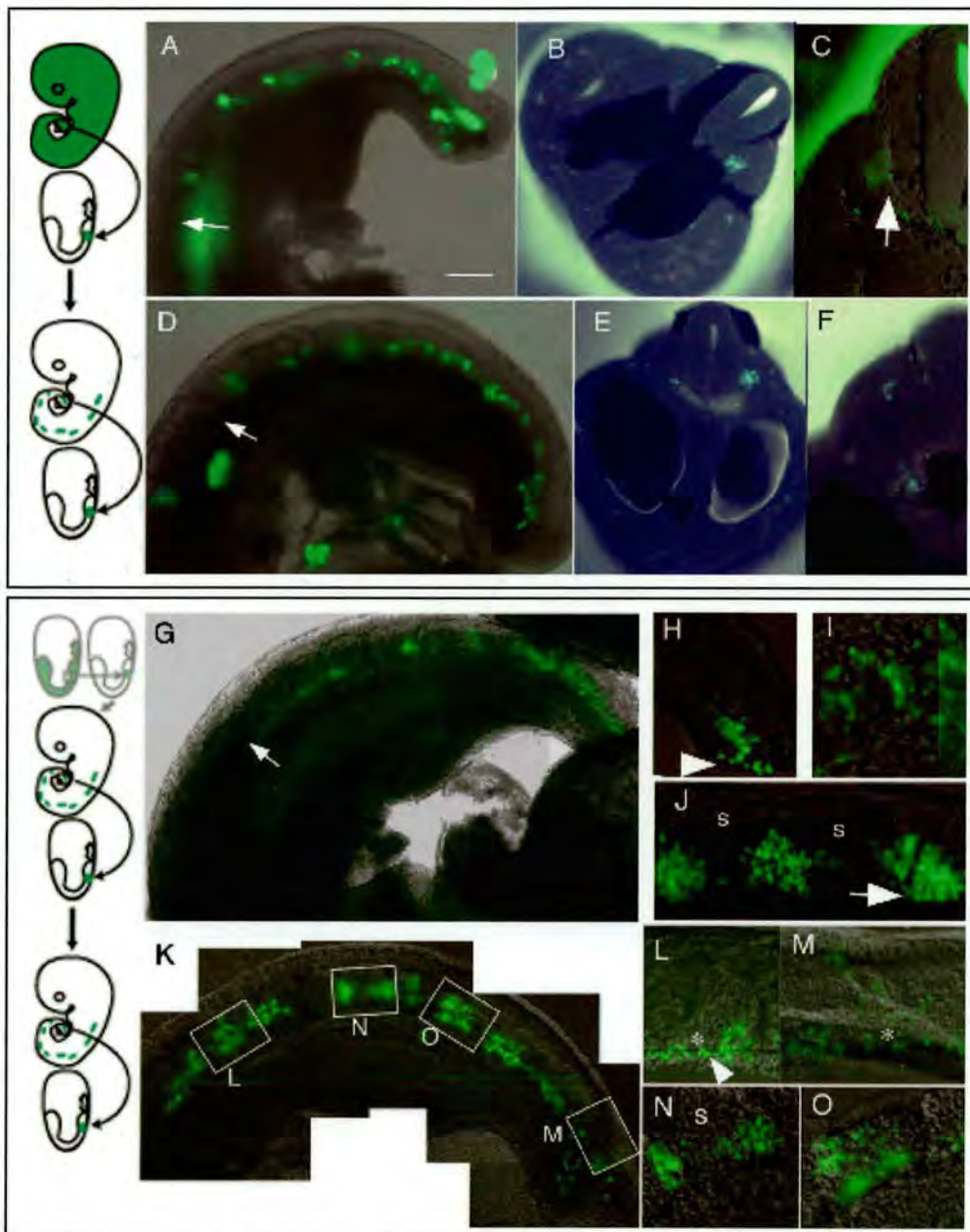
Figure 3.4 Regrafting of GFP-labelled CNH results in contribution to both the axis and tail bud in up to three generations

Diagrams illustrate the history of grafted cells in the cultured embryo shown immediately to the right. **Top panel**: whole mount **(A)** and transverse sections **(B, C)** of an embryo that received a graft of 10.5 dpc GFP-labelled CNH. In the axis, cells populated the paraxial mesoderm exclusively and either formed medial graft- derived somites **(B)**, or incorporated into wild-type tissue **(C, arrow)**. **D-F)** Whole mount **(D)** and sections **(E-F)** of an embryo grafted with CNH cells from the embryo in A-C. Grafted cells populate axial derivatives that are identical to the parent graft. **Bottom panel**: whole mount **(G)**, dissected neural tube/notochord **(H)** and paraxial mesoderm **(I, J)** from embryos that had received a graft of 10.5 dpc CNH, derived from an intitial 8.5 dpc node graft. Labelled cells populated the posterior end of the notochord and CNH (arrowhead, **H**), incorporate in paraxial mesoderm **(I)**, but also from small medially located somites that are epithelial posteriorly (arrow in J) and disperse anteriorly, and are located out of register with the endogenous somites (s). **K-O)** A third generation graft. Whole mount **(K)**, dissected neural tube and notochord **(L, M)**, and paraxial mesoderm **(N, O)**, showing contribution to notochord (arrowhead in L), posterior neurectoderm (asterisks in L and M), and both ectopic somites located between host somites (s) **(N)** and interspersed GFP-labelled cells **(O)** in host somites. Arrows in A, D, G indicate the position of somite 20. Bar: 280µm in A, D; 88µm in B, E; 43µm in C, F, H, I, J, L, M, N, O; and 200µm in G, K.

109

The CNH, but not TBM, is serially transplantable

The contribution to host CNH by grafted CNH cells separated by up to 4 days in developmental stage from the host (in the case of 12.5 dpc CNH grafts into 8.5 dpc embryo hosts), together with their ability to participate in differentiated axial tissue formation, suggested that axial stem cells reside there, and not in the TBM. Such stem cells should also contribute cells to the axis and repopulate CNH on multiple passages through host embryos. We therefore tested this by regrafting GFP-labelled CNH and TBM to 8.5 dpc embryos.

In second generation grafts, groups of cells containing labelled TBM derived from initial anterior streak grafts were also disadvantaged relative to CNH from incorporating in the axis. Similar to the results above, when they did incorporate in the axis, they did so only over short axial distances (Fig. 3.3 C, D), and only one embryo showed label in the tail bud. In this embryo, no contribution to more anterior positions in the axis were observed, and it is therefore impossible to determine whether these grafted cells truly retained potential to contribute to the axis. Thus, even though these cells were now retained in the tail bud 48h after transplant to the node/anterior streak border, this did not select for greater ability to generate descendants both in axis and tail bud.

As shown above, labelled CNH from 10.5 dpc embryos grafted to 8.5 dpc node/anterior streak border resulted in contribution throughout the axis and in the tail bud in the CNH. The labelled cells in the CNH were regrafted to an 8.5 dpc host, which contributed to the same axial tissues and the CNH (Fig. 3.4 A-F). Similar results were obtained when the grafted 10.5 dpc CNH was derived from an initial 8.5 dpc node graft (Fig. 3.4 G-J). These second generation embryos predominantly showed contribution to somites, but also to notochord and ventral neural tube. Although intermingling of host and wild-type cells could be observed in paraxial mesoderm, formation of small medial, grafted-derived somites within the somite territory was also apparent (Fig. 3.4 B, E, arrow in J). The majority of grafted embryos showed repopulation of both CNH and TBM, supporting the hypothesis that TBM is derived from CNH. These second generation CNH were grafted a third time, and incorporation was

110

observed both in axial tissues and the tail bud, in CNH and TBM (Fig. 3.4 K-O). The grafted tissue shows a somewhat reduced rate of incorporation. However, the pattern of incorporation in notochord, somites and neural tube was similar in 3rd generation grafts to that observed in the 2nd generation and in the grafts of 10.5-12.5 dpc CNH described above. TBM derived from second generation CNH grafts showed similar properties to other 10.5 dpc TBM grafts.

In general, the anterior limit of contribution (approx. somite 17 onwards) was similar for the 1st, 2nd and 3rd generations of CNH grafts, showing that the stage of the donor tail bud (not the absolute age of the cells) determined this anterior border.

In summary, grafted TBM either does not incorporate or differentiates as paraxial mesoderm and cells are not retained in the tail bud. In contrast, grafted CNH can incorporate in all the dorsal host axial tissues and still retain progenitor cells in the tail bud. Moreover, the CNH is serially transplantable. Therefore, the CNH, but not TBM, has the characteristics of a population of axial stem cells.

No difference in contribution was obvious between CNH derived from anterior streak versus that from node. However it was striking that contribution to 3 generations was seen only where the first generation grafts were from nodes that contributed not only to notochord, but also to paraxial mesoderm. This suggested that a population of axial progenitors with capacity for self-renewal and extensive contribution to somites, notochord and neurectoderm was located close to the node at 8.5 dpc, and that these continued to be associated with the CNH in successive generations. The localisation of the axial stem cells at primitive streak stages will be discussed in the next chapter.

3.2 AIMS AND EXPERIMENTAL APPROACH

In the results presented above we showed that the CNH can be serially transplanted for at least 3 generations contributing to the dorsal host axial tissues and still retain progenitor cells in the tail bud. Therefore, the CNH may contain a population of axial stem cells.

However, it remained to be verified whether these apparently well-

integrated donor tissues indeed differentiated appropriately in their new host environment. As mentioned above, on some occasions unincorporated tissues were also found. Thus, an experiment was set up to confirm that differentiation was occurring appropriately: a subset of 8.5 dpc embryos were grafted with cells from 8.5 dpc node or 10.5 dpc CNH expressing the transgenic marker *Zin40*, a developmentally neutral gene trap integration containing a ubiquitously expressed LacZ gene (Munsie *et al.*, 1998). This histologically stable marker allowed processing of grafted embryos for *in situ* hybridisation to markers of differentiation in axial tissues (Tajbakhsh and Houzelstein, 1995). Coexpression of LacZ and the differentiation marker was scored in serial transverse microtome sections. The riboprobes that we used were: *T (Brachyury)* (Herrmann *et al.*, 1991) for notochord, CNH and TBM; *Sonic hedgehog (Shh)* (Echelard *et al.*, 1993) for notochord and floor plate; *Pax3* (Goulding *et al.*, 1991) for dermomyotome and dorsal neural tube; *Pax6* (Walther and Gruss, 1991) for neural tube; and *Delta-like1 (Dll1)* (Dunwoodie *et al.*, 1997) for unsegmented paraxial mesoderm. To allow visualisation of the grafted cells while in culture, the donor tissues were also labelled with DiI. Dissections, grafts and culture were performed as described in Chapter 6 of materials and methods or Cambray and Wilson (2002).

Also from the results presented above, it was suggested that the TBM was a descendant of the CNH. Before posterior neuropore closure, the posterior neural plate is a source of mesoderm for somites (Wilson and Beddington, 1996). As labelled anterior streak contributed descendants to both the posterior neurectoderm and mesoderm, it was of interest to determine whether the posterior neural plate continues to produce mesoderm after neuropore closure. To test this, the entire neurectoderm of dissected 10.5 dpc tail pieces that had undergone posterior neuropore closure was labelled using DiI. After 48 hours culture, we sectioned the tails in a vibratome and looked for labelling in the mesoderm as well as in neurectoderm. Culture conditions for tail pieces were the same as for whole embryos (Tam and Tan, 1992; Cambray and Wilson, 2002).

3.3 RESULTS

Grafted cells express markers of differentiation correctly

In embryos that received an 8.5 dpc node graft, *T* and *Shh* were expressed appropriately in donor cells in the notochord (Fig. 3.5 A-D; Table 3.1), and graft-derived cells in the floorplate expressed *Shh* but not *T*. Cells immediately dorsal to the floorplate express the neural marker *Pax6*, and graft-derived cells populating this region also appropriately expressed *Pax6* (Table 3.1). Medially located donor cells in the paraxial mesoderm showed no ectopic *T* expression (data not shown). The tail buds of embryos A and C had been removed prior to processing and were not assayed for marker gene expression. This apparently normal differentiation therefore correlates well with the morphological assessment of incorporation in tissue derived from isochronic grafts.

To determine whether this was true of grafted 10.5 dpc CNH tissue, the expression of *T, Shh* and two additional markers of paraxial mesoderm differentiation, *Dll1* and *Pax 3* were assayed. Within the axis, where donor cells appeared morphologically incorporated in a tissue, they correctly co-expressed all differentiation markers assayed (Fig. 3.5 E-H; Table 3.1). Furthermore, the incorporated cells did not ectopically express differentiation markers (Fig. 3.5 arrow in H). In the tail bud mesoderm and CNH, many donor cells also expressed *T*, showing that these cells also express markers appropriate for tail bud (data not shown).

Table 3.1. Correct gene expression in grafted cells anterior to the TB

Graft type	Embryo	Probe	Appropriate expression of marker by donor cells in:		
			nch	nt	pxm
8.5 dpc node	1	*T*	Y		
	2	*Shh*	Y	Y	
	3	*Pax6*		Y	
10.5 dpc CNH	4	*T*	Y		
	5	*Shh*	Y		
	6	*Shh*	Y*	Y*	
	7	*Dll1*			Y
	8	*Pax3*		Y	Y

*Rodlike groups of donor cells near the notochord could be followed through serial sections in this embryo. When lying beside the notochord, they did not express *Shh*, but became physically incorporated over several sections in notochord and ventral neural tube, and concomitantly expressed *Shh*. nch: notochord; nt: neural tube; pxm: paraxial mesoderm; CNH: chordoneural hinge; *T: Brachyury; Shh: Sonic hedgehog; Dll1: Delta-like1*.

Unincorporated tissues

As mentioned in the introduction of this chapter, although a high proportion of control isochronic grafts had incorporated well in the axis, a reduction in the proportion of heterotopic TBM grafts that incorporated correctly was observed, with cells remaining predominantly as morphologically undifferentiated clumps. No incorporation was seen in the axis or TB of these embryos (Fig. 3.3 A, B). By contrast, embryos receiving CNH grafts showed extensive incorporation in the axis. However, some unincorporated tissues could be also found. Although differentiation towards somites was apparent in many of the CNH grafted embryos, the grafted tissue did not always intersperse well with host tissue. Typically, some regions of the grafted embryos contained small groups of medially located somitic tissue, sometimes out of register with those of the host (Fig. 3.4 B, E, arrow in J).

In the grafts that were performed using *Zin40* donors, some unincorporation was also observed. Embryo 6, which had received a 10.5 dpc CNH graft, showed rodlike groups of donor cells near the notochord. These cells could be followed through serial sections, when lying beside the notochord they did not express the differentiation marker for the notochord *Shh*, but became physically incorporated over several sections in the notochord and ventral neural tube, and concomitantly expressed *Shh* (Table 3.1; Fig. 3.5 F).

DiI labelling did not coincide with X-gal staining

The *Zin40* donor tissues were also labelled with DiI to allow visualisation of the grafted cells while in culture. Unexpectedly, after X-gal staining, the β-gal activity observed in these embryos did not coincide with the DiI labelling (Fig. 3.6). The number of cells labelled with DiI was much higher than the number of β-gal expressing cells, whereas the opposite result was expected, as we were labelling 3D pieces of tissue and DiI, according to the manufacturers, can only label the cells at the surface. Moreover, this marker should be diluted through cell division.

The posterior neural plate generates mesoderm after posterior neuropore closure

The entire neurectoderm of 10.5 dpc tail pieces was labelled using DiI. After 48 hours, labelled mesoderm was detected in the posterior region of six out of six cultured tail pieces. The most posterior notochord appeared also to be labelled (Fig. 3.7).

3.4 DISCUSSION

Grafted cells are able to incorporate appropriately in the host axis as shown by differentiation markers, but clumps of unincorporated cells were also found

As presented in these results, node and CNH cells are able to incorporated and differentiate appropriately when grafted to the border between the node and anterior streak either isochronically or heterochronically. However, in a few of the CNH grafted embryos, alongside incorporation, ectopic structures were also found. One embryo, at least, that received a 10.5 dpc CNH graft contained rod-like groups of donor cells near the notochord (Table 3.1; Fig. 3.5 F). Furthermore, some regions of the CNH grafted embryos, presented in the introduction, contained small groups of medially located somitic tissue, sometimes out of register with those of the host (Fig. 3.4 B, E, arrow in J). It is possible that the cluster of grafted cells in the streak may retain information on the periodicity of somites to be formed. An alternative possibility is that as the CNH ectoderm is much smaller than the primitive streak, the grafted cells may include the progenitors of entire somites, effectively creating a heterotopic graft of lateral somite precursors to a location where cells normally exit to medial somites.

In contrast grafted TBM is only capable of populating short axial stretches that corresponds to a distance of a few somites. It shows a low frequency of incorporation in axial tissues, and fails to contribute to tail bud. In most embryos only clumps of unincorporated cells were found where incorporation should have started in the axis, no incorporation was observed in the axis or TB (Fig. 3.3). The capacity of TBM cells to

contribute to anterior axial positions has also been studied by Tam and Tan (1992), who grafted small number of cells from the tail bud of embryos up to 13.5 dpc. These grafts were capable of contributing to much more anterior positions than they would have done in situ. As these authors do not distinguish CNH from TBM in the grafts, it may be that it is a small population of CNH cells included in their grafted population that retain potency, especially to contribute to the tail bud. The relatively low frequency observed by these authors of grafted cell retention in the tail bud (around 20%) supports this idea. Alternatively, the smaller number of grafted cells used by Tam and Tan (1992) may intermingle more extensively with the host cells than the TBM grafts in our study. Larger TBM grafts may therefore be subject to greater community effects that preserve either specification as mesoderm or anteroposterior information. As recently ingressed mesoderm earlier in gastrulation is more restricted in potency than the cells from the ectoderm that produced it (Tam *et al.*, 1997), it is likely that TBM cells that have undergone ingression from the posterior neural plate, are also restricted in potency.

The categories of unincorporated cell clumps presented in this chapter, either ectopic structures or clumps, will be further discussed in the discussion of the next chapter.

Larger numbers of DiI labelled cells compared to β-gal expressing ones was observed in *Zin40* grafted embryos

Unexpectedly, in *Zin40* transgenic embryos labelled with DiI, the amount of cells expressing β-gal was reduced compared to the number of DiI labelled cells (Fig. 3.6), whereas the opposite result was expected, as we were labelling 3D pieces of tissue and DiI, according to the manufacturers, can only label the cell surface. Moreover, this marker should be diluted through cell division. Therefore, two things could be happening: either the LacZ staining was not labelling all cells appropriately or the DiI was being transferred cell to cell differently to how the manufacturers propose. 10.5 dpc *Zin40* embryos have been previously stained and shown β-gal expression in all the cells (Jenny

Nichols, personal communication, and Munsie *et al.*, 1998). Therefore, we would not expect this to be the cause.

On the other hand, DiI is a lipophilic dye. Therefore, it is not expected to be passed from cell to cell through gap junctions, instead it becomes incorporated in the lipid membrane of the cells. During division, each daughter cell inherits part of the label when it inherits its membrane. One possibility is that DiI labelled cells that have died naturally, become incorporated to neighbouring cells when they die, passing on the dye as membrane components are recycled. A further explanation is that when cells are labelled with DiI, precipitated crystals often form in the surface of the labelled cells. These crystals might label other cells at the time of the graft.

In any case, these findings made us very suspicious about the use of DiI in these studies, particularly in experiments where a piece of tissue is labelled with DiI and then grafted. We therefore abandoned its usage in our grafts and used GFP transgenic mice as donors instead.

Ingression of cells from the neural plate to the mesoderm layer continues after posterior neuropore closure

The dramatic involution movements during *Xenopus* gastrulation cease by the neural plate stage (Gont *et al.*, 1993), as does the transit of a large part of the epiblast through the streak and node/organiser to generate mesoderm in mouse by the equivalent headfold stage (Kinder *et al.*, 2001; Snow, 1981). In chick, passage of lateral epiblast cells early during gastrulation through Hensen's node ceases prior to node regression (Joubin and Stern, 1999). Thus, at the start of somitogenesis in vertebrates, the neural, mesodermal and notochordal precursors are no longer in mass transit from the ectoderm but are contained in the region of ingression. I have extended previous studies in the mouse (Wilson and Beddington, 1996) to show that this ingression of cells to the mesoderm layer continues even after posterior neuropore closure around the 35-somite stage (Fig. 3.7). In chick, ingression movements after posterior neuropore closure have also been observed (Knezevic *et al.*, 1998). These can apparently occur from the dorsal surface, perhaps indicating subtle

differences in the organisation and/or movements of vertebrate tail bud tissues.

The notochord appeared also labelled at its most posterior end (Fig. 3.7 C). Therefore, there is some evidence to support that the most posterior notochord is populated by ectoderm descendants. From the experiments discussed in the Introduction, we had already found labelled cells in the most posterior end of the notochord when labelling or grafting the anterior streak. In chick, too, there is evidence that some notochord progenitors reside in the ectodermal layer, rather than in the ventral node region (Catala *et al.*, 1995; Catala *et al.*, 1996; Psychoyos and Stern, 1996). Furthermore, while passage through Hensen's node is a prerequisite for incorporation in the notochord, some notochord progenitors originate outside Hensen's node in the anterior primitive streak and are only incorporated there later, presumably during node regression (Psychoyos and Stern, 1996). Therefore, the ventral node itself may not contain all notochord progenitors. Instead, the notochord may be supplied from cells in the ectoderm layer that represent more primitive notochord precursors at primitive streak stages and later in the tail bud.

In chick therefore, as in mouse, the posterior neural plate may merely represent a localised remnant of the outer layer of the primitive streak, which continues a form of ingression after gastrulation. Therefore, the passage of cells from the ectoderm of the CNH towards the most posterior TBM is conserved among vertebrates. This would raise an interesting parallel with the situation in *Xenopus*, where as discussed in the Introduction (chapter 1), the posterior part of the neural plate gives rise to tail somites (Bitjel, 1936). Nonetheless, the question whether these somite fate cells are being produced by an ongoing process of specification to mesoderm by cell ingression or merely differentiation of a previously committed population, as postulated by Gont *et al.* (1993), has not yet been answered.

In this experiment, DiI was applied to the cells *in situ* rather than by grafting labelled cells, and is therefore less likely to have ectopic labelled cells due to adherent DiI crystals. However, it remains a caveat that

perhaps not all internally labelled cells were derived from the ectoderm layer.

3.5 SUMMARY

In this chapter, I have extended previous studies in the mouse to show that the ingression of cells to the mesoderm layer from the ectoderm continues even after posterior neuropore closure around the 35-somites stage. In chick, ingression movements after posterior neuropore closure have also been observed (Knezevic *et al.*, 1998). Therefore, the posterior neural plate may merely represent a localised remnant of the outer layer of the primitive streak, which continues a form of ingression after gastrulation.

Furthermore, in previous studies, summarised in the introduction, we had shown that the CNH region can incorporated in all the host axial tissues and repopulated the host CNH itself and TBM for at least 3 generations. In addition, I have proven that the incorporated cells differentiate appropriately, according to several tissue specific markers. Therefore, this region has the characteristics of a stem cell population for the axis.

In the next chapter, I will describe the results of the experiments performed to locate this putative axial stem cell population at primitive streak stages.

Chapter 4

LOCALISATION AND POTENCY OF AXIAL PROGENITORS AT PRIMITIVE STREAK STAGES

4.1 INTRODUCTION

It has been hypothesised in chick and mouse that cells remaining in the streak or tail bud at the termination of prospective lineage labelling studies represent a minority population composed of self-renewing stem cells (Beddington, 1994; Psychoyos and Stern, 1996; Tam and Beddington, 1987; Wilson and Beddington, 1996). In the last chapter, I have expanded some of these fate maps to locate these progenitors in the tail bud. The descendants of primitive streak and node populate different regions in the tail. Ventral node descendants in the tail bud label the end of the notochord, which corresponds to the ventral part of the chordoneural hinge (CNH), whereas anterior streak descendants label the posterior neural plate, corresponding to the dorsal part of the CNH and also the tail bud mesoderm (TBM) (chapter 3, see Fig. 3.1). Therefore, the CNH contains descendants of ventral node and anterior streak, while the TBM contains only anterior streak descendants. It was possible to dissect the loose TBM from the CNH. Grafting experiments showed that the TBM either does not integrate or differentiates as paraxial mesoderm and cells are not retained in the tail bud (chapter 3, see Fig. 3.3). In contrast, the CNH region can integrate in all the dorsal host axial tissues and repopulate the host CNH itself and the TBM for at least 3 generations (chapter 3, see Fig. 3.4). These results showed that the primitive streak/tail bud can retain descendants of cells initially located near the node over a total of around 90 somites made by the hosts, and strongly suggests that a stem cell population resides in the CNH region.

Interestingly, the grafts that gave rise to three generations of integration in the axis and CNH were descended from initial node grafts that showed integration to both notochord and paraxial mesoderm. This, together with the observation that many node grafts did not show such integration, suggests that it is not the node itself, but cells immediately abutting it that were included with the grafted tissue, that demonstrate stem cell-like properties.

The mouse node is clearly visible as a depression at the distal tip of the embryo between early headfold stages (7.5 dpc) until the 7-somite stage (8.5 dpc). It is composed of two layers separated by a basal

membrane. The ventral layer contains meso-endodermal cells and is composed of two regions: the cells in the depression, also called 'pit cells', and the cells sourrounding them, called 'crown cells'. 'Pit cells' are columnar and monociliated, as is the contiguous head process more anteriorly. On the other hand, 'crown cells' are radially oriented, perpendicular to the dorso-ventral axis. Both ventral regions are characterised by a low proliferative rate. Bellomo *et al.* (1996) proposed that this low proliferation rate was not compatible with the existence of a stem cell population residing in this layer, as suggested by Beddington (1994). Conversely, the dorsal layer of the node contains a highly proliferative ectodermal population of cells, indistinguishable from the anterior neurectoderm and anterior primitive streak ectoderm at the level of BrdU incorporation. Taking into account these results and the already hypothesised existence of a resident population in the anterior primitive streak, Bellomo *et al.* (1996) proposed that a proliferative stem cell population could exist in the dorsal layer of the node/anterior primitive streak, which would then differentiate, stop proliferating, and migrate to the ventral layer of the node to contribute to the non-proliferative population. This ventral part would then form the head process and the notochord, as well as acting as the organiser. In transplantation experiments, Beddington (1994) showed that the ventral layer of the node was necessary to induce a secondary axis when transplanted ectopically, revealing it has Spemann organiser function as does the frog dorsal lip of the blastopore and the chick Hensen's node.

Interestingly, there are differences between the anterior and posterior part of the node ectoderm. As reported by Bellomo *et al.* (1996), the basal lamina is continuous at the anterior part of the node, containing the 'pit cells', but becomes discontinuous at its posterior part. Moreover, genes such as T, Fgf8, Wnt3a and Evx1 are only expressed in the ectoderm of the posterior node, as seen in our gene expression analysis (chapter 2). It would be therefore interesting to compare the fate, potency and specification of this most posterior region of the node with its surrounding regions in the anterior node and anterior primitive streak. Could this posterior node region with such a heterogeneous gene expression

represent a stem cell population for the axial, paraxial and ectodermal tissues? One could imagine then, that the inclusion of this posterior region of the node in some of the node grafts, presented in the last chapter, resulted in these node grafts giving rise to 3 generations of integration in the axis and CNH, whereas the grafts that contained only the anterior part of the node did not show this ability.

An interesting parallel to these experiments is seen in studies of the chick node and anterior streak (Charrier *et al.*, 1999). The junction of Hensen's node and the anterior primitive streak (the axial-paraxial hinge (APH) shows overlapping expression of genes characteristic of the node (*Foxa2* and *Chordin*) and those characteristic of the streak (*Ch-Tbx6L*) (Fig. 4.1). Cells from this region are capable of generating notochord, neural tube or somites. Normally this contribution is limited to small regions of the axis, and cells are retained in the tail bud. Deletion of the bulk of Hensen's node (region b, excluding the APH) results in the interruption of notochord formation, but this resumes further posteriorly. However, deletion of the APH (region c) results in embryos in which notochord formation continues for a short distance, but is followed by axial truncation. These results imply that this region is important as a signalling centre allowing maintenance of axial elongation, and/or that it contains stem cells for the axis.

Therefore, it would be interesting to know whether the posterior node region is equivalent to the axial-paraxial hinge described in chick and whether it contributes to the CNH in the tail bud.

4.2 AIMS AND EXPERIMENTAL APPROACH

The aim of the experiments was to test the hypothesis that it is the posterior node, which corresponds to the border between the node and anterior primitive streak (APS), that contains the self-renewing population at early primitive streak stages. For simplicity, we will refer to this region as border, meaning the border between the anterior node and the contiguous anterior primitive streak. We were also interested in distinguishing between 3 possibilities: 1) the border region is equivalent to a stem cell "niche", acting as a signalling centre allowing the maintenance

of axial elongation, 2) it contains the axial stem cells, or 3) both possibilities are true.

In the mouse embryo, the border can be distinguished morphologically, as a hinge between the end of the pit of the node (anterior node) and the anterior primitive streak, between 2 to 8 somites (8.5 dpc) (Fig. 4.2). Therefore, we performed a series of homotopic and heterotopic grafts of this region and the surrounding ones. All grafts were done isochronically; donor and host were dissected at 8.5 dpc. Homotopic grafts should show the fate of the different regions. Heterotopic grafts ask about the potency of the tissue we graft and also the influence of the new environment. Donor tissues, containing groups of about 100-150 cells, were dissected from GFP transgenic mice and were grafted into wild-type hosts. The primitive streak was dissected by making two longitudinal lateral cuts, isolating a thin strip of tissue containing the entire primitive streak and node and retaining both ectodermal and endodermal layers. Node, border and APS fragments were further dissected by making transverse cuts. It is important to note that the limitations of working with the mouse embryo meant that the grafted tissue did not replace the tissue at the graft site. The grafts were performed by blowing a small hole at the graft site to insert the new tissue. Therefore, the tissue at the graft site was disrupted but not completely removed, which means that the number of cells at the graft site was increased by the addition of the new grafted cells.

To prove that these regions could be dissected accurately, after dissection, some pieces were kept to be analysed by *in situ* hybridisation for markers such as *Foxa2* (Sasaki and Hogan, 1993), *Fgf8* (Mahmood et al., 1995) and *T* (Herrmann, 1991), which are known to be expressed in these regions, as seen in the gene expression chapter 2. The rest of the pieces were used in homotopic and heterotopic grafts, which were performed as described in the materials and methods chapter (chapter 6) or as Cambray and Wilson (2002). All host embryos used in this study were dissected and cultured as described previously (Wilson and Beddington, 1996). After culture, the embryos were dissected out of their membranes and their head and heart were removed, leaving the trunk and the tail to be photographed, before embedding for vibratome sectioning. Usually the tip

of the tail was separated from the rest to allow transverse sections to be made through the entire labelled region. Embryos were sectioned transversely at 100 μm. Integration in each dorsal axial tissue was scored in each section using confocal microscopy.

To allow quantification, a scoring system was developed where I divided the number of sections that had integration in a specific tissue, like the notochord, by the total number of sections that had any labelled cells. If integration was found in more than 50% of the sections, it was scored as high level integration. In each embryo scored in this way, label was detected in at least 10 out of a total of ~20 sections scored, corresponding to 1000 μm and approximately 10 somite lengths. If integration was found in 20% to 50% of sections, integration was considered low. Integration found in less than 20% of the sections was scored as zero, because less than 20% usually corresponds to integration seen in 1 to 3 sections out of ~20 sections in the axis. This usually corresponds to scattered or small clumps of cells found around where the graft has started to integrate and it is difficult to know whether these cells have integrated well in the tissue where they are found. The tail bud was scored differently from the axis as some of the axial tissues are indistinguishable. Moreover, there are fewer sections in the tail bud so any integration was scored as high level for either the CNH and/or the TBM. This scoring system was complemented with diagrams showing representative integration in the axial (notochord, neural tube and CNH) and paraxial (somites, paraxial mesoderm and TBM) tissues along the axis and the tail bud, for each type of graft (Fig. 4.4). This shows how the integration of GFP-labelled cells changes along the axis in the different types of grafts. It was possible to draw these diagrams because all embryos for each type of graft were very similar. Nevertheless, for more detailed information, an appendix has also been included, containing tables with each embryo's summary of scoring and its wholemount picture after culture (Appendix I).

To ask about the specification of these regions, I dissected node, border and APS, as described above, from 129, CBA and C57BL/6 strains of mice. Teratocarcinomas are produced from pluripotent stem cells or

embryonic carcinoma cells, and it was therefore of interest to determine whether the putative axial stem cells also produced such cells. Although embryo-derived teratocarcinomas can be produced in many mouse strains (teratoma-permissive), a few strains, such as C57BL/6 (teratoma non-permissive), are resistant. The regions alone or the three together were grafted under the kidney capsule to allow terminal differentiation and/or teratocarcinoma production at a neutral site. The grafts were left in place for a period of 4 or 6 weeks, after which the animals were sacrificed and both kidneys removed for examination. All grafts were performed on the left kidney so the right could be used as a negative control. No growths were observed in any right kidney. The growths were removed by cutting the part of the kidney that contained the growth and embedding them in paraffin for sectioning at 7 μm. Sections were either haematoxylin and eosin or Masson's trichrome stained to reveal the different cell types produced. Finally, we scored tissues that could be recognised histologically.

4.3 RESULTS

Validation

Node, border and anterior primitive streak can be accurately dissected by morphology, as confirmed by *in situ* hybridisation

To confirm that node, border and APS regions could be precisely dissected, after dissection, *in situ* hybridisation was performed for genes that are known to be exclusively expressed in some of these regions, as seen in the gene expression chapter (chapter 2).

As seen in Fig. 4.3, the node region expresses *Foxa2* in its ventral layer. *Fgf8* is not expressed in this region. In contrast, the APS expresses *Fgf8* in the ectoderm and nascent mesoderm, whereas *Foxa2* is not expressed in this region. The border region expresses the 2 genes: *Foxa2* is expressed in the ventral layer of this region as in the node; *Fgf8* is expressed in the ectoderm in a similar manner to the expression in the APS. *T* is expressed in both border and APS; in the border it is principally present in the ventral layer of this region as in the node, but some cells expressing high levels of *T* can also be seen in the ectodermal layer.

Therefore, dissection of these regions can separate the regions identified on the basis of gene expression. Node and APS can clearly be defined by the mutually exclusive expression of *Foxa2* and *Fgf8*. The border region instead expresses all 3 genes tested, as expected.

Fate of the cells (homotopic grafts)

Homotopic grafts of node, border and APS show that these regions produce different cell types

In node to node grafts, GFP-labelled cells integrated mainly into the notochord in the axis (Table 4.1; Fig. 4.4; Fig. 4.5 B, c, d). Border to border grafts integrated into all the dorsal tissues of the axis: the main integration is in the ventral neurectoderm and medial paraxial mesoderm; integration of cells in the notochord was also observed in 7 out of 8 embryos but was lower and intermittent compared to the integration seen in the other tissues (Table 4.1; Fig. 4.4; Fig. 4.5 H, i, j). Homotopic grafts of APS cells integrated into the somites and presomitic mesoderm only (Table 4.1; Fig. 4.4; Fig. 4.5 N, o, p).

The consistent integration in different tissues by these different types of grafts further corroborates that these regions can be accurately dissected and grafted.

Derivatives of the border, but not the node or APS, populate the CNH

As integration of node cells grafted homotopically is followed into the tail, it becomes more sporadic and eventually disappears (Fig. 4.5 e, f). Only 1 out of 5 embryos had integrated in the CNH, but only 2 labelled cells were observed in this structure (Table 4.1). Therefore, node appears to not contain cells destined for long-term contribution to the axis, as I will discuss later.

On the other hand, interestingly, border cells integrate into all the dorsal axial tissues as far as the tail bud, where a high concentration of labelled cells can be observed in the most posterior ventral neurectoderm and notochord of the tail, which corresponds to the CNH (Fig. 4.5 k, l). This region sometimes appears enlarged due to the high integration of grafted cells. Integration of border cells can also be seen in the TBM.

Table 4.1 Homotopic and heterotopic grafts

	Total eb graft.	Total eb integ.	Axis			Tail bud		Non-integ.
			NCH	NT	PXM	CNH	TBM	
Node to Node	5	5	5	0	0	1 (2cells)	0	0
Border to Border	8	8	7 (5low)	8	8	8	8	0
APS to APS	6	6	0	1 (low)	6	1	6	3 (2 clumps, TB; 1 ectopic nt, axis)
Border to Node	4	4	4	2 (1low)	2 (1low)	4	1 (few cells)	1 (ectopic nt/noto, TB)
Border to APS	7	7	4 (low)	6 (4low)	7	7	7	6 (4 clumps, TB; 2 ectopic nt/noto, axis and/or TB)
Node to Border	7	7	7 (low, TB)	7	1 (low)	7	3 (few cells)	4 (ectopic nt/noto, axis and TB)
Node to APS	7	7	6 (5low)	5	3 (low)	7	4	7 (6 ectopic nt/noto,axis and/or TB; 1clump, TB)
APS to Border	7	7	0	4 (TB) (2low)	7	6	7	3 (2 clumps, TB; 1 ectopic nt/noto, TB)
APS to Node	9	5	4 (2low, TB)	3 (2low)	4 (1low)	3	3	10 (2clumps axis; 3 ectopic s. on dnt, axis; 5 ectopic nt/noto,axis and/or TB)

Integration of grafted GFP-transgenic cells in the axis and tail bud after culture. eb. graft.: embryo grafted, eb. integ.: embryos that contained integrated GFP-labelled cells, NCH: notochord, NT: neural tube, PXM: paraxial mesoderm, CNH: chordoneural hinge, TBM: tail bud mesoderm, non-integ: non-integrated cells, APS: anterior primitive streak, TB: tail bud, nt: neural-like tissue, nt/noto: neural-like structure or cavitated notochord, s: somite, dnt: dorsal neural tube.

133

RECIPIENT

APS

border

vnt →

not →

node

node

s

nt

psm

am

DONOR

border

m

m

APS

paraxial

axial

TBM

paraxial

axial

paraxial

axial

Figure 4.4 Diagrams showing integration into the tail of GFP-labelled cells from homotopic and heterotopic grafts
Red letters described the type of graft performed; for each type of graft, a sagittal section through the axial (notochord, neural tube and CNH) or paraxial (somites, presomitic mesoderm and TBM) regions of the tail is presented. Black continuous fill represents high integration of GFP-labelled cells into the different tissues, whereas interrupted fill represents low integration. Red broken box defines the CNH region. s: somites, not: notochord, nt: neural tube, psm: presomitic mesoderm, vnt: ventral neural tube, m: medial contribution to the somites, ml: mediolateral contribution to the somites, am: axial mesoderm, TBM: tail bud mesoderm.

In contrast, APS to APS grafted cells populate the tail bud, usually integrating only in the TBM (Fig. 4.5 q, r). Only one out of 6 embryos had integrated in the CNH (Table 4.1), although this embryo had a totally different pattern of integration to the rest, probably due to an early non-integrated clump of cells in the dorsal neural tube that seem to create at first a double neural tube, then cells were integrated in the host neural tube in only one site, before populating the ventral neural tube and finally reaching the CNH region. One explanation could be that the dissection of the donor APS in this embryo included part of the border as the outcome of the graft is very similar to a border to APS graft as described later.

Potency of the cells (heterotopic grafts)

Border can differentiate as node and APS derivatives

2 out of the 4 embryos that contained a border to node graft had integrated cells in all the dorsal tissues in the anterior axis (Table 4.1), but in the following sections towards the tail, integration becomes restricted to the notochord; the other two embryos have integrated cells only in the notochord. Integration in the tail bud was concentrated in the notochord part of the CNH (Fig. 4.4; Fig. 4.6 A-f). Consequently, border is capable of differentiating as a node derivative when grafted to the node, but integrates more posteriorly in the notochord than node itself.

Border tissue when grafted to the APS integrates mainly into the presomitic mesoderm and somites as streak homotopics grafts do (Fig. 4.4; Fig. 4.6 G-l) Therefore, border can differentiate as APS derivatives when grafted in the APS. However, in 4 out 7 embryos we also observed low integration in the notochord, and in 6 out 7 we could see integration (low in 4 out of the 6) in the neural tube of the host (Table 4.1). In the tail bud, labelled cells were observed in both, the CNH and the TBM in all the embryos.

Node can integrate in the ventral neural tube when grafted to the border or APS

As described above, node homotopic grafts only integrated into the notochord. However, node to border and node to APS grafts integrated mainly into the floor plate and the ventral neural tube in the axis (Fig. 4.7 A-f). The integration in the floor plate was almost exclusively from donor-derived cells, whereas the ventrolateral segments of the neural tube contained a mixture of cells (Fig. 4.7 c, i). Node to border and node to APS grafts also integrated into the notochord to a lesser extent. Intriguingly, node to border grafts integration in this tissue was consistently found at the end of the tail (Fig. 4.4).

Therefore, node is able to integrate in the ventral neural tube when grafted to the border or the APS, a potency not observed when grafted homotopically. Thus, node environment might be suppressing neural differentiation, in favour of notochordal fate, as discussed later.

Node or APS homotopic grafts did not have any labelled cells in the most posterior notochord and CNH. However, node to border and node to APS grafts can integrate in the most posterior notochord and CNH (Table 4.1, Fig. 4.7 e, f, k, l).

Integration of cells in the presomitic mesoderm and somites in the axis was almost absent in node to border grafts. However, in 3 out of 7 embryos integration in the TBM was found in a very few cells scattered close to the CNH. In node to APS grafts, 3 out 7 embryos had low integration in the presomitic mesoderm and somites as far as the tail bud, whereas integration was observed all over this structure in the remaining 4 embryos (Table 4.1).

It is interesting to note that all node to APS grafts contained non-integrated ectopic structures, as I will discuss later.

The APS is partially but not completely committed

APS into border grafts closely resemble APS homotopic grafts, as they integrate mainly into the paraxial mesoderm and TBM (Fig. 4.8 A-f). However, 4 out of 7 embryos resulting from these grafts also contained labelled cells in the ventral neural tube mostly at the end of the tail and 6
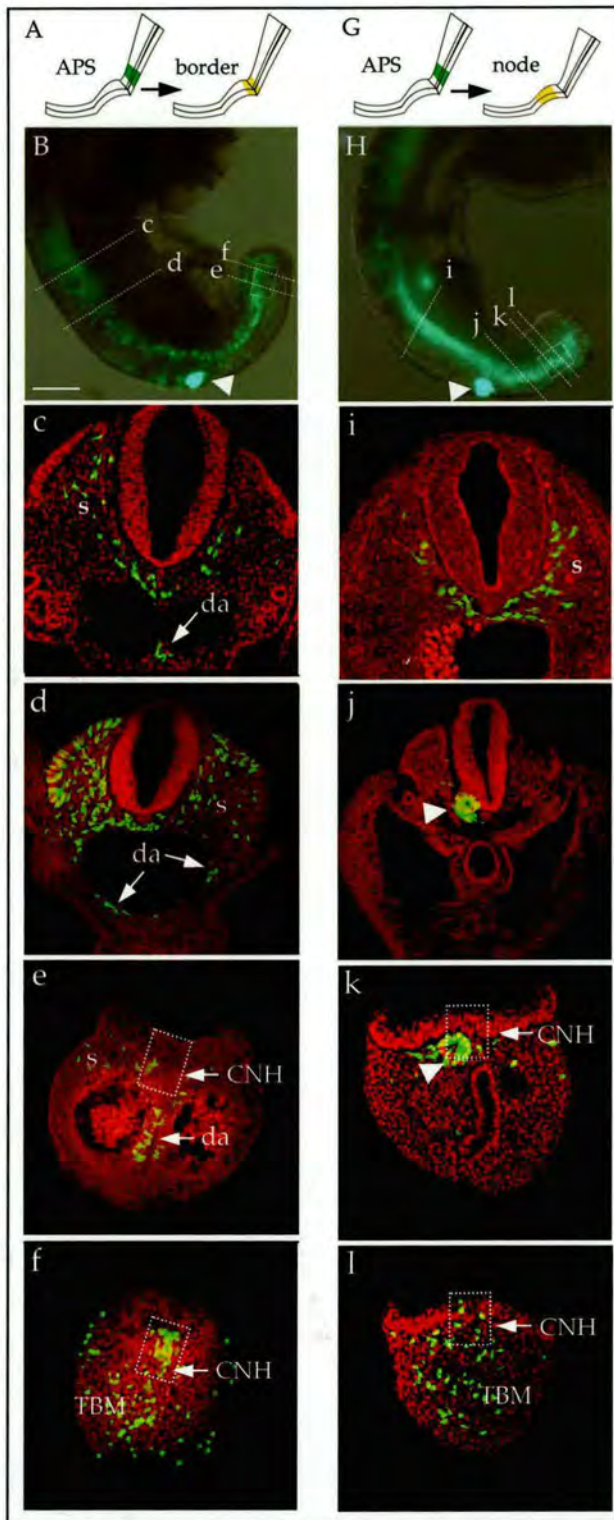
Figure 4.8 Heterotopic grafts (streak to border, streak to node) at 8.5 dpc
Diagrams in **A, G** describe the type of graft, either streak to border or streak to node. Whole trunks and tails in **B, H** show integrated GFP-labelled cells in the axis and tail bud. Confocal microscopy of transverse sections in **c, d, e, f** are from embryo in B; sections in **i, j, k, l** are from embryo in H. The nuclear stain TO-PRO-3 is shown in red. Broken boxes in B, H, e, f, k, l mark the CNH region. Arrowheads in B, H mark clumps of non-integrated cells in the neural tube in the tail bud. Arrowheads in j, k mark what seems an ectopic ring-like neural derived tissue or cavitated notochord next to the endogenous ventral neural tube in the axis. s: somite, da: dorsal aorta, CNH: chordoneural hinge, TBM: tail bud mesoderm. Bar: 375μm in B, H; and 100μm in c, d, e, f, i, j, k, l.

140

out of 7 had integrated in the CNH (Table 4.1). There was only one embryo that showed no integration in the ventral neural tube or CNH, this embryo was extremely similar to an APS homotopic graft, more likely due to an inaccurate graft. No labelled cells in the notochord were observed in any of these embryos.

Interestingly, APS to border grafts are the only type of grafts where integrated cells were observed in mesodermal cells that appear to form the dorsal aorta in the tail (Fig. 4.8 c, d, e).

Strikingly, in contrast to all other graft types, APS cells grafted to the node showed a very poor level of integration (Table 4.1). Non-integrated cells were present either as defined clumps, but also as ectopic structures, as described later. Of the cells that integrated approprietly in the axis, most formed paraxial mesoderm and TBM, although some examples of apparently appropriate integration in other axial tissues were present towards the tail bud (Fig. 4.8 j, k). In the 5 embryos that showed integration at some level along the axis, 3 colonised the CNH in the tail bud (Table 4.1).

Therefore, APS when grafted to the border or the node differentiates as streak homotopic grafts, although some integration can also be seen in other axial structures to a lesser extent towards the tail bud, which suggest that streak is partially but not completely determined.

Almost all heterotopic grafts integrate into the CNH

Surprisingly, most of the heterotopic grafts integrate into the CNH, whereas only border to border homotopic grafts integrate into this structure.

However, interestingly, the pattern of colonisation of this structure seen in border to border grafts is different to heterotopic grafts. Border homotopic grafts integrate equally into the most central region of the ventral neurectoderm and the notochord in the CNH, without showing signs of non-integrated cells (Fig. 4.5 k, l). However, border to node grafts and node to border grafts integrate mostly or exclusively into the notochord part of the CNH (Fig. 4.6 e; Fig. 4.7 f); APS to border grafts integrate mainly into the ventral neurectoderm of this structure (Fig. 4.8 f);

border to APS grafts integrate into both the ventral neurectoderm and the notochord, but they also contain clumps of non-integrated cells in the medial neural tube (Fig. 4.6 k, l); finally APS to node and node to APS grafts also integrate similarly to border homotopic grafts, but they also have ectopic structures (Fig. 4.7 k, l; Fig. 4.8 k, l), as discussed later.

The mediolateral integration in the somites depends on the route of exit taken by the cells at the graft site

In homotopic grafts, as integration starts in the axis, border cells tend to integrate mainly into the medial part of the somites (Fig. 4.5 i; Fig. 4.4), whereas APS cells integrate into medial and lateral parts (Fig. 4.5 o; Fig. 4.4). These observations are in agreement with previous fate maps in chick and mouse (Selleck and Stern, 1991; Wilson and Beddington, 1996; Eloy-Trinquet and Nicolas, 2002). However, posteriorly towards the tail, cells from border and APS seem to be scattered all around the somites, thus integrating into all parts of the somites (Fig. 4.5 j, k, l, q, r; Fig. 4.4).

On the other hand, when the border cells are grafted to the APS, integration in the somites in the axis is seen to the medial and lateral parts of the somite indistinguishably (Fig. 4.6 j; Fig. 4.4), similar to APS homotopic grafts. In addition, when APS is grafted to the border or to the node, integration in the somites in the axis becomes more medial. This is more clearly seen in streak to node grafts (Fig. 4.8 c, i; Fig. 4.4).

This shift in integration seen in heterotopic grafts is probably due to the fact that cells grafted in this way follow a route of exit from the midline similar to the cells at the graft site, as discussed later.

Nonetheless, the tail bud integration of these heterotopic grafts is unchanged, as in homotopic grafts labelled cells integrate into all parts of the somites or presomitic mesoderm (Fig. 4.6 j, k, l; Fig. 4.8 d, e, f, k, l; Fig. 4.4).

Non-integrated cells are mostly seen in heterotopic grafts

As presented in the last chapter, CNH and TBM to border grafts contained non-integrated tissues in some cases. In the present results, the same was observed in isochronic heterotopic grafts. Putting together the

results from the last chapter and this chapter, we find two major types of non-integrated tissues in these grafts:

- self-adherent clumps
- ectopic axial structures

Neither node nor border homotopic grafts contained non-integrated cells. Only 3 out of 6 APS homotopic grafts contained non-integrated cells, 2 of these were self-adherent clumps that did not disrupt the axis. Similar types of clumps were seen in border to APS and APS to border grafts, whereas node to border, border to node, APS to node and node to APS had mainly ectopic axial structures (Table 4.1).

Self-adherent clumps

Self-adherent clumps are usually found either: in the axis where integration is expected to have started, or in the tail bud as if they have been carried along on the neural tube (externally or in the lumen) through axial elongation.

-Clumps found in the axis were seen in heterochronic grafts of TBM to border, as described in the last chapter. Usually all grafted cells stay as a clump and there are not any integrated cells in any dorsal axial tissues. However, occasionally, in a very few embryos, some cells from the clump integrate into short stretches of the paraxial mesoderm in the axis. These types of clumps were also found in 2 out of 9 embryos that received an APS to node graft (Table 4.1). In this occasion, similar to what was observed in TBM grafts, one embryo had not any integrated cells in the axis, whereas the other embryo had integrated cells in the notochord in the axis for just a few sections (see chapter 3, Fig. 3.3 A, B).

-On the other hand, in embryos that contained a tail bud clump, appropriate integration was also observed in the axis and TB. This type of clump was found in a few CNH to border and APS to border (see chapter 3, Fig. 3.1 arrowhead in D; Fig. 3.4 A) grafted embryos presented in the last chapter and also in homotopic and heterotopic grafts presented in this chapter. This type of clump is often found at the most posterior end of the neural tube in the tail bud: in 2 out of 6 APS homotopic grafts, the clump was found inside the neural tube partly attached to the dorsal part of it; in

4 out of 7 border to APS grafts, the clump was found inside the neural tube partly attached to the ventral part of it; in 2 out of 7 APS to border grafts, the clump was found inside the neural tube partly attached to the ventral part of it; and in 1 out of 7 node to APS grafts, the clump was found inside the neural tube partly attached to the dorsal part of it (Fig4.5 N, q; Table 4.1).

Ectopic axial structures

A different type of non-integrated tissues occurs when part of the graft, instead of integrating appropriately in the axis, produces ectopic structures.

-3 out of 9 embryos that received an APS to node graft contained an ectopic structure in the dorsal (external) part of the neural tube that extended along part of the axis and resembled ectopic somites. In these embryos, appropriate integration of cells in the axial tissues was not observed (Fig. 4.9 F, g; Table 4.1).

-Internally located ectopic somites were found in a few embryos that received a CNH to border graft, as described in the last chapter. In this case, some regions of the grafted embryo contained small groups of medially located somitic tissue, sometimes out of register with those of the host. Appropriate integration in the somites was also observed in these embryos (see chapter 3, Fig. 3.4 B, E, arrow in J).

-The last type of ectopic structure was the most commonly found. It is composed of a rod of tissue resembling either neurectoderm of a cavitated notochord.

-A neural-like tissue or double notochord was found in a few CNH to border grafts, as presented in the last chapter. It resembled a rod-like structure derived entirely from donor cells near the notochord that at some points seemed to join the endogenous notochord and/or ventral neural tube and only when this happened it expressed Shh (see chapter 3, Table 3.1 embryo 6; and Fig. 3.5 F).

-In 2 out of 7 border to APS grafts and in 4 out of 7 node to border grafts, I believe that this ectopic structure was composed of neural tissue. In these embryos, in sections preceding the start of this structure, appropriate

integration is observed only to one site of the neural tube. From three-dimensional reconstructions of all the optical sections taken from some of the sections of these embryos, it looks like this ectopic structure dettaches from the labelled part of the host neural tube, creating an independent ring-like structure. In 1 out of 4 embryos that received a border to node graft we observed a similar ectopic structure after observing strong labelling to the host floorplate (Fig. 4.9 b-d; Fig. 4.6 j; Table 4.1).

-One out of 7 embryos only that received an APS to border graft also had a ring-like structure. However, this ectopic ring was almost as big as the host neural tube. Moreover, this embryo seem to have two host notochords, one underneath the host neural tube and one underneath this ectopic structure. Therefore, in this case, it might represent an ectopic neural tube. However, this embryo also had a big clump on the top of its neural tube, which might had been also involved in the disruption of neural tube formation.

-Five out of 9 APS to node and 6 out of 7 node to APS grafted embryos also contained a similar ring-like structure. In APS to node embryos, integration in mostly paraxial mesoderm and/or ventral neural tube was found in sections preceding the start of this ectopic structure. In node to APS embryos, integration in the floor plate and the ventral neural tube was observed in sections preceding the start of this ectopic structure (Fig. 4.8 j, k; Fig. 4.7 j, k; Table 4.1).

However, the exact nature of the ectopic tissues should be verified using different tissue markers by *in situ* hybridisation.

Grafts to a neutral site

Node, border and APS regions show different potency when grafted to a neutral site

Node, border and APS regions were grafted under the kidney capsule to allow differentiation at a neutral site. All grafted kidneys contained disorganised growth of well differentiated somatic tissues, apart from a few occasions when we could not find any growth, probably due to the loss of the tissue during grafting (Fig. 4.10). No teratoma-like cells were observed, whatever the strain. No difference in size between

grafts from the different strains of mice used was observed: 129, CBA (teratoma-permissive) and C57BL/6 (teratoma non-permissive) and no major differences were observed when the grafts were left in place for either 4 or 6 weeks, apart from the extent of cartilage contribution, which was slightly reduced in favour of bone differentiation after 6 weeks. This is in agreement with the gradual replacement of the cartilage model of the skeleton by bone during normal development. Therefore, all the results could be pooled together and shown graphically (Fig. 4.11). Node, border and APS regions were either grafted separately or together. The difference in size of the tissue grafted between grafts of the regions alone or together was compensated by dissecting 2-3 pieces from different mice when the regions were grafted alone compared to only one piece when node, border and APS were grafted together. Nonetheless, a slight increase in the size of the growth was observed when the intact node, border and APS region was grafted compared to the growth seen from the isolated regions, even though the starting material was of equivalent size (compare Fig. 4.10 A, D, G with J).

The tissue types produced reflect the origin of the graft

The tissues types produced are different depending on the origin of the graft: node produces mainly neural tissue and to a lesser extent bone (Fig. 4.10 A-c; Fig. 4.11); APS produces mainly adipocytes (Fig. 4.10 G-i; Fig. 4.11); whereas border produces all axial tissues expected: muscle, bone, cartilage, adipocytes and neural tissue as we observed when the 3 regions are grafted together (Fig. 4.10 D-f; Fig. 4.11).

4.4 DISCUSSION

Is the border region in mouse equivalent to the axial paraxial hinge in chick?

As presented in chapter 3, the region of the border between the node and APS shows overlapping expression of genes characteristic of the node (*Foxa2*) and the anterior streak (*Evx1, Wnt3a* and *Fgf8*). The border region can be distinguished morphologically, as a hinge between the end of the pit of the node and the anterior primitive streak, between 2 to 8

% of growths containing each
type of tissue
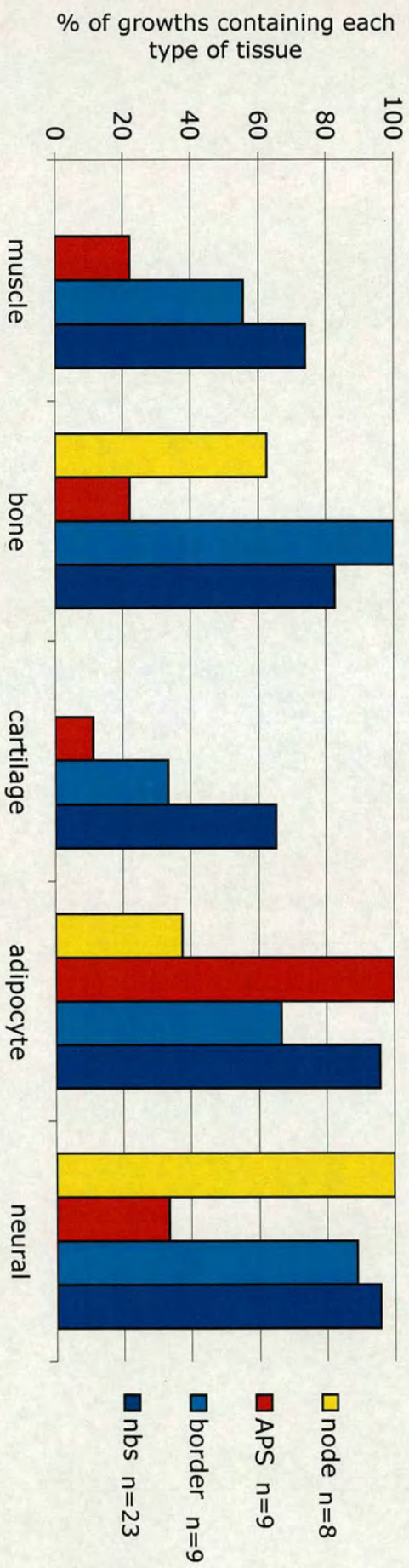
Figure 4.11 The tissue type produced by node, border and APS reflect the origin of the graft
Node produces mainly neural tissue and to a lesser extent bone; APS produces mainly adipocytes; whereas border produces all axial tissues expected: muscle, bone, cartilage, adipocytes and neural tissue, as observed when the 3 regions are grafted together (nbs). n: indicates the total number of grafts performed for each region.

somites (8.5 dpc). In the present chapter, I have dissected apart these 3 regions: node, border and APS and I have shown that they express the correct markers of gene expression: *Foxa2* is exclusively expressed in the node and border pieces, whereas *Fgf8* is expressed in the streak and border pieces (Fig. 4.3). This further proves that we can accurately dissect these regions. Furthermore, we have shown, by performing homotopic grafts, that the different regions (node, border and APS) integrate appropriately in 100% of the embryos and contribute to different cell types: node differentiates to notochord, border differentiates to ventral neurectoderm, notochord and paraxial mesoderm, and APS differentiates to paraxial mesoderm (Fig. 4.5; Table 4.1). In addition, when grafted to a neutral site, the tissue types that node, border and APS produce reflect the graft origin; border can generate all axial tissues expected: muscle, bone, cartilage, adipocytes and neural tissue, whereas node mainly forms neural tissue and APS differentiates mainly into adipocytes (Fig. 4.10; Fig. 4.11). Therefore, from these experiments, border cells are able to contribute to and produce all dorsal axial tissues, compared to the restricted capacity of node or APS cells. Moreover, from the homotopic grafts, I have shown that derivatives of the border, but not those of APS or node, are capable of integrating in all the dorsal axial tissues and yet retain labelled cells in the CNH (compare Fig. 4.5 e, f, q, r with k, l; Table 4.1). As described in the introduction of this chapter, the border region might be similar to the axial paraxial hinge (APH) described in chick. Both express genes characteristic of notochord and somite precursors. Here, I have shown that the border also shares the lineage hallmarks of the APH, which can differentiate to neural tube, somites and notochord, but produces rather few of these tissues if grafted homotopically. Only when challenged in Charrier *et al.*'s experiments (1999), by removal of region b in front of it, does it reconstitute large segments of notochord (Fig. 4.1).

Node contains only committed progenitors

Surprisingly, node homotopic grafts integrate only into the notochord in the axis and part of the tail bud, but integration ends before reaching the CNH, suggesting that by 10.5 dpc all the node cells grafted

have already differentiated into notochord (Fig. 4.5 B-f, Table 4.1, Fig. 4.4). The mouse ventral node has been identified previously as a putative self-renewing progenitor region for the notochord (Beddington, 1994; Wilson and Beddington, 1996), as its posterior extremity contains labelled cells after culture. As discussed in the previous chapter, it is likely that the ventral node may not contain all the notochord progenitors, but they may instead be located in the ectoderm layer. The present study would further refine the location of these primitive progenitors to the border, not the node. This idea is further supported by the sporadic integration of border grafts in the notochord and their retention in the CNH (Fig. 4.5 k, l). In chick, too, there is evidence that some notochord progenitors reside in the ectodermal layer, rather than in the ventral node region (Catala *et al.*, 1995; Catala *et al.*, 1996; Selleck and Stern, 1991; Psychoyos and Stern, 1996).

Moreover, Davis and Kirschner (2000) studies in *Xenopus* showed that when labelling very small numbers of cells (1-3) in the dorsal CNH, contribution to the axis was observed in different axial tissues. Interestingly, notochord contribution was only observed when other tissues were also labelled. This argues that in *Xenopus*, the primitive notochord progenitors are either in very close contact with other axial progenitors, or are in fact neural tube or somite progenitors themselves, and therefore located in the ectoderm layer.

Intriguingly, in the fate maps described in the last chapter and in Cambray and Wilson (2002), we showed that when labelling the ventral region of the node, contribution was found to the whole notochord including the CNH (see chapter 3, Fig. 3.1 A). This is probably due to the fact that in those experiments we were labelling all the ventral node cells and the most posterior node or border, which might contained a reserve of more undifferentiated notochordal cells. Interestingly, Selleck and Stern (1991) reported that some (but not all) single cell injections in the node resulted in sporadic contribution to the notochord. It is possible that the notochord is supplied by two different sources from early on, one specified notochord supply residing in the bulk of the node and an undifferentiated reserve residing at its most posterior end or in the Sox1GFP expressing cells on both sides of it, as suggested in chapter 2.

State of commitment of cells in the different regions

The heterotopic grafts performed were informative about the state of commitment of the different tissues grafted and also the influence of the new environment.

Border homotopic grafts showed integrated cells into all axial tissues, although notochord integration was low compared to the other tissues (Table 4.1). However, when border was grafted to the node, integrated cells were seen mainly in the notochord and to a much lower extent to the other tissues. In border to APS grafts, integration is mainly seen in paraxial mesoderm and TBM. Therefore, node or APS influences the cell types to which the border differentiates. Moreover, after heterotopic grafting, border tissue also suppresses its capacity to differentiate to inappropriate cell types, for example, little paraxial mesoderm is formed by border to node grafts. Moreover, there is little evidence that a large proportion of the border cells on these heterotopic grafts remain consistently non-integrated, as the frequency of non-integrated tissues was not significantly higher than homotopic node or APS grafts (Table 4.1). Therefore, border cells exhibit a low state of commitment.

On the other hand, when grafting node or APS to border, node and APS cells show some versatility in differentiation towards the cell types formed by the new environment, but they continued to produce the tissues they would ordinarily do in homotopic grafts, thus showing at least partial commitment to their original fate. For example, node to border grafts integrate mainly into the ventral neural tube and notochord, whereas APS to border grafts integrate mainly into the paraxial mesoderm and to a lower extent to the ventral neural tube (Table 4.1). This partial commitment of node and APS cells is more exaggerated in node to APS or APS to node grafts. Both of these types of grafts provoke the highest rate of non-integrated tissues (Table 4.1). At the anterior end of the graft-derived integration, APS to node grafts differentiate to paraxial mesoderm, while node to APS grafts produce notochord and ventral neural tube. However, usually towards the posterior end of the axis, cells integrate into tissues that the grafted site would normally produce (Fig.

152

4.4), emphasizing the importance of the new environment's influence on these partially committed tissues.

Influence of the new environment

In the last chapter, all the tissues were grafted to the border between the node and APS, since this graft site seemed to allow the grafted tissue to integrate into the node or the anterior streak, in agreement with the fate maps. The heterotopic grafts performed in this chapter, further corroborate this idea.

Node and APS to border grafts integrate into the same tissues to which their respective homotopic grafts would intagrate in. However, in node to border grafts, there is a consistent integration into the floor plate and ventral neural tube by the node tissue (Table 4.1). The potential of the node tissue to produce floor plate and neural tube is well established from fate map studies (Wilson and Beddington, 1996; Catala *et al.*, 1996). Moreover, the ability of the node to produce neural tissue was indeed observed when grafting this region under the kidney capsule (Fig. 4.10 b, c). However, in our node homotopic grafts, node integrated only into the notochord. This suggests that node has the potential to integrate into notochord, floor plate and ventral neural tube, although when grafted to the node, this graft site must be inhibiting continued floor plate and ventral neural tube integration.

The strong influence of node and APS environments can be observed from looking at node to APS and APS to node grafts. As mentioned before, these are the grafts that produce the highest rate of non-integrated tissues (Table 4.1), which in part might be due to the state of commitment of the cells grafted but also to incompatibility between the signals produced by node or APS environments and the competence of APS or node cells, respectively, to respond to them.

Incompatibility between cell commitment and the new environment result in non-integrated tissues

Heterochronic grafts tend to contain non-integrated tissues alongside integrated cells as presented in the results of this chapter and

last chapter. However, the degree of non-integrated tissues found seems to depend on the tissue grafted and the place where it is grafted, as some types of heterochronic grafts created more non-integrated tissues than others.

Some of these non-integrated tissues represent self-adherent clumps that travelled along the axis during elongation and are found in the tail bud. These are usually located externally or in the lumen on the neural tube in the tail bud. These were found in APS homotopic grafts, in border to APS and APS to border grafts as well as in some CNH grafts to border. This type of clump probably occurs from self-association due to grafting large numbers of cells (100-150 cells), and could be avoided by grafting smaller numbers (10-20). However, it is not clear why it only occurs in isochronic grafts involving APS as donor or host tissue since similar sized tissue fragments were dissected for all grafts. Perhaps the graft site healing and/or APS cell behaviours result in the rapid excision of part of the grafted tissue. This type of clump does not seem to affect or disrupt axis formation (Fig. 4.5 N, q; Table 4.1; chapter 3, Fig. 3.1 arrowhead in D; Fig. 3.4 A).

Other self-adherent clumps were found in APS to node grafts and TBM to border grafts (presented in the last chapter). However, in these types of grafts, all cells seemed to have stayed in the original clump, as the clump was found where normal integration would have expected to start, and we often did not find any integrated cells into the axis or tail. This type of clump probably occurs from the incompatibility between the state of commitment of the grafted cells and the new environment, and usually leads to a very few integrated cells into the axis or any integration at all (chapter 3, Fig. 3.3 A, B).

APS to node grafts also had another type of non-integrated tissue. In this case, the non-integrated clumps seem to elongate and became an ectopic structure in the dorsal part of the neural tube that extended along part of the axis and resembled ectopic somites. No integration was found in these embryos either, which suggests that a similar mechanism to that above is in operation (Fig. 4.9 F, g; Table 4.1).

Other ectopic somites were found in a few embryos that had received a CNH to border graft (presented in the last chapter). In this case, the ectopic somites were more medial than those of the host. However, appropriate integration in the host somites was also observed in these embryos. One possibility presented in the discussion of the last chapter was that these ectopic somites occurred because the CNH ectoderm is much smaller than the primitive streak, thus the grafted cells may include the progenitors of entire somites, effectively creating a heterotopic graft of medial and lateral somite precursors to a location where cells normally exit to medial somites. However, I have shown in this chapter that although border seems to participate in only medial somites, when grafted to the APS it can integrate into all mediolateral segments of the somites. The opposite happens when APS is grafted to border or node, now APS cells tend to integrate into more medial somites. Therefore, it is more likely that the reason why APS to node and CNH to border create ectopic somites is because APS, like CNH, has an intrinsic capacity to segment. The different location of the ectopic somites: externally in the dorsal neural tube in the case of APS to node grafts or inside the axis next to the host somites in CNH grafts, are because the CNH actually integrates but its timing of somite formation is different to the border location, while the APS to node grafts are essentially incompatible, as mentioned above, and so healing tends to exclude the streak tissue from the node (chapter 3, Fig. 3.4 B, E, arrowhead in J; Fig. 4.9 F, g; Table 4.1).

The last type of ectopic structure was the most commonly found. It resembled a ring-like neural derived tissue or cavitated notochord, although in some types of grafts its diameter was almost as large as that of the host neural tube and might have represented an ectopic neural tube.

This type of ectopic structure was found in some CNH to border grafts (presented in the last chapter), in border to node or node to border grafts and in APS to node or node to APS grafts.

In node to border, border to node, node to APS and CNH grafts, these ectopic structures could be explained by the fact that node, border and CNH in situ can produce neural tissue and therefore, in these grafts the number of cells that can integrate into this structure was increased,

which might explain the ectopic neural tissues observed in some of the embryos (Fig. 4.9 b-d; Fig. 4.6 j; Table 4.1; chapter 3, Fig. 3.5 F; Table 3.1). However, this cannot be the only reason, as border homotopic grafts where the number of neural progenitors is also increased, do not present ectopic structures. Therefore, it is likely that part of these ectopic structures are also due to incompatibilities between the state of commitment of the grafted cell and the new environment. And in the case of APS to node and node to APS these incompatibilities must be even more pronounced as they tend to create the higher rate of non-integrated tissues. It is conceivable that partially committed cells take longer to respond to environmental cues because they must reverse their state of commitment, in terms of the set of genes they express (Fig. 4.8 j, k; Fig. 4.7 j, k; Table 4.1).

However, the exact nature of the ectopic tissues should be verified using different tissue markers by *in situ* hybridisation.

Grafted cells follow a route of exit from the midline similar to the cells at the graft site

In homotopic grafts, anteriorly in the axis, border cells tend to integrate mainly into the medial part of the somites, whereas APS cells integrate into medial and lateral parts. Posteriorly in the tail, cells from border and APS seem to be scattered all around the somites, thus integrate into all parts of the somites (compare Fig. 4.5 i with o; compare Fig. 4.5 j, k, l with p, q, r; Fig. 4.4). This posterior integration suggests that both border and APS have the ability to integrate into all parts of at least some somites, although anteriorly, because somite progenitors are dispersed over a longer distance in the streak than in the tail bud, there is more medial or lateral integration, depending on the position of the progenitors in the midline. Time-lapse video-microscopy in chick has shown that anterior primitive streak cells will follow routes of exit more close to the midline than more posterior positioned cells, which will therefore integrate into more lateral position (Yang *et al.*, 2002). This could also explain why we saw medial versus mediolateral integration in border versus APS, whereas in chick fate maps, Selleck and Stern (1991) found exclusively medial

integration from the node versus exclusively lateral integration from the streak. In their study they labelled cells in the streak 200 μm behind the node, which due to their posterior position are probably taking more lateral routes of exit from the midline.

In heterotopic grafts, by changing the route of exit of the cells, border to APS cells seem to integrate into the medial and lateral parts of the somites indistinguishably (Fig. 4.6 j; Fig. 4.4), similar to what is seen in APS homotopic grafts. This shift in integration of border cells is probably due to the new slightly more posterior location of the cells in the midline. On the other hand, in APS to border grafts, the opposite is seen, now changing the route of exit of streak more anteriorly, more integration into the medial somites is seen (Fig. 4.8 d; Fig. 4.4), although there are also examples of integration into lateral and even whole somites.

Eloy-Trinquet and Nicolas (2002) suggested that the mediolateral regionalisation in the integration of primitive (stem cell) clones observed in their studies comes from regionalisation of the progenitors already present in the primitive streak. However, our heterotopic grafts have shown that cell integration can be changed by modifying their position in the midline. Thererefore, both border and APS cells have the potential to integrate into all the parts of the somites, as shown by changing the route of the cells in heterotopic grafts, which further suggests that regionalised progenitors are not committed to a particular mediolateral fate.

Nevertheless, all this analyses were done by grafting groups of cells, and should be complemented with single cell studies to fully prove this hypothesis.

Interestingly, these different types of grafts integrate into all parts of the tail somites in a similar non-exclusive manner (Fig. 4.5 j, k, l, p, q, r; Fig. 4.6 k, l; Fig. 4.8 e, f; Fig. 4.4) suggesting that both border and APS tissues have the potential to integrate into all the parts of the somites. Moreover, it suggests that the progenitors of the tail somites are more close together than in the APS.

Surprisingly, APS to border grafts are the only type of grafts where integration is observed in mesodermal cells that appear to form the dorsal aorta in the tail (Fig. 4.8 c, d, e). Although neither border nor streak

homotopic grafts integrate into these mesodermal cells, a change in the route of exit of the cells might explain this integration. However, this needs further investigation.

Border cells do not provoke the formation of teratocarcinomas when grafted under the kidney capsule

Unlike embryonic stem cells, node, border and APS grafts showed no evidence of teratocarcinoma cell growth (Fig. 4.10). This reinforces the conclusion reached in chapter 2 that primitive streak stem cells have different potency and are controlled by different factors than pluripotent stem cells. The majority of the tissue types found were those expected to be derived from the axis. Node cells produced mainly neural tissue and to a lower extent bone, whereas APS cells, that will normally integrate into the somites, differentiated mainly into adipocytes. However, it is well documented that both sclerotome and myotome induction are dependent on the presence of midline structures. *Sonic hedgehog* signalling from the notochord is essential for sclerotome induction (Chiang *et al.*, 1996; Johnson *et al.*, 1994), and neural tube and notochord are required for the induction of myotome, possibly due to a combination of *Sonic hedgehog* and *Wnt* signalling (Munsterberg *et al.*, 1995; Munsterberg and Lassar, 1995). Thus the failure of APS cells to form skeletal muscle, bone and cartilage is probably a function of the absence of signals from the notochord and neural tube. Intriguingly, mice that lack skeletal muscle due to the absence of the myogenic factors *Myf5* and *Mrf* have ectopic areas of adipocyte formation in place of the muscles (Kablar *et al.*, 2003). In this study it was not clear whether this was because the prospective myotomes defaulted to an adipocyte fate, or whether this tissue had expanded into the region from elsewhere. Our study would suggest that adipocyte differentiation in the absence of activation of the myogenic programme in somite precursors is a possible outcome.

On the other hand, border cells can produce all the dorsal axial tissues expected: muscle, bone, cartilage, adipocytes and neural tissue, as is seen in growths derived from grafts containing the three regions

together (Fig. 4.11), which further suggest that axial progenitors reside in the border region at primitive streak stages.

Interestingly, 10.5 dpc CNH cells grafted under the kidney capsule differentiate in a similar manner to border cells, whereas grafted surrounding tail bud mesoderm only produces adipocytes, as APS does (data not shown); a result consistent with the identity of the CNH as the descendant of the border region in the tail. On the other hand, most 13.5 CNH kidney capsule grafts showed no growth at all (data not shown). This suggests that by this stage, CNH cells have lost their ability to sustain continued growth.

Does the border constitute the progenitors, the 'niche', or both?

In homotopic grafts, the border region is capable of integrating into all the expected axial tissues: ventral neurectoderm, notochord and paraxial mesoderm. In addition, when this region was grafted under the kidney capsule, it was able to produce all the tissues expected. Moreover, derivatives of the border, but not those of streak or node, retain labelled cells in the CNH. Together these results imply that this region of the border in mouse is equivalent to the axial-paraxial hinge described in chick, containing the progenitors for the axis and perhaps also the factors to sustain axis elongation.

Interestingly, as shown in the results, border cells can differentiate more towards a notochord (axial mesoderm) or somite (paraxial mesoderm) fate, depending whether it is grafted in the node or APS environment (Fig. 4.6; Table 4.1; Fig. 4.4). The fact that this can occur without creating major non-integrated tissues suggests that multipotent cells reside in this region.

On the other hand, in the last chapter, all the tissues were grafted to the border between the node and APS, since this site seems to allow the grafted tissue to integrate into either node or the APS derivatives, depending on the origin of the graft. The more detailed investigation in these experiments confirms the tissue integration of node and APS when grafted to the border. However, it is now clear that the graft site actually modified the fate of the graft, both types of graft integrated into ventral

neural tube along the axis, and to the CNH, where they do not do this *in situ*. Therefore, the border tissue or its surrounds might also be important as a signalling centre allowing maintenance of axial elongation.

Consequently, I believe that possibly the border region contains the progenitors for the axis and at the same time is acting as a 'niche'.

Do all the cells integrating into the CNH in heterotopic grafts represent progenitors?

Surprisingly, most of the heterotopic grafts integrated into the CNH, whereas only border homotopic grafts integrated into the CNH. This creates a paradox: as seen in the last chapter, cells integrating into the CNH can be grafted for 3 generations. It is also known from homotopic grafts performed in this chapter that the CNH derives from the border region, as only border derivatives integrate into the CNH. Moreover, these results suggest that border tissue contains a stem cell population that later reside in the CNH. Therefore, are these cells in heterotopic grafts becoming stem cells, or are they simply more differentiated node-like or streak-like progenitor cells that are unable to execute a program of differentiation because of their ectopic location?

Interestingly, if we look carefully at the integration into the CNH by heterotopic grafts and compare it to the border homotopic integration, we see differences in the pattern of colonisation. Border homotopic grafts integrate equally to the most central region of the ventral neurectoderm and the notochord in the CNH, without creating non-integrated tissues (Fig. 4.5 k, l). In contrast, border to node and node to border grafts integrate mostly or exclusively into the notochord in the CNH (Fig. 4.6 e; Fig. 4.7 e); APS to border grafts integrate mainly into the ventral neurectoderm of this structure (Fig. 4.8 e, f); border to APS grafts integrate into both the ventral neurectoderm and the notochord, but they also contain clumps in the medial neural tube (Fig. 4.6 k, l); finally APS to node and node to APS grafts also integrate similarly into border homotopic grafts, but they also have ectopic ring-like structures (Fig. 4.8 k, l; Fig. 4.7 k, l). Therefore, it remains an open question whether these cells found in the CNH represent progenitor cells that could be grafted for several

generations or because we have changed their route of exit, these cells are delayed in their the exit from the midline or cannot exit and therefore they are not true stem cells. One way to distinguish between these possibilities is to perform 2nd and 3rd generation grafts to see whether these cells now behave like progenitors integrating into all the dorsal tissues and repopulate the CNH. We should then compare these results to the 2nd and 3rd generation grafts obtained from border homotopic grafts. Another alternative would be to extend the time of culture of these embryos. At the moment, 8.5 embryos can be only cultured for 48 hours, but after this period we could isolate their tails and culture them for another 48 hours. Tam and Tan experiments (1992) showed that 10.5 dpc tails can be cultured for 48 hours producing all tail tissues. The somites are usually smaller than in wild type embryos, making the whole tail smaller, but the overall morphology looks the same. Therefore we might be able to see if after 4 days in culture these cells have now left the midline and differentiated or if they are still located in the CNH.

Insights to previous experiments provided by these results

The results described in this chapter clarified some of the unexplained results described in the introduction of chapter 3 and 4 and in Cambray and Wilson (2002).

As described in chapter 3, it was the observation that node grafts contributing descendants to the paraxial mesoderm appeared the most potent that suggested that it was not the node itself that contains the axial stem cells, but cells immediately beside it. From results described in this chapter, now we know that the fate of the node is to give rise to notochord only *in situ*, as seen in node homotopic grafts. Moreover, node grafts do not give descendants to the CNH. However, border homotopic grafts are able to integrate into notochord, ventral neural tube and somites and retain cells in the CNH. Therefore, it is probably the border cells included with the node to border grafts described in the last chapter that allowed integration for three generations.

4.5 SUMMARY

The region of the border between the node and APS shows overlapping expression of genes characteristic of the node (*Foxa2*) and the anterior streak (*Evx1*). This region can be distinguished morphologically as a hinge between the end of the pit of the node and the APS, between 2 to 8 somites (8.5 dpc). I have accurately dissected apart these 3 regions: node, border and APS as shown by their correct expression of known markers: *Foxa2* is exclusively expressed in the node, whereas *Fgf8* is expressed in the APS, the border region expresses both markers. Furthermore, I have shown, by performing homotopic grafts, that the different regions: node, border and APS integrate well in all the dorsal axial tissues and produce different cells types: node produces notochord, border produces ventral neurectoderm, notochord and paraxial mesoderm, and APS produces paraxial mesoderm; without creating non-integrated tissues. Moreover, from these homotopic grafts, I have shown that derivatives of the border, but not those of APS or node, are capable of integrating into all the dorsal axial tissues and yet retain labelled cells in the CNH. In addition, when grafted to a neutral site, the tissue types that node, border and APS produce reflect the graft origin; besides border can differentiate into all axial tissues expected: muscle, bone, cartilage, adipocytes and neural tissue, whereas node forms mainly neural tissue and streak differentiates mainly into adipocytes. Interestingly, I have shown that border cells can differentiate as node and APS derivatives in heterotopic grafts. Therefore, the ventral layer of the node contains committed notochord progenitors, while cells in the border constitute less committed (stem cell) progenitors. APS cells are also partially committed as shown by APS to node grafts: APS cells try to differentiate into paraxial mesoderm in their new node environment creating a lot of non-integrated tissues. Moreover, grafted cells follow a route of exit from the APS similar to the cells at the graft site.

Consequently, APS and node regions represent influential environments in which cells are partly committed, although some plasticity is observed; whereas, the border region in the mouse and the axial-paraxial hinge in chick might contain both the progenitors for the

axis and also the 'niche', i.e. the factors to allow these progenitors to self-renew and sustain axis elongation.

Chapter 5

CONCLUDING REMARKS AND PERSPECTIVES

The general purpose of my project was to locate and define the stem cell progenitors for the anteroposterior axis that had been proposed from previous experiments (Lawson *et al.*, 1991; Tam and Beddington, 1897; Tam and Tan, 1992; Wilson and Beddington, 1995; Nicolas *et al.*, 1996; Mathis and Nicolas, 2000). I used homotopic and heterotopic grafting experiments to locate and define the potency of the progenitors at early (primitive streak) and late (tail bud) stages. In separate experiments, I carefully mapped gene expression relative to these regions. The major experimental findings and future perspectives are discussed below.

The border and later its derivative the CNH is the best candidate to contain a population of axial stem cells for the mouse anteroposterior axis

We have shown that at late tail bud stages, the chordoneural hinge (CNH) region can be grafted for at least 3 generations to younger embryos and contribute to all the dorsal axial tissues and again contribute to the CNH, a potency not shown by any other parts of the tail. Therefore, the CNH has the characteristics of a population of axial stem cells.

Homotopic grafts have shown that at early primitive streak stages, only the border region, not the node or the anterior primitive streak (APS), is able to contribute to all the dorsal axial tissues and to the CNH. Moreover, when grafted to a neutral site, this region, the CNH, can produce all the expected derivatives of the anteroposterior axis: muscle, bone, cartilage, adipocytes and neural tissue.

Putting all these results together, we can conclude that the CNH is the derivative of the border in the tail bud, and that these two tissues contain the putative axial stem cells for the mouse anteroposterior axis. It might also act as a 'niche' to allow self-renewal, and/or continued axial elongation (see Fig. 5.1 broken white boxes and arrows for summary of location and potency of the putative axial stem cells).
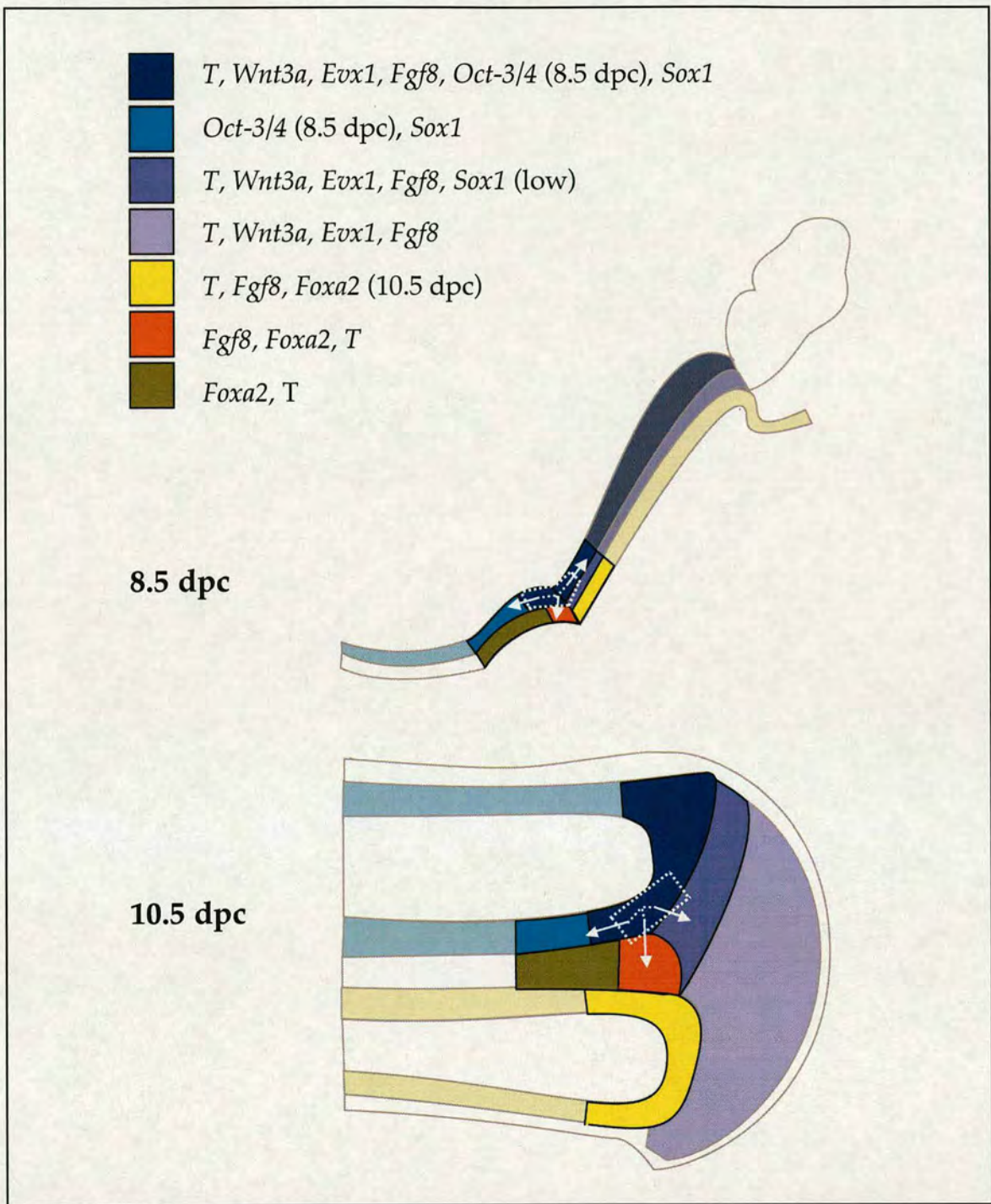
Figure 5.1 Summary of location, potency and gene expression of axial stem cells
White boxes represent the border region at 8.5 dpc and the CNH region at 10.5 dpc where the stem cell-like population resides. Descendants populate notochord, neural tube and somites (white arrows), and may originate from a common stem cell axial progenitor (broken lines). Light blue corresponds to the anterior part of the node at 8.5 dpc and anterior neurectoderm at 10.5 dpc, dark blue corresponds to the posterior region of the node (border) and the adjacent anterior primitive streak at 8.5 dpc and the most posterior neurectoderm at 10.5 dpc, brown corresponds to the anterior prospective notochordal cells in the node and the anterior notochord in the tail bud, orange corresponds to the most posterior prospective notochordal cells in the node and tail bud, the two tones of purple corresponds to the primitive streak mesoderm at 8.5 dpc and the tail bud mesoderm at 10.5 dpc, yellow corresponds to the endoderm in the primitive streak and the posterior hindgut at tail bud stages.

165

Characteristics of the putative axial stem cells

Based on these experiments, we can construct a profile for the putative axial stem cells.

Small numbered and Oligopotent

Nicolas *et al.* (1996) proposed that the population of axial progenitors for the myotome was composed of only around 100 to 150 cells. This number is rather similar to the number of cells used in border (as well as node and APS) grafts. Our results strongly suggest that all the axial stem cells are localised in the border at 8.5 dpc. Therefore, if Nicolas *et al.*'s estimates are correct, the number of stem cells for the myotome is approximately equal to the number of axial stem cells. This in turn implies that the myotome stem cells are capable of producing neural and notochord tissue, since all border grafts produce robust quantities of these tissues. This conclusion is supported by the observation that border cells readily differentiate to predominantly notochord or somites on heterotopic grafts to the node or APS, respectively, with few unincorporated cells.

However, despite their apparent potency to produce both neurectoderm and mesoderm, these cells are not equivalent to pluripotent ES cells. They only transiently express *Oct-3/4*, and do not express *Nanog* at the stages examined. They never formed teratocarcinomas on kidney capsule grafts. Surface ectoderm structures (skin, hair follicles) and glandular tissue reminiscent of gut that is often seen on grafts of embryonic stem cells, were conspicuously absent from the growths formed by border and CNH cells. Instead, well-differentiated ectoderm and mesoderm was produced.

However, lateral plate mesoderm contribution was not observed in any of our grafts. This population of cells arises from the posterior streak at primitive streak stages (Wilson and Beddington, 1996) and might be supplied by a different population of cells.

Therefore, it is likely that these cells are a novel, oligopotent progenitor population.

Self-renewing

While Nicolas *et al.*'s (1996) and Mathis and Nicolas (2000) experiments proposed self-renewal as a characteristic of stem cells for the axis, this cannot be properly tested *in situ* in the embryo, since different axial tissues are produced at successively later times. Our experiments show that successive generations of 10.5 dpc CNH grafts, as well as 12.5 dpc grafts to the border show a similar anterior extent of contribution and tissue types colonised by donor cells. This demonstrates that there is no irreversible 'ageing' process in the stem cells.

Located in the ectoderm of border and CNH

We have seen that at all stages during axis elongation, ectodermal cells contribute to mesoderm. The presence of strongly *Sox1*-GFP positive cells in the notochord, apparently associated with cells immediately above it in the neurectoderm is strongly suggestive of traffic of cells from the ectodermal layer into the notochord. Moreover, some cells of this ectodermal layer appear also to express genes such as *Not* (Plouhinec *et al.*, 2004) and *Foxa2* (data not shown), which are predominantly expressed in the ventral node, corresponding to the notochord precursors. Therefore, the ectodermal region of the border and CNH expresses genes characteristic of the notochord and neurectoderm, which might account for the oligopotent character of cells in these regions. This conclusion was reached independently in the chick by Selleck and Stern (1991), who saw contribution of single cells to two or more tissues when labelling cells in the ectodermal layer of the chick node. Furthermore, in *Xenopus*, Davis and Kirschner (2000) saw a high proportion of contribution to different tissues when labelling small groups of cells (up to 3) in the dorsal CNH, but not when labelling the ventral part of this structure. Therefore, multipotent progenitors appear to be located in the ectodermal layer of these tissues.

Finally, if we accept the argument that most border cells are stem cells, in order for them to contribute to neurectoderm as well as mesoderm, it would be reasonable to assume that they are located in the ectoderm.

Express a characteristic set of genes

If it is the case that most border cells are axial stem cells and they are located in the ectoderm, then the gene expression profile of border ectoderm is predominantly that of the stem cells. The expression of the markers tested were relatively homogeneous, i.e. there were no detectable gaps in their region of expression. Therefore, stem cells would express *Wnt3a, Fgf8, Evx1, T, Cdx2* and *Sox1* throughout axis elongation. They would express *Oct-3/4* at 8.5 dpc but not thereafter (see Fig. 5.1 for summary of gene expression).

Surrounded by a 'niche'

Charrier *et al.* (1999) propose that the equivalent to the border region in the chick, the axial paraxial hinge (APH), is a region that contains self-renewing progenitors and/or contains the gene products responsible to mediate caudalward extension of the axis and to assure survival of the embryonic structures formed. This suggests that the APH region is acting as a 'niche' or is surrounded by a 'niche' to assure axial elongation. This hypothesis could also be true for the mouse embryo. It is easy to imagine that axial stem cells might be situated in a 'niche' that provides them the appropriate environment to self-renew.

Conserved at least among amniotes

The experiments of Selleck and Stern (1991) demonstrate that single cells at the lateral border of the node apparently show stem cell properties. Our evidence indicates essentially the same in the mouse. Davis and Kirschner (2000) results, although not clonal suggest similar oligopotent/resident cells in the tail bud. However, the experiments of Tucker and Slack (1995b) suggesting the interaction of 3 separate populations, thus contrast with these data. Can they be reconciled?

Firstly, the N/M/C model for 'tail' outgrowth is proposed to act at stage 13, essentially the equivalent of a mouse late headfold stage/early somite stage embryo. Therefore, this is more correctly a model for axial extension rather than tail outgrowth. If axial stem cells were to exist in *Xenopus*, we could place them at the N/M junction in the ectoderm, the

topological equivalent of the border. However, the N/M junction is not a visible border, neither does it correspond to regions of mutually exclusive gene expression at stage 13. Therefore, there is no clonal data to exclude that cells at the N/M junction are confined to either neural or mesodermal fates. It might thus be similar to the border region in the mouse. In this case, it would be worthwhile testing the inductive properties of the border cells. Our heterotopic grafts showed no evidence of extra tails, although it is possible that some of the ectopic structures observed may have arisen essentially due to the creation of new, transient 'N/M' junctions.

Future prespectives

Nonetheless, these characteristics proposed for axial stem cells need further investigation:

-Reaching a clear distinction between multipotent or single restricted progenitors would require the graft of a single labelled cell from the CNH for at least 2 generations, which is technically very demanding to achieve by grafting techniques. Nevertheless, there are other techniques that can be used to label single cells. Experiments are underway in the lab to conditionally activate the expression of the site-specific recombinase cre, in order to indelibly mark descendants of single cells in the primitive streak and tail bud.

-A way to further confirm the self-renewing behaviour of axial stem cells would be to perform 2nd generation grafts from 12.5 dpc CNH, as it was done for 10.5 dpc CNH. In a self-renewing mode 12.5 dpc CNH would be expected to behave as 10.5 dpc ones, and contribute to all dorsal axial tissues and retain cells in the CNH. Moreover the most anterior labelling in the axis should be always the same.

-Confirmation of the location of these axial progenitors to the ectoderm layer of the border and the CNH, and to define between true axial stem cells and putative supporting cells forming a 'niche' could be done by fine analysis using single cell PCR, which might allow finding differences between cells in different layers or even between neighbouring cells. If this technique is successful it could be followed by a microarray

analysis, which would add new light to the putative genes regulating these cells.

-Determination of the exact nature of the ectopic tissues found in our heterotopic grafts would require *in situ* hybridisation using known markers for axial tissues.

Finally, the ultimate goal of this research would be to culture these axial stem cells *in vitro* to establish clonal cell lines, which would allow us to learn more about the regulation mechanisms that control their self-renew and differentiation. A way to start culturing these cells could be to perform explants of border, CNH or even from cells recovered from the growths formed in kidney capsule grafts, as some undifferentiated cells might be left in those cultures. To start they could be grown in feeders or using conditioned media from feeders, and use factors known to be important to maintain axial elongation such as Fgfs or Wnts to find a way to maintain these cells undifferentiated.

Chapter 6

Materials and Methods

6.1 MATERIALS

Standard molecular biology solutions were made according to Sambrook *et al.* (1989). All chemicals were of analytical grade and supplied by BDH or Sigma. Electrophoresis grade agarose was supplied by GibcoBRL. Restriction enzymes and modifying enzymes were supplied by Roche and New England Biolabs. All bacterial media components were supplied by Difco laboratories. CellTracker CM-DiI and nucleic acid marker TO-PRO-3 were supplied by Molecular Probes. Embryo culture media (GMEM or DMEM), non-essential aminoacids (NEAA), glutamine and sodium pyruvate were supplied by GibcoBRL. M2 medium was made as described in Hogan *et al.* (1994). Rat serum was prepared in-house according to Hogan *et al.* (1994).

Probes for hybridisation

T (Brachyury) (Herrmann, 1991)

Fgf8 (Mahmood et al., 1995)

Cdx2 (Tanaka et al., 1998)

Wnt3a (Takada et al., 1994)

Evx1 (Dush and Martin, 1992)

Foxa2 (Sasaki and Hogan, 1993)

Nodal (Conlon et al., 1994)

Sox1 (Aubert et al., 2003; probe made by Su Ling Zhao in Meng Li's lab)

Oct-3/4 (Scholer et al., 1990b)

Nanog (Chambers et al., 2003)

Sonic hedgehog (Shh) (Echelard *et al.*, 1993)

Pax3 (Goulding *et al.*, 1991)

Pax6 (Walther and Gruss, 1991)

Delta like 1 (Dll1) (Dunwoodie *et al.*, 1997)

Mice strains

MF1

C57BL/6

129

CBA

TgN(beta-actEGFP)04Obs (Okabe *et al.*, 1997) (here termed 'GFP transgenic')
Zin40 (Munsie *et al.*, 1998)
Sox1-GFP (Ying *et al.*, 2003)

Escherichia coli strains
XL1-blue

6.2 EMBRYOLOGY
Maintenance of mice stocks

Mice were housed and bred within the animal unit of the Institute for Stem Cell Research according to the provisions of the Animals (Scientific Procedures) Act (1986). They were maintained in a stabilised environment on a 14 hours light/ 10 hours dark cycle.

Recovery of embryos

For the collection of embryos at specific stages of gestation, matings were set up overnight and the females examined for the presence of a vaginal plug the next morning. Noon on the day of finding a vaginal plug was designated 0.5 dpc. Embryos were dissected from the uterus in PBS to be fixed for *in situ* hybridisation or M2 medium when embryos were to be cultured. Dissection and culture was performed as described (Copp and Cockroft, 1990; Cambray and Wilson, 2002)

Dissection of tissues for grafting

GFP transgenic × MF1 embryos containing the transgene were selected in a Zeiss Stemi SV11 dissecting microscope with fluorescence attachment (green filter: GFP 525 filter). The anterior and posterior halves of *Zin40* × MF1 embryos were first separated using fine forceps, the anterior structures were then used to perform X-gal staining. Embryos containing the transgene were then used as donors.

8.5 dpc embryos

The posterior half of the embryo containing the primitive streak was dissected using fine forceps. The primitive streak was dissected using an eyelash tool or fine glass needles by making two longitudinal lateral cuts, isolating a thin strip of tissue containing the entire primitive streak, the border region and node, retaining all 3 germ layers. Node, border and anterior primitives streak (APS) fragments were further dissected by making transverse cuts with the eyelash tool or glass needle. The final size of the fragments grafted to wild-type embryos contained groups of about 100-150 cells. The position of these regions in the intact embryo and in a schematic representation is shown in Fig. 4.2.

10.5 dpc embryos

Regions of the 10.5 tail bud were dissected by first isolating the whole tail bud using fine forceps. The chordoneural hinge (CNH) was dissected using an eyelash tool or fine glass needles. First, the extreme end of the tail was excised, and two dorsoventral longitudinal cuts made to remove the paraxial mesoderm. To dissect the CNH, the hindgut and dorsal neurectoderm were then removed by similar longitudinal cuts in the mediolateral plane. Dissected CNH was trimmed and divided into two to three pieces containing groups of about 200-300 cells to graft to wild-type hosts. The position of these tissues in the intact and partially dissected tail is shown in Fig. 3.2.

Dissection of recipient embryos

Wild-type MF1 embryos were dissected from the decidua. Reichert's membrane was then removed by peeling it off the embryo with two pairs of very fine forceps leaving the yolk sac and amnion intact.

DiI labelling

Embryos were labelled with CellTracker CM-DiI (Molecular Probes) as described in Wilson and Beddington (1996). CM-DiI was dissolved in 10µl of Ethanol and then diluted 1/10 in 0.3M sucrose.

Dissected 8.5 dpc node and 10.5 dpc CNH

Dissected node and CNH from Zin40 embryos were labelled by expelling DiI from a pipette held directly above the tissue to be labelled for a few seconds. The graft was then washed in fresh M2.

Dissected 10.5 dpc tails

Dissected tail pieces were labelled in the neural tube by inserting a fine pipette into the lumen and expelling a small amount of dye, which covered most of all of the luminal surface. Labelling of the most posterior end was checked either by observing a faint pink colour under brightfield illumination, or by viewing in a dissecting microscope with fluorescence attachment (red filter: rhodamine).

Grafting labelled tissues

Grafts were performed using a hand-drawn micropipette. The embryo was held loosely in place with forceps while suction was gently applied with the micropipette to the region of interest to create an opening for the graft (Fig. 3.2 c shows the site of grafting). The tissue to be grafted was then drawn into the pipette, and the pipette inserted in the opening. The graft was gently expelled as the pipette was drawn out of the embryo, leaving the tissue lodged in the opening.

Culture of embryos and tails

Embryos

After grafting the embryos were then placed in a universal container (Nunc) in 50% rat serum, 50% GMEM or DMEM supplemented with 1% NEAA (100x) and 2mM I-Glutamine and 1mM Sodium pyruvate. The universal was kept in an incubator gassed at 5% CO_2 in air for 30 minutes to allow the grafts to heal. Embryos were then gassed at the right concentrations needed depending on the stage of development: 5% oxygen, 5% CO_2 in nitrogen for embryos with 0-6 somites, and 5% CO_2 in air for embryos with >6 somites, before sealing the universal and placing it in a roller culture apparatus at 37°C overnight. Embryos which had developed normally were cultured for a further 24 hours in 75% rat

174

serum, 25% GMEM or DMEM in 5% CO_2 in air if they had undergone turning or in 50% rat serum, 50% GMEM or DMEM in 5% CO_2 in air if they had not yet turned.

DiI labelled tails

Tails were cultured as Tam and Tan (1992). After DiI labelling the tails were placed in a universal container in 50% rat serum, 50% GMEM or DMEM supplemented with 1% NEAA (100x) and 2mM I-Glutamine and 1mM Sodium pyruvate. The tails were then gassed at 5% CO_2 in air before sealing the universal and placing it in a roller culture apparatus at 37°C overnight. Tails which had developed normally were cultured for a further 24 hours in 75% rat serum in 40% oxygen, 5% CO_2, 55% nitrogen.

Whole mount imaging

Images of whole mount embryos or tails before embedding for sectioning were captured using Openlab software (Improvision) with a digital camera attached to a Zeiss Stemi SV11 dissecting microscope with fluorescence attachment (green filter: GFP 525 or red filter: rhodamine). Images were processed using Adobe Photoshop CS (Adobe Systems Inc.)

6.3 *IN SITU* HYBRIDISATION

Embryos

Wild type embryos were dissected in PBS and then transferred to 12 mm Diameter nets (12.0 μm pore size) (Corning Inc.) Whole mount *in situ* hybridisation was performed as described previously (Wilkinson, 1992) with the following modifications: embryos were treated with 10 μg/ml of Proteinase K for different times depending on the stage of the embryo/tail: 7.5 dpc embryos for 7 min, 8.5 dpc embryos for 10 min, 9.5 dpc embryos for 12 min, 10.5 dpc embryos (neuropore open) for 15 min, 10.5 dpc embryos (neuropore close) for 16 min, 11.5 dpc tails for 16 min, 12.5 dpc tails for 17 min and 13.5 dpc tails for 18 min. Probes were used at 1/50 dilution and were denatured for 10 min at 80°C and then cooled down on ice before being added to the hybridisation solution. Treatment with levamisole to inhibit endogenous alkaline phosphatase activity was

omitted and the anti-DIG antibody was not preadsorbed with embryo powder. The probes used were: *T, Fgf8, Cdx2, Wnt3a, Evx1, Foxa2, Nodal, Sox1, Oct-3/4,* and *Nanog.*

Node, border and APS fragments

Fragments of node, border and APS from wild-type embryos were dissected as described above. Whole mount *in situ* hybridisation was performed as described above for whole embryos and tails, with the following modifications: fragments were treated with 10 μg/ml of Proteinase K for 5 min. The probes used were: *T, Fgf8* and *Foxa2.*

X-gal staining with *in situ* hybridisation

Embryos carrying the ubiquitously expressed *Zin40* gene trap integration were first stained with X-gal as described previously (Tajbakhsh and Houzelstein, 1995) with the following modifications: 10.5 dpc embryos were fixed in fresh 4% PFA at 4°C for 30 min; in the β-gal staining procedure the concentration of PFA was reduced by half to 2%. Embryos were then subjected to *in situ* hybridisation as described by (Wilkinson, 1992) and modified as above, with probes specific for *T, Shh, Dll1, Pax3* and *Pax6.* Embryos were then dehydrated via an ethanol series and processed for paraffin wax histology as described below.

6.4 HISTOLOGY

Vibratome sectioning

Fluorescent embryos: DiI-labelled embryos or tails, embryos that received grafts of GFP transgenic cells or Sox1-GFP embryos, were first embedded in 20% gelatin in PBS (heated at 37°C to melt) and 20% albumin in PBS at a final embedding mixture of 1:1. Embryos were oriented in a microscope on a surface of dry ice to allow the albumin-gelatin mixture to set. Small square blocks were cut and fixed overnight in 4% PFA. These blocks were then embedded in a 'setting solution' with 10% glutaraldehyde to create a harder outer layer that was more resistant to tearing than the gelatin block. Transverse sections were cut in a Series 1000 Vibratome at 50 μm, then mounted under coverslips in an aqueous

mountant (Aquamount, BDH) for conventional fluorescent microscopy. For detailed analysis, embryos or tails were embedded in the same way and sectioned at 100 µm and then incubated with a nucleic acid marker, TO-PRO-3 (Molecular Probes) for 30 min before being mounted under coverslips in Vectashield (Vector Laboratories) for confocal microscopy. Confocal microscopy on the sections was performed within 48 hours of sectioning to prevent autofluorescence caused by diffusion of glutaraldehyde from the block onto the specimen.

The 'setting solution' is made by combining 450 ml PBS, 2.2 g gelatin, 70 g bovine serum albumin (minimum 96% electrophoresis) (BSA), 90 g sucrose. The gelatin is added to the PBS and heated to dissolve and allowed to cool slightly. The BSA is then added, allowing a thin layer of albumin to form on the surface that dissolves very slowly. Once this is dissolved, the sucrose is added. The final solution can be then aliquoted and stored at -20°C.

Microtome sectioning

After fixation overnight in 4% PFA, *in situ* hybridised embryos or embryos subjected to X-gal staining with *in situ* hybridisation were dehydrated through an ethanol series (70%, 90%, 95%, 2×100%, 45 min each) and incubated in xylene twice for 30 min each. The embryos were then incubated in paraffin wax for 1 hour total, changing the wax 3 times. Embryos were oriented in a dissecting microscope with the help of a fine point tool. After orienting, they were left at 4°C overnight and trimmed the next day before being sectioned transversally at 7µm in a microtome (Anglia Scientific 0325). Sections were then dewaxed in for 2x5 min xylene washes and mounted under coverslips in DPX mountant (Agar Scientific)

Paraffin sections were performed by Ron Wilkie.

Imaging sections

Images from vibratome sections were captured using Openlab software (Improvision) with a digital camera attached to a Zeiss Stemi SV11 dissecting microscope with fluorescence attachment (green filter: GFP 525 or red filter: rhodamine).

For more detailed analysis, GFP and TO-PRO-3 fluorescence were detected using laser excitation wavelengths of 488 nm for GFP and 633 nm for TO-PRO-3 and were detected at 500-600 nm and 650-700 nm, respectively, in an inverted confocal microsope (Leica DM IRE2; Leica Microsystems). Images were captured using Leica Confocal Software v2.61 (Leica Microsystems), before being noise filtered in a Workstation G5 using Volocity LE software (Improvision).

Images of microtome sections were captured onto 100 ASA print film (Fujifilm) using an Olympus Vanox AHBT3 compound microscope. Negatives were scanned using Paintshop Pro software.

All images were processed using Adobe Photoshop CS (Adobe Systems Inc).

6.5 GRAFTING UNDER THE KIDNEY CAPSULE

Dissection of tissues for grafting

Wild-type (C57BL/6, 129 and CBA) embryo fragments were dissected in M2 using a dissecting microscope (Olympus SZ40). 8.5 dpc tissues containing the node, border and APS regions together or node, border and APS separated fragments were dissected as described previously in this chapter.

Grafting under the kidney capsule

The engraftments were performed by Dr. Val Wilson as described by Roberson (1987), with the following modifications. Surgical operations were carried out on mice of the same strain as the fragments grafted in a Class II laminar flow hood under sterile conditions using a dissecting microscope (Olympus SZ40). Mice were anaesthetised with an intraperitoneal injection of 0.5 ml of Avertin. 0.1ml 1% Toborgesic was also injected intraperitoneally. An incision was made in the flank on the left side and the corresponding kidney exposed. A small tear was made in the kidney capsule using fine forceps and fragments were transferred using a glass pipette controlled by mouth suction. The kidney was then replaced, the peritoneal cavity sutured and the skin clipped to close the wound.

Recovery of Kidneys

4-6 weeks after the graft was performed, the mice were sacrificed and the kidneys removed in PBS. Growth could be seen by eye or in some cases a dissecting microscope was used. After imaging, the growth and the surrounding part of the kidney were fixed overnight in 4% PFA.

Histology

After fixing, the kidneys were dehydrated through ethanol series, cleared in xylene and embedded in paraffin wax before being sectioned in a microtome as described previously.

Staining of paraffin sections

The following methods were adapted from Bancroft and Gamble (2002).

Haematoxylin and eosin

Slides were dewaxed in xylene twice for 5 min and rehydrated through an ethanol series (2×4 min in 100%, followed by 2 min change in each 90%, 70%, 50% and 30% ethanol, then running tap water). Sections were then stained for 5 min in Mayer's hematoxylin (Sigma), washed in running tap water and treated in saturated Lithium Carbonate solution for a few seconds. After a further wash in running tap water, sections were stained for 15 seconds in eosin (0.05% solution) and washed again in running tap water. Finally, sections were placed in 100% ethanol for 2×1 min, cleared for 2×5 min in xylene and mounted using DPX (BDH).

After haematoxylin and eosin staining, nuclei are stained in blue/black, cytoplasm in varying shades of pink, muscle fibers in deep pink/red, red blood cells in orange/red, and fibrin in deep pink.

Masson's trichrome

Slides were dewaxed in xylene for 5 min and rehydrated through an ethanol series (5 min in 100%, followed by 2 min change in each 90%, 70%, 50% and 30% ethanol, then running tap water). Sections were then stained for 20 min in Alcian blue solution, rinsed in distilled water,

stained Mayer's haematoxylin solution for 3 min and washed in running tap water for 10 min. Sections were then stained with Xylidine Red for 4 min, rinsed in distilled water, followed by a treatment with Phosphomolybdic acid for 5 min. Sections were rinsed in distilled water, before staining with Light Green for 4-5 sec. Finally sections were rehydrated in ethanol (70% for 3 sec, 90% for 1-2 min and 5 min in 100% ethanol) then cleared in xylene for 5 min and mounted using DPX (BDH).

Solutions (for 250 ml):

Alcian blue: 0.25 g Alcian blue (BDH), 7.5 mls acetic acid, in distilled water.

Haematoxylin: 250 ml Mayer's haematoxylin (BDH).

Xylidine Red: Ponceaude xylidine (BDH) 0.25 g, acetic acid 2.5 ml, in distilled water.

Phosphomolybdic acid: Phosphomolybdic acid (BDH) 2.5 g in 250 mls of distilled water.

Light Green: Light Green (BDH) 5 g, acetic acid 2.5 ml, in distilled water.

After staining using this technique: nuclei are stained blue-black; cytoplasm, muscle, bone and erythrocytes red; collagen, cartilage light green/blue.

Haematoxylin and eosin staining and Masson's trichrome technique were performed by Ron Wilkie.

Imaging

Images of whole kidneys and stained sections were captured using Openlab software (Improvision) with a digital camera attached to a Zeiss Stemi SV11 dissecting microscope.

All images were processed using Adobe Photoshop CS (Adobe Systems Inc.).

6.6 MOLECULAR BIOLOGY

The following methods were adapted form Sambrook *et al.* (1989).

Preparation of chemically competent cells

100 ml of LB broth were inoculated with 1 ml of an overnight bacterial culture and grown until O.D.$_{550}$ reached 0.3-0.6. Cells were centrifuged at 4000g for 10 min at 4°C and the pellet resuspended in a 5 ml solution (LB broth pH 6.1, 10% PEG, 5% DMSO, 10mM $MgCl_2$, 10 mM $MgSO_4$). Cells were kept on ice for 10 min and either used directly for transformation or glycerol was added to a final concentration of 10% and 200 µl aliquots were snap frozen in a dry ice/ethanol bath before stored at -70°C.

Plasmid transformation on competent bacteria (Chemical transformation)

0.5 ng of supercoiled plasmid DNA was used for transformation. The DNA was made up to 80 µl with H_2O and mixed on ice with 20 µl of 5×KCM solution (0.5 M KCl, 150 mM $CaCl_2$, 250 mM $MgCl_2$). The DNA solution was added to 100 µl of chemically competent cells and the mix was kept on ice for 20 min then at RT for 10 min. 1 ml of LB broth was added and the cells were incubated at 37°C for 1 hour before being plated in the appropriate selective medium

Plasmid DNA preparation

For small-scale plasmid preparation, a single bacterial colony was inoculated using a sterile pipette tip and grown in 5 ml of LB containing 100 mg/ml of the appropriate antibiotic overnight at 37 °C. 1.5 ml of the bacterial suspension was transferred to an eppendorf tube and centrifuged for 10 min. Qiagen Mini-prep Kit was used to extract DNA according to manufacturer's instructions.

For medium-scale or large-scale plasmid preparation, a single bacterial colony was inoculated using a sterile pipette tip and grown in 5 ml of LB containing 100 mg/ml of the appropriate antibiotic for several hours (7-8 h). 500 µl of this growth were then transferred to 50 ml (for

medium-scale) or to 250 ml (for large-scale) of LB containing 100 mg/ml of the appropriate antibiotic and shaken overnight at 37 °C. Qiagen Midi- and Maxi-prep Kit were used to extract DNA according to manufacturer's instructions.

Restriction enzyme digestion

10 μg of DNA were digested using the corresponding restriction enzymes and the appropriate buffers commercially supplied and following the specifications of time of reaction and temperatures recommended by the manufacturer (Roche and New England Biolabs) in a 40 μl digestion mix.

Phenol/Chloroform extraction and ethanol precipitation of DNA template for *in vitro* transcription

To purify nucleic acid from proteins, a mixture of phenol:chloroform was added in a 1:1 volume ratio to the nucleic acid solution and vortexed for 30 sec. Following 1-2 min of centrifugation, two phases can be differentiated, the upper aqueous phase and the lower phenol-chloroform phase. The upper phase was transferred into a new sterile eppendorf tube. DNA was precipitated from the aqueous phase with 1/10 volume of 3 M NaOAc pH 5.2 and 2.5 volumes of 100% (v/v) EtOH for 30 min on ice. The mixture was centrifuged for 30 min at 13,000 rpm and the pellet washed in 70% (v/v) EtOH, dried and resuspended in DEPC- treated water.

In vitro transcription (RNA for riboprobes)

The reaction was performed in sterile eppendorf tubes with 1-3 μg of linearised and purified DNA template, 2 μl of 10x transcription buffer (Roche), 2 μl of 10x digoxigenin RNA labelling mix (Roche), 1 μl of RNase inhibitor (Roche), 2 μl of the appropriate RNA polymerase and DEPC-treated water for a total mixture of 20 μl. After a 2 h incubation period at 37 °C, 2 μl of DNase I (Roche) was added and the reaction was incubated for a further 20 min at 37 °C. At this point, 1 μl of 0.5 mM EDTA was added to stop the reaction, which was purified from the mixture by

Chroma Spin-100 columns (Clontech). RNA integrity was verified by agarose gel electrophoresis and the RNA concentration determined by spectrophotometry.

Fgf8 and *Shh* were linearised by *Hind*III digestion and RNA transcribed with T3 polymerase; *T* and *Nanog* by *Bam*HI and T7; *Nodal* and *Oct-3/4* by *Eco*RI and T3; *Evx1* and *Pax3* by *Hind*III and T7; *Cdx2* by *Xho*I and T7; *Wnt3a* by *Eco*RI and Sp6; *Foxa2* by *Bam*HI and T3; *Sox1* by *Sac*I and T3; *Pax6* by *Xba*I and T7; *Dll1* by *Not*I and T3.
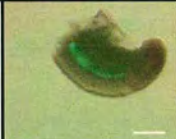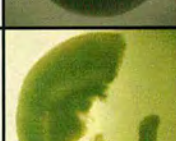
Agarose gel electrophoresis of DNA and RNA

DNA or RNA separation was performed by electrophoresis using agarose gels. Gels were prepared with agarose melted in 1xTAE in the appropriate concentration that was usually 0.8% (w/v). For RNA gels, all solutions were made in DEPC-treated water. Ethidium bromide (0.5 mg/ml) was added to the gel in order to visualise the nucleic acids. Gel loading buffer was added at 1x to the DNA/RNA samples. The resolved nucleic acid was visualised using UV light and the size was estimated by comparison with known size molecular markers (1 Kb ladder from Invitrogen).
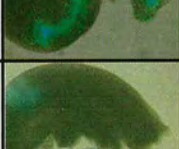
APPENDIX I
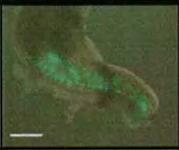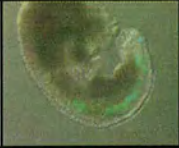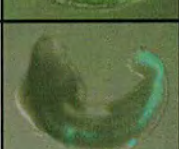
Table A. Results of the integration of GFP-transgenic cells in homotopic and heterotopic grafts, embryo by embryo

Node to node

Embryo		Integ.	Axis			Tail bud		Non-integ.
			NCH	NT	PXM	CNH	TBM	
1		1	1	0	0	0	0	0
2		1	1	0	0	1 (2cells)	0	0
3		1	1	0	0	0	0	0
4		1	1	0	0	0	0	0
5		1	1	0	0	0	0	0
Total		5	5	0	0	1 (2cells)	0	0
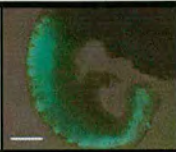
Integ: embryo that contained integrated GFP-labelled cells, NCH: notochord, NT: neural tube, PXM: paraxial mesoderm, CNH: chordoneural hinge, TBM: tail bud mesoderm, non-integ: non-integrated cells. Bar: 500μm.

Border to border

Embryo		Integ.	Axis			Tail bud		Non-integ.
			NCH	NT	PXM	CNH	TBM	
1		1	1	1	1	1	1	0
2		1	1 (low)	1	1	1	1	0
3		1	1	1	1	1	1	0
4		1	1 (low)	1	1	1	1	0
5		1	1 (low)	1	1	1	1	0
6		1	1 (low)	1	1	1	1	0
7		1	0	1	1	1	1	0
8		1	1 (low)	1	1	1	1	0
Total		8	7 (5 low)	8	8	8	8	0

Integ: embryo that contained integrated GFP-labelled cells, NCH: notochord, NT: neural tube, PXM: paraxial mesoderm, CNH: chordoneural hinge, TBM: tail bud mesoderm, non-integ: non-integrated cells. Bar: 500μm.

APS to APS

Embryo		Integ.	Axis			Tail bud		Non-integ.
			NCH	NT	PXM	CNH	TBM	
1		1	0	0	1	0	1	0
2		1	0	1 (low)	1	1	1	1 (ectopic nt, axis)
3		1	0	0	1	0	1	0
4		1	0	0	1	0	1	1 (clump in dnt, TB)
5		1	0	0	1	0	1	0
6		1	0	0	1	0	1	1 (clump in dnt, TB)
Total		6	0	1 (low)	6	1	6	3 (2 clumps, TB; 1 ectopic nt, axis)

Integ: embryo that contained integrated GFP-labelled cells, NCH: notochord, NT: neural tube, PXM: paraxial mesoderm, CNH: chordoneural hinge, TBM: tail bud mesoderm, non-integ: non-integrated cells, APS: anterior primitive streak, nt: neural-like tissue, dnt: dorsal neural tube, TB: tail bud. Bar: 500μm.
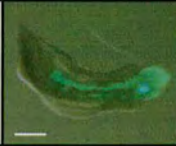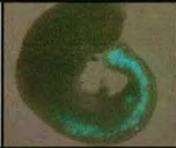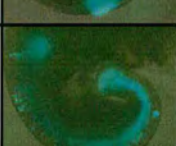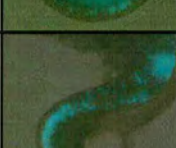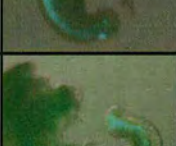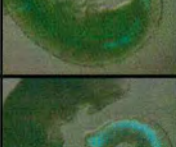
Border to node

Embryo		Integ.	Axis			Tail bud		Non-integ.
			NCH	NT	PXM	CNH	TBM	
1		1	1	1	1	1	1 (few cells)	1 (ectopic nt/noto, TB)
2		1	1	1 (low)	1 (low)	1	0	0
3		1	1	0	0	1	0	0
4		1	1	0	0	1	0	0
Total		4	4	2 (1 low)	2 (1 low)	4	1 (few cells)	1 (ectopic nt/noto, TB)
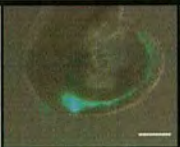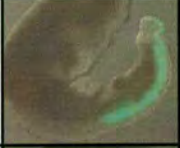
Integ: embryo that contained integrated GFP-labelled cells, NCH: notochord, NT: neural tube, PXM: paraxial mesoderm, CNH: chordoneural hinge, TBM: tail bud mesoderm, non-integ: non-integrated cells, nt/noto: neural-like structure or cavitated notochord, TB: tail bud. Bar: 500μm.

Border to APS

Embryo		Integ.	Axis			Tail bud		Non-integ.
			NCH	NT	PXM	CNH	TBM	
1		1	0	1 (low)	1	1	1	1 (clump in vnt, TB)
2		1	1 (low)	1 (low)	1	1	1	1 (ectopic nt/noto, TB)
3		1	0	0	1	1	1	1 (clump in vnt, TB)
4		1	1 (low)	1 (low)	1	1	1	1 (ectopic nt/noto, axis and TB)
5		1	0	1	1	1	1	1 (clump in vnt, TB)
6		1	1 (low)	1 (low)	1	1	1	0
7		1	1 (low)	1	1	1	1	1 (clump in vnt, TB)
Total		7	4 (low)	6 (4 low)	7	7	7	6 (4 clumps, TB; 2 ectopic nt/noto, axis and/or TB)
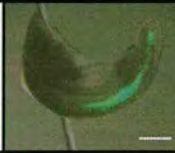
Integ: embryo that contained integrated GFP-labelled cells, NCH: notochord, NT: neural tube, PXM: paraxial mesoderm, CNH: chordoneural hinge, TBM: tail bud mesoderm, non-integ: non-integrated cells, vnt: ventral neural tube, nt/noto: neural-like structure or cavitated notochord, TB: tail bud, APS: anterior primitive streak. Bar: 500μm.

Node to border

Embryo		Integ.	Axis			Tail bud		Non-integ.
			NCH	NT	PXM	CNH	TBM	
1		1	1 (low, TB)	1	0	1	0	0
2		1	1 (low, TB)	1	0	1	1 (few cells)	0
3		1	1 (low, TB)	1	0	1	1 (few cells)	1 (ectopic nt/noto, axis and TB)
4		1	1 (low, TB)	1	0	1	0	1 (ectopic nt/noto, axis and TB)
5		1	1 (low, TB)	1	0	1	0	1 (ectopic nt/noto, axis and TB)
6		1	1 (low, TB)	1	1 (low)	1	1 (few cells)	1 (ectopic nt/noto, axis and TB)
7		1	1 (low, TB)	1	0	1	0	0
Total		7	7 (low, TB)	7	1 (low)	7	3 (few cells)	4 (ectopic nt/noto, axis and TB)
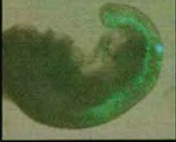
Integ: embryo that contained integrated GFP-labelled cells, NCH: notochord, NT: neural tube, PXM: paraxial mesoderm, CNH: chordoneural hinge, TBM: tail bud mesoderm, non-integ: non-integrated cells, nt/noto: neural-like structure or cavitated notochord, TB: tail bud. Bar: 500μm.

189

Node to APS

Embryo		Integ.	Axis			Tail bud		Non-integ.
			NCH	NT	PXM	CNH	TBM	
1		1	1 (low)	1	0	1	0	1 (ectopic nt/noto, axis and TB)
2		1	1	0	0	1	0	1 (ectopic nt/noto, axis and TB)
3		1	0	0	0	1	1	1 (clump in TB)
4		1	1 (low)	1	1 (low)	1	1	1 (ectopic nt/noto, TB)
5		1	1 (low)	1	1 (low)	1	1	1 (ectopic nt/noto, TB)
6		1	1 (low)	1	1 (low)	1	1	1 (ectopic nt/noto, TB)
7		1	1 (low)	1	0	1	0	1 (ectopic nt/noto, TB)
Total		7	6 (5 low)	5	3 (low)	7	4	7 (6 ectopic nt/noto, axis and/or TB; 1 clump, TB)
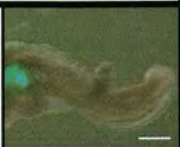
Integ: embryo that contained integrated GFP-labelled cells, NCH: notochord, NT: neural tube, PXM: paraxial mesoderm, CNH: chordoneural hinge, TBM: tail bud mesoderm, non-integ: non-integrated cells, nt/noto: neural-like structure or cavitated notochord, TB: tail bud. Bar: 500μm.

APS to border

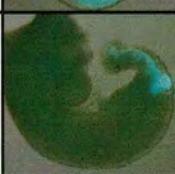| Embryo		Integ.	Axis			Tail bud		Non-integ.
			NCH	NT	PXM	CNH	TBM	
1		1	0	1 (low, TB)	1	1	1	1 (ectopic nt/noto, TB)
2		1	0	0	1	1	1	0
3		1	0	1 (low, TB)	1	1	1	1 (clump in vnt, TB)
4		1	0	1 (TB)	1	1	1	1 (clump in vnt, TB)
5		1	0	0	1	1	1	0
6		1	0	1 (TB)	1	1	1	0
7		1	0	0	1	0	1	0
Total		7	0	4 (TB) (2 low)	7	6	7	3 (2 clumps, TB; 1 ectopic nt/noto, TB)

Integ: embryo that contained integrated GFP-labelled cells, NCH: notochord, NT: neural tube, PXM: paraxial mesoderm, CNH: chordoneural hinge, TBM: tail bud mesoderm, non-integ: non-integrated cells, nt/noto: neural-like structure or cavitated notochord, vnt: ventral neural tube, TB: tail bud. Bar: 500μm.

APS to node

Embryo		Integ.	Axis			Tail bud		Non-integ.
			NCH	NT	PXM	CNH	TBM	
1		0	0	0	0	0	0	1 (clump mnt, axis)
2		0	0	0	0	0	0	2 (ectopic on dnt+ectopic nt/noto,axis)
3		1	1 (low, TB)	1 (low)	1 (low)	0	0	1 (ectopic nt/noto, axis)
4		1	1	0	0	0	0	1 (clump pm, axis)
5		1	1	1	1	1	1	1 (ectopic nt/noto, TB)
6		0	0	0	0	0	0	1 (ectopic on dnt, axis)
7		0	0	0	0	0	0	1 (ectopic on dnt, axis)
8		1	1 (low, TB)	1 (low, TB)	1	1	1	1 (ectopic nt/noto, TB)
9		1	0	0	1	1	1	1 (ectopic nt/noto, axis and TB)
Total		5	4 (2 low, TB)	3 (2 low)	4 (1 low)	3	3	10 (2 clump axis; 3 ectopic on dnt, axis; 5 ectopic nt/noto, axis and /or TB)

Integ: embryo that contained integrated GFP-labelled cells, NCH: notochord, NT: neural tube, PXM: paraxial mesoderm, CNH: chordoneural hinge, TBM: tail bud mesoderm, non-integ: non-integrated cells, nt/noto: neural-like structure or cavitated notochord, dnt: dorsal neural tube, mnt: middle neural tube, pm: paraxial mesoderm, TB: tail bud. Bar: 500μm.

APPENDIX II

Axial progenitors with extensive potency are localised to the mouse chordoneural hinge

Noemí Cambray and Valerie Wilson*

Centre for Genome Research, Kings Buildings, West Mains Road, Edinburgh EH9 3JQ, UK
*Author for correspondence (e-mail: v.wilson@ed.ac.uk)

SUMMARY

Elongation of the mouse anteroposterior axis depends on a small population of progenitors initially located in the primitive streak and later in the tail bud. Gene expression and lineage tracing have shown that there are many features common to these progenitor tissues throughout axial elongation. However, the identity and location of the progenitors is unclear. We show by lineage tracing that the descendants of 8.5 d.p.c. node and anterior primitive streak which remain in the tail bud are located in distinct territories: (1) ventral node descendants are located in the widened posterior end of the notochord; and (2) descendants of anterior streak are located in both the tail bud mesoderm, and in the posterior end of the neurectoderm. We show that cells from the posterior neurectoderm are fated to give rise to mesoderm even after posterior neuropore closure. The posterior end of the notochord, together with the ventral neurectoderm above it, is thus topologically equivalent to the chordoneural hinge region defined in *Xenopus* and chick. A stem cell model has been proposed for progenitors of two of the axial tissues, the myotome and spinal cord. Because it was possible that labelled cells in the tail bud represented stem cells, tail bud mesoderm and chordoneural hinge were grafted to 8.5 d.p.c. primitive streak to compare their developmental potency. This revealed that cells from the bulk of the tail bud mesoderm are disadvantaged in such heterochronic grafts from incorporating into the axis and even when they do so, they tend to contribute to short stretches of somites suggesting that tail bud mesoderm is restricted in potency. By contrast, cells from the chordoneural hinge of up to 12.5 d.p.c. embryos contribute efficiently to regions of the axis formed after grafting to 8.5 d.p.c. embryos, and also repopulate the tail bud. These cells were additionally capable of serial passage through three successive generations of embryos in culture without apparent loss of potency. This potential for self-renewal in chordoneural hinge cells strongly suggests that stem cells are located in this region.

Key words: Mouse, Anteroposterior axis, Tail bud, Stem cell, Chordoneural hinge

INTRODUCTION

After the formation of the most rostral tissues, the extension of the mouse anteroposterior axis is undertaken by the primitive streak and subsequently by the tail bud (reviewed by Hogan et al., 1994). These two progenitor tissues share many common features. First, the morphology and topological relationship between the axial tissues that they produce is similar from the most rostral to the most caudal level. Some 60 somites flank two central tissues, the neural tube and notochord, and lie dorsal to the endoderm and lateral mesoderm. Secondly, the sites of mesoderm formation at gastrulation and in the tail bud later in axial elongation in vertebrates share expression of many genes (Chapman et al., 1996; Crossley and Martin, 1995; Dunwoodie et al., 1997; Gawantka et al., 1998; Ruiz and Robertson, 1994; Wilson et al., 1995). Third, several genes such as brachyury and *Wnt3a*, which have a crucial role in primitive streak morphogenesis revealed by null mutations, affect only tail development when function is partially lost (Chesley, 1935; Greco et al., 1996; Wilson et al., 1995). Thus,

in these respects, the extension of the anteroposterior axis caudal to the head can be viewed, at least to some extent, as a continuum from its inception at 8.0 days postcoitum (d.p.c.) to its termination 5 days later.

In support of this, groups of 10-20 cells from the primitive streak and tail bud of 9.5 d.p.c.-13.5 d.p.c. embryos are able to incorporate in the streak of 8.5 d.p.c. embryos (Tam and Tan, 1992). However, there is evidence from the above study to suggest that cells in the primitive streak and tail bud are not completely interchangeable, as grafted cells from older tail buds contribute to more posterior somites than cells from the streak. In the past, it has been suggested that cells in the tail bud not only have different potency, but also proliferate according to different rules from those that pertain to the streak. Holmdahl (Holmdahl, 1925), from studies in chick, suggested that the vertebrate tail bud constitutes a blastema of undifferentiated cells with little or no regional specification of the progenitors. However, later fate mapping analysis in *Xenopus* showed regionalisation of distinct progenitors of neural tube, notochord and somites within a small area of the

blastopore (the *Xenopus* equivalent of the late primitive streak) and tail bud (Gont et al., 1993). In the tail bud, this region was termed the chordoneural hinge (CNH), and it is able to produce ectopic tails when grafted to host embryos. Gene expression within the tail bud is also strongly localised amongst the regionalised progenitors (Beck and Slack, 1998; Gawantka et al., 1998).

Intriguingly, however, it appears that there may be some cells in the tail bud whose fate is not specified, as marking very small groups of cells in the tail bud can result in descendants in more than one tissue type (Davis and Kirschner, 2000). Thus, while much of the tail bud in *Xenopus* is composed of regionalised progenitors, it is unclear whether these constitute all the axial progenitors. Alternatively, a second population of multi-fated progenitors may exist, which raises the possibility that these give rise to regionally specified progenitors.

In mouse, the descendants of single cells in the epiblast destined for the streak at early streak stage are not confined to any single tissue type (Lawson et al., 1991). Even later, mesoderm progenitors in the epiblast, although regionalised in fate, are not highly restricted in potency (Beddington, 1981). Whether the same multipotency is conserved in the later streak and tail bud in the mouse is unknown. The ontogeny of two of the axial tissues, the myotome, a paraxial mesoderm derivative, and spinal cord, derived from neural plate, has been studied using a retrospective single cell marking technique (Nicolas et al., 1996; Mathis and Nicolas, 2000). In these studies, descendants of single cells that have undergone a rare somatic recombination event and are located in either myotome or spinal cord are marked. In the myotome, those descendants of single cells that populate large anteroposterior axial distances are located bilaterally, showing that their progenitors originate in the primitive streak and tail bud (Nicolas et al., 1996). These studies indicate the existence of stem cell progenitors of both myotome and spinal cord. However, they do not give detailed information on their position and identity.

In lineage tracing experiments in cultured mouse embryos, most cells in the streak are destined for exit to differentiating axis tissues (Lawson et al., 1991; Tam and Beddington, 1987). However, a small proportion remain in the tail bud at the end of the culture period, in some cases after the formation of some 32 somites (Wilson and Beddington, 1996). Because we know that axial progenitors reside there, some or all of these may represent stem cells. Because stem cells are characterised by the ability to self-renew, they should be distinguishable from other cells in the axis by their capacity to contribute to both anterior and posterior differentiated tissues, and the ability to be serially passaged.

We have refined previous fate maps to show that the tail bud contains regionally separated descendants of cells in the streak using topically applied lipophilic dyes. We have exploited transgenic strains of mice that express green fluorescent protein (GFP) (Okabe et al., 1997) or *lacZ* (Munsie et al., 1998) ubiquitously to explore the potency of these cells. We show that cells in the vicinity of the node and their descendants are found in an equivalent structure to the *Xenopus* CNH. These cells fulfil the above criteria expected of stem cells. By contrast, cells in the more ventrally located tail bud mesoderm, which were found to be descended from the CNH, are more limited in their potency.

MATERIALS AND METHODS

Maintenance of mouse stocks and culture of embryos

MF1, *Zin40* (Munsie et al., 1998) and *TgN(beta-actEGFP)04Obs* (Okabe et al., 1997) (here termed 'GFP transgenic') mice were maintained on a 14 hour light, 10 hour dark cycle. Noon on the day of finding a vaginal plug was designated 0.5 days postcoitum (d.p.c.). Dissection and culture was performed as described (Cockroft, 1990).

Dissection of tissues for grafting

GFP transgenic×MF1 litters were dissected in M2 medium and those containing the transgene selected in a Nikon SMZ-U dissecting microscope with fluorescence attachment. The posterior half of the embryo containing the primitive streak was dissected using fine forceps. The primitive streak was dissected using an eyelash tool by making two longitudinal lateral cuts, isolating a thin strip of tissue containing the entire primitive streak and node and retaining both ectodermal and endodermal layers. Node and primitive streak fragments were further dissected by making transverse cuts with the eyelash tool. A schematic diagram of the sites dissected is shown in Fig. 1A.

Regions of the 10.5-12.5 d.p.c. tail bud were dissected by first isolating the whole tail bud using fine forceps. The CNH and tail bud mesoderm (TBM) were dissected using an eyelash tool or fine glass needles. First, the end of the tail was excised, and two dorsoventral longitudinal cuts made to remove the paraxial mesoderm. To dissect CNH, the hindgut and dorsal neurectoderm were then removed by similar longitudinal cuts in the mediolateral plane. The TBM was separated by a transverse cut posterior to the neural tube and hindgut. Dissected CNH was trimmed and divided into two to three pieces to graft to wild-type hosts. The surface ectoderm was removed from TBM and it was divided into two to three pieces for grafting. The position of these tissues in the intact and partially dissected tail is shown in Fig. 1A,B.

DiI labelling

Embryos were labelled with CellTracker CM-DiI and CMFDA (Molecular Probes) as described previously (Wilson and Beddington, 1996). Dissected CNH and TBM were labelled by expelling DiI from a pipette held directly above the tissue to be labelled for a few seconds. The graft was then washed in fresh M2. Dissected 10.5 d.p.c. tail pieces were labelled in the neural tube by inserting a fine pipette into the lumen and expelling a small amount of dye, which covered most or all of the luminal surface. Labelling of the most posterior end was checked either by observing a faint pink colour under brightfield illumination, or by viewing in a dissecting microscope with fluorescence attachment. Label sites are shown in Fig. 1A.

Grafting labelled tissue

Grafts were performed using a hand-drawn micropipette. The embryo was held loosely in place with forceps while suction was gently applied with the micropipette to the anterior primitive streak immediately abutting the node to create an opening for the graft. The tissue to be grafted was then drawn into the pipette, and the pipette inserted in the opening. The graft was gently expelled as the pipette was drawn out of the embryo, leaving the tissue lodged in the opening (Fig. 1C). The embryos were then placed in a universal container in 50% rat serum, 50% GMEM or DMEM in an incubator gassed at 5% CO_2 in air for 30 minutes to allow the grafts to heal before sealing the Universals and placing them in a roller culture apparatus at 37°C overnight. Embryos which had developed normally were cultured for a further 24 hours in 75% rat serum in 40% oxygen, 5% CO_2, 55% nitrogen. At the end of the culture period fluorescence was assessed either in a Nikon SMZ-U dissecting microscope or, for more detailed analysis, in a Zeiss Axiovert inverted microscope. Images were captured using Improvision Openlab software and processed using Adobe Photoshop.

X-gal staining with in situ hybridisation

Embryos carrying the ubiquitously expressed *Zin40* gene trap integration were used as donors for experiments testing the gene expression of grafted cells. Grafted embryos were first stained with X-gal and then subjected to in situ hybridisation (Tajbakhsh and Houzelstein, 1995) with probes specific for *T* (Wilkinson et al., 1990), sonic hedgehog (Echelard et al., 1993), Delta like 1 (*Dll1*) (Dunwoodie et al., 1997) and *Pax3* (Goulding et al., 1991). Embryos were then dehydrated via a methanol series and processed for paraffin wax histology.

Histology

DiI-labelled embryos and embryos that received grafts of GFP transgenic cells were sectioned transversely in a Series 1000 Vibratome at 50 μm as and images obtained as described above. Embryos subjected to X-gal staining with in situ hybridisation were sectioned transversely at 7 μm and photographed in an Olympus Vanox compound microscope.

RESULTS

All host embryos used in this study were dissected for labelling or grafting at 8.5 d.p.c. (three to eight somites) and cultured for 48 hours, forming a total of 30-35 somites, as described previously (Wilson and Beddington, 1996).

Regionalisation of primitive streak descendants in the tail bud

Previous studies have shown that some descendants of cells in the node and primitive streak at 8.5 d.p.c. are present in the tail bud at 10.5 d.p.c. (Wilson and Beddington, 1996). To determine whether there is any relationship between origin of the cells in the streak and their subsequent location in the tail bud, two distinct sites were labelled: the ventral layer of the node and anterior primitive streak. In accordance with previous fate-mapping studies, the descendants of cells in the node were located in the notochord (Fig. 2A,E), whereas those of the anterior streak were predominantly somitic (Fig. 2B,G). Descendants of anterior streak were also located in the ventral neurectoderm, but not notochord (Fig. 2F). The anterior limit of labelling was around somite 12. In the tail bud after node labelling, the labelled notochord widened and ended abruptly beneath the neural tube, anterior to the end of the tail such that the mesoderm in the tail bud (Fig. 2A,K) was unlabelled. Descendants of the anterior streak were located in the tail bud in two domains: the posterior ectoderm continuous with the ventral posterior neural tube (termed posterior neural plate) and the TBM. (Fig. 2B,M).

We next compared this fate map information with the contribution of GFP transgenic node and primitive streak cells when grafted to stage-matched embryos. These were grafted to the anteriormost extreme of the primitive streak, touching the outer rim of the node (Fig. 1A,C), to allow incorporation of the grafted tissue in either the host node or streak. In general, these grafts mirrored the tissue contribution seen after DiI labelling, showing that, when grafted to this position, cells can incorporate efficiently in either tissue from this site, and that
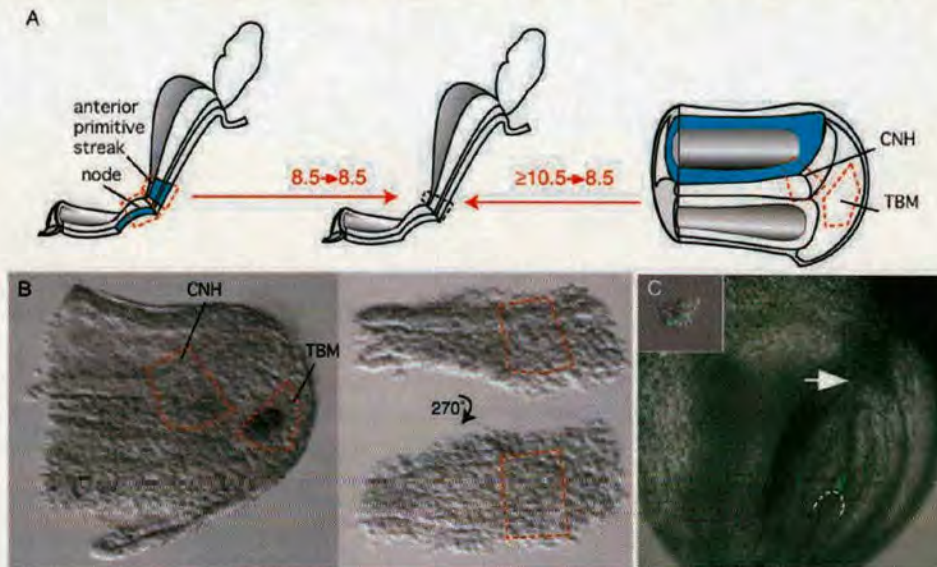
Fig. 1. Labelling sites, donor origin and graft sites. (A) Schematic showing labelling and grafting experiments. Blue fill denotes sites of DiI label. In 8.5 d.p.c. embryos, the ventral layer of node is exposed as a hiatus in the endoderm and can therefore be labelled separately from the ectoderm layer immediately above it, whereas anterior primitive streak is labelled by inserting a pipette through the endoderm and thus labels all layers. The entire neural ectoderm surface, including the posterior ventral neural plate that overlies the notochord is labelled in 10.5 d.p.c. cultured tail pieces. Broken red lines outline sites dissected for grafting. The broken black line outlines plug of tissue at the node/streak border replaced by graft in host embryo. (B) Dissection of 10.5 d.p.c. tail bud: (left) lateral view of tail bud after removal of paraxial mesoderm, overlaid with position of CNH and TBM (broken red lines); (right, top) the same embryo after removal of dorsal neural tube and hindgut; (right, bottom) the same piece rotated so that the widened end of the notochord is upwards. CNH is outlined in red. (C) Inset shows a dissected clump containing eight GFP-labelled cells amongst ~200 unlabelled cells from the CNH of the embryo in Fig. 2C,H,L. Main panel: posterior view of an embryo containing this clump grafted immediately posterior to the node (outlined by a broken white line) at the anterior of the primitive streak, the posterior limit of which is marked by a white arrow.
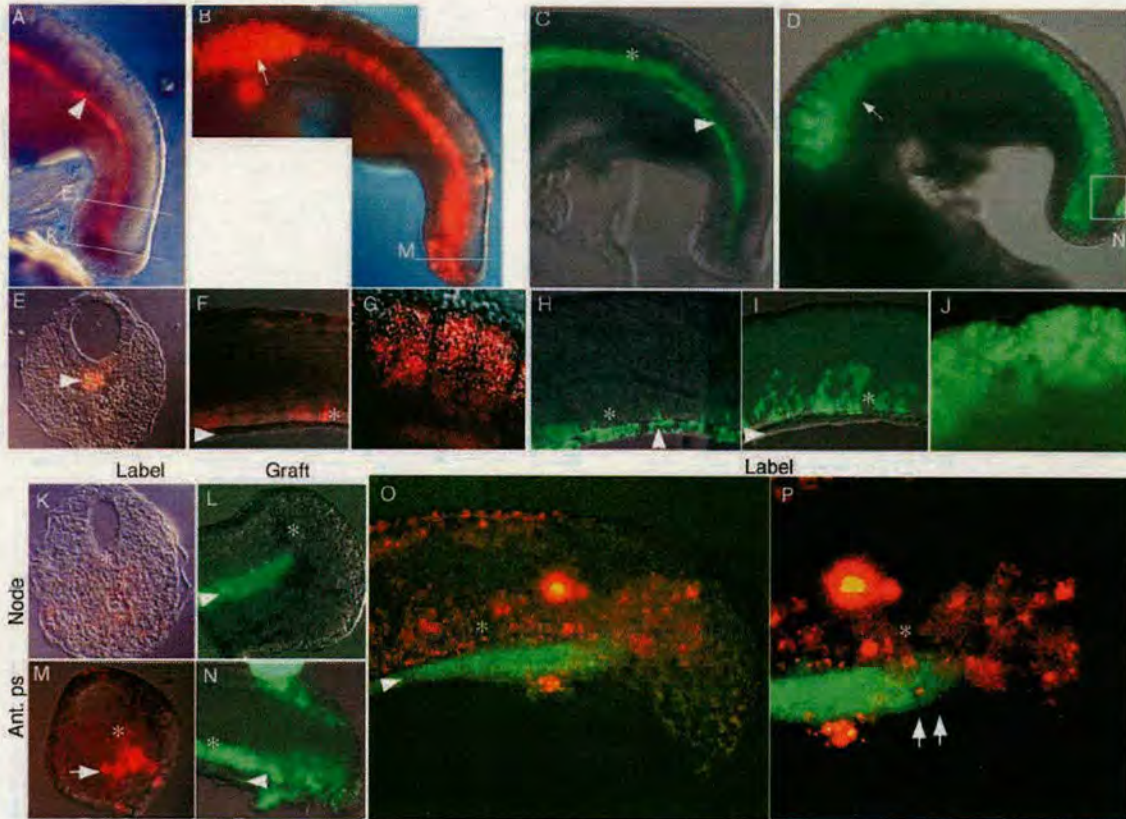
Fig. 2. Descendants of the anterior streak and node populate different regions of the tail bud. Embryos were DiI labelled or grafted with GFP-expressing cells at 8.5 d.p.c. and cultured for 48 hours. (A-D) Lateral views of the posterior ends of manipulated embryos. (A) Embryo labelled with DiI in the ventral node. Labelled cells populate the notochord (arrowhead) and end short of the tail tip, just anterior to the line showing the plane of section in K. (B) Embryo labelled with DiI in the anterior primitive streak. Labelled descendants colonise somites and are widespread in the tail bud. Arrow, position of somite 20. (C) Embryo grafted with 8.5 d.p.c. node. Label is similarly located to the label in A, but also includes the ventral neurectoderm (asterisk). (D) Embryo grafted with 8.5 d.p.c. anterior primitive streak. Label is similar to that in B. Arrow indicates position of somite 20. (E) Transverse section of the embryo shown in A, showing label in the notochord. (F) Neural tube and notochord, and (G) paraxial mesoderm of dissected embryo shown in B. Labelled cells are present in ventral neural tube, but not notochord (F), and in somites (G). (H) Dissected neural tube and notochord of embryo shown in C, where labelled cells populate notochord and ventral neural tube. (I) Dissected neural tube and notochord, and (J) paraxial mesoderm of the embryo shown in D. Labelling is similar to that in F,G. (K) Transverse section of distal tail bud of embryo in A. No labelling is seen. (L) Dissected tail tip of embryo shown in C. Labelling is confined to notochord and ends short of the tail tip. (M) Dissected neural tube and notochord (transverse view) of embryo in B. Labelled cells are present in posterior neurectoderm and mesoderm (arrow). (N) Dissected distal neural tube and underlying mesoderm of embryo in D. Labelled cells are present in ventral neurectoderm. (O,P) Embryo labelled with DiI in anterior primitive streak (red) and CMFDA in ventral node (green). (O) Fluorescent overlay on brightfield image, and (P) fluorescent image, of dissected neural tube and notochord. Node descendants end sharply under the neural tube. Anterior streak descendants populate the ventral neurectoderm and underlying mesoderm and, posteriorly, encroach on the notochord territory (arrows). Arrowheads indicate notochord; asterisks indicate ventral neural tube.

Table 1. Isochronic and heterochronic grafts

	Total embryos	Total incorporated	Number (%) of incorporated embryos with label in				
			Axis			Tailbud	
			NCH	NT	PXM	CNH	TBM
8.5 d.p.c. node	22	18 (82)	17 (94)	16 (89)	8 (44)	17 (94)	4 (22)
8.5 d.p.c. ant. streak	10	8 (80)	1 (12)	4 (50)	8 (100)	5 (62)	6 (75)
10.5 d.p.c. CNH	18	15 (83)	9 (60)	6 (40)	13 (87)	14 (93)	11 (73)
12.5 d.p.c. CNH	8	6 (75)	4 (66.7)	3 (50)	6 (100)	4 (67)	4 (67)
10.5-12.5 d.p.c. TBM	11	1 (9)	0	0	1 (100)	0	0

Contribution of DiI-labelled or GFP transgenic grafts to the axis of 8.5 d.p.c. (three to eight somite) embryos after grafting to the border of the node and anterior streak and culturing for 48 hours.

NCH, notochord; NT, neural tube; PXM, paraxial mesoderm; CNH, host chordoneural hinge; TBM, host tail bud mesoderm.

the pattern of incorporation reflects the site of origin of the cells. Grafts of node contributed predominantly to notochord (Fig. 2C,H; Table 1) and anterior streak to somites (Fig. 2D,J; Table 1). In eight embryos, contribution from grafted node to predominantly medial paraxial mesoderm was observed (Table 1). This is consistent with fatemaps of the chick node, where cells in lateral regions of the node contribute to somites (Psychoyos and Stern, 1996; Selleck and Stern, 1991). However, the majority of embryos receiving node grafts contained little or no contribution to somites, indicating that it is possible to physically separate somite from notochord progenitors. Both graft types contributed descendants to the ventral neural tube (Fig. 2H,I), although node grafts tended to contribute to more ventral descendants than anterior streak ones, consistent with existing fate maps. In the tail bud, the contribution from GFP transgenic cells (Fig. 2L,N) was essentially as seen with the fluorescent lineage tracers (Fig. 2K,M). In anterior streak grafts, GFP-labelled cells were absent from the notochord, except for a small number of cells at its posterior end in the CNH (Fig. 2N).

To confirm the distinct locations of streak and node descendants, anterior streak cells were labelled in situ with DiI (red) and ventral node with CMFDA (green). Here, the CMFDA-labelled notochord ends sharply beneath the neural plate, while anterior streak descendants are found in the posterior neural plate and mesoderm directly beneath it (Fig. 2O,P). Dorsal labelling in surface ectoderm is probably a result of DiI spreading in the amniotic cavity on initial labelling. Interestingly, although a sharp posterior border is seen in the notochord descended from ventral node, primitive streak descendants appear to encroach on this territory. This suggests that anterior streak descendants may contribute to posterior notochord.
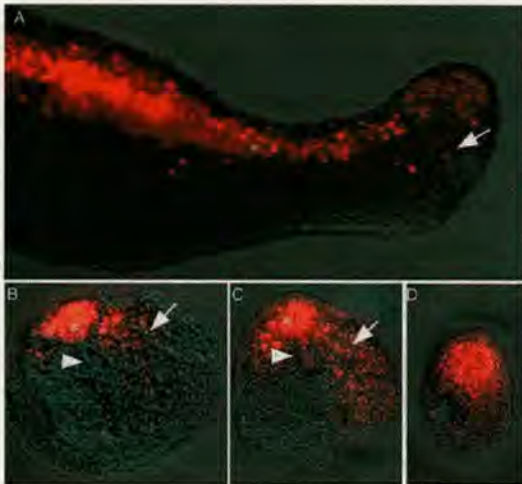
Fig. 3. The posterior neural plate generates mesoderm after posterior neuropore closure. (A) 10.5 d.p.c. tail piece labelled with DiI in neurectoderm and cultured for 48 hours. Labelled descendants are present in neurectoderm (asterisk) and posterior mesoderm (arrow). (B-D) successively more posterior transverse sections of a second embryo, showing label in neurectoderm (asterisks), mesoderm (arrow) and in the posterior, but not more anterior, notochord (arrowheads in B,C).

Before posterior neuropore closure, the posterior neural plate is a source of mesoderm for somites (Wilson and Beddington, 1996). As labelled anterior streak contributed descendants to both posterior neurectoderm and mesoderm, it was of interest to determine whether the posterior neural plate continues to produce mesoderm after posterior neuropore closure. To test this, the entire neurectoderm of dissected 10.5 d.p.c. tail pieces that had undergone posterior neuropore closure was labelled using DiI. After 48 hours, labelled mesoderm was detected in the posterior region of six out of six cultured tail pieces (Fig. 3). Here, too, there is some evidence that the most posterior notochord is populated by ectoderm descendants (compare notochord in Fig. 3B with that in 3C) Therefore, a region continuous with the neurectoderm – most probably the posterior ventral neurectoderm, which is descended from the streak (Fig. 2M) – contributes to the mesoderm of the tail. The region composed of the posterior neural plate and the posterior end of the notochord is thus topologically equivalent to the CNH defined in *Xenopus*.

In the CNH, the ventral node descendants identified by lineage labelling are morphologically indistinguishable from more posterior axial mesoderm beneath the neurectoderm in the tail bud. By contrast, mesoderm located in more posterior, ventral and paraxial regions in the tail bud is composed of loose mesenchyme. It was therefore possible to dissect apart the loose tail bud mesoderm (TBM) from the CNH. As shown above, the CNH contains descendants of ventral node and anterior streak, while the TBM contains only anterior streak descendants. The location of these cells in the tail bud suggests that they may constitute a self-renewing subset of the labelled or grafted tissue. This has been tested in two ways: (1) we have grafted CNH and TBM from tail buds up to 12.5 d.p.c. into 8.5 d.p.c. embryos, and (2) labelled 10.5 d.p.c. CNH or TBM have been serially passaged into successive 8.5 d.p.c. embryos. In each case, a self-renewing population would be expected to contribute descendants both to the differentiated axial tissues formed by the host and the tail bud itself.

Potency depends on location in the tail bud

We compared the capacity of dissected 10.5-12.5 d.p.c. CNH or TBM to differentiate relative to control isochronic grafts, when grafted to the 8.5 d.p.c. primitive streak/node border (Table 1). The donor tissues were derived either from GFP transgenic embryos, *Zin40* embryos or wild-type tissue labelled with DiI. Although a high proportion of control isochronic grafts had incorporated well in the axis (Table 1), we observed a reduction in the proportion of grafts from the TBM that incorporated correctly, with cells remaining predominantly as morphologically undifferentiated clumps (Fig. 4A,B). Differentiation of only one out of 11 heterochronic grafts of TBM, derived from a 10.5 d.p.c. embryo, was observed. In this embryo, labelled cells were restricted to a short unilateral stretch of somitic mesoderm and did not populate the tail bud (data not shown).

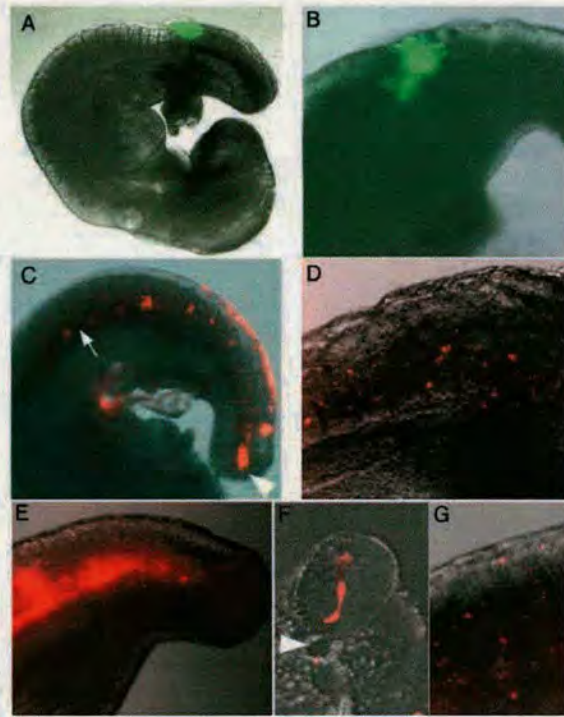By contrast, a high proportion of embryos receiving up to 12.5 d.p.c. CNH cells showed extensive contribution to the axis (Fig. 4C-G; Table 1). Most successfully grafted embryos contained label in somites (Fig. 4C,D,G), with a lower proportion showing label in notochord and/or neural tube (Fig. 4E,F). All embryos showed bilateral contribution from the labelled cells. In general, the anterior limit of contribution

tended to be more posterior than in isochronic grafts (approx. somite 17 onwards; Fig. 4C). Unlike TBM, they also populated the tail bud with high frequency (Fig. 4C,E; Table 1), and were located in both the CNH and in TBM.

To verify that these apparently well-integrated donor tissues indeed differentiated appropriately, a subset of the embryos were grafted with cells expressing the transgenic marker *Zin40*, a developmentally neutral gene trap integration containing a ubiquitously expressed *lacZ* gene (Munsie et al., 1998). This histologically stable marker allowed processing of grafted embryos for in situ hybridisation to markers of differentiation in axial tissues (Tajbakhsh and Houzelstein, 1995). Co-expression of *lacZ* and the differentiation marker was scored in serial transverse sections.

Within the axis, brachyury (*T*) and sonic hedgehog (*Shh*) are expressed in the notochord, and Shh is additionally expressed in the floorplate (Echelard et al., 1993; Wilkinson et al., 1990). In embryos that received an 8.5 d.p.c. node graft, both *T* and *Shh* were expressed appropriately in donor cells in

the notochord, and graft-derived cells in the floorplate expressed *Shh* but not *T* (Fig. 5A-D; Table 2). Cells

Fig. 5. Grafted cells express markers of differentiation correctly. Embryos are doubly stained with X-gal (light blue; donor cells), and antisense riboprobes as indicated (purple). (A,C,E,G) Whole embryo; (B,D,F,H) transverse section of the adjoining embryo at the level shown by the lines in A,C,E,G. Left hand insets in B,D,F,H show high power images of the regions indicated by black arrowheads. Co-expressing cells are indicated by blue arrowheads. (A-D) Embryos resulting from graft of 8.5 d.p.c. node. (A,B) Embryo hybridised with *T* riboprobe. Like unlabelled host cells, donor cells in the notochord express *T*, while those in the ventral neural tube (asterisk and upper right-hand corner of inset) do not. (C,D) Embryo hybridised with *Shh* riboprobe. Donor cells correctly express *Shh* in the floorplate (compare floorplate in B with that in D). A comparable high magnification image in a control unlabelled embryo is shown (right-hand inset in D). (E-H) Embryos receiving grafts of 10.5 d.p.c. CNH. (E,F) Embryo hybridised with a *Shh* riboprobe. Donor cells in the notochord express *Shh*. (G,H) Embryo hybridised with *Dll1* riboprobe. Donor cells in dorsal paraxial mesoderm express *Dll1*, while those outside the region of host cells expressing *Dll1* do not (arrow). Asterisks indicate ventral neural tube.

Fig. 4. The CNH, but not the TBM, generate labelled descendants in axis, CNH and tail bud. (A,B) Cultured embryos that received a graft of 10.5 d.p.c. (A) and 12.5 d.p.c. (B) TBM. Grafts remain as distinct clumps and do not incorporate in the host. (C,D) Whole embryo (C) and dissected paraxial mesoderm from a second embryo (D) that received a graft of DiI-labelled 10.5 d.p.c. CNH. Labelled cells are present in CNH (arrowhead) and paraxial mesoderm. Arrow indicates position of somite 20. Labelled cells are also present along the dorsal neural tube, possibly because of incomplete incorporation of the graft during posterior neuropore closure. (E-G) Embryos receiving a graft of DiI-labelled 12.5 d.p.c. CNH. Tail (E) and transverse section (F) of a second embryo showing incorporation in notochord (arrowhead). (G) Dissected paraxial mesoderm of a third embryo showing label in somites.

Table 2. Gene expression in grafted cells anterior to the tail bud

Graft type	Embryo	Probe	Expression of marker by donor cells in		
			NCH	NT	PXM
8.5 d.p.c. node	1	*T*	Yes	No	No
	2	*Shh*	Yes	Yes	No
	3	*Pax6*	No	Yes	No
10.5 d.p.c. CNH	4	*T*	Yes	No	No
	5	*Shh*	Yes	No	No
	6	*Shh*	Yes*	Yes*	No
	7	*Dll1*	No	No	Yes
	8	*Pax3*	No	Yes	Yes

*Rodlike groups of donor cells near the notochord could be followed through serial sections in this embryo. When lying beside the notochord, they did not express *Shh*, but became physically incorporated over several sections in notochord and ventral neural tube, and concomitantly expressed *Shh*.

NCH, notochord; NT, neural tube; PXM, paraxial mesoderm; CNH, host chordoneural hinge.

Fig. 6. Regrafting of GFP-labelled TBM (derived from an anterior streak graft) results in contribution to short stretches of somites, not the tail bud. (A) Whole embryo and (B) dissected paraxial mesoderm (enlarged) of embryo shown in A. Cells have incorporated over a distance of six somites unilaterally. Arrows indicate anterior and posterior borders of labelled cell incorporation.

immediately dorsal to the floorplate express the neural marker *Pax6*, and graft-derived cells populating this region also appropriately expressed *Pax6* (Table 2). Medially located donor cells in the paraxial mesoderm showed no ectopic *T* expression (data not shown). The tail buds of the embryos shown in Fig. 5A-D had been removed prior to processing and were not assayed for marker gene expression. This apparently normal differentiation therefore correlates well with the morphological assessment of incorporation in tissue derived from isochronic grafts. To determine whether this was true of grafted 10.5 d.p.c. tissue, the expression of *T*, *Shh* and two additional markers of paraxial mesoderm differentiation, *Dll1* (Dunwoodie et al., 1997) and *Pax3* were assayed. Within the axis, where donor cells appeared morphologically incorporated in a tissue, they correctly co-expressed all differentiation markers assayed (Fig. 5E-H; Table 2). Furthermore, the incorporated cells did not ectopically express differentiation markers (Fig. 5H, arrow). In the tail bud mesoderm and CNH, many donor cells also expressed *T*, showing that these cells also express markers appropriate for tail bud (data not shown).

Although differentiation towards somites was apparent in many of the embryos, the grafted tissue did not always intersperse well with host tissue. Typically, some regions of the grafted embryos contained small groups of medially located

somitic tissue, sometimes out of register with those of the host (Fig. 4C). However, it is clear that some regions – even in embryos where this abnormal differentiation was apparent – do mix well with host tissue (Fig. 4D,G). Taken together, these results suggest that the grafted CNH is at least partially equivalent to its earlier counterpart in the node and anterior streak. These results show that the CNH has the potential both to contribute widely to the axis, and to repopulate the CNH itself and the TBM.

The CNH, but not TBM, is serially transplantable

The population of host CNH by grafted CNH cells separated by up to 4 days in developmental stage from the host (Table 1; Fig. 4), together with their ability to participate in differentiated axial tissue formation, suggested that axial stem cells reside there, and not in the TBM. Such stem cells should also contribute cells to the axis and repopulate CNH on multiple passages through host embryos. We therefore tested this by regrafting GFP-labelled CNH and TBM to 8.5 d.p.c. embryos.

In second generation grafts, groups of cells containing labelled TBM derived from initial anterior streak grafts were also disadvantaged relative to CNH from incorporating in the axis (Table 3). Similar to the results above, when they did incorporate in the axis, they did so only over short axial

Table 3. Serial grafting of CNH and TBM

	Total embryos	Total incorporated	No. (%) of incorporated embryos with label in				
			Axis			Tailbud	
			NCH	NT	PXM	CNH	TBM
2nd generation							
CNH	10	8 (80)	2 (25)	1 (12)	6 (75)	6 (75)	4 (50)
TBM	11	6 (55)	0	0	5 (83)	0	1 (17)
3rd generation							
CNH	10	4 (40)	3 (75)	2 (50)	3 (75)	3 (75)	2 (50)
TBM	4	0					

Contribution of CNH or TBM derived from original GFP transgenic node and anterior streak grafts to the axis of 8.5 d.p.c. (three to eight somite) embryos after grafting to the border of the node and anterior streak and culturing for 48 hours..

NCH, notochord; NT, neural tube; PXM, paraxial mesoderm; CNH, host chordoneural hinge; TBM, host tail bud mesoderm.

Fig. 7. Regrafting of GFP-labelled CNH results in contribution to both the axis and tail bud in up to three generations. Diagrams illustrate the history of grafted cells in the cultured embryo shown immediately to the right. (A-C) Whole mount (A) and transverse sections (B,C) of an embryo that received a graft of 10.5 d.p.c. GFP-labelled CNH. In the axis, cells populated the paraxial mesoderm exclusively and either formed small medial graft-derived somites (B), or incorporated into wild-type tissue (C, arrow). (D-F) Whole mount (D) and sections (E,F) of an embryo grafted with CNH cells from the embryo in A-C. Grafted cells populate axial derivatives that are identical to the parent graft. (G-J) Whole mount (G), dissected neural tube/notochord (H) and paraxial mesoderm (I,J) from embryos that had received a graft of 10.5 d.p.c. CNH, derived from an initial 8.5 d.p.c. node graft. Labelled cells populate the posterior end of the notochord and CNH (arrowhead, H), incorporate in paraxial mesoderm (I), but also form small medially located somites that are epithelial posteriorly (arrow in J) and disperse anteriorly, and are located out of register with the endogenous somites (s). (K-O) A third generation graft. Whole mount (K), dissected neural tube and notochord (L,M), and paraxial mesoderm (N,O), showing contribution to notochord (arrowhead in L), posterior neurectoderm (asterisks in L and M), and both ectopic somites located between host somites (s) (N) and interspersed GFP-labelled cells (O) in host somites. Arrows in A,D,G indicate the position of somite 20.
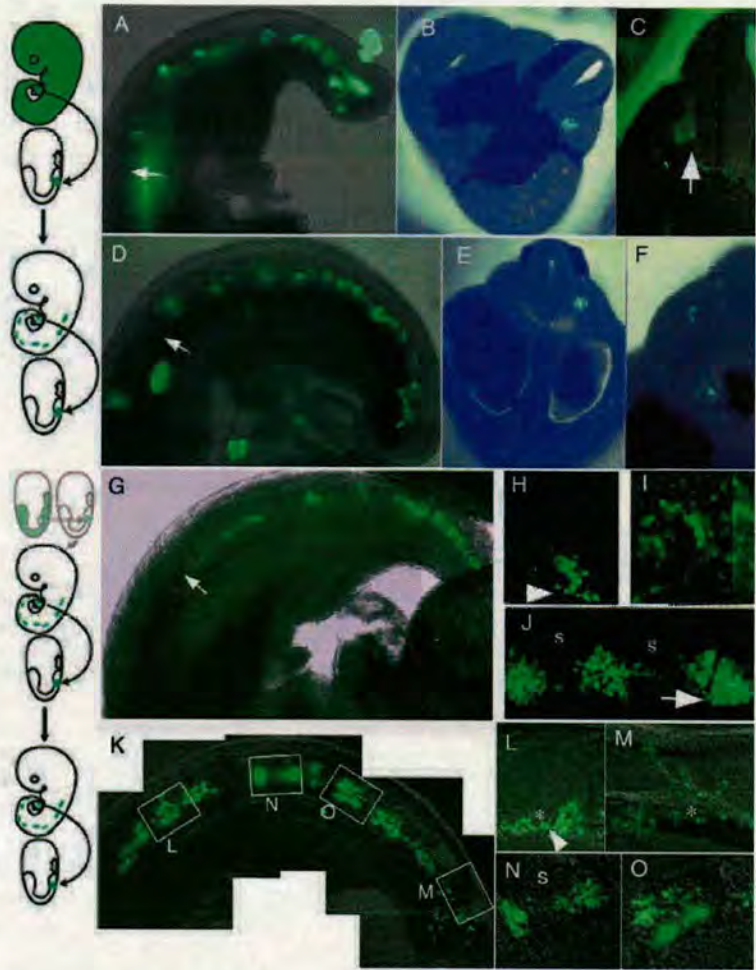
distances (Fig. 6), and only one embryo showed label in the tail bud. In this embryo, no contribution to more anterior positions in the axis were observed, and it is therefore impossible to determine whether these grafted cells truly retained potential to contribute to the axis. Thus, even though these cells were now retained in the tail bud 48 hours after transplant to the anterior primitive streak, this did not select for greater ability to generate descendants both in axis and tail bud.

As shown above, labelled CNH from 10.5 d.p.c. embryos grafted to 8.5 d.p.c. primitive streak resulted in contribution throughout the axis and in the tail bud. Labelled cells from the CNH of the embryo shown in Fig. 7A were regrafted to an 8.5 d.p.c. host, which contributed to the same axial tissues and the CNH, although there may be some depletion of cells from the CNH itself (Fig. 7D). Sections revealed contribution to somites in both generations (Fig. 7B,C,E,F). Similar results were obtained when the grafted 10.5 d.p.c. CNH was derived from an initial 8.5 d.p.c. node graft. These second generation embryos predominantly showed contribution to somites, but also to notochord and ventral neural tube (Fig. 7G-J; Table 3). Although intermingling of host and wild-type cells could be observed in paraxial mesoderm (Fig. 7H), formation of small, medial, graft-derived somites within the somite territory was also apparent (Fig. 7J). The majority of grafted embryos showed repopulation of both CNH and TBM, supporting the hypothesis that TBM is derived from CNH. These second generation CNH were grafted a third time, and incorporation was observed both in axial tissues and the tail bud, in CNH and

TBM (Fig. 7K-O). The grafted tissue shows a somewhat reduced rate of incorporation (Table 3). However, the pattern of incorporation in notochord, somites and neural tube was similar in these 3rd generation grafts to that observed in the second generation and in the grafts of 10.5-12.5 d.p.c. CNH described above. TBM derived from second generation CNH grafts showed similar properties to other 10.5 d.p.c. TBM grafts (Table 3).

In general, the anterior limit of contribution (approx. somite 17 onwards; Fig. 7A,D,G) was similar for the 1st, 2nd and 3rd generations of CNH grafts, showing that the stage of the donor tail bud (not the absolute age of the cells) determined this anterior border. No difference in contribution was obvious between CNH derived from anterior streak versus that from node. However, it was striking that contribution to 3 generations was seen only where the first generation grafts were from nodes that contributed not only to notochord, but also to paraxial mesoderm. This suggested that a population of axial progenitors with capacity for self-renewal and extensive contribution to somites, notochord and neurectoderm were located close to the node at 8.5 d.p.c., and that these continued to be associated with the CNH in successive generations.

DISCUSSION

Regionalisation in the tail bud

We have shown that the descendants of primitive streak and node populate different regions in the tail bud. The descendant of the mouse anterior primitive streak in the posterior neural plate is composed of both neural and somitic progenitors that overlie the posterior end of the notochord. This layout is similar to that in the *Xenopus* tail bud (Tucker and Slack, 1995), where neural (N) progenitors abut precursors of mesoderm within the posterior neural plate (M) and notochord (C) progenitors underlie both. Thus, it is valid to term the mouse posterior neural plate and notochord region 'CNH'. In *Xenopus*, cells from the M region in the CNH pass posteriorly in the tail bud before exiting laterally in the paraxial mesoderm. Similar posterior and lateral movement from the equivalent chick CNH have been observed (Catala et al., 1996; Catala et al., 1995). Thus, the passage of cells from the ectoderm of the CNH towards the more posterior TBM is conserved among vertebrates.

The dramatic involution movements during *Xenopus* gastrulation cease by the neural plate stage (Gont et al., 1993), as does the transit of a large part of the epiblast through the streak and node/organiser to generate mesoderm in mouse by the equivalent headfold stage (Kinder et al., 2001; Snow, 1981). In chick, passage of lateral epiblast cells early during gastrulation through Hensen's node ceases prior to node regression (Joubin and Stern, 1999). Thus, at the start of somitogenesis in vertebrates, the neural, mesodermal and notochordal precursors are no longer in mass transit from the ectoderm but are contained in the region of ingression. We have extended previous studies in the mouse to show that this ingression of cells to the mesoderm layer continues even after posterior neuropore closure around the 35-somite stage. In chick, ingression movements after posterior neuropore closure have also been observed (Knezevic et al., 1998). These can apparently occur from the dorsal surface, perhaps indicating subtle differences in the organisation and/or movements of vertebrate tail bud tissues. In *Xenopus* and chick therefore, as in mouse, the posterior neural plate may merely represent a localised remnant of the outer layer of the marginal zone/primitive streak, which continues a form of ingression after gastrulation.

The mouse ventral node has been identified previously as a putative self-renewing progenitor region for the notochord (Beddington, 1994; Wilson and Beddington, 1996), as its posterior extremity contains labelled cells after culture. In the present study, the apparent population of the posterior end of the notochord by anterior streak derivatives and the posterior neural plate (Fig. 2N,P; Fig. 3C) suggests that the ventral node itself may not contain all notochord progenitors. Instead, the notochord may be supplied from cells in the ectoderm layer that represent more primitive notochord precursors. In chick, too, there is evidence that some notochord progenitors reside in the ectodermal layer, rather than in the ventral node region (Catala et al., 1996; Catala et al., 1995; Psychoyos and Stern, 1996). Furthermore, while passage through Hensen's node is a prerequisite for incorporation in the notochord, some notochord progenitors originate outside Hensen's node in the anterior primitive streak and are only incorporated there later, presumably during node regression (Psychoyos and Stern,

1996). The hypothesis that the mouse ventral node does not contain all notochord progenitors is supported by the relative quiescence of cells in the node and notochord (as few as 10% appear to cycle), while cells around the node are dividing rapidly (Bellomo et al., 1996). Furthermore, the ability of grafted 8.5 d.p.c. node to give rise to notochord in the present study, even when grafted to the anterior streak, suggests that the ventral node contains committed notochord precursors. Therefore the ventral node may contain cells destined only for exit to the notochord, and although dramatic elongation of this structure occurs, mediolateral intercalation (Wilson and Keller, 1991) may account for much of this elongation. This therefore suggests that notochord, somite and neural progenitors are located close together in the ectoderm layer near the node at 8.5 d.p.c., and we show that these progenitors remain closely apposed in the later CNH.

In the *Xenopus* tail bud, there is also evidence from labelling very small groups of around one to three cells in the CNH itself during tail elongation that the progenitors of notochord, muscle and neural tube are located close together, or represent single multilineage cells (Davis and Kirschner, 2000). Earlier, during blastopore closure at the neural plate stage, there appear to be more regionally separated cells (Gont et al., 1993). However, if multilineage cells were located in only a small proportion of the blastopore, lineage labelling larger groups of cells using DiI may not have highlighted such a population.

A stem cell population in the CNH ectoderm?

It has been hypothesised in chick and mouse that cells remaining in the streak or tail bud at the termination of prospective lineage labelling studies represent a minority population composed of self-renewing stem cells in the streak (Beddington, 1994; Psychoyos and Stern, 1996; Tam and Beddington, 1987; Wilson and Beddington, 1996). Evidence for stem cell precursors of myotome (Nicolas et al., 1996) and spinal cord (Mathis and Nicolas, 2000) located in or near the posterior midline of the embryo strengthens this hypothesis. However, so far, evidence showing that the prospective lineage labelled cells in the streak are indeed stem cells, and not dead or quiescent cells, has been lacking. We tested whether the two major areas colonised by primitive streak descendants in the tail bud, the TBM and CNH, fulfilled criteria expected of axial stem cells by grafting GFP transgenic cells to 8.5 d.p.c. embryos.

Potency of tail bud in contributing to anterior axial positions

In this study we have shown that the tissues in the tail bud are not developmentally equipotent. Unlike TBM, CNH cells can efficiently incorporate in the axis, differentiating into somites, ventral neural tube and notochord, and giving rise to descendants in the tail bud itself. Within the tail bud, CNH descendants are found in both CNH and TBM, consistent with the observation that the posterior neural plate continues to generate mesoderm long into axial elongation. There was no apparent difference between 10.5 and 12.5 d.p.c. CNH in the anterior extent of labelling or the tissue types colonised. It is therefore likely that this region contains self-renewing progenitors.

The strong bias towards contribution to somites by CNH cells compared with their node-derived antecedents is

intriguing. This may result from the composition of the graft. Somites form most of the bulk of the tail, while the neural tube and notochord are a relatively minor population. Alternatively, cells or growth factors at the graft site, at the anterior of the primitive streak, may influence the CNH population to differentiate towards somites. A further characteristic of the graft-derived somites was the occurrence of medially located ectopic somites, sometimes in embryos that also had bona fide intermingling of grafted cells with wild type cells in somites. It is possible that the cluster of grafted cells in the streak may retain information on the periodicity of somites to be formed. An alternative possibility is that as the CNH ectoderm is much smaller than the primitive streak, the grafted cells may include the progenitors of entire somites, effectively creating a heterotopic graft of lateral somite precursors to a location where cells normally exit to medial somites.

In contrast to CNH, TBM is only capable of populating short axial stretches that corresponds to a distance of a few somites. It shows a low frequency of incorporation in axial tissue, and fails to contribute to tail bud. The capacity of TBM cells to contribute to anterior axial positions has also been studied by Tam and Tan (Tam and Tan, 1992), who grafted of small numbers of cells from the tail bud of embryos up to 13.5 d.p.c. These grafts are capable of contributing to much more anterior positions than they would have done in situ. As these authors do not distinguish CNH from TBM in the grafts, it may be that it is a small population of CNH cells included in their grafted population that retain potency, especially to contribute to the tail bud. The relatively low frequency observed by these authors of grafted cell retention in the tail bud (around 20% of embryos) supports this idea. Alternatively, the smaller number of grafted cells used by Tam and Tan (Tam and Tan, 1992) may intermingle more extensively with the host cells than the TBM grafts in the present study. Larger TBM grafts may therefore be subject to greater community effects that preserve either specification as mesoderm or anteroposterior information. As recently ingressed mesoderm earlier in gastrulation is more restricted in potency than the cells from the ectoderm that produced it (Tam et al., 1997), it is likely that TBM cells that have undergone ingression from the posterior neural plate, are also restricted in potency.

Serial passage of axial progenitors

When CNH cells are passaged through a second and third generation of embryos in culture, at least some cells retain the capacity to colonise the axis in an identical manner to first generation CNH. These results show that the primitive streak/tail bud can retain descendants of cells initially located near the node over a total of around 90 somites made by the hosts, and strongly suggests that a stem cell population resides in the CNH. When we tested TBM in the same way, this showed the same pattern of incorporation as grafts from fresh 10.5 d.p.c. TBM, albeit a slight increase in the frequency of grafts that incorporate in the axis (compare TBM grafts in Tables 1 and 3). However, this subpopulation of TBM cells that originated from anterior streak does not show any greater tendency for retention in the tail bud than the bulk population of TBM, and argues against stem cells residing in any part of the TBM.

It is interesting to note that the grafts that gave rise to three generations of incorporation in the axis and CNH were descended from initial node grafts that showed contribution to both notochord and paraxial mesoderm. This, together with the observation that many node grafts did not show such contribution, suggests that it is not the node itself, but cells immediately abutting it that were included with the grafted tissue, that demonstrate stem cell-like properties. This would correspond well with the hypothesis, discussed earlier, that the ventral layer of the node contains committed notochord progenitors, while cells in its vicinity in the ectoderm layer constitute less committed (stem cell) progenitors. An interesting parallel to these experiments is seen in studies of the chick node and anterior streak (Charrier et al., 1999). The junction of Hensen's node and the anterior primitive streak (the axial-paraxial hinge) shows overlapping expression of genes characteristic of the node (*Hnf3b* and chordin) and those characteristic of the streak (chicken *Tbx6l*). Cells from this region are capable of generating notochord, neural tube or somites. Normally this contribution is limited to small regions of the axis, and cells are retained in the tail bud. Deletion of the bulk of Hensen's node (excluding the axial-paraxial hinge) results in the interruption of notochord formation, but this resumes further posteriorly. However, deletion of the axial-paraxial hinge results in embryos in which notochord formation continues for a short distance, but is followed by axial truncation. These results imply that this region is important as a signalling centre allowing maintenance of axial elongation, and/or that it contains stem cells for the axis. This is consistent with lineage data in the chick that places progenitors contributing to the entire mediolateral extent of all somites at the anterior end of the streak, in a region overlapping with notochord precursors (Psychoyos and Stern, 1996).

The hypothesis that stem cells are highly localised at the anterior streak, however, presents a paradox. If stem cells are so highly localised, why do fate maps show that most cells in
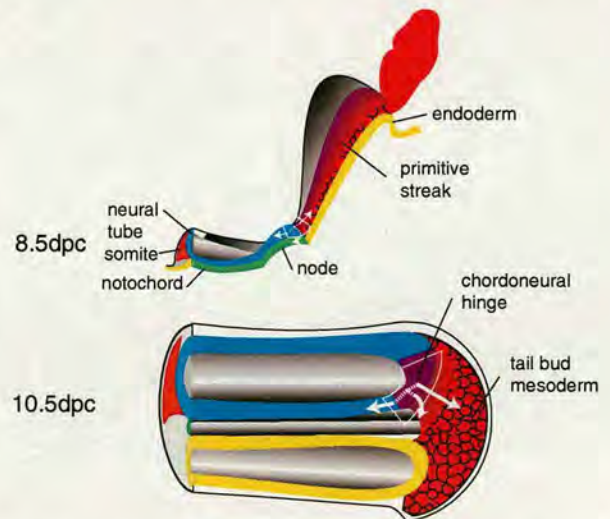
Fig. 8. Location of the progenitor cells during axis elongation. White boxes represent the regions in 8.5 d.p.c. and 10.5 d.p.c. embryos where the stem cell-like population resides. Descendants populate notochord, neural tube and somites (white arrows), and may originate from a common stem cell axial progenitor (broken lines).

the anterior streak close to the node give rise only to the medial portion of somites? The precursors of lateral somites lie more posteriorly in the streak at 8.5 d.p.c. (Wilson and Beddington, 1996). Descendants of these also contribute to the tail bud after 24-48 hours culture (Wilson and Beddington, 1996) (results not shown). However, they do not contribute to the CNH, but instead lie ventrally in the TBM. In contrast, the CNH can generate ventral tail bud mesoderm (Fig. 3A,D; Fig. 7A,K). Therefore, the cells in more posterior regions of the 8.5 d.p.c. streak may represent progenitors already committed to a mesoderm fate, which have themselves arisen earlier from a stem cell population near the node. Nonetheless, the contribution of cells in posterior regions of the 8.5 d.p.c. streak to relatively long axial distances without generating a population in which we can demonstrate extensive potency leaves open the possibility that not all of the postcranial axis is generated by node/streak border and CNH derived-stem cells.

The stem cell progenitors suggested by Nicolas and colleagues for the myotome and spinal cord may therefore reside close together in the regions we have identified: the junction of the node and streak at 8.5 d.p.c., and the CNH at 10.5-12.5 d.p.c. (Fig. 8). Their close physical proximity raises the possibility that a single multipotent axial stem cell type may exist, consistent with the observation that some cells in the *Xenopus* CNH appear to contribute to neurectoderm, somites and notochord (Davis and Kirschner, 2000). In the myotome, stem cell-derived clones are almost exclusively bilateral (Nicolas et al., 1996), consistent with our observation that CNH cells contribute bilaterally to host embryos. Our analysis also suggests a location for progenitor cells that contribute to up to six consecutive somites (either unilaterally or bilaterally) in the myotome observed by Nicolas et al. (Nicolas et al., 1996). The present study would locate such clones posterior to the axial-paraxial hinge at 8.5 d.p.c., and in the TBM from 10.5 d.p.c. Like these progenitors identified by Nicolas et al. (Nicolas et al., 1996) TBM derived cells contributed to one or both sides of the midline (results not shown). Our identification of the position of putative stem cells in the node/streak junction and the CNH will make it possible to characterise their potency in more detail via single cell transplantation or other forms of clonal analysis.

REFERENCES

Beck, C. W. and Slack, J. M. (1998). Analysis of the developing Xenopus tail bud reveals separate phases of gene expression during determination and outgrowth. *Mech. Dev.* **72**, 41-52.

Beddington, R. S. (1994). Induction of a second neural axis by the mouse node. *Development* **120**, 613-620.

Beddington, S. P. (1981). An autoradiographic analysis of the potency of embryonic ectoderm in the 8th day postimplantation mouse embryo. *J. Embryol. Exp. Morphol.* **64**, 87-104.

Bellomo, D., Lander, A., Harragan, I. and Brown, N. A. (1996). Cell proliferation in mammalian gastrulation: the ventral node and notochord are relatively quiescent. *Dev. Dyn.* **205**, 471-485.

Catala, M., Teillet, M. A. and le Douarin, N. M. (1995). Organization and development of the tail bud analyzed with the quail-chick chimaera system. *Mech. Dev.* **51**, 51-65.

Catala, M., Teillet, M. A., de Robertis, E. M. and le Douarin, M. L. (1996). A spinal cord fate map in the avian embryo: while regressing, Hensen's node lays down the notochord and floor plate thus joining the spinal cord lateral walls. *Development* **122**, 2599-2610.

Chapman, D. L., Agulnik, I., Hancock, S., Silver, L. M. and Papaioannou, V. E. (1996). Tbx6, a mouse T-Box gene implicated in paraxial mesoderm formation at gastrulation. *Dev. Biol.* **180**, 534-542.

Charrier, J. B., Teillet, M. A., Lapointe, F. and le Douarin, N. M. (1999). Defining subregions of Hensen's node essential for caudalward movement, midline development and cell survival. *Development* **126**, 4771-4783.

Chesley, P. (1935). Development of the short-tailed mutant in the house mouse. *J. Exp. Zool.* **70**, 429-459.

Cockroft, D. L. (1990). Dissection and culture of postimplantation embryos. In *Postimplantation Mammalian Embryos: A Practical Approach* (ed. A. J. Copp and D. L. Cockroft), pp. 15-40. Oxford: Oxford University Press.

Crossley, P. H. and Martin, G. R. (1995). The mouse Fgf8 gene encodes a family of polypeptides and is expressed in regions that direct outgrowth and patterning in the developing embryo. *Development* **121**, 439-451.

Davis, R. L. and Kirschner, M. W. (2000). The fate of cells in the tailbud of Xenopus laevis. *Development* **127**, 255-267.

Dunwoodie, S. L., Henrique, D., Harrison, S. M. and Beddington, R. S. (1997). Mouse Dll3: a novel divergent Delta gene which may complement the function of other Delta homologues during early pattern formation in the mouse embryo. *Development* **124**, 3065-3076.

Echelard, Y., Epstein, D. J., St-Jacques, B., Shen, L., Mohler, J., McMahon, J. A. and McMahon, A. P. (1993). Sonic hedgehog, a member of a family of putative signaling molecules, is implicated in the regulation of CNS polarity. *Cell* **75**, 1417-1430.

Gawantka, V., Pollet, N., Delius, H., Vingron, M., Pfister, R., Nitsch, R., Blumenstock, C. and Niehrs, C. (1998). Gene expression screening in Xenopus identifies molecular pathways, predicts gene function and provides a global view of embryonic patterning. *Mech. Dev.* **77**, 95-141.

Gont, L. K., Steinbeisser, H., Blumberg, B. and de Robertis, E. M. (1993). Tail formation as a continuation of gastrulation: the multiple cell populations of the Xenopus tailbud derive from the late blastopore lip. *Development* **119**, 991-1004.

Goulding, M. D., Chalepakis, G., Deutsch, U., Erselius, J. R. and Gruss, P. (1991). Pax-3, a novel murine DNA binding protein expressed during early neurogenesis. *EMBO J.* **10**, 1135-1147.

Greco, T. L., Takada, S., Newhouse, M. M., McMahon, J. A., McMahon, A. P. and Camper, S. A. (1996). Analysis of the vestigial tail mutation demonstrates that Wnt-3a gene dosage regulates mouse axial development. *Genes Dev.* **10**, 313-324.

Hogan, B., Beddington, R., Constantini, F. and Lacy, E. (1994). *Manipulating the Mouse Embryo: A Laboratory Manual*. Cold Spring Harbor: Cold Spring Harbor Laboratory Press.

Holmdahl, D. E. (1925). Experimentelle Untersuchungen über die Lage der Grenze zwischen primärer und sekundärer Körperentwicklung beim Hühn. *Anat. Anz.* **59**, 393-396.

Joubin, K. and Stern, C. D. (1999). Molecular interactions continuously define the organizer during the cell movements of gastrulation. *Cell* **98**, 559-571.

Kinder, S. J., Tsang, T. E., Wakamiya, M., Sasaki, H., Behringer, R. R., Nagy, A. and Tam, P. P. (2001). The organizer of the mouse gastrula is composed of a dynamic population of progenitor cells for the axial mesoderm. *Development* **128**, 3623-3634.

Knezevic, V., de Santo, R. and Mackem, S. (1998). Continuing organizer function during chick tail development. *Development* **125**, 1791-1801.

Lawson, K. A., Meneses, J. J. and Pedersen, R. A. (1991). Clonal analysis of epiblast fate during germ layer formation in the mouse embryo. *Development* **113**, 891-911.

Mathis, L. and Nicolas, J. F. (2000). Different clonal dispersion in the rostral and caudal mouse central nervous system. *Development* **127**, 1277-1290.

Munsie, M., Peura, T., Michalska, A., Trounson, A. and Mountford, P. (1998). Novel method for demonstrating nuclear contribution in mouse nuclear transfer. *Reprod. Fertil. Dev.* **10**, 633-637.

Nicolas, J. F., Mathis, L., Bonnerot, C. and Saurin, W. (1996). Evidence in the mouse for self-renewing stem cells in the formation of a segmented longitudinal structure, the myotome. *Development* **122**, 2933-2946.

Okabe, M., Ikawa, M., Kominami, K., Nakanishi, T. and Nishimune, Y. (1997). 'Green mice' as a source of ubiquitous green cells. *FEBS Lett.* **407**, 313-319.

Psychoyos, D. and Stern, C. D. (1996). Fates and migratory routes of primitive streak cells in the chick embryo. *Development* **122**, 1523-1534.

Ruiz, J. C. and Robertson, E. J. (1994). The expression of the receptor-protein tyrosine kinase gene, eck, is highly restricted during early mouse development. *Mech. Dev.* **46**, 87-100.

Selleck, M. A. and Stern, C. D. (1991). Fate mapping and cell lineage analysis of Hensen's node in the chick embryo. *Development* **112**, 615-626.

Snow, M. H. (1981). Autonomous development of parts isolated from primitive-streak-stage mouse embryos. Is development clonal? *J. Embryol. Exp. Morphol.* **65 Suppl**, 269-287.

Tajbakhsh, S. and Houzelstein, D. (1995). In situ hybridization and beta-galactosidase: a powerful combination for analysing transgenic mice. *Trends Genet.* **11**, 42.

Tam, P. P. and Tan, S. S. (1992). The somitogenetic potential of cells in the primitive streak and the tail bud of the organogenesis-stage mouse embryo. *Development* **115**, 703-715.

Tam, P. P. and Beddington, R. S. (1987). The formation of mesodermal tissues in the mouse embryo during gastrulation and early organogenesis. *Development* **99**, 109-126.

Tam, P. P., Parameswaran, M., Kinder, S. J. and Weinberger, R. P. (1997). The allocation of epiblast cells to the embryonic heart and other mesodermal lineages: the role of ingression and tissue movement during gastrulation. *Development* **124**, 1631-1642.

Tucker, A. S. and Slack, J. M. (1995). Tail bud determination in the vertebrate embryo. *Curr. Biol.* **5**, 807-813.

Wilkinson, D. G., Bhatt, S. and Herrmann, B. G. (1990). Expression pattern of the mouse T gene and its role in mesoderm formation. *Nature* **343**, 657-659.

Wilson, P. and Keller, R. (1991). Cell rearrangement during gastrulation of Xenopus: direct observation of cultured explants. *Development* **112**, 289-300.

Wilson, V. and Beddington, R. S. (1996). Cell fate and morphogenetic movement in the late mouse primitive streak. *Mech. Dev.* **55**, 79-89.

Wilson, V., Manson, L., Skarnes, W. C. and Beddington, R. S. (1995). The T gene is necessary for normal mesodermal morphogenetic cell movements during gastrulation. *Development* **121**, 877-886.

REFERENCES

Abdelkhalek, H. B., Beckers, A., Schuster-Gossler, K., Pavlova, M. N., Burkhardt, H., Lickert, H., Rossant, J., Reinhardt, R., Schalkwyk, L. C., Muller, I. et al. (2004). The mouse homeobox gene Not is required for caudal notochord development and affected by the truncate mutation. Genes Dev 18, 1725-36.

Ang, S. L. and Rossant, J. (1994). HNF-3 beta is essential for node and notochord formation in mouse development. Cell 78, 561-74.

Aubert, J., Stavridis, M. P., Tweedie, S., O'Reilly, M., Vierlinger, K., Li, M., Ghazal, P., Pratt, T., Mason, J. O., Roy, D. et al. (2003). Screening for mammalian neural genes via fluorescence-activated cell sorter purification of neural precursors from Sox1-gfp knock-in mice. Proc Natl Acad Sci U S A 100 Suppl 1, 11836-41.

Aulehla, A., Wehrle, C., Brand-Saberi, B., Kemler, R., Gossler, A., Kanzler, B. and Herrmann, B. G. (2003). Wnt3a plays a major role in the segmentation clock controlling somitogenesis. Dev Cell 4, 395-406.

Bancroft, J. D. and Gamble, M. (2002). Theory and Practice of Histological Techniques: Churchill Livingstone.

Barnes, J. D., Crosby, J. L., Jones, C. M., Wright, C. V. and Hogan, B. L. (1994). Embryonic expression of Lim-1, the mouse homolog of Xenopus Xlim-1, suggests a role in lateral mesoderm differentiation and neurogenesis. Dev Biol 161, 168-78.

Bastian, H. and Gruss, P. (1990). A murine even-skipped homologue, Evx 1, is expressed during early embryogenesis and neurogenesis in a biphasic manner. Embo J 9, 1839-52.

Beck, C. W. and Slack, J. M. (1998). Analysis of the developing Xenopus tail bud reveals separate phases of gene expression during determination and outgrowth. Mech Dev 72, 41-52.

Beck, C. W. and Slack, J. M. (1999). A developmental pathway controlling outgrowth of the Xenopus tail bud. Development 126, 1611-20.

Beck, C. W., Whitman, M. and Slack, J. M. (2001). The role of BMP signaling in outgrowth and patterning of the Xenopus tail bud. Dev Biol 238, 303-14.

Beddington, R. S. (1994). Induction of a second neural axis by the mouse node. Development 120, 613-20.

Beddington, S. P. (1981). An autoradiographic analysis of the potency of embryonic ectoderm in the 8th day postimplantation mouse embryo. J Embryol Exp Morphol 64, 87-104.

Bellomo, D., Lander, A., Harragan, I. and Brown, N. A. (1996). Cell proliferation in mammalian gastrulation: the ventral node and notochord are relatively quiescent. Dev Dyn 205, 471-485.

Bitjel, J. H. (1936). Die Mesodermbildungspotenzen der hinteren Medullarplatten bezirke bei Amblystoma mexicanum in Bezug auf die Schwanzbildung. Wilhelm Roux' Arch F EntwMech Org 134, 262-282.

Bonnerot, C. and Nicolas, J. F. (1993). Clonal analysis in the intact mouse embryo by intragenic homologous recombination. C R Acad Sci III 316, 1207-17.

Bonnerot, C., Rocancourt, D., Briand, P., Grimber, G. and Nicolas, J. F. (1987). A beta-galactosidase hybrid protein targeted to nuclei as a marker for developmental studies. Proc Natl Acad Sci U S A 84, 6795-9.

Brennan, J., Lu, C. C., Norris, D. P., Rodriguez, T. A., Beddington, R. S. and Robertson, E. J. (2001). Nodal signalling in the epiblast patterns the early mouse embryo. Nature 411, 965-9.

Cambray, N. and Wilson, V. (2002). Axial progenitors with extensive potency are localised to the mouse chordoneural hinge. Development 129, 4855-66.

Cao, Y., Knochel, S., Donow, C., Miethe, J., Kaufmann, E. and Knochel, W. (2004). The POU factor Oct-25 regulates the Xvent-2B gene and counteracts terminal differentiation in Xenopus embryos. J Biol Chem 279, 43735-43.

Catala, M., Teillet, M. A., De Robertis, E. M. and Le Douarin, M. L. (1996). A spinal cord fate map in the avian embryo: while regressing, Hensen's node lays down the notochord and floor plate thus joining the spinal cord lateral walls. Development 122, 2599-610.

Catala, M., Teillet, M. A. and Le Douarin, N. M. (1995). Organization and development of the tail bud analyzed with the quail-chick chimaera system. Mech Dev 51, 51-65.

Chambers, I., Colby, D., Robertson, M., Nichols, J., Lee, S., Tweedie, S. and Smith, A. (2003). Functional expression cloning of Nanog, a pluripotency sustaining factor in embryonic stem cells. Cell 113, 643-55.

Chapman, D. L., Agulnik, I., Hancock, S., Silver, L. M. and Papaioannou, V. E. (1996). Tbx6, a mouse T-Box gene implicated in paraxial mesoderm formation at gastrulation. Dev Biol 180, 534-42.

Charrier, J. B., Lapointe, F., Le Douarin, N. M. and Teillet, M. A. (2001). Anti-apoptotic role of Sonic hedgehog protein at the early stages of nervous system organogenesis. Development 128, 4011-20.

Charrier, J. B., Lapointe, F., Le Douarin, N. M. and Teillet, M. A. (2002). Dual origin of the floor plate in the avian embryo. Development 129, 4785-96.

Charrier, J. B., Teillet, M. A., Lapointe, F. and Le Douarin, N. M. (1999). Defining subregions of Hensen's node essential for caudalward movement, midline development and cell survival. Development 126, 4771-83.

Chawengsaksophak, K., de Graaff, W., Rossant, J., Deschamps, J. and Beck, F. (2004). Cdx2 is essential for axial elongation in mouse development. Proc Natl Acad Sci U S A 101, 7641-5.

Chawengsaksophak, K., James, R., Hammond, V. E., Kontgen, F. and Beck, F. (1997). Homeosis and intestinal tumours in Cdx2 mutant mice. Nature 386, 84-7.

Chesley, P. (1935). Development of the short-tailed mutant in the house mouse. J Exp Zool 70, 429-459.

Chiang, C., Litingtung, Y., Lee, E., Young, K. E., Corden, J. L., Westphal, H. and Beachy, P. A. (1996). Cyclopia and defective axial patterning in mice lacking Sonic hedgehog gene function. Nature 383, 407-13.

Ciruna, B. and Rossant, J. (2001). FGF signaling regulates mesoderm cell fate specification and morphogenetic movement at the primitive streak. Dev Cell 1, 37-49.

Ciruna, B. G., Schwartz, L., Harpal, K., Yamaguchi, T. P. and Rossant, J. (1997). Chimeric analysis of fibroblast growth factor receptor-1 (Fgfr1) function: a role for FGFR1 in morphogenetic movement through the primitive streak. Development 124, 2829-41.

Collignon, J., Varlet, I. and Robertson, E. J. (1996). Relationship between asymmetric nodal expression and the direction of embryonic turning. Nature 381, 155-8.

Colvin, J. S., Feldman, B., Nadeau, J. H., Goldfarb, M. and Ornitz, D. M. (1999). Genomic organization and embryonic expression of the mouse fibroblast growth factor 9 gene. Dev Dyn 216, 72-88.

Conlon, F. L., Lyons, K. M., Takaesu, N., Barth, K. S., Kispert, A., Herrmann, B. and Robertson, E. J. (1994). A primary requirement for nodal in the formation and maintenance of the primitive streak in the mouse. Development 120, 1919-28.

Conlon, R. A., Reaume, A. G. and Rossant, J. (1995). Notch1 is required for the coordinate segmentation of somites. Development 121, 1533-45.

Copp, A. J. and Cockroft, D. L. (1990). Postimplantation Mammalian embryos. Oxford: IRL PRESS.

Crossley, P. H. and Martin, G. R. (1995). The mouse Fgf8 gene encodes a family of polypeptides and is expressed in regions that direct outgrowth and patterning in the developing embryo. Development 121, 439-51.

Dale, J. K., Maroto, M., Dequeant, M. L., Malapert, P., McGrew, M. and Pourquie, O. (2003). Periodic notch inhibition by lunatic fringe underlies the chick segmentation clock. Nature 421, 275-8.

Dale, L. and Slack, J. M. (1987). Fate map for the 32-cell stage of Xenopus laevis. Development 99, 527-51.

Davis, R. L. and Kirschner, M. W. (2000). The fate of cells in the tailbud of Xenopus laevis. Development 127, 255-67.

Downs, K. M. and Davies, T. (1993). Staging of gastrulating mouse embryos by morphological landmarks in the dissecting microscope. Development 118, 1255-66.

Dubrulle, J. and Pourquie, O. (2004). fgf8 mRNA decay establishes a gradient that couples axial elongation to patterning in the vertebrate embryo. Nature 427, 419-22.

Dufort, D., Schwartz, L., Harpal, K. and Rossant, J. (1998). The transcription factor HNF3beta is required in visceral endoderm for normal primitive streak morphogenesis. Development 125, 3015-25.

Dunwoodie, S. L., Henrique, D., Harrison, S. M. and Beddington, R. S. (1997). Mouse Dll3: a novel divergent Delta gene which may complement the function of other Delta homologues during early pattern formation in the mouse embryo. Development 124, 3065-76.

Dush, M. K. and Martin, G. R. (1992). Analysis of mouse Evx genes: Evx-1 displays graded expression in the primitive streak. Dev Biol 151, 273-87.

Echelard, Y., Epstein, D. J., St-Jacques, B., Shen, L., Mohler, J., McMahon, J. A. and McMahon, A. P. (1993). Sonic hedgehog, a member of a family of putative signaling molecules, is implicated in the regulation of CNS polarity. Cell 75, 1417-30.

Economides, K. D., Zeltser, L. and Capecchi, M. R. (2003). Hoxb13 mutations cause overgrowth of caudal spinal cord and tail vertebrae. Dev Biol 256, 317-30.

Ekonomou, A., Kazanis, I., Malas, S., Wood, H., Alifragis, P., Denaxa, M., Karagogeos, D., Constanti, A., Lovell-Badge, R. and Episkopou, V. (2005). Neuronal migration and ventral subtype identity in the telencephalon depend on SOX1. PLoS Biol 3, e186.

Eloy-Trinquet, S. and Nicolas, J. F. (2002). Cell coherence during production of the presomitic mesoderm and somitogenesis in the mouse embryo. Development 129, 3609-19.

Faure, S., Lee, M. A., Keller, T., ten Dijke, P. and Whitman, M. (2000). Endogenous patterns of TGFbeta superfamily signaling during early Xenopus development. Development 127, 2917-31.

Fleming, R. J., Gu, Y. and Hukriede, N. A. (1997). Serrate-mediated activation of Notch is specifically blocked by the product of the gene fringe in the dorsal compartment of the Drosophila wing imaginal disc. Development 124, 2973-81.

Forss-Petter, S., Danielson, P. E., Catsicas, S., Battenberg, E., Price, J., Nerenberg, M. and Sutcliffe, J. G. (1990). Transgenic mice expressing beta-galactosidase in mature neurons under neuron-specific enolase promoter control. Neuron 5, 187-97.

Gajovic, S. and Kostovic-Knezevic, L. (1995). Ventral ectodermal ridge and ventral ectodermal groove: two distinct morphological features in the developing rat embryo tail. Anat Embryol (Berl) 192, 181-7.

Gawantka, V., Pollet, N., Delius, H., Vingron, M., Pfister, R., Nitsch, R., Blumenstock, C. and Niehrs, C. (1998). Gene expression screening in Xenopus identifies molecular pathways, predicts gene function and provides a global view of embryonic patterning. Mech Dev 77, 95-141.

Gofflot, F., Hall, M. and Morriss-Kay, G. M. (1997). Genetic patterning of the developing mouse tail at the time of posterior neuropore closure. Dev Dyn 210, 431-45.

Goldman, D. C., Martin, G. R. and Tam, P. P. (2000). Fate and function of the ventral ectodermal ridge during mouse tail development. Development 127, 2113-23.

Gont, L. K., Steinbeisser, H., Blumberg, B. and de Robertis, E. M. (1993). Tail formation as a continuation of gastrulation: the multiple cell populations of the Xenopus tailbud derive from the late blastopore lip. Development 119, 991-1004.

Goulding, M. D., Chalepakis, G., Deutsch, U., Erselius, J. R. and Gruss, P. (1991). Pax-3, a novel murine DNA binding protein expressed during early neurogenesis. Embo J 10, 1135-47.

Greco, T. L., Takada, S., Newhouse, M. M., McMahon, J. A., McMahon, A. P. and Camper, S. A. (1996). Analysis of the vestigial tail mutation demonstrates that Wnt-3a gene dosage regulates mouse axial development. Genes Dev 10, 313-24.

Griffith, C. M., Wiley, M. J. and Sanders, E. J. (1992). The vertebrate tail bud: three germ layers from one tissue. Anat Embryol (Berl) 185, 101-13.

Gruneberg, H. (1957). Genetical studies on the skeleton of the mouse. XIX. Vestigial-tail. J Genet 55, 181-194.

Gruneberg, H. (1958). Genetical studies on the skeleton of the mouse. XXIII. The development of brachyury and anury. J Embryol Exp Morphol 6, 424-43.

Gruneberg, H. and McLaren, A. (1972). The skeletal phenotype of some mouse chimaeras. Proc R Soc Lond B 182, 9-23.

Gruneberg, H. and Wickramaratne, G. A. (1974). A re-examination of two skeletal mutants of the mouse, vestigial-tail (vt) and congenital hydrocephalus (ch). J Embryol Exp Morphol 31, 207-22.

Gubbay, J., Collignon, J., Koopman, P., Capel, B., Economou, A., Munsterberg, A., Vivian, N., Goodfellow, P. and Lovell-Badge, R. (1990). A gene mapping to the sex-determining region of the mouse Y chromosome is a member of a novel family of embryonically expressed genes. Nature 346, 245-50.

Hamburger, V. (1988). The Heritage of Experimental Embryology: Oxford, England: Oxford University Press.

Hamburger, V. and Hamilton, H. L. (1992). A series of normal stages in the development of the chick embryo (1951). Dev Dyn 195, 231-72.

Herrmann, B. G. (1991). Expression pattern of the Brachyury gene in whole-mount TWis/TWis mutant embryos. Development 113, 913-7.

Herrmann, B. G., Labeit, S., Poustka, A., King, T. R. and Lehrach, H. (1990). Cloning of the T gene required in mesoderm formation in the mouse. Nature 343, 617-22.

Heston, W. E. (1951). The "vestigial tail" mouse; a new recessive mutation. J Hered 42, 71-4.

Hogan, B., Beddington, R., Constantini, F. and Lacy, E. (1994). Manipulating the Mouse Embryo: A Laboratory Manual. Cold Spring Harbor, NY, USA: Cold Spring Harbor Laboratory Press.

Holmdahl, D. E. (1925). Experimentelle Untersuchungen über die Lage der Grenze zwischen primärer und sekundärer Körperentwicklung beim Huhn. Anat Anz 59, 393-396.

Hopper, A. F. and Hart, N. H. (1985). Foundations of Animal Development: New York: Oxford University Press.

Hukriede, N. A., Tsang, T. E., Habas, R., Khoo, P. L., Steiner, K., Weeks, D. L., Tam, P. P. and Dawid, I. B. (2003). Conserved requirement of Lim1 function for cell movements during gastrulation. Dev Cell 4, 83-94.

Huppert, S. S., Ilagan, M. X., De Strooper, B. and Kopan, R. (2005). Analysis of Notch function in presomitic mesoderm suggests a gamma-secretase-independent role for presenilins in somite differentiation. Dev Cell 8, 677-88.

Izpisua-Belmonte, J. C., De Robertis, E. M., Storey, K. G. and Stern, C. D. (1993). The homeobox gene goosecoid and the origin of organizer cells in the early chick blastoderm. Cell 74, 645-59.

James, R. and Kazenwadel, J. (1991). Homeobox gene expression in the intestinal epithelium of adult mice. J Biol Chem 266, 3246-51.

Jen, W. C., Gawantka, V., Pollet, N., Niehrs, C. and Kintner, C. (1999). Periodic repression of Notch pathway genes governs the segmentation of Xenopus embryos. Genes Dev 13, 1486-99.

Johnson, R. L., Laufer, E., Riddle, R. D. and Tabin, C. (1994). Ectopic expression of Sonic hedgehog alters dorsal-ventral patterning of somites. Cell 79, 1165-73.

Joly, J. S., Joly, C., Schulte-Merker, S., Boulekbache, H. and Condamine, H. (1993). The ventral and posterior expression of the zebrafish homeobox gene eve1 is perturbed in dorsalized and mutant embryos. Development 119, 1261-75.

Joubin, K. and Stern, C. D. (1999). Molecular interactions continuously define the organizer during the cell movements of gastrulation. Cell 98, 559-71.

Kablar, B., Krastel K., Tajbakhsh, S. and Rudnicki, M. A. (2003). Myf5 and MyoD activation define independent myogenic compartments during embryonic development. Dev Biol 258, 307-18.

Kanki, J. P. and Ho, R. K. (1997). The development of the posterior body in zebrafish. Development 124, 881-93.

Keller, R., Shih, J., Wilson, P. and Sater, A. (1991). Pattern and function of cell motility and cell interactions during convergence and extension in Xenopus: New York: Wiley-Liss.

Kerr, J. G. (1919). Textbook of Embryology Vol. II: London: Macmillan and Co.

Kinder, S. J., Tsang, T. E., Wakamiya, M., Sasaki, H., Behringer, R. R., Nagy, A. and Tam, P. P. (2001). The organizer of the mouse gastrula is composed of a dynamic population of progenitor cells for the axial mesoderm. Development 128, 3623-34.

Kingsbury, B. F. (1932). The 'law' of cephalocaudal differential growth in its application to the nervous system. J Comp Neur 56, 431-463.

Kispert, A. and Herrmann, B. G. (1993). The Brachyury gene encodes a novel DNA binding protein. Embo J 12, 3211-20.

Kispert, A. and Herrmann, B. G. (1994). Immunohistochemical analysis of the Brachyury protein in wild-type and mutant mouse embryos. Dev Biol 161, 179-93.

Kispert, A., Ortner, H., Cooke, J. and Herrmann, B. G. (1995). The chick Brachyury gene: developmental expression pattern and response to axial induction by localized activin. Dev Biol 168, 406-15.

Klarsfeld, A., Bessereau, J. L., Salmon, A. M., Triller, A., Babinet, C. and Changeux, J. P. (1991). An acetylcholine receptor alpha-subunit promoter conferring preferential synaptic expression in muscle of transgenic mice. Embo J 10, 625-32.

Knezevic, V., De Santo, R. and Mackem, S. (1998). Continuing organizer function during chick tail development. Development 125, 1791-801.

Koizumi, K., Nakajima, M., Yuasa, S., Saga, Y., Sakai, T., Kuriyama, T., Shirasawa, T. and Koseki, H. (2001). The role of presenilin 1 during somite segmentation. Development 128, 1391-402.

Laufer, E., Dahn, R., Orozco, O. E., Yeo, C. Y., Pisenti, J., Henrique, D., Abbott, U. K., Fallon, J. F. and Tabin, C. (1997). Expression of Radical fringe in limb-bud ectoderm regulates apical ectodermal ridge formation. Nature 386, 366-73.

Lawson, K. A., Meneses, J. J. and Pedersen, R. A. (1991). Clonal analysis of epiblast fate during germ layer formation in the mouse embryo. Development 113, 891-911.

Lawson, K. A. and Pedersen, R. A. (1992). Clonal analysis of cell fate during gastrulation and early neurulation in the mouse. Ciba Found Symp 165, 3-21; discussion 21-6.

Le Douarin, N. M. (1969). Particularités du noyau interphasique chez la Caille japonaise (Coturnix coturnix japonica). Utilisation de ces particularités comme 'marquage biologique' dans les recherches sur les interactions tissulaires et les migrations cellulaires au cours de l' ontogénèse. Bull Biol Fr Belg 103, 435-452.

Liu, C., Knezevic, V. and Mackem, S. (2004). Ventral tail bud mesenchyme is a signaling center for tail paraxial mesoderm induction. Dev Dyn 229, 600-6.

Lopez, S. L., Paganelli, A. R., Siri, M. V., Ocana, O. H., Franco, P. G. and Carrasco, A. E. (2003). Notch activates sonic hedgehog and both are involved in the specification of dorsal midline cell-fates in Xenopus. Development 130, 2225-38.

Lopez, S. L., Rosato-Siri, M. V., Franco, P. G., Paganelli, A. R. and Carrasco, A. E. (2005). The Notch-target gene hairy2a impedes the involution of notochordal cells by promoting floor plate fates in Xenopus embryos. Development 132, 1035-46.

Lowe, L. A., Supp, D. M., Sampath, K., Yokoyama, T., Wright, C. V., Potter, S. S., Overbeek, P. and Kuehn, M. R. (1996). Conserved left-right asymmetry of nodal expression and alterations in murine situs inversus. Nature 381, 158-61.

Lowe, L. A., Yamada, S. and Kuehn, M. R. (2001). Genetic dissection of nodal function in patterning the mouse embryo. Development 128, 1831-43.

Mahmood, R., Bresnick, J., Hornbruch, A., Mahony, C., Morton, N., Colquhoun, K., Martin, P., Lumsden, A., Dickson, C. and Mason, I. (1995). A role for FGF-8 in the initiation and maintenance of vertebrate limb bud outgrowth. Curr Biol 5, 797-806.

Malas, S., Postlethwaite, M., Ekonomou, A., Whalley, B., Nishiguchi, S., Wood, H., Meldrum, B., Constanti, A. and Episkopou, V. (2003). Sox1-deficient mice suffer from epilepsy associated with abnormal ventral forebrain development and olfactory cortex hyperexcitability. Neuroscience 119, 421-32.

Maruoka, Y., Ohbayashi, N., Hoshikawa, M., Itoh, N., Hogan, B. L. and Furuta, Y. (1998). Comparison of the expression of three highly related genes, Fgf8, Fgf17 and Fgf18, in the mouse embryo. Mech Dev 74, 175-7.

Mathis, L. and Nicolas, J. F. (2000). Different clonal dispersion in the rostral and caudal mouse central nervous system. Development 127, 1277-90.

Mathis, L., Sieur, J., Voiculescu, O., Charnay, P. and Nicolas, J. F. (1999). Successive patterns of clonal cell dispersion in relation to neuromeric subdivision in the mouse neuroepithelium. Development 126, 4095-106.

McWhirter, J. R., Goulding, M., Weiner, J. A., Chun, J. and Murre, C. (1997). A novel fibroblast growth factor gene expressed in the developing nervous system is a downstream target of the chimeric homeodomain oncoprotein E2A-Pbx1. Development 124, 3221-32.

Mitsui, K., Tokuzawa, Y., Itoh, H., Segawa, K., Murakami, M., Takahashi, K., Maruyama, M., Maeda, M. and Yamanaka, S. (2003). The homeoprotein Nanog is required for maintenance of pluripotency in mouse epiblast and ES cells. Cell 113, 631-42.

Moore, K. (1977). The Developing Human: Philadelphia: W. B. Saunders Company.

Munsie, M., Peura, T., Michalska, A., Trounson, A. and Mountford, P. (1998). Novel method for demonstrating nuclear contribution in mouse nuclear transfer. Reprod Fertil Dev 10, 633-7.

Munsterberg, A. E., Kitajewski, J., Bumcrot, D. A., McMahon, A. P. and Lassar, A. B. (1995). Combinatorial signaling by Sonic hedgehog and Wnt family members induces myogenic bHLH gene expression in the somite. Genes Dev 9, 2911-22.

Munsterberg, A. E. and Lassar, A. B. (1995). Combinatorial signals from the neural tube, floor plate and notochord induce myogenic bHLH gene expression in the somite. Development 121, 651-60.

Nichols, J., Zevnik, B., Anastassiadis, K., Niwa, H., Klewe-Nebenius, D., Chambers, I., Scholer, H. and Smith, A. (1998). Formation of pluripotent stem cells in the mammalian embryo depends on the POU transcription factor Oct4. Cell 95, 379-91.

Nicolas, J. F., Mathis, L., Bonnerot, C. and Saurin, W. (1996). Evidence in the mouse for self-renewing stem cells in the formation of a segmented longitudinal structure, the myotome. Development 122, 2933-46.

Nieuwkoop, P. D. and Faber, J. (1967). Normal Table of Xenopus laevis: Amsterdam: North Holland.

Nievelstein, R. A., Hartwig, N. G., Vermeij-Keers, C. and Valk, J. (1993). Embryonic development of the mammalian caudal neural tube. Teratology 48, 21-31.

Niewkoop, P. D. a. F. J. (1967). Normal Table of Xenopus laevis Development. Amsterdam: North-Holland.

Nishiguchi, S., Wood, H., Kondoh, H., Lovell-Badge, R. and Episkopou, V. (1998). Sox1 directly regulates the gamma-crystallin genes and is essential for lens development in mice. Genes Dev 12, 776-81.

Niswander, L. and Martin, G. R. (1992). Fgf-4 expression during gastrulation, myogenesis, limb and tooth development in the mouse. Development 114, 755-68.

Okabe, M., Ikawa, M., Kominami, K., Nakanishi, T. and Nishimune, Y. (1997). 'Green mice' as a source of ubiquitous green cells. FEBS Lett 407, 313-9.

Okamoto, K., Okazawa, H., Okuda, A., Sakai, M., Muramatsu, M. and Hamada, H. (1990). A novel octamer binding transcription factor is differentially expressed in mouse embryonic cells. Cell 60, 461-72.

Panin, V. M., Papayannopoulos, V., Wilson, R. and Irvine, K. D. (1997). Fringe modulates Notch-ligand interactions. Nature 387, 908-12.

Panthier, J. J. and Condamine, H. Mitotic recombination in mammals. BioEssays 13, 351-56.

Pasteels, J. (1937). Etudes sur la gastrulation des vertébrés méroblastiques. III. Oiseaux.IV. Conclusions générales. Archives de Biologie 48, 381-488.

Pasteels, J. (1943). Proliférations et croissance dans la gastrulation et la formation de la queue des Vertébrés. Archives de Biologie 54, 1-51.

Perea-Gomez, A., Vella, F. D., Shawlot, W., Oulad-Abdelghani, M., Chazaud, C., Meno, C., Pfister, V., Chen, L., Robertson, E., Hamada, H. et al. (2002). Nodal antagonists in the anterior visceral endoderm prevent the formation of multiple primitive streaks. Dev Cell 3, 745-56.

Pevny, L. H., Sockanathan, S., Placzek, M. and Lovell-Badge, R. (1998). A role for SOX1 in neural determination. Development 125, 1967-78.

Plouhinec, J. L., Granier, C., Le Mentec, C., Lawson, K. A., Saberan-Djoneidi, D., Aghion, J., Shi, D. L., Collignon, J. and Mazan, S. (2004). Identification of the mammalian Not gene via a phylogenomic approach. Gene Expr Patterns 5, 11-22.

Pollet, N., Muncke, N., Verbeek, B., Li, Y., Fenger, U., Delius, H. and Niehrs, C. (2005). An atlas of differential gene expression during early Xenopus embryogenesis. Mech Dev 122, 365-439.

Pourquie, O. (2004). The chick embryo: a leading model in somitogenesis studies. Mech Dev 121, 1069-79.

Przemeck, G. K., Heinzmann, U., Beckers, J. and Hrabe de Angelis, M. (2003). Node and midline defects are associated with left-right development in Delta1 mutant embryos. Development 130, 3-13.

Psychoyos, D. and Stern, C. D. (1996). Fates and migratory routes of primitive streak cells in the chick embryo. Development 122, 1523-34.

Rashbass, P., Cooke, L. A., Herrmann, B. G. and Beddington, R. S. (1991). A cell autonomous function of Brachyury in T/T embryonic stem cell chimaeras. Nature 353, 348-51.

Robertson, E. J. (1987). Teratocarcinomas and embryonic stem cells a practical approach. Oxford-Washington DC: IRL PRESS.

Rodriguez-Esteban, C., Schwabe, J. W., De La Pena, J., Foys, B., Eshelman, B. and Belmonte, J. C. (1997). Radical fringe positions the apical ectodermal ridge at the dorsoventral boundary of the vertebrate limb. Nature 386, 360-6.

Roelink, H. and Nusse, R. (1991). Expression of two members of the Wnt family during mouse development--restricted temporal and spatial patterns in the developing neural tube. Genes Dev 5, 381-8.

Rosner, M. H., Vigano, M. A., Ozato, K., Timmons, P. M., Poirier, F., Rigby, P. W. and Staudt, L. M. (1990). A POU-domain transcription factor in early stem cells and germ cells of the mammalian embryo. Nature 345, 686-92.

Ruiz i Altaba, A. and Melton, D. A. (1989). Interaction between peptide growth factors and homoeobox genes in the establishment of antero-posterior polarity in frog embryos. Nature 341, 33-8.

Sambrook, J., Fritsch, E. F. and Maniatis, T. (1989). Molecular Cloning: A Laboratory Manual. Cold Spring Harbor, NY, USA: Cold Spring Harbor Laboratory Press.

Sasaki, H. and Hogan, B. L. (1993). Differential expression of multiple fork head related genes during gastrulation and axial pattern formation in the mouse embryo. Development 118, 47-59.

Sasaki, H. and Hogan, B. L. (1994). HNF-3 beta as a regulator of floor plate development. Cell 76, 103-15.

Schoenwolf, G. C. (1977). The tail (end) bud contribution to the posterior region of the chick embryo. Anat Rec 192, 289-296.

Schoenwolf, G. C. (1984). Histological and ultrastructural studies of secondary neurulation in mouse embryos. Am J Anat 169, 361-76.

Schoenwolf, G. C. and Delongo, J. (1980). Ultrastructure of secondary neurulation in the chick embryo. Am J Anat 158, 43-63.

Schoenwolf, G. C. and Smith, J. L. (1990). Mechanisms of neurulation: traditional viewpoint and recent advances. Development 109, 243-70.

Scholer, H. R., Ruppert, S., Suzuki, N., Chowdhury, K. and Gruss, P. (1990a). New type of POU domain in germ line-specific protein Oct-4. Nature 344, 435-9.

Scholer, H. R., Dressler, G. R., Balling, R., Rohdewohld, H. and Gruss, P. (1990b). Oct-4: a germline-specific transcription factor mapping to the mouse t-complex. Embo J 9, 2185-95.

Selleck, M. A. and Stern, C. D. (1991). Fate mapping and cell lineage analysis of Hensen's node in the chick embryo. Development 112, 615-26.

Shawlot, W. and Behringer, R. R. (1995). Requirement for Lim1 in head-organizer function. Nature 374, 425-30.

Shih, J. and Keller, R. (1992). Cell motility driving mediolateral intercalation in explants of Xenopus laevis. Development 116, 901-14.

Sive, H. L., Grainger, R. M. and Harland, R. M. (2000). Early Development of Xenopus laevis - A laboratory manual: Cold Spring Harbor, New York.

Slusarski, D. C., Corces, V. G. and Moon, R. T. (1997). Interaction of Wnt and a Frizzled homologue triggers G-protein-linked phosphatidylinositol signalling. Nature 390, 410-3.

Snow, M. H. (1981). Autonomous development of parts isolated from primitive-streak-stage mouse embryos. Is development clonal? J Embryol Exp Morphol 65 Suppl, 269-87.

Spemann, H. (1931). Über den Anteil von Implantat und Wirtskeim an der Orientierung und Beschaffenheit der induzierten Embryonalanlage. Wilhelm Roux' Arch F EntwMech Org 123, 389-517.

Spemann, H. and Mangold, H. (1924). Über Induktion von Embryonalanlagen durch Implantation artfremder Organisatoren. Wilhelm Roux' Arch F EntwMech Org 100, 599-638.

Spyropoulos, D. D. and Capecchi, M. R. (1994). Targeted disruption of the even-skipped gene, evx1, causes early postimplantation lethality of the mouse conceptus. Genes Dev 8, 1949-61.

Stewart, R. and Gerhart, J. (1991). Induction of notochord by the organizer in Xenopus. Roux's Arch Dev Biol 199, 341-348.

Sun, X., Meyers, E. N., Lewandoski, M. and Martin, G. R. (1999). Targeted disruption of Fgf8 causes failure of cell migration in the gastrulating mouse embryo. Genes Dev 13, 1834-46.

Tabin, C. J. and Vogan, K. J. (2003). A two-cilia model for vertebrate left-right axis specification. Genes Dev 17, 1-6.

Taira, M., Jamrich, M., Good, P. J. and Dawid, I. B. (1992). The LIM domain-containing homeo box gene Xlim-1 is expressed specifically in the organizer region of Xenopus gastrula embryos. Genes Dev 6, 356-66.

Tajbakhsh, S. and Houzelstein, D. (1995). In situ hybridization and beta-galactosidase: a powerful combination for analysing transgenic mice. Trends Genet 11, 42.

Takada, S., Stark, K. L., Shea, M. J., Vassileva, G., McMahon, J. A. and McMahon, A. P. (1994). Wnt-3a regulates somite and tailbud formation in the mouse embryo. Genes Dev 8, 174-89.

Tam, P. P. (1986). A study of the pattern of prospective somites in the presomitic mesoderm of mouse embryos. J Embryol Exp Morphol 92, 269-85.

Tam, P. P. (1989). Regionalisation of the mouse embryonic ectoderm: allocation of prospective ectodermal tissues during gastrulation. Development 107, 55-67.

Tam, P. P. and Beddington, R. S. (1987). The formation of mesodermal tissues in the mouse embryo during gastrulation and early organogenesis. Development 99, 109-26.

Tam, P. P., Parameswaran, M., Kinder, S. J. and Weinberger, R. P. (1997). The allocation of epiblast cells to the embryonic heart and other mesodermal lineages: the role of ingression and tissue movement during gastrulation. Development 124, 1631-42.

Tam, P. P. and Tan, S. S. (1992). The somitogenetic potential of cells in the primitive streak and the tail bud of the organogenesis-stage mouse embryo. Development 115, 703-15.

Tanaka, S., Kunath, T., Hadjantonakis, A. K., Nagy, A. and Rossant, J. (1998). Promotion of trophoblast stem cell proliferation by FGF4. Science 282, 2072-5.

Thibert, C., Teillet, M. A., Lapointe, F., Mazelin, L., Le Douarin, N. M. and Mehlen, P. (2003). Inhibition of neuroepithelial patched-induced apoptosis by sonic hedgehog. Science 301, 843-6.

Tucker, A. S. and Slack, J. M. (1995a). The Xenopus laevis tail-forming region. Development 121, 249-262.

Tucker, A. S. and Slack, J. M. (1995b). Tail bud determination in the vertebrate embryo. Curr Biol 5, 807-13.

von Dassow, G., Schmidt, J. E. and Kimelman, D. (1993). Induction of the Xenopus organizer: expression and regulation of Xnot, a novel FGF and activin-regulated homeo box gene. Genes Dev 7, 355-66.

Walther, C. and Gruss, P. (1991). Pax-6, a murine paired box gene, is expressed in the developing CNS. Development 113, 1435-49.

Weigel, D. and Jackle, H. (1990). The fork head domain: a novel DNA binding motif of eukaryotic transcription factors? Cell 63, 455-6.

Weinstein, D. C., Ruiz i Altaba, A., Chen, W. S., Hoodless, P., Prezioso, V. R., Jessell, T. M. and Darnell, J. E., Jr. (1994). The winged-helix transcription factor HNF-3 beta is required for notochord development in the mouse embryo. Cell 78, 575-88.

Westin, J. and Lardelli, M. (1997). Three novel Notch genes in zebrafish: Implications for vertebrate Notch gene evolution and function. Dev Genes Evol 207, 51-63.

Wilkinson, D. G. (1992). Whole mount in situ hybridisation of vertebrate embryos. Oxford: IRL PRESS.

Wilkinson, D. G., Bhatt, S. and Herrmann, B. G. (1990). Expression pattern of the mouse T gene and its role in mesoderm formation. Nature 343, 657-9.

Wilkinson, D. G., Peters, G., Dickson, C. and McMahon, A. P. (1988). Expression of the FGF-related proto-oncogene int-2 during gastrulation and neurulation in the mouse. Embo J 7, 691-5.

Wilson, V. and Beddington, R. S. (1996). Cell fate and morphogenetic movement in the late mouse primitive streak. Mech Dev 55, 79-89.

Wilson, V., Manson, L., Skarnes, W. C. and Beddington, R. S. (1995). The T gene is necessary for normal mesodermal morphogenetic cell movements during gastrulation. Development 121, 877-86.

Wong, P. C., Zheng, H., Chen, H., Becher, M. W., Sirinathsinghji, D. J., Trumbauer, M. E., Chen, H. Y., Price, D. L., Van der Ploeg, L. H. and Sisodia, S. S. (1997). Presenilin 1 is required for Notch1 and Dll1 expression in the paraxial mesoderm. Nature 387, 288-92.

Woo, K. and Fraser, S. E. (1995). Order and coherence in the fate map of the zebrafish nervous system. Development 121, 2595-609.

Wood, H. B. and Episkopou, V. (1999). Comparative expression of the mouse Sox1, Sox2 and Sox3 genes from pre-gastrulation to early somite stages. Mech Dev 86, 197-201.

Yamaguchi, T. P., Bradley, A., McMahon, A. P. and Jones, S. (1999a). A Wnt5a pathway underlies outgrowth of multiple structures in the vertebrate embryo. Development 126, 1211-23.

Yamaguchi, T. P., Takada, S., Yoshikawa, Y., Wu, N. and McMahon, A. P. (1999b). T (Brachyury) is a direct target of Wnt3a during paraxial mesoderm specification. Genes Dev 13, 3185-90.

Yang, X., Dormann, D., Munsterberg A. E. and Weijer, C. J. (2002). Cell movement patterns during gastrulation in the chick are controlled by positive and negative chemotaxis mediated by FGF4 and FGF8. Dev Cell 3, 425-37.

Ying, Q. L., Stavridis, M., Griffiths, D., Li, M. and Smith, A. (2003). Conversion of embryonic stem cells into neuroectodermal precursors in adherent monoculture. Nat Biotechnol 21, 183-6.

Yntema, C. L. (1968). A series of stages in the embryonic development of Chelydra serpentina. J Morphol 125, 219-51.

Yoshikawa, Y., Fujimori, T., McMahon, A. P. and Takada, S. (1997). Evidence that absence of Wnt-3a signaling promotes neuralization instead of paraxial mesoderm development in the mouse. Dev Biol 183, 234-42.

Zhang, N. and Gridley, T. (1998). Defects in somite formation in lunatic fringe-deficient mice. Nature 394, 374-7.

Zhou, X., Sasaki, H., Lowe, L., Hogan, B. L. and Kuehn, M. R. (1993). Nodal is a novel TGF-beta-like gene expressed in the mouse node during gastrulation. Nature 361, 543-7.